

University of West Bohemia
Faculty of Applied Sciences

THREE FILAMENT CROSS-BRIDGE MODEL OF SARCOMERE

Ing. Václav Čibera

A dissertation thesis submitted to obtain
the academic degree Doctor of Philosophy
in the field of Applied Mechanics

Supervisor: Assoc. Prof. Dr. RNDr. Miroslav Holeček
Department: Department of mechanics

Plzeň 2016

Západočeská univerzita v Plzni
Fakulta aplikovaných věd

CROSS-BRIDGE MODEL SARKOMERY SKLÁDAJÍCÍ SE ZE TŘÍ FILAMENT

Ing. Václav Čibera

Disertační práce předložená
k získání akademického titulu doktor
v oboru Aplikovaná mechanika.

Školitel: doc. Dr. RNDr. Miroslav Holeček
Katedra: Katedra mechaniky

Plzeň 2016

Declaration of authorship:

I declare that this submitted work is the product of my own work. All sources I have used and quoted have been indicated in references.

Václav Čibera

Acknowledgement:

First of all, I would like to thank for the consultations and help namely to Dr. Walter Herzog and to everyone in his working group at the University of Calgary in Canada. It is necessary to point out that the topic of submitted dissertation thesis emerged during my internship at the University of Calgary. The crucial parts of the thesis were created during this internship. I am very thankful that I could participate in very interesting and actual research.

Further, I would like to thank for the continuous support and consultations to my supervisors and colleagues at the University of West Bohemia. Namely I would like highlight the help of my supervisor doc. Dr. RNDr. Miroslav Holeček and my colleagues doc. Ing. Luděk Hynčík Ph.D. and prof. Ing. Josef Rosenberg DrSc. Further, I would like to thank also for the consultations in physiology to doc. Mudr. Milan Štengl Ph.D. and his working group at Faculty of Medicine in Pilsen.

Last but not least, I would like to thank to my parents, friends and namely to my girlfriend Veronika for their patience with me.

I would like to acknowledge the financial support of the The International Travel Grant Program by International Society of Biomechanics, SGS-2013-026 the internal grant at the University of West Bohemia, Pilsen, Czech Republic and Freemovers grant provided by the Ministry of Education, Youth and Sports in Czech Republic.

As soon as I mention this, people tell me about miniaturization, and how far it has progressed today. They tell me about electric motors that are the size of the nail on your small finger. And there is a device on the market, they tell me, by which you can write the Lord's Prayer on the head of a pin. But that's nothing; that's the most primitive, halting step in the direction I intend to discuss. It is a staggeringly small world that is below. In the year 2000, when they look back at this age, they will wonder why it was not until the year 1960 that anybody began seriously to move in this direction.

Richard Phillips Feynman, 1959 [24]

Abstract

The submitted dissertation thesis is focused on a theoretical mathematical model describing contractile activity of skeletal muscles. More specifically, the main subject of interest is the mathematical model of a structure called sarcomere. Sarcomere is traditionally considered as the basic contractile unit at the lowest level of muscle structural hierarchy (scale of units of μm). Sarcomere itself is a natural mechanism consisting namely of three specialized proteins in a shape of filaments - myosin, actin and titin.

Firstly, the basic contractile properties of muscles (sarcomere) are introduced in general. Considerable part of the thesis is devoted to the description of myosin and its interaction with actin, where the single myosins as molecular motors are able to develop discrete movements in a range of units of nm . Further, the protein titin and its role in sarcomere is described more profoundly. Namely, the important information about currently observed special properties of this protein is introduced.

On account of mathematical modelling, the thesis follows the classical cross-bridge theory and two sliding filament theory as developed during 1950s. More concretely, the cross-bridge theory was proposed and mathematically described in 1957 by A.F. Huxley. In brief, theoretical models based on those two approaches more or less succeeded in the elucidation of the nature of isometric contraction (force at constant muscle length) and concentric contraction (shortening). Till nowadays, the most challenging part of the mentioned theories remains the explanation of eccentric contraction (stretch). The another insufficiently explained properties of muscle contraction are history-dependent phenomenons namely force depression following after concentric contraction and force enhancement following after eccentric contraction.

To summarize the main aims of dissertation thesis, the main goals were to modify and enhance the classical Huxley's mathematical model according to the latest experimental results obtained on a single myosin molecule (single cross-bridge) and according to the experimental results on a single sarcomere. Further on account of the description of eccentric contraction and force enhancement, the pivotal modification is the integration of the currently discovered special titin properties into classical approaches.

Therefore, one of the main results of the presented thesis is the derived *mathematical three filament cross-bridge model* of skeletal muscle (sarcomere) contraction. Based on this model, the main goal of the thesis is to show convincing results that the crucial mechanical properties of muscle contraction have their origin on a sarcomere or more specifically on a half-sarcomere level. In particular, simulations of eccentric contraction and force enhancement on a half-sarcomere level were performed. Further, the results of simulation of isometric contraction, concentric contraction, sudden shortening and sudden stretch are presented. The achieved results are compared to various experimental results as published in literature. The important conclusion of the thesis is that the results achieved

by the derived three filament cross-bridge model might significantly contribute namely to the explanation of the nature of eccentric contraction and its intrinsic phenomenon called force enhancement.

keywords: muscle contraction, eccentric contraction, sarcomere, myosin, titin, molecular motors, Huxley's cross-bridge model, two sliding filament theory.

Abstrakt

Předkládaná disertační práce se zabývá teoretickým matematickým modelem, který popisuje kontrakci kosterního svalstva. Hlavním předmětem zájmu je konkrétně matematický model struktury nazývané sarkomera. Sarkomera je tradičně považována jako základní funkční jednotka svalové kontrakce na nejnižší úrovni strukturální hierarchie svalstva (škála jednotek μm). Sarkomera samotná je přírodní mechanismus, který se skládá především ze tří speciálních proteinů - myosinu, aktinu a titinu.

V práci jsou nejdříve obecně popsány základní vlastnosti kontrakce svalu (sarkomery). Velká část práce je věnována popisu myosinu a jeho interakci s aktinem, kde jednotlivé myosiny jakožto molekulární motory jsou schopny vyvinout diskrétní pohyb v řádu jednotek nm . V následující části práce je podrobněji popsán protein titin a jeho úloha v sarkomere. Tato část dizertace také obsahuje důležité informace o v současné době pozorovaných speciálních vlastnostech tohoto proteinu.

Způsob matematického modelování uvedené problematiky vychází z klasické cross-bridge teorie (cross-bridge theory) a klasické "teorie dvou filament" (two sliding filament theory), které byly navrženy v padesátých letech 20. století. Cross-bridge teorii konkrétně navrhl a zachytil do matematického modelu A.F. Huxley v roce 1957. Teoretické modely založené na těchto dvou teoriích více či méně uspěly ve vysvětlení podstaty izometrické kontrakce (síla při konstantní délce svalu) a koncentrické kontrakce (zkracování svalu). Do současnosti zůstává obtížnou částí výše uvedených teorií vysvětlení excentrické (eccentric, tažení svalu) kontrakce. Další vlastnosti, které nejsou dostatečně vysvětleny, jsou jevy závislé na historii kontrakce. Konkrétně se jedná o nižší než očekávanou velikost síly (force depression) následující po koncentrické kontrakci a vyšší než očekávanou velikost síly (force enhancement) následující po excentrické kontrakci.

Shrnutí hlavních cílů dizertace je následující. Hlavním cílem bylo modifikovat a vylepšit klasický Huxleyho matematický model vzhledem k aktuálním experimentálním výsledkům obrženým na úrovni jednotlivých molekul myosinu (na úrovni jednoho cross-bridge) a vzhledem k experimentálním výsledkům získaných na úrovni jedné sarkomery. Další důležitou úpravou s ohledem na popis excentrické kontrakce je začlenění nově objevených speciálních vlastností titinu do klasických teorií.

Jedním z hlavních výsledků práce je proto odvozený matematický model založený na cross-bridge teorii, který popisuje kontrakci kosterního svalstva (sarkomery) jako interakci tří filament. Na základě tohoto modelu je hlavním cílem disertační práce ukázat přesvědčivé výsledky o tom, že klíčové mechanické vlastnosti svalové kontrakce mají svůj původ na úrovni sarkomery nebo ještě přesněji na úrovni poloviny sarkomery. Především byly provedeny simulace excentrické kontrakce a jevu nazývaného force enhancement. Dále jsou v práci prezentovány výsledky ze simulací izometrické kontrakce, koncentrické kontrakce, náhlého zkrácení sarkomery (sudden shortening) a náhlého natažení sarkomery (sudden

stretch). Výsledky ze simulací byly porovnány s různými experimentálními výsledky publikovanými v literatuře. Důležitým závěrem dizertační práce je, že výsledky získané pomocí odvozeného cross-bridge modelu, který popisuje interakci tří filament, mohou podstatně přispět k vysvětlení podstaty excentrické kontrakce a s ní spojeným jevem nazývaným force enhancement.

klíčová slova: svalová kontrakce, excentrická kontrakce, myosin, titin, sarkomera, molekulární motory, Huxleyho cross-bridge model, two sliding filament teorie.

Resumen

La presente tesis doctoral está centrada en la descripción de un modelo matemático capaz de predecir la actividad contráctil de músculos esqueléticos, específicamente la actividad de su unidad básica denominada sarcómero. El sarcómero es la unidad contráctil del músculo (en una escala de μm) que a su vez se constituye de tres proteínas filamentosas: la miosina, la actina y la titina.

En primer lugar se describe en esta tesis, en términos generales, las propiedades básicas contráctiles de los músculos. Gran parte del texto está centrada en la descripción de la miosina y su interacción con la actina, donde las estructuras de miosina actúan como motores moleculares que son capaces de desarrollar movimientos discretos en la escala nanométrica. También se describe con gran profundidad el papel que juega la titina en el sarcómero, proteína en la que se han observado recientemente ciertas propiedades especiales.

Respecto a la modelización matemática, la presente tesis se basa en la teoría clásica de cross-bridge, descrita por el Nobel Sir Andrew F. Huxley, y en la teoría de filamentos deslizantes (sliding filament theory), ambas desarrolladas durante la década de 1950. Modelos matemáticos posteriores que se basan en las dos anteriores teorías han predicho con éxito tales procesos naturales como la contracción isométrica (fuerza con longitud muscular constante) o la contracción concéntrica (acortamiento). Sin embargo, hasta hoy en día, estas teorías fallan en la modelización de la contracción concéntrica (estiramiento) del músculo. Otra de las carencias de estos modelos es la descripción de la de tales propiedades que dependen de la historia muscular, concretamente depresión de fuerza (force depression) después de la contracción concéntrica y el desarrollo de fuerzas (force enhancement) después de la contracción excéntrica.

Los principales objetivos de esta tesis han sido modificar y mejorar el clásico modelo matemático descrito por Huxley de acuerdo con los recientes resultados experimentales sobre la molécula miosina (single cross-bridge) y sobre la unidad básica muscular (sarcómero). Considerando la carente descripción de la contracción excéntrica y desarrollo de fuerzas (force enhancement), la central modificación del modelo se basa en la inclusión de las mencionadas propiedades especiales de la titina dentro del modelo clásico.

Asimismo, uno de los principales resultados de esta tesis doctoral es el desarrollo del denominado modelo matemático del cruzamiento de tres filamentos (mathematical three filament cross-bridge model) durante la contracción de músculos esqueléticos (sarcómero). Basándose en este modelo, el principal objetivo de esta investigación yace en la obtención de resultados convincentes que arrojen luz a que las propiedades mecánicas de la contracción muscular tienen su origen en su unidad básica, es decir, en el sarcómero. Para ello, se han realizado simulaciones del modelo sobre la contracción excéntrica y del desarrollo de fuerzas (force enhancement). De la misma manera se presentan resultados de simulaciones de

contracción isométrica, contracción concéntrica, rápido acortamiento y rápido estiramiento. Los resultados obtenidos se comparan con varios resultados experimentados publicados en la literatura científica.

La conclusión más importante de esta investigación es que los resultados obtenidos del modelo matemático desarrollado para esta investigación pueden contribuir significativamente a la explicación de la naturaleza de la contracción excéntrica y a su fenómeno intrínseco llamado desarrollo de fuerzas (force enhancement).

Palabras clave: contracción muscular, contracción excéntrica, sarcómero, miosina, titina, motores moleculares, modelo cross-bridge de Huxley, teoría del deslizamiento de dos filamentos.

Contents

1	Introduction and Motivation	24
2	Sarcomere - An Amazing Nanomachine	32
2.1	General Description of Sarcomere	35
2.2	Structure of Sarcomere	37
2.2.1	A-band	37
2.2.2	I-band	38
2.3	Contraction properties	38
2.3.1	Three main types of contraction	39
2.3.2	Force-velocity relationship	41
2.3.3	Isometric contraction, Gordon's graph: force-length relationship . .	43
2.3.4	Concentric contraction	46
2.3.5	Eccentric contraction	49
3	Myosin II - Muscle Molecular Motor	57
3.1	Molecular Motors in General	57
3.1.1	Mechanochemical cycle - conformation states and power stroke . . .	59
3.1.2	Movement on molecular motor tracks	61
3.1.3	Processive vs. non-processive motors	61
3.1.4	Thermodynamics of molecular motors	62
3.1.5	Myosin family	65
3.2	Myosin II - Muscle Propelling Engine	67
3.2.1	Single myosin II molecule	68
3.2.2	Power-stroke and myosin II conformation cycle	71
3.2.3	Single myosin II molecule mechanics	77
3.2.4	Myosin filament, thick filament	81
3.2.5	Actin - A Linear Track for Molecular Motor Myosin, thin filament .	83

3.2.6	Spatial arrangement of myosin and actin filaments	84
3.3	Contraction - Interaction between Myosin and Actin Filaments	87
3.3.1	Contraction velocity	87
3.3.2	Regulation of contraction - regulation of cross-bridge cycling activity	88
4	Titin - An Entropic Molecular Spring	91
4.1	Repetitive building blocks of titin	93
4.2	Titin in Sarcomere	93
4.2.1	Titin in I-band	94
4.2.2	Titin in A-band of sarcomere	95
4.3	Titin Mechanics	95
4.3.1	Single titin molecule mechanics	96
4.3.2	Unfolding and refolding of single protein	97
4.3.3	Changing of mechanical properties of titin molecule	100
4.4	Binding of titin to actin filament - a clue to modification of classical Huxley's cross-bridge model and hint to explanation of eccentric contraction	101
5	Mathematical Models - A Brief Overview	104
5.1	Single myosin molecule mechanics	105
5.1.1	Force production of single cross-bridges	105
5.1.2	Strongly bound duration	106
5.2	State models of molecular motors	107
5.3	Hill's model of the force-velocity relationship	108
5.4	Huxley's cross-bridge model and Huxley type of models	112
5.4.1	Common modifications of Huxley's model	117
5.4.2	Results of Huxley's model	118
5.4.3	Conclusion on Huxley's type of models	119
5.5	Zahalak's Distribution Moment Model	120
5.6	Mathematical Models of Titin	123
5.6.1	Worm-like-chain model	123
5.6.2	Unfolding and refolding of proteins	125
5.6.3	Three filament model - stochastic model of IG domain unfolding	127
6	Proposed Three Filament Cross-Bridge Model	131
6.1	Derivation of the Three Filament Cross-bridge Model	131

6.1.1	Active force: force F_{CB} generated by cross-bridges in actin-myosin overlap	133
6.1.2	Another quantities describing properties of cross-bridge mechanism	147
6.1.3	Preservation of cross-bridges error in classical Huxley's cross-bridge model	149
6.1.4	Passive force: force F_T generated by the bunch of titin filaments . .	151
6.2	Three Filament Cross-Bridge Model of Sarcomere	154
6.2.1	Dynamic form of Three Filament Cross-Bridge Model	154
6.2.2	Steady-state model	156
6.2.3	Initial and boundary conditions:	158
7	Simulation and results	160
7.1	Model parameters and half-sarcomere properties	164
7.2	Isometric Contraction	167
7.3	Concentric Isotonic Contraction	171
7.3.1	Sudden shortening	177
7.4	Eccentric Contraction (stretch of half-sarcomere)	181
7.4.1	Properties of steady-state force enhancement	191
7.4.2	Sudden stretch	195
8	Conclusion and summary on the achieved results	199

List of Figures

2.1	Arrangement of contractile proteins in smooth muscle cell.	33
2.2	Schematic diagram of skeletal muscle structural hierarchy in vertebrate striated muscle. The picture was adapted from [47].	34
2.3	Structure of sarcomere with three main structural filaments: actin, myosin and titin. The picture was adapted from [33].	36
2.4	Molecular structure of vertebrate striated muscle sarcomere's A-band. Seven myosin filaments and twelve actin filaments are shown during contraction. The source of picture is [111].	37
2.5	Concentric (shortening), isometric (force production at constant length) and eccentric (lengthening) contraction of skeletal muscle and relevant dynamic force-time relationship with length-time relationship. The picture was adapted from [23].	40
2.6	Illustrative curves of force-velocity relationship and muscle power. A) Force-velocity relationships for the domain of concentric contraction. B) Power curves of muscle. Modified from [10].	42
2.7	General shape of force-velocity relationship. The force-velocity relationship in both eccentric contraction domain and concentric contraction domain. The case for $V = 0$ corresponds to isometric contraction. Source of picture [10].	42
2.8	Illustrative force production of muscle during isometric contraction, when the muscle is kept at constant length. At $t = 0$ the muscle is activated and starts to produce the force. After a while, the force production reaches its maximum. This maximum is kept by muscle until it is deactivated or subjected to the changes of surroundings. Adapted from [35].	44

- 2.9 **Gordon's graph:** Force-length relationship. Summary of the results of force production of isometric contraction conducted along the sarcomere lengths by which actin and myosin filaments have various degree of overlap. The arrows with numbers in the top part of the graph are intrinsic to the numbered stages as depicted in figure 2.10. The picture was modified from [29]. 45
- 2.10 Critical lengths of sarcomere according to Gordon's graph. The picture shows significant stages of actin-myosin overlap. The picture was modified from [29]. 45
- 2.11 Force-length relationship for isometric contraction obtained from measurement on single sarcomeres. The open circles represent the force obtained at $15^{\circ}C$ and closed circles represent the forces measured at $20^{\circ}C$. The continuous lines represents results of least squares fitting and fitting with linear regression. The picture with its description was adapted from [95]. 46
- 2.12 Illustrative transient state of force during concentric contraction followed by steady-state isometric force. At $t = 0$ the muscle is activated and force production is approaching its maximum force intrinsic to isometric contraction at particular length. Then the muscle is subjected to shortening accompanied by characteristic decrease in a force. After a while, the shortening is stopped and the force production approach the steady-state magnitude of force related to isometric contraction at new corresponding length. Modified from [35]. 47
- 2.13 Force-time histories of concentric contraction conducted for various shortening speed in the range of $4 - 128\text{mms}^{-1}$, depicted as lines $b - f$ regarding to magnitudes of speed. The shortening distance of muscle was 8mm for all speeds and the final length of sarcomere was the same for all speeds. The resulted forces are compared to isometric force at corresponding resulted length, depicted as line a . Adapted from [42]. 47
- 2.14 Example of force depression. The top line represents an isometric force achieved at constant length. The bottom line represents the concentric contraction followed by isometric contraction at the same length like isometric contraction of top line. ΔF represents the force depression. The picture was adapted from [35]. 48

2.15	Transient force respond of muscle exposed to sudden shortening step. The top line represents sudden shortening step in length. The bottom line represents the corresponding force-time relationship. The picture was adapted as published by Huxley in 1971 in [54].	49
2.16	Illustrative force-time relationship of eccentric contraction. The muscle is first activated at constant length. Consequently, the muscle is lengthened by external force to the new length. Adapted from [41].	50
2.17	The stretches of 9, 6, 3 mm conducted by speed of 9 mms^{-1} , f denotes reference isometric contraction. The picture was adapted from [41].	51
2.18	The stretches of 9, 6, 3 mm conducted by speed of 27 mms^{-1} , f denotes reference isometric contraction. The picture was adapted from [41].	51
2.19	Force enhancement ΔF : the top line represents force-time relationship of eccentric contraction. The bottom line represents isometric contraction. The force produced by muscle after stretch is higher than the force produced during isometric contraction at corresponding (same) length. The picture was adapted from [35].	52
2.20	The dependence of the magnitude of force enhancement on the magnitude of stretch. f represents the reference isometric contraction. The lines 9, 6, 3 represent the force-time relationship for stretches conducted for 9, 6 and 3 mm. All stretches were conducted for the same speed of 3 mms^{-1} . The picture was adapted from [41].	53
2.21	Force enhancement on three structural levels of skeletal muscle. A shows force enhancement in an entire muscle. B depicts force enhancement on isolated myofibril. C represents force enhancement in a single, mechanically isolated sarcomere. The grey lines in A refers to isometric reference force and length. The black lines in A represents course of force during stretches. The grey trace in B is a passive stretch while the black trace is an active stretch of a myofibril. The picture and the annotations are adapted from [37], [38], [43].	54
2.22	Illustration of passive force enhancement ΔP . ΔF is force enhancement after stretch. The top line represents eccentric contraction. The middle line represents isometric contraction at corresponding length of the final length of eccentric contraction. The bottom line represents stretch of passive muscle. Adapted from [35].	55

2.23	Sudden stretch of muscle as published by Huxley in 1971 [54]. The top line represents sudden change of muscle length - ramp stretch. The bottom line represents the corresponding force-time relationship during response on ramp stretch.	55
3.1	Mechanochemical cycles of myosin (left) and kinesin (right). The myosin force-producing step occurs with P_i release. In contrary, ATP binding is thought to be the force-producing step for kinesin based motors. Modified from [73].	60
3.2	a) Lever arm movement of myosin molecular motors. b) Movement of myosins in hand-over-hand fashion. The picture was adapted from [27]. . .	67
3.3	The two headed structure of single myosin molecule (single cross-bridge). The scheme depicts following parts: MHC - myosin heavy chains, essential light chains (LC), regulatory light chains (LC), ATP binding loop, actin binding loop, carboxyl terminal subfragment-1 (S1) part, subfragment-2 part(S2). MHC can be cleaved to into α -helical light meromyosin (LMM), S2 and S1. The picture adapted from [18].	69
3.4	The N-terminal 25-kDa domain is labeled green. The upper and lower 50-kDa domains are red. The C-terminal 20-kDa is blue. The regulatory light chain is (RLC) light blue. The essential light chain (ELC) is purple. The picture with its description was adapted from [120].	70
3.5	Myosin power-stroke mechanism as proposed by H. E. Huxley in 1969. He proposed that the source of force production is rotation of head $S1$, where the movement of rotation is transmitted to the actin filament by the S-2 part of single myosin molecule. The picture is adapted from [56], [49]. . . .	73
3.6	A.F. Huxley and Simmons further enhanced proposals [54] on mechanism as depicted in figure 3.5. They incorporated elastic element and stepwise-shortening elements into force-producing model. The picture is adapted from [49].	73
3.7	Schematic representation of cross-bridge cycle during contractile activity. The picture is adapted from [101].	75
3.8	Myosin conformation cycle. Picture shows $10nm$ power-stroke. The picture is adapted from [113].	75

3.9	Biochemical and structural states of ATPase cycle. A = actin, M = myosin, T = ATP, D = ADP, P = P_i . Upper case K_i denotes equilibrium kinetics rates of state transitions, k_i denotes kinetics rates of various state transitions. Adapted from [87].	76
3.10	The interaction of myosin with actin. The green, red and blue segments represent the heavy chain. Yellow segment represent essential light chains. The magenta segment represent regulatory light chain. The picture is adapted from [101].	77
3.11	The structure of actomyosin. Adapted from [87].	77
3.12	Stretch of elastic element by power stroke. The picture is adapted from [21].	79
3.13	Force-length relationship for single myosin molecule as measured and published in [62].	80
3.14	Force-length relationship for single myosin molecule as measured and published in [63].	80
3.15	Stiffness-force relationship. Adapted from [63].	81
3.16	Myosin thick filament and its bipolar structure. Source of picture [2]. . . .	82
3.17	Comparison of skeletal muscle myosin filament (A) and smooth muscle myosin filament B . Skeletal muscle filament is a bipolar structure with a central bare zone without myosin heads. Myosin filament in smooth muscle is believed to be "side polar". Adapted from [18].	82
3.18	Structure of actin (F-actin, where "F" stands for filamentous). Four main components are: actin monomer (referred as G-actin), tropomyosin and troponin complex consisting of three components: troponin-C, troponin-I and troponin-T. The picture is adapted from [2].	85
3.19	Atomic model of F-Actin filament. The arrangement of troponin (Tn), tropomyosin and actin in the skeletal muscle thin filament. The various troponin subunits are color coded - TnC(red), TnT(yellow) and TnI(green). The picture is adapted from [28].	86
3.20	Schematic drawing of a cross-section through the myosin and action filaments lattices within the A-band parts of sarcomere. (A) fish skeletal muscle, (B) insect fibrillar flight muscle, (C) scallop pecten muscle. Adapted from [2].	86
3.21	Assumed arrangement of myosin and actin filaments in smooth muscle cell. Modified from [104].	87
4.1	Titin's domains and titin's parts in its structure. Modified from [98]. . . .	91

4.2	Sarcomere structure and the titin structure in the skeletal and heart muscle. The picture was adapted from [30].	92
4.3	Structure of titin Ig domains as solved by x-ray crystallography. These domains are representative for proximal Ig domain segment <i>I1</i> , distal Ig domain segment <i>I27</i> , and the segment in A-band <i>M5</i> . The picture is adapted from [118].	94
4.4	Typical response to force of protein unfolding achieved by Atomic force microscope. The graph is adapted from [26].	98
4.5	Measured single titin molecule hysteresis. The graph is adapted from [67].	99
4.6	Unfolding of seven (of eight possible) distal cardiac Ig domains with atomic force microscopy. Broken line represent $200pN$. Left part of graph shows control force-length curve without presence of calcium. Right part of graph shows force-length curve with presence of calcium. The graph was adapted from [17].	100
4.7	Titin-induced force enhancement. A: Left part of picture represents stretch of deactivated half-sarcomere. Right part of picture represents stretch of activated half-sarcomere (eccentric contraction). B: The effects of titin's modulated properties illustrated in force-length graph. Adapted from [43].	102
5.1	Strongly vs. weakly bound duration. The picture was modified from [120].	106
5.2	Diagram of a four state model with states A, B, C, D and kinetic rates $k_i, i = 1, \dots, 8$	107
5.3	Length and force during isotonic contraction, which started from isometric contraction. Time course of the length response to a force step during an isotonic quick release. The shape of phases 1-2-3 is caused by transient behaviour of elastic element in muscle and cross-bridge transient behaviour. The phase 4 is characterized by linear slope during steady-state isotonic shortening. The picture was adapted from [110].	109
5.4	Relation between load and speed of shortening in isotonic contraction. The curve is calculated from the equation $(P + 14.35)(v + 1.03) = 87.6$. Hence $a = 14.35, b = 1.03cm/sec = 0.27length/sec$. The graph with its description is adapted from [44].	110
5.5	The dashed line and closed circles depict power output ($= F.v$) of muscle. The solid line and open circles is force-velocity relationship. The graph is adapted from [110] where it was modified originally from [44].	111

5.6	Historical diagram showing the arrangement of the filaments, which was suggested during the 1950s. Note that in comparison to recent schemes as in picture 2.3 on page 36 and in picture 4.2 on page 92 the titin filaments are completely missing. Further, the single actin filaments were assumed to connect both Z-lines across sarcomere. The pictures was adapted from Huxley's 1957 article [48].	112
5.7	Diagram illustrating the mechanism of contraction (tension generation) as suggested by Huxley in 1957 [48]. The part of a fibril which is shown is in the right-hand half of an A band, so that the actin filament is attached to a Z line which is out of the picture to the right. The arrows give the direction of the relative motion between the filaments when the muscle shortens. The picture with its description is adapted from [48].	113
5.8	The shapes of kinetic rates: f - bounding rate, g unbinding rate as proposed by Huxley in [48].	116
5.9	Results for Huxley's 1957 n distribution for various values of velocity v . The top part shows the distribution for $v = 0$, i.e. for isometric contraction. Adapted from [48].	118
5.10	Huxley's model comparison to Hill's model as published in [48]. The continuous line is Hill's model. The circles are results of Huxley's model. The graph depicts results of concentric isotonic contraction.	119
5.11	Results of Zahalak's distribution model as published in [128]. The picture depicts tension-length for a muscle subjected to constant-velocity stretches starting from isometric states corresponding to various initial lengths and stimulus rates. The interrupted curves represents isometric force of various activation. The thin curves are stretches labelled with corresponding velocities in $mm s^{-1}$	124
5.12	The results of eccentric contraction simulation as achieved with stochastic function as presented in [108]. The top panel depicts the forces from regular cross-bridge as simulated in [108]. The second panel depicts results considering three filaments. The last panel depict corresponding length of sarcomere. For comparison with measured data see figure 2.16 on page 50, figure 2.17 on page 51, figure 2.18 on page 51 and figure 2.19 on page 52. . .	129

6.1	Conceptual model of titin's force regulation during eccentric contraction as proposed and published in [40]. Nowadays experimental research indicate that titin actively bind to actin and further titin increase its stiffness in the presence of calcium ions. Both of these new emerging properties give to the titin more important role than originaly thought in classical cross-bridge theory.	132
6.2	Force- x end-to-end relationship of single cross-bridge. In comparison to original measured data as published in [62], [63] the x-axis was moved according to the length of S2 part of cross-bridge. This modification allowed to use the end-to-end distance of cross-bridge's ends (compare with figures 3.13 and 3.14 on page 80).	135
6.3	Diagram of two states model with states N_{ax} and N_{ux} with bound kinetic rate f_x and unbound kinetic rate g_x	138
7.1	Selected properties of sarcomere and its parameters.	166
7.2	Properties of isometric contraction.	167
7.2	Properties of isometric contraction.	168
7.2	Properties of isometric contraction.	169
7.3	Properties of concentric contraction.	171
7.3	Properties of concentric contraction.	172
7.3	Properties of concentric contraction.	173
7.4	Properties of contraction during sudden shortening.	177
7.4	Properties of contraction during sudden shortening.	178
7.4	Properties of contraction during sudden shortening.	179
7.5	Properties of eccentric contraction.	181
7.5	Properties of eccentric contraction.	182
7.5	Properties of eccentric contraction.	183
7.6	Proportion of the number of cross-bridges in $n(x, t)$ distribution during stretches of speeds $v = 0, 100, 150, 200, 300 \text{ nm s}^{-1}$	186
7.7	Force distribution $f_{cb}(x)n(x, t)$ during stretches of speeds $v = 0, 100, 150, 200, 300 \text{ nm s}^{-1}$	187
7.8	Simulation of eccentric contraction for length of stretches 60, 120, 180 nm with speeds of $-100, -150, -200, -300 \text{ nm s}^{-1}$	189
7.9	Comparison between classical two sliding filament theory (classical Huxley's approach) and three filament theory (proposed three filament cross-bridge model).	190

7.10	Demonstration of force enhancement achieved in simulation. The blue line represents the force-time relationship during eccentric contraction. The black line represents the isometric force at sarcomere length corresponding to the length of sarcomere after stretch.	191
7.11	Simulation of force enhancements conducted for stretches of 60, 120, 180 nm with speeds $-100, -150, -200, -300 \text{ nm s}^{-1}$	193
7.12	Force enhancements performed for stretches of 60nm, 120nm, 180nm with speeds of $-100, -150, -200 \text{ nm s}^{-1}$	194
7.13	Properties of contraction during sudden stretch.	195
7.13	Properties of contraction during sudden stretch.	196
7.14	$n(x, t)$ time evolution during simulation of sudden stretch $v = -1800 \text{ nm s}^{-1}$	197

List of Symbols, Abbreviations and Nomenclature

\AA	Ångström
ADP	adenosine diphosphate
AFM	atomic force microscope
a in c-b model	longest end-to-end distance of attached cross-bridge in wrong direction
a in Hill's eq.	constant within Hill's equation of force-velocity relationship
A	persistence length of wlc chain
ATP	adenosine triphosphate
ATPase	adenosine triphosphatase
b in c-b model	longest end-to-end distance of attached cross-bridge in right direction
b in Hill's eq.	constant within Hill's equation of force-velocity relationship
c-b	cross-bridge
Da, kDa	Dalton, kiloDalton, unit used for indicating mass on molecular level
d_e	elongation of cross-bridge's elastic part
ΔG_{ATP}	Gibbs free energy released through the hydrolysis of ATP
ΔL	chain's contour length increment after Ig-domain unfolding
Δx	distance of the stretch over which the force must be applied to reach unfolding/fold
d_s	step-size (shortening step) after power-stroke
d_w	magnitude of power-stroke
E_a	activation energy for unfolding (energy barrier of bond)
ELC	essential light chains
f_{Ca}	parameter in bound rate $f(x)$ depending on concentration of Ca^{2+}
F_{CB}	active force produced by cross-bridges
F_{CBS}	steady-state force exerted by cross-bridges
$f_{cb}(x)$	force exerted by single cross-bridge according to its x end-to-end distance
F_E	external force acting on Z-line
F	force produced by sarcomere/muscle
F_{max}	maximal force achieved by sarcomere
Fn-3	fibronectin-3, part of titin
F_S	(half-) sarcomere force acting on Z-line
F_{SS}	steady-state (reference isometric) force of (half) sarcomere
F_T	passive force exerted by titins upon stretch
F_{TS}	steady-state force exerted by titins

F_{wlc}	force described by worm-like-chain model
$f(x)$	bound rate [s^{-1}]
f_x	the value of bound kinetic rate for particular x
g_{ATP}	part of unbound rate $g(x)$ depending on concentration of ATP
G	Gibbs free energy
$g_L(x)$	part of unbound rate $g(x)$ depending on load of cross-bridge
g_x	the value of unbounding kinetic rate for particular x
$g(x)$	unbound rate [s^{-1}]
h	Huxley's interval (a, b) within cross-bridges bound with particular x
HMM	Heavy meromyosin, part of myosin
Ig	immunoglobulin, part of titin
k_B	Boltzmann constant
k_{cb}	stiffness of single cross-bridge
$k_n, n \in N$	rate constants in state models [s^{-1}]
LC	essential and regulatory light chains
L	contour length of wlc chain, protein
L_f	contour length of folded Ig domain
L_f	contour length of single folded Ig-domain
l	length of actin-myosin overlap
l_{max}	maximal length of actin-myosin overlap
LMM	light meromyosin
l_{plato}	length of plato (bare zone) of myosin filament
l_S	length of (half) sarcomere
l_{S0}	initial (half) sarcomere length
l_T	end-to-end distance of titin's ends, length of titin stretch
l_{T0}	initial stretch of titin
L_u	contour length of single unfolded Ig-domain
L_u	contour length of unfolded Ig domain
l_0	initial actin-myosin overlap
m_{cb}	number of cross-bridges in (half) sarcomere
MHC	myosin heavy chains
MLC ₁	myosin light chain-1
MLC ₂	myosin light chain-2
MLC ₃	myosin light chain-3
μ	parameter in log-normal distribution of bound kinetic rate $f(x, [Ca^{2+}])$

μ_T	parameter in distribution of in initial lengths of l_T
N_{ax}	number (proportion) of attached cross-bridges with particular x
N_{fIg}	number of folded Ig domains
N_{fIg}	number of folded Ig-domains
N_{Ig}	number of Ig-domains
$n_s(x)$	steady-state (isometric) distribution of the number (proportion) of cross-bridges
N_T	number of titin filaments in (half) sarcomere
N_{uIg}	number of unfolded Ig domains
N_{uIg}	number of unfolded Ig-domains
N_{ux}	number (proportion) of unattached cross-bridges at particular x
$n_u(x, t)$	distribution of unattached cross-bridges end-to-end distances at time t
$n(x, t), n_a(x, t)$	distribution of attached cross-bridges x end-to-end distances at time t
N2A	non-repetitive part of titin
N2B	non-repetitive part of titin
ω, ω_0	natural or attempt frequency of oscillation
PEVK	proline, glutamate, valine and lisyne -rich domain non-repetitive part of titin
P_i	inorganic phosphate
P_m	sarcomere/muscle power
P	tension developed by sarcomere/muscle
Q	parameter in $g_{ATP}(x)$ unbound function
RLC	regulatory light chains
R	parameter in $g_{ATP}(x)$ unbound function
σ	parameter in log-normal distribution of bound kinetic rate $f(x, [Ca^{2+}])$
σ_T	parameter in distribution of in initial lengths of l_T
S1	subfragment-1, the part of myosin molecule
S2	subfragment-2, the part of myosin molecule
τ_{-ADP}	time constant for ADP release
τ_{+ATP}	time of the ATP binding to myosin
τ_{on}	time that myosin spends strongly bound to the actin
τ	time of contraction end
Tm	tropomyosin
TnC	troponin-C
TnI	troponin-I
Tn	troponin
TnT	troponin-T

v_{max}, V_{max}	maximal shortening (concentric contraction) velocity of sarcomere
v, V	velocity of contraction
WLC, wlc	worm-like-chain model
x	shortest end-to-end distance between cross-bridge's ends
x_0	end-to-end distance by which cross-bridge exerts zero force

Chapter 1

Introduction and Motivation

The possibility to conduct a directed movement is one of the most striking features of the living organisms. It can be resolved on a macro-scale level as well as on a micro-scale and nano-scale level. In a fact, the active movement of all living organisms on the macro-scale, as we can observe without special equipment, is in summary superposition of the movements generated at nano-scale level. In the realm of biological nano-world, the source of an active movement are special proteins called *molecular motors* - biological engines.

Molecular motors are small mechanisms developed during the millions years of evolution. They are responsible for intracellular transport, organization of (in) cells, organelle movements, cell division, mitose, muscle contraction and other physiological processes. It might be said that these mechanisms are one of the crucial parts that create "life nature" because their physiological activity fundamentally contributes to the "maintaining of the life" on a cellular level.

In contrast to macroscopic engines, molecular motors operate mainly at the single molecule level in Brownian environment, thermodynamically nonequilibrium but isothermal conditions [71]. Due to their operating environment which is strongly affected by thermal noise, their features differ in many properties in comparison to macro-scaled engines. But as a great surprise might be a fact that these small mechanisms has also a lot of in common with "ordinary" macroscopic engines. Regarding to this comparison, there

can be found biological motors conducting linear translational motion as well as rotational motion. In comparison to “classical engines”, molecular motors are also cyclic machines. During their activity, molecular motors undergo specified working cycle. The single molecular motors must go through this cycle and reach again the same initial state before it can produce work again. Within their working cycle, these biological nanometer-sized motors consume energy released from chemical reaction to produce mechanical work. On account of the huge number of living organisms, this results for example in a fact that more energy is transformed each day by biological engines than by all artificial engines including the cars [97].

The beginning of understanding to molecular motors is strictly connected with the research on muscles and experiments in physiology. The pivotal results which significantly contributed to the progress in understanding of molecular motors were achieved during the 1950s in the experiments on striated skeletal muscles. Although that time the terms as molecular motors were not used, it was already apparent that at the nano-scale level of biological systems is occurring something, which soon started to attract attention not only of physiologists but also of specialists in other scientific fields as physic, math, chemistry etc. As a proof might be that for instance already in 1959, well-known physicist Richard Phillips Feynman mentioned in his famous talk Plenty of Room at the Bottom [24] the "*marvellous biological systems*" as an example and great source of inspiration for technology.

Nowadays, after of almost seventy years of intensive research, with new observation and measuring techniques, it is possible and feasible to examine these small mechanisms in more details. During the 1990s, two main techniques were introduced: Optical tweezers and glass needles. These tools allowed to conduct experiments on single molecules. Further experiments with atomic force microscope allowed to measure length-force relationships of proteins in the length range of Å. Therefore, it is now possible to observe and even control the motion of a single motor-protein molecule under a variety of conditions and with a high spatial and time resolution [71]. The popularity and the importance of the topic of molecular motors was also highlighted by the Nobel Prize in Chemistry 2016 awarded to Jean-Pierre Sauvage, Sir J. Fraser Stoddart and Bernard L. Feringa "for the design and

synthesis of molecular machines".

Although many types of molecular motors are still being discovered, the most currently known are the families of: dynein, kinesin, myosin, DNA and RNA polymerases and helicases [71]. The main subject of interest in the following pages is a molecular motor from myosin family, concretely molecular motor *myosin II*. Myosin II molecular motor is the main propelling engine of all kind of muscles. As an inherent part of musculoskeletal system and cardiac tissue, the myosin II constitutes with another two functional and structural proteins *actin* and *titin* regular structures called *sarcomeres*.

Single sarcomeres are objects at the lowest level of regular organisation of skeletal and heart muscles. The higher levels of organisation in skeletal and heart muscles are always basically serially linked sarcomeres into parts called myofibriles. The final contractile activity of the whole muscle is then the superposition of contractile activity of great amount of sarcomeres in each myofibrile. The various properties of single sarcomeres are therefore the subjects of the intensive and manifold researches in muscle science. Also due to this reason, the mechanical properties of a single sarcomere, considered as a mechanism powered by molecular motor myosin II, are the main subject matter in this submitted thesis.

The presented work is especially devoted to a theoretical mathematical model describing activity of bunch of myosins II, actins and titins proteins in a single sarcomere. The main aim of presented work was to show convincing results that the crucial mechanical properties of muscles have their origin on sarcomere or more specifically half-sarcomere level. The submitted dissertation thesis followed an approach and theories called *sliding filament theory* and especially *cross-bridge* theory as developed and discussed during the decades mainly in [48], [51], [54], [56].

In brief, the sliding filament theory was established during 1950s by two independent teams leaded by Andrew Fielding Huxley¹ and Hugh E. Huxley and their co-workers. The first basic assumption of this theory was (is) that proteins actin and myosin in the shape of filaments slide relative to one another during contractile activity of sarcomeres. In 1950s, this assumption came directly of microscopy observation, but the exact propelling

¹The Nobel Prize in Physiology or Medicine 1963

mechanism of sliding was still not known. In the later of 1950s, Andrew Fielding Huxley suggested an idea of a molecular interaction among the contractile proteins based on the sliding filament theory. His idea resulted in so called cross-bridge theory which was later supported by the experiments and persisted as a major explanation of muscle contraction till nowadays.

In cross-bridge theory approach, there is a strong effort to explain the muscle mechanics out of the processes taking place on the molecular level. The original Huxley's cross-bridge theory describes the interaction between two main contractile elements in sarcomere which are represented by two proteins myosin and actin. Myosin and actin molecules, as already noted above, form a shape of filaments. Along the myosin filaments protrude the specific parts of myosin molecules. These parts of myosin are able to cyclically bind and unbind at actin filaments and shift actin filaments in the direction to the centre of sarcomere. Active shifting of actin by myosin is in brief the main principle of muscle shortening - contraction and muscle force production against the external force. Once the protruding myosin parts attach at actin, they form transient connection among myosin and actin filaments. These connection are traditionally and illustratively called cross-bridges, which gave the name to this theory. Every single cross-bridge is nothing else then the molecular motor myosin II.

The cross-bridge theory and its developed mathematical description can be denoted as a bridge connecting molecular mechanics with the mechanics of the whole muscle (continuum mechanics) and with chemical kinetics. The first mathematical model related to this theory was published already in 1957 by its founder A. F. Huxley [48]. Nowadays, his 1957 paper is recognised as a classic work in cross-bridge theory, which helped to uncover and understand molecular basis of muscle contraction and helped to set the direction of the muscle research. As the time progressed, the original Huxley's cross-bridge hypothesis and model were improved into various forms and many of its variations were published as the research was bringing actual results. But the main idea about the cyclical interaction of two main contractile proteins actin and myosin remained the same till nowadays.

The classical cross-bridge model involving interaction of two filaments was a long time considered as a universal tool to clarify and simulate the contractile activity and energetic

properties of muscles. Many attempts can be found to modify this model for explaining all physiology related to contraction of the muscles even nowadays. In brief, models based on the classical cross-bridge theory more or less succeeded in the explanation of concentric contraction - shortening of the muscles and isometric contraction - force production of muscles, where the length of muscle is kept constant. Till nowadays, among the most challenging part of cross-bridge theory remains the explanation of the properties of *eccentric contraction* - stretch of active muscle, and history dependent properties of contraction as phenomena called *force enhancement* followed after stretch of activated muscle and *force depression* followed after active shortening of muscle.

Regarding to eccentric contraction, there were proposed a few models, but no one of them was more widely and universally accepted till nowadays. Among the most successful and discussed might be mentioned the theories with sarcomere length non-uniformities [86] or model called distribution-moment model [128]. Although these and other models brought better insight and description into muscle science, the universal mathematical description involving sufficient explanation of all physiological processes regarding to contractile activity is still missing.

As the latest experiments uncovered and suggested new properties of sarcomere activity and discovered new mechanical properties of proteins inside sarcomere, it might be worthwhile to return to the original Huxley's cross-bridge mathematical model and include to this model the new information achieved namely in last two decades. In last two decades, one of the most important investigation related to the sarcomere was done on protein titin and myosin. On account of titin's recently discovered properties, titin is very often referred as "molecular spring". As proposed in [40], one of the reasons of insufficiently explained problems of eccentric contraction might be the fact that the role of this third most abundant protein in sarcomere might be much more important than originally thought in classical cross-bridge theory. Recently, titin was found to bind calcium ions upon activation of sarcomere, thereby increasing its structural stability. This way its stiffness increases and the force production is higher than originally thought when it is stretched [43] during eccentric contraction. Furthermore, there is an increasing evidence that the specific parts

of titin binds to actin in an activation, thereby shortening its "free-length" [43], [37].

Further important results which might be used to improve classical cross-bridge model comes from experiments on single myosin molecules and single sarcomeres. In first mentioned, the nonlinear force-length relationship was measured on single myosin molecules uncovering then non-linear stiffness of single cross-bridges [62], [63]. In latter mentioned, it was for instance experimentally showed that the history-dependent properties as force enhancement followed after eccentric contraction is property observable also on a single sarcomere level [79], [95], [99]. These and other results introduced in the following chapters indicated the way the classical cross-bridge theory and its mathematical description could be enhanced.

To summarize the goals of presented work, the main aim was to modify and enhance the classical Huxley's mathematical model according to the latest experimental results obtained on a single myosin molecule (cross- bridge) [62], [63], according to the experimental results on single sarcomere [80], [79] and according to the way of the third filament titin implementation in sarcomere activity as proposed in [40].

Before all, the work was focused namely on the improve of classical cross-bridge model with respect on properties of eccentric contraction - stretch of active sarcomere. Regarding this aim, the main goal was to show that the phenomena of force enhancement has its origin on half-sarcomere level. Besides other, the aim of thesis was also to describe and introduce myosin II in the context of another molecular motors. Further, the aim was to introduce the sarcomere as an amazing nano-machine developed by nature. The reason for this latest mentioned aims is to point out that the classical Huxley's cross-bridge model can be understood as one of the first and maybe the first mathematical model describing the activity of molecular motors.

Information summarized in the following chapters was selected especially with the respect on mechanical and physical properties of sarcomere in skeletal muscle although some information about the other muscle tissues is also presented. Due to the complexity of studied problem, namely the part involving chemical properties of sarcomere had to be neglected.

The presented work is organised as follows. First the sarcomere's structure and its relation to the contractile activity and force production is described in detail in chapter 2. This chapter comprises mainly of information about the basic properties of sarcomere. The information was selected namely with regard on contraction related to the skeletal muscle. But some information related to the contractile properties of other two kinds of muscle tissues, i.e. about cardiac and smooth muscle, is also presented for better insight into muscle science. The crucial part for better comprehension of the main subject of this work is the section about the contractile properties of eccentric contraction. The sources of information in this chapter were predominantly texts [6], [10], [15], [19], [20], [23], [29], [28], [37], [38], [36], [35], [39], [40], [41], [42], [43], [44], [49], [53], [55], [56], [58], [57], [59], [60], [72], [80], [79], [87], [86], [89], [95], [97], [99], [100], [104], [106], [111], [114], [126].

Molecular motors concept and muscle propelling molecular motor myosin II is introduced in chapter 3. The chapter devoted to molecular motors gives a brief overview about one of the most amazing structures in nature - about molecular motors. This part of the text presents mainly information related to the molecular motor myosin II. Furthermore, the important concept of *power stroke* [56] is introduced here. Further, information given in this part of text describes the molecular mechanism of muscle contraction as a biomechanical cycle of single cross-bridge. The information about the myosin molecule and molecular motors comes namely from [1], [2], [3], [4], [5], [8] [15], [16], [18], [25], [26], [27], [46], [52], [51], [50], [48], [54], [56], [61], [63], [62], [68], [69], [71], [73], [74], [76], [81], [82], [83], [88], [90], [92], [96], [97], [101], [102], [105], [109], [110], [113], [112], [115], [120], [121], [122], [125], [127].

Molecular spring protein titin and its elastic properties are presented in chapter 4. The chapter presents structure of this biggest natural protein and its relation to the sarcomere contractile activity. The last part of chapter about titin introduces an important concepts and clue for modification of classical cross-bridge theory as proposed in [40]. The information about the titin comes predominantly from [9], [11], [17], [26], [30], [31], [33], [37], [38], [40], [43], [64], [66], [67], [72], [75], [80], [84], [85], [91], [103], [116], [117], [119], [118].

The next chapter 5 introduces selected mathematical models and their results. Among

the others, chapter introduces classical Huxley's mathematical model, models of titin mechanics, distribution-moment model and few more models for better insight into considered problems. The main source of information and also the main sources of the inspiration for the changes of classical Huxley's model are primarily texts [3], [6], [9], [11], [12], [13], [14], [21], [34], [40], [44], [45], [52], [48], [54], [61], [70], [71], [76], [77], [78], [83], [84], [85], [88], [93], [94], [97], [107], [108], [110], [116], [125], [123], [124], [128], [129], [130], [132], [131].

The chapter 6 following after introduction and brief description of the crucial parts of sarcomere, myosin II and titin introduces the modified Huxley's cross-bridge model. In this chapter, the mathematical model was derived from the scratch for better and clearer insight into the model purpose. This chapter contains one of the most important results of the thesis.

The proposed model was used to simulate the basics and various contractile activity of sarcomere. Therefore, in the following chapter 7 are presented another important results of thesis. In particular, the simulation of concentric, isometric and eccentric contraction were conducted. Further, the special cases of concentric and eccentric contraction as sudden release and sudden shortening of sarcomere, were simulated. The chapter with results also contains the important results on simulated properties of phenomenon of force enhancement. The graphical results of developed mathematical model are compared to the results obtained in experiments.

Chapter 2

Sarcomere - An Amazing Nanomachine

The cause and propelling source of human and animal movement are muscles. In addition to movement such as walking, muscles act also as the crucial regulators of various physiological processes as digestion, blood circulation and other important life supporting processes. Based on the specialized functions of muscles and the external appearance, the muscle tissues are traditionally divided into three classes:

1. striated (skeletal) muscles,
2. cardiac muscles,
3. smooth muscles.

Striated muscles are involved in skeletal motion, lip motion, eyelid motion and eyeball motion [32]. Skeletal muscles are under conscious control, although some move without voluntary control. Skeletal muscles constitute of the long cylindrical cells, which have many nuclei. Cardiac muscles are found in heart. They have one nucleus. In contrary to skeletal muscles, the cell structure of cardiac muscles is often branched [32]. Cardiac muscles are not under conscious control. The last kind of muscles are smooth muscles. Smooth muscle

cells are the basic structural elements of blood vessel, digestive and urogenital organs and retina. Smooth muscles are not under conscious control. They have one cell nucleus.

Arrangement of all kind of muscles, considered as a whole tissues, comprises of a few distinctive units at different level of order and scale. Regardless of the muscle type, the main mechanism causing the ability of muscle contractile activity is found at the lowest level of muscle structure. Contractile mechanism consists of two main contractile proteins myosin and actin. These two proteins are capable to trigger contraction activity and force production of muscles. The main contractile proteins are accompanied by structural proteins of elementary contractile apparatus.

Notwithstanding the contraction of smooth muscle is not the main subject of presented work, at least the information about the elementary contractile structure in smooth muscle tissue is introduced here for the better insight into considered problem. In smooth muscles, the contractile proteins are organized in smooth muscle cells. Smooth muscle cells are the main units constituting tissue of smooth muscle. Although the arrangement of the contractile proteins in smooth muscle cell prevails in the direction along the longest "axis" of smooth muscle cell, the organization of these proteins look like random or irregular arrangement with no deeper specific structure. Illustrative arrangement of contractile proteins in smooth muscle cell is shown in figure 2.1.

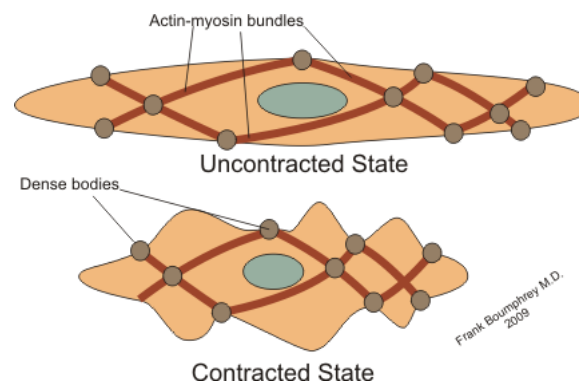


Figure 2.1: Arrangement of contractile proteins in smooth muscle cell.

In contrary to arrangement of contractile proteins in smooth muscle cell, the arrangement of contractile proteins in striated and cardiac muscles is highly organized. The

contractile proteins in these two kinds of muscles are organized in the structure called **sarcomere**. Albeit sarcomeres in cardiac and skeletal muscle are very similar, the following text is predominantly focused on sarcomere in skeletal striated muscle. Nevertheless, some information given in the following chapters are also valid for cardiac and even for smooth muscle.

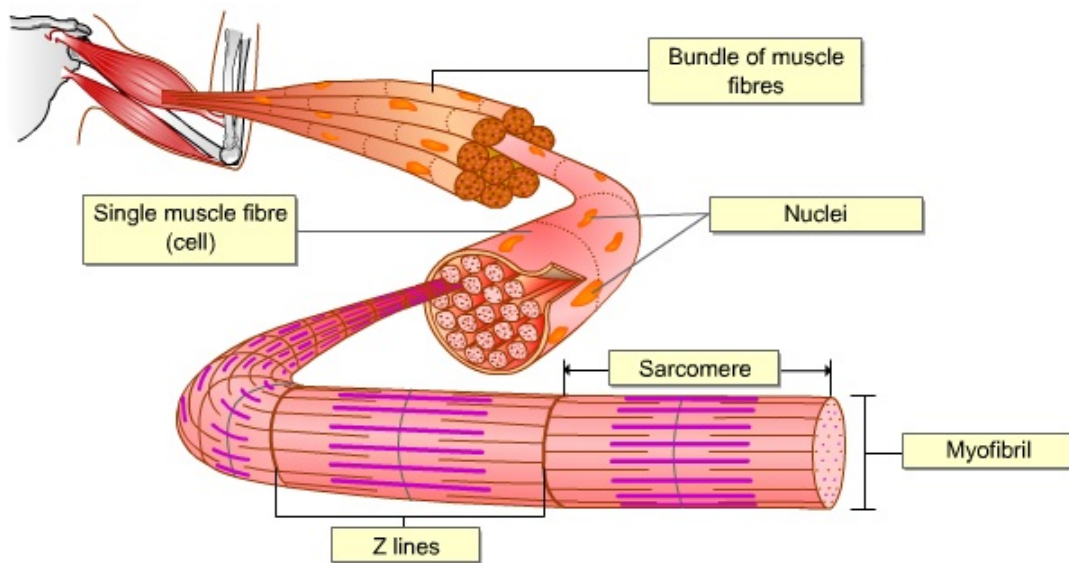


Figure 2.2: Schematic diagram of skeletal muscle structural hierarchy in vertebrate striated muscle. The picture was adapted from [47].

Structural hierarchy of skeletal muscle parts is depicted in figure 2.2. Sarcomere (sarco = muscle, mere = unit) is the basic functional contractile unit of striated and heart muscle. It affects the crucial mechanical properties of muscle contractile activity. Sarcomere is found at the lowest level of skeletal muscle regular hierarchy. Sarcomere never exists in isolation [97]. Sarcomeres are always organized in series into filaments called myofibrils. Myofibrils are further bundled into fibers. Fibers anchor serially linked sarcomeres in myofibrils into muscle. This serially linkage of sarcomeres induces the characteristic periodic external appearance of striated muscle. Therefore, the skeletal muscles are called *striated*. Each muscle fiber has millions of sarcomeres [95].

The characteristic striation pattern was first observed with the light microscope by Dutchman van Leeuwenhoek in seventeenth century [97]. Further the most important investigation on sarcomeres was performed already with electron microscope during the 1950s by two independent teams led by Hugh Huxley and Andrew F. Huxley. They and their colleagues showed that the striation pattern arose out of the arrays of overlapped filaments. Even with this profound insight to structure, the mechanism of contraction was still not understood.

Since the regular structure of striated muscle was always the motivation to develop easy and transparent model describing the properties of contraction from molecular level to tissue level, in 1957 Andrew Fielding Huxley published a theoretical model supported by mathematical model. Nowadays, Huxley's work is well known as cross-bridge theory. At this time, during 1950s, the technology did not allow to confirm A. F. Huxley's theory. Either way, Huxley's theoretical work directed and paved the way of muscle research, which prevails till nowadays.

2.1 General Description of Sarcomere

As already mentioned above, myofibrillar sarcomere is a highly regular structure. Its regularity is the key feature of the effective contractile process [97]. The typical striation pattern consists of the periodically sequences of the **dark** and **light** bands. During the early time of muscle investigation, the scientist conducting observations with microscopes started to call the dark band as **A-band** and light band as **I-band**.

Although the structure of sarcomere varies little bit from species to species, the main scheme of protein structure stays similar. Nowadays, three kind of proteins in the shape of filaments are considered as the main structural parts of sarcomere. These proteins affect the crucial mechanical and contractile properties of sarcomere and consequently the mechanical properties of the whole muscle tissue. These three filaments consist in particular from proteins myosin, actin and titin [43]. The bunches of these three kinds of filaments lay in parallel in sarcomere as depicted in figure 2.3. Regarding to the myofibrile's striated

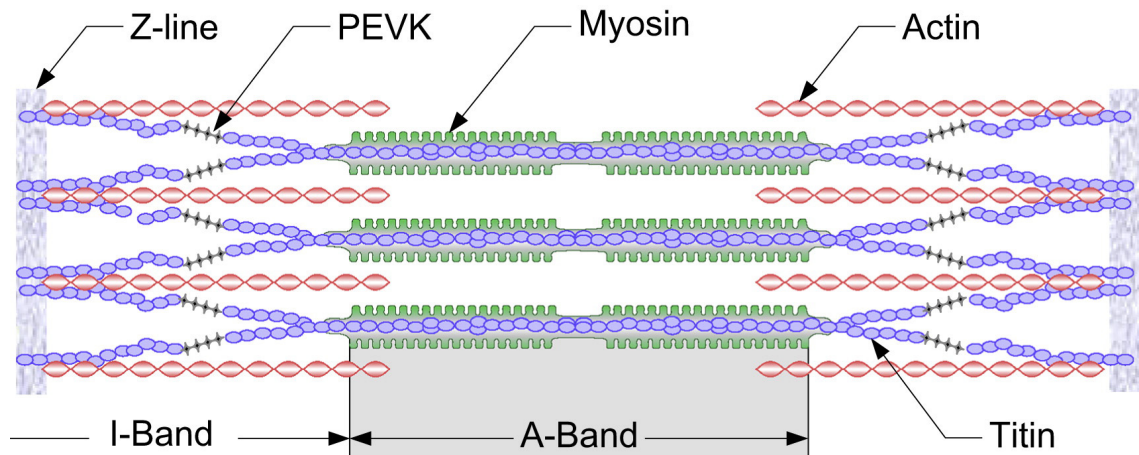


Figure 2.3: Structure of sarcomere with three main structural filaments: actin, myosin and titin. The picture was adapted from [33].

patterns of A-bands and I-bands, single sarcomere consists of one A-band in the centre of sarcomere and two halves of I-bands. Each of one half of I-band is structurally connected at the side of A-band (see the figure 2.3). The sarcomere is confined on the both sides with parts called Z-lines. The Z-lines on both sides of sarcomere determine the sarcomere's boundary. Each sarcomere is approximately $2.0 - 2.5\mu m$ [87] long and is symmetric. Along the fiber length and in cross-sectional area are observed significant length non-uniformities of sarcomeres.

On account of the contractile activity, individual parts (proteins) of sarcomere can be sorted to two classes: active and passive parts. The first mentioned are called active since they are capable to actively contribute to the contractile activity. These are namely myosin and actin. Whereas the later mentioned are called passive, because they are able to affect the mechanical properties only "passively" with their natural mechanical properties as elasticity or viscous properties. The main example of these is predominantly titin.

2.2 Structure of Sarcomere

2.2.1 A-band

A-band is the region of sarcomere, where the active contractile force is produced. A-band is dense and dark due to the great amount of proteins myosin and actin. It consists of parallel arrays of overlapped thin (actin) and thick (myosin) filaments. During contraction, the size of A-band remains approximately of the same length. In 1950s, the observed length conservation of A-band was one of the main concepts that led to the proposals of "sliding filament theory" [53], [57] and understanding of molecular basis of contraction. On the other hand, some experiments and texts argue with conservation of A-band length during the sarcomere activity, see for instance [97]. Nowadays, it is known that the length of this region slightly changes. This change is considered rather as consequence of contractile activity than the active contributor to contraction.

In this part of sarcomere, the titin is the internal part of myosin filament [118]. The actin filaments protrude to A-band part from I-band region (see figure 2.3 on page 36).

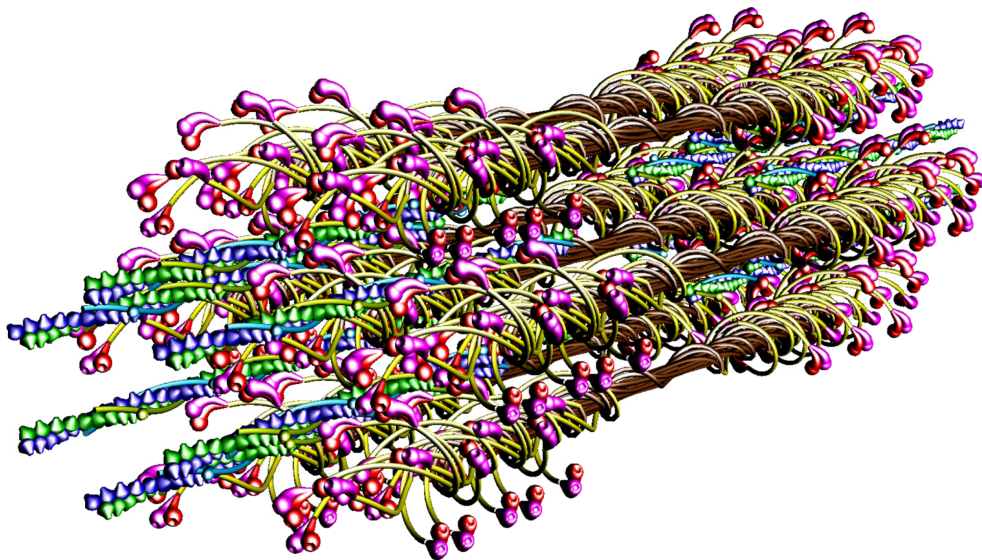


Figure 2.4: Molecular structure of vertebrate striated muscle sarcomere's A-band. Seven myosin filaments and twelve actin filaments are shown during contraction. The source of picture is [111].

Myosin - the molecular motor The most interesting and important part of A-band is the protein myosin. Myosin is the main propelling source of sarcomere contractile activity. It acts as motor - molecular motor. Myosin as a crucial part affecting contraction is presented in detail in chapter 3 Myosin II - Muscle Molecular Motor .

2.2.2 I-band

In contrary to A-band, I-band changes its length during the contraction significantly. This part of sarcomere is composed mainly of the ordered arrays of actin filaments and titin filaments. Actin filaments are at one sides anchored to the Z-line and cross through the I-band part to the A-band part. Further, I-band of sarcomere is spanned by protein titin. Titin filaments connect Z-lines with myosin filaments. The bunches of titin filaments are traditionally thought to be the main source of the passive forces and viscoelasticity [119] since the titin is considered as "molecular spring".

During last two decades, more deeper and more sophisticated experiments were conducted on the titin filaments and their structure. Latest results suggest that the role of titin in sarcomere is not only passive, but also active [40], [43]. Although the viscous properties are arguable under normal physiological conditions of sarcomere. The properties of titin are introduced more deeply in one of the following chapters 4 Titin - An Entropic Molecular Spring.

2.3 Contraction properties

In the rest part of this chapter, the basic contraction properties are introduced from the macroscopic (continuum) point of view. The description given bellow is presented regardless of the deeper insight into molecular mechanism of the contractile activity. The detailed molecular mechanism of contraction is more profoundly described in following chapter 3 Myosin II - Muscle Molecular Motor. But, for the better comprehension of the contraction properties as introduced in the following parts of this chapter, the elementary properties of

sarcomere's contractile mechanism are here briefly introduced. The basic theories of muscle contraction are cross-bridge theory and two sliding-filament theory. Nowadays, both of these theories have plausible experimentally substantiated background.

Cross-bridge theory Cross-bridge hypothesis is widely accepted theory to explain muscle contraction. Cross-bridge theory proposes that muscle force is produced as a consequence of direct physical contact between the the part of myosin molecules, called illustratively **cross-bridges**, and the actin units in the thin filaments [56]. $1mg$ of muscle contains 10^{14} of cross-bridges [5].

Sliding filament theory The interaction of cross-bridges with actin filaments results in the process, where the myosin and actin filaments slide along each other. One of the most significant sarcomere's property regarding the contractile activity is that the sarcomere **can only shorten not lengthen actively**. This results from the fact that cross-bridges can pull the actin filaments only in one direction. This direction is to the centre of sarcomere. According to the sliding-filament theory, the force exerted by actin-myosin interaction then depends on the degree of actin-myosin overlap.

To achieve the elongation of activated sarcomere, external force must be applied to overcome activity of contractile proteins. Beyond the $4\ \mu m$ of sarcomere length there is no myosin and actin overlap. Therefore, cross-bridge theory predicts no active force in this range.

2.3.1 Three main types of contraction

The force-time relationships of muscles/sarcomeres depend on the types of contraction. Characteristic force evolutions during all kinds of contraction are depicted in figure 2.5. Three kinds of contraction are traditionally stated:

1. **concentric** - muscle shortening,
2. **isometric** - muscle exerts force at constant length,

3. **eccentric** - activated muscle is stretched by an external force, which overwhelm the force exerted by muscle.

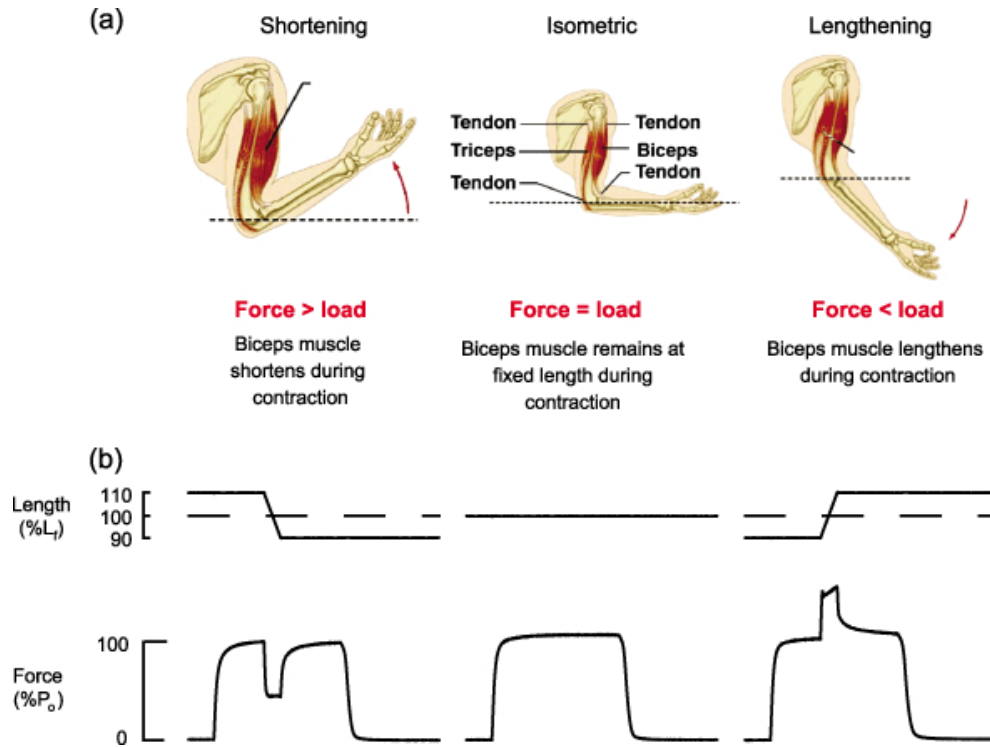


Figure 2.5: Concentric (shortening), isometric (force production at constant length) and eccentric (lengthening) contraction of skeletal muscle and relevant dynamic force-time relationship with length-time relationship. The picture was adapted from [23].

The experiments on muscles contraction are performed either on intact or on skinned muscle fibers [87] and nowadays also on single sarcomeres [79]. In the case of intact muscle, the cells are dissected from a tissue leaving the cell membrane intact. In this case, the excitation of muscle is achieved through the physical processes on cell membrane, which is excited to allow the inflow of Ca^{2+} from internal and external surroundings into cell. In contrast, the membrane of skinned muscle cell is removed allowing the myoflament environment to be controlled from the bath [87].

2.3.2 Force-velocity relationship

The force-velocity relationship of muscle contraction (see figures 2.6 and 2.7) is well known through the Hill's pioneering work from 1938 [44]. The properties of force-velocity relationship are important because they reflect and provide deeper insight into muscle physiology. The force-velocity relationship determines the theoretical limits of the amount of work and power of muscle in vivo [96]. The shape of force-velocity relationship is known to be affected by intracellular concentration of substrate ATP and metabolites (ADP, inorganic phosphate, H^+) [12]. The velocities as depicted in force-velocity relationship are the maximal velocities that can be achieved regarding to the particular magnitudes of force. In other interpretation, the force-velocity relationship captures the properties of isotonic contraction, where the muscle contract under constant force.

The force-velocity relationship represents the muscle's basic properties as [10]:

- description of the spectrum of all possible force-velocity interactions,
- determines the instantaneous power $P = Fv$,
- determines the enthalpy change ($\Delta heat + \Delta work$) during contraction,
- dictates the rate of adenosine triphosphate hydrolysis,
- dictate efficiency.

Shortening (concentric) domain of force-velocity relationship Skeletal muscles shorten rapidly when the load is low. Whereas when the muscle contracts against the higher load, the velocity of shortening is much lower [44], [10].

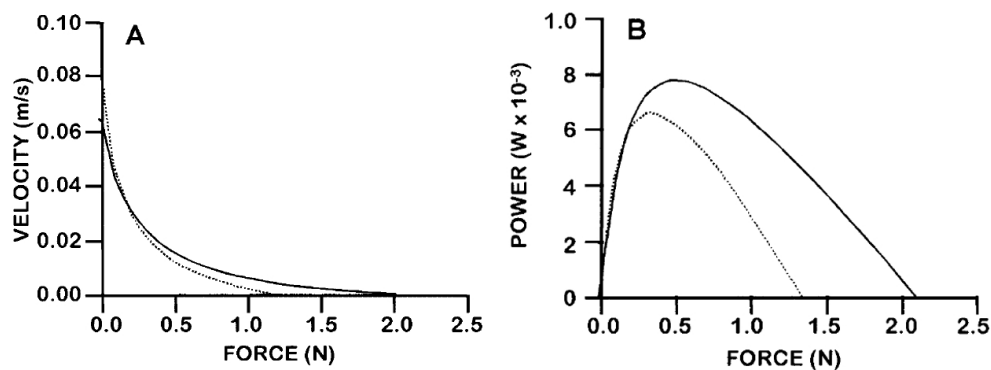


Figure 2.6: Illustrative curves of force-velocity relationship and muscle power. **A)** Force-velocity relationships for the domain of concentric contraction. **B)** Power curves of muscle. Modified from [10].

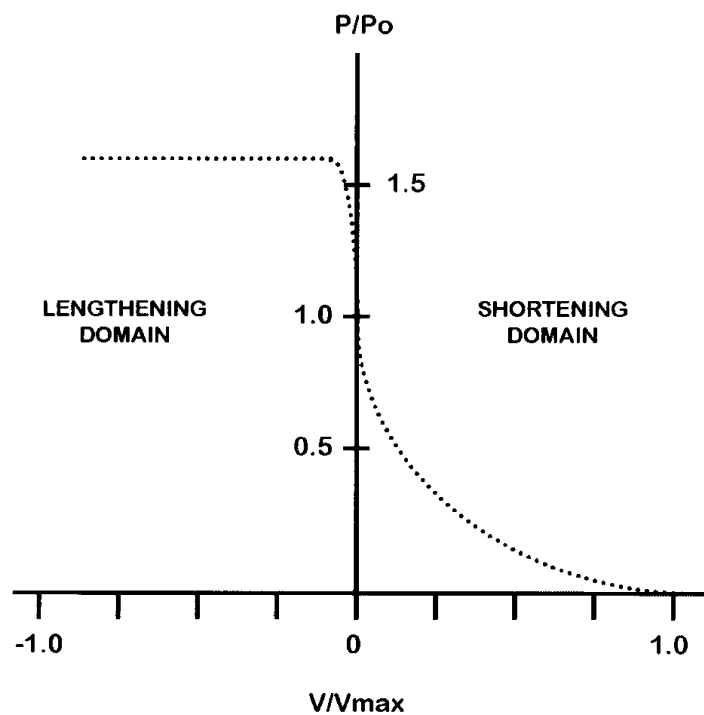


Figure 2.7: General shape of force-velocity relationship. The force-velocity relationship in both eccentric contraction domain and concentric contraction domain. The case for $V = 0$ corresponds to isometric contraction. Source of picture [10].

Isometric domain of force-velocity relationship Isometric domain of force-velocity relationship is simply one point, where the velocity of contraction is zero. The force-velocity relationship is traditionally normalized to the force related to zero velocity.

Lengthening (eccentric) domain of force-velocity relationship The exact shape of force-velocity relationship in lengthening domain is hard to establish universally since the lengthening is caused primarily by external force. The external force can have in general arbitrary magnitude. Therefore, the general shape of force-velocity relationship during eccentric contraction is hard to establish. Sometimes this part force-velocity relationship is referred rather as plane determined by various factors than simple line. The approximate shape of this part of the force-velocity relationship can be seen in figure 2.7.

2.3.3 Isometric contraction, Gordon's graph: force-length relationship

Isometric contraction occurs in a case, when the force produced by cross-bridges is the same as external force. This happens in the case, when the muscle is kept at constant length and is simultaneously activated to exert the force. Isometric contraction triggered at different lengths of sarcomere produces different forces related to the particular sarcomere lengths and degree of actin-myosin filaments overlap. During the isometric contractions are achieved the maximal forces that can be produced by actin-myosin interaction. Isometric forces reach a maximum at average sarcomere lengths about $2\mu m$ (frog sarcomere) [39]. The average force per single cross-bridge during isometric contraction is assumed to be $6pN$ [63]. Isometric contraction is also considered as sufficiently understood in cross-bridge theory. For characteristic force-time evolution of isometric contraction see figure 2.8.

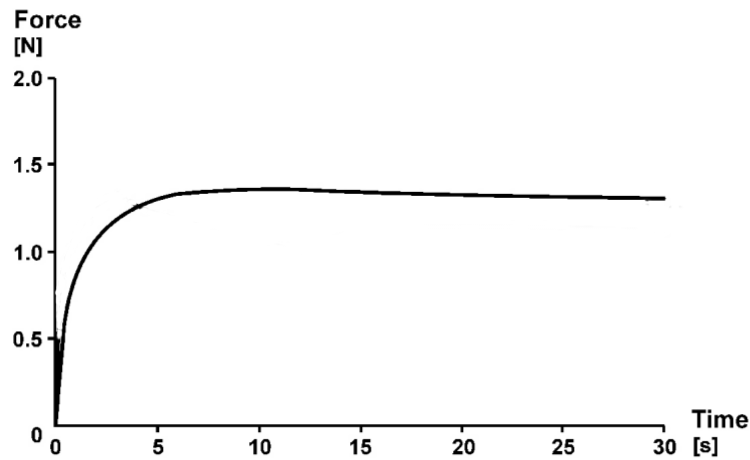


Figure 2.8: Illustrative force production of muscle during isometric contraction, when the muscle is kept at constant length. At $t = 0$ the muscle is activated and starts to produce the force. After a while, the force production reaches its maximum. This maximum is kept by muscle until it is deactivated or subjected to the changes of surroundings. Adapted from [35].

Gordon's graph: Force-length relationship Regarding to the various magnitudes of forces intrinsic to particular lengths of sarcomere during isometric contraction, the force-length relationship of isometric contraction of sarcomeres was measured in 1966 by Gordon et. all. [29]. Gordon's graph, as is the force-length relationship often called, was obtained by the measurements on a single fibre from frog striated muscle. Due to the experimental equipment used in 1960s, Gordon was not able to measure directly the lengths of sarcomeres in fibre. Instead of sarcomere's length, he was able to measure the distances among the neighbouring A-bands (neighbouring striations). Based on these results, he reconstructed force-length relationship for isometric contraction of single sarcomeres. Gordon's force-length relationship covers the whole range within the myosin and actin filaments overlap. Force-length relationship can be simply explained by sliding filament theory as can be seen from following pictures 2.9 and 2.10.

Gordon's graph is traditionally divided into three distinctive regions (see the figure 2.9):

1. ascending limb region,

- 2. plateau region,
- 3. descending limb region.

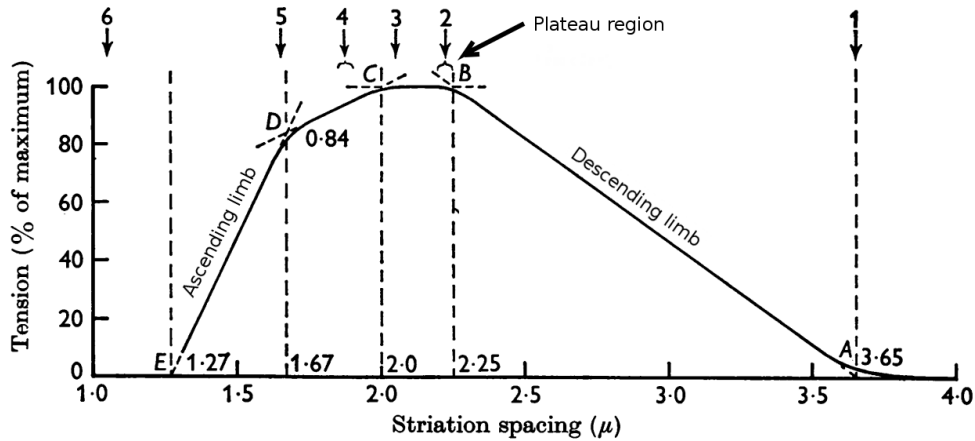


Figure 2.9: **Gordon's graph**: Force-length relationship. Summary of the results of force production of isometric contraction conducted along the sarcomere lengths by which actin and myosin filaments have various degree of overlap. The arrows with numbers in the top part of the graph are intrinsic to the numbered stages as depicted in figure 2.10. The picture was modified from [29].

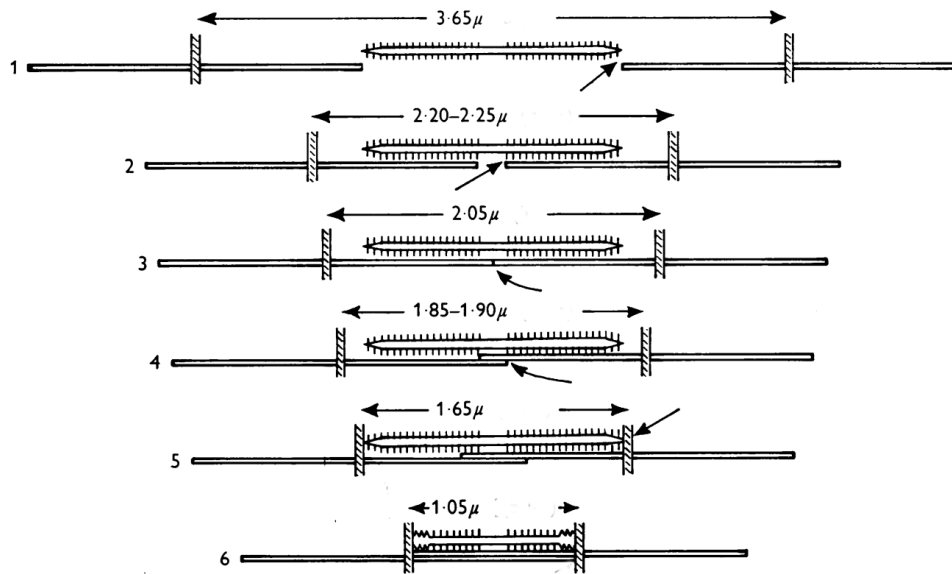


Figure 2.10: Critical lengths of sarcomere according to Gordon's graph. The picture shows significant stages of actin-myosin overlap. The picture was modified from [29].

The characteristic shape of Gordon's graph can be traced to the lowest level of muscle structural hierarchy. The experimental measurements of force-length relationship at the sarcomere level give the same profile of this property as the results on higher level of the structural hierarchy of muscle. See the results of measurements on a single sarcomere in figure 2.11 from year 2009.

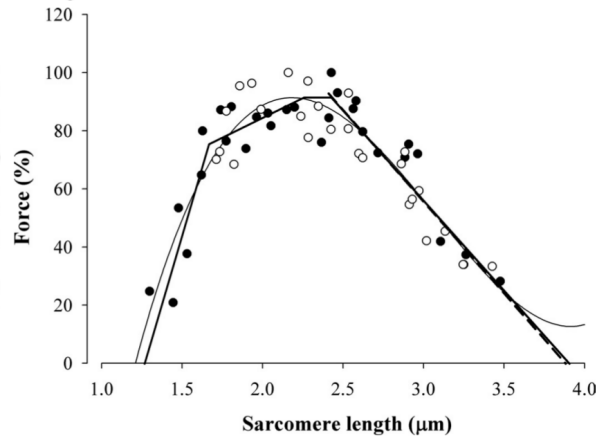


Figure 2.11: Force-length relationship for isometric contraction obtained from measurement on single sarcomeres. The open circles represent the force obtained at 15°C and closed circles represent the forces measured at 20°C . The continuous lines represents results of least squares fitting and fitting with linear regression. The picture with its description was adapted from [95].

2.3.4 Concentric contraction

Concentric contraction occurs if the force produced by cross-bridge mechanism overcomes external force acting on sarcomere. This also includes the case, when the external force equals to zero. The work produced during concentric contraction is often called positive work. In this type of contraction sarcomere shortens, which results in the whole muscle contraction. This kind of contraction is assumed to be sufficiently understood in cross-bridge theory with exception of history-dependent phenomena called force depression as described below.

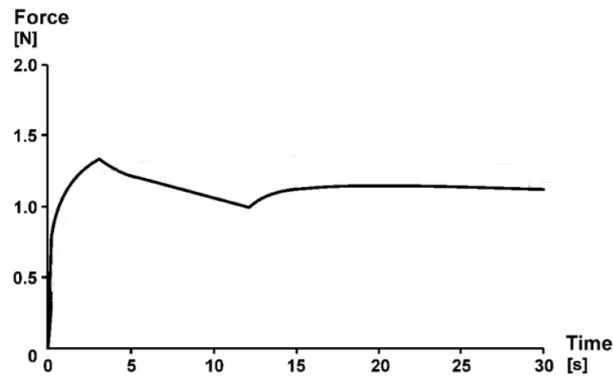


Figure 2.12: Illustrative transient state of force during concentric contraction followed by steady-state isometric force. At $t = 0$ the muscle is activated and force production is approaching its maximum force intrinsic to isometric contraction at particular length. Then the muscle is subjected to shortening accompanied by characteristic decrease in a force. After a while, the shortening is stopped and the force production approach the steady-state magnitude of force related to isometric contraction at new corresponding length. Modified from [35].

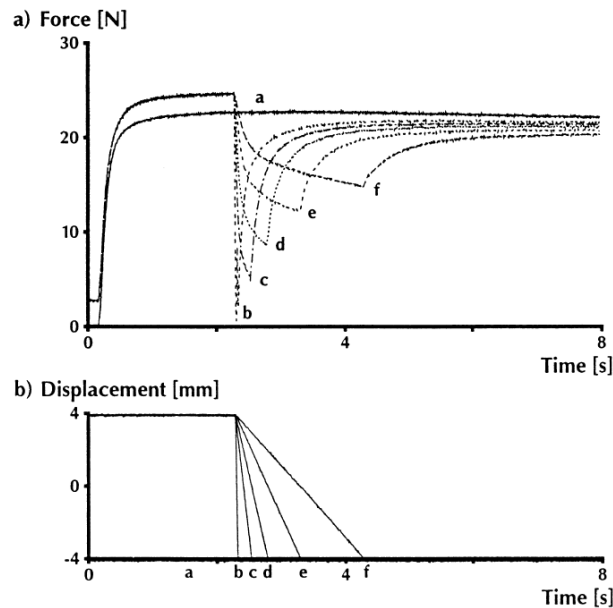


Figure 2.13: Force-time histories of concentric contraction conducted for various shortening speed in the range of $4 - 128 \text{ mm s}^{-1}$, depicted as lines $b - f$ regarding to magnitudes of speed. The shortening distance of muscle was 8 mm for all speeds and the final length of sarcomere was the same for all speeds. The resulted forces are compared to isometric force at corresponding resulted length, depicted as line a . Adapted from [42].

The characteristic property of concentric contraction is the force decrease once the concentric contraction is triggered. This force decrease is dependent on the magnitude of shortening velocity. The decrease in force production is higher for higher velocities and vice versa. See the results in figure 2.13, where the muscle was shortened for the same amount of length but with different magnitudes of speed.

Force depression

Force depression is an absolute or percentage decrease in the steady-state isometric force following a shortening contraction compared to the purely isometric force at the corresponding length [35]. The force depression increases with increasing magnitudes of shortening. It increases also with decreasing speed of shortening and with increasing force during the shortening phase [35].

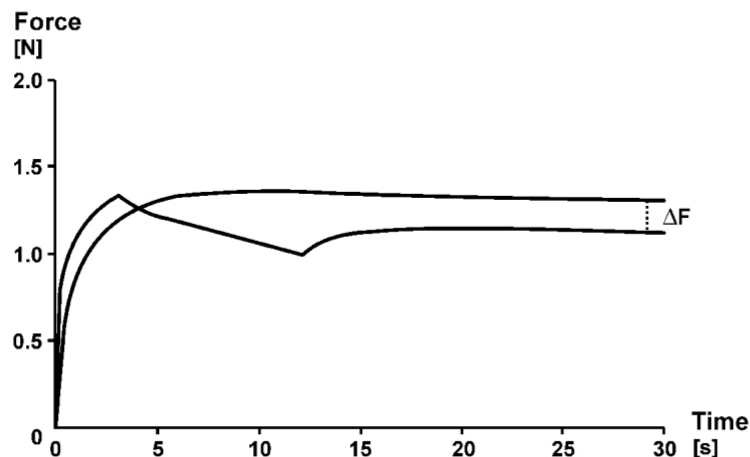


Figure 2.14: Example of force depression. The top line represents an isometric force achieved at constant length. The bottom line represents the concentric contraction followed by isometric contraction at the same length like isometric contraction of top line. ΔF represents the force depression. The picture was adapted from [35].

The mechanism underlying force depression is still not sufficiently explained although several mechanisms have been proposed. One of the most probable theories suggests that during the concentric contraction the actin filaments might be shifted to the opposite site

behind the centre of sarcomere. There they might reduce the probability of cross-bridge attachments [42] of cross-bridges from opposite side of sarcomere. In addition, the actin filaments from opposite side of sarcomere may encounter and collide. The force depression then might come from myofilament deformation [42].

Sudden shortening step

Sudden shortening step is a special case of eccentric contraction, where the muscle/sarcomere is suddenly released from its isometric contraction. The force-time relationship then corresponds with results for high velocity shortening. The results of sudden shortening step can be seen in figure 2.15 as published by Huxley in 1971.

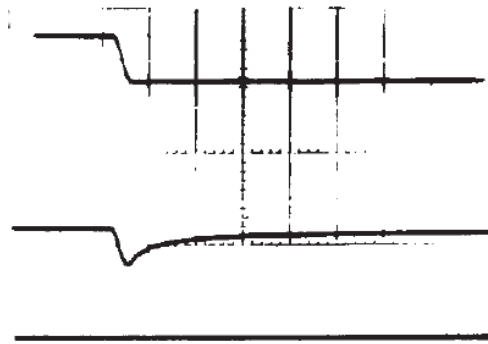


Figure 2.15: Transient force response of muscle exposed to sudden shortening step. The top line represents sudden shortening step in length. The bottom line represents the corresponding force-time relationship. The picture was adapted as published by Huxley in 1971 in [54].

2.3.5 Eccentric contraction

Eccentric contraction is one of the most challenging themes for cross-bridge theory and two sliding filament approach. Already Huxley, when he proposed cross-bridge theory in 1957, was aware that his hypothesis has limitation on the explanation of this kind of contraction. Eccentric contraction occurs if the external force is greater than the cross-bridge mechanism is able to develop. The external force then overwhelms the force developed by inner

mechanism in sarcomere. Sarcomere is consequently stretched. The work done during the eccentric contraction is often called negative work since it is done by external force.

The most insufficiently understood property of this kind of contraction is the explanation of the nature of the phenomena called **force enhancement**. The typical force-time relationship of eccentric contraction is characterized by the quick force increase once the muscle is stretched by external force from its initial isometric state. After that, with the continuous lengthening by external force, the force monotonically increases until the external force stop to stretch the muscle. Once the external force disappears, the force relaxes to a lower value of steady-state force (see figure 2.16). Force-time relationship of eccentric contraction is then characterized by following components [100], [41], [37]:

1. sudden increase in the force once the stretch begins (transient state of force enhancement),
2. continuous monotonous increase in the force (transient state of force enhancement),
3. gradual dissipation of the force once the external force disappears (transient state of force enhancement),
4. stable steady-state increased force that remains constant until the end of the sarcomere activation (steady-state force enhancement).

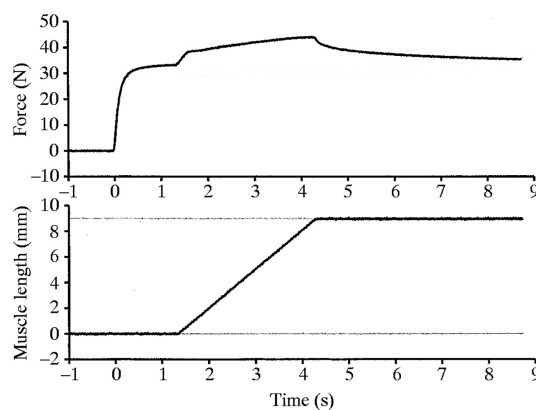


Figure 2.16: Illustrative force-time relationship of eccentric contraction. The muscle is first activated at constant length. Consequently, the muscle is lengthened by external force to the new length. Adapted from [41].

Transient state of force enhancement

As can be compared from experimentally measured results in figures 2.17, 2.18 as well as in figure 2.20, the magnitude of force developed by muscle in the transient state of eccentric contraction depends on the magnitude of speed. More concretely, the value of force in transient state of eccentric contraction increases with the speed of stretch (lengthening). This effect is the most apparent at the beginning of eccentric contraction, where the quick increase of force occurs.

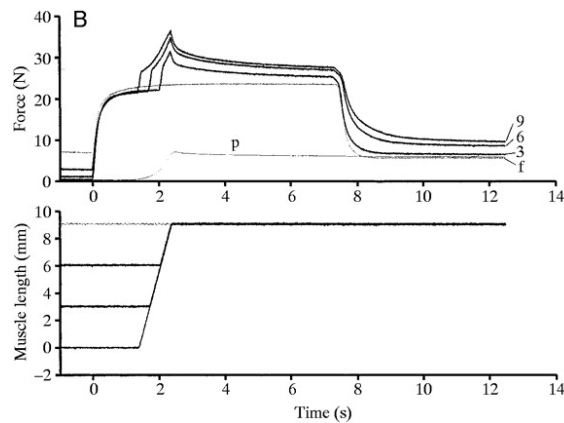


Figure 2.17: The stretches of 9, 6, 3 mm conducted by speed of 9 mms^{-1} , f denotes reference isometric contraction. The picture was adapted from [41].

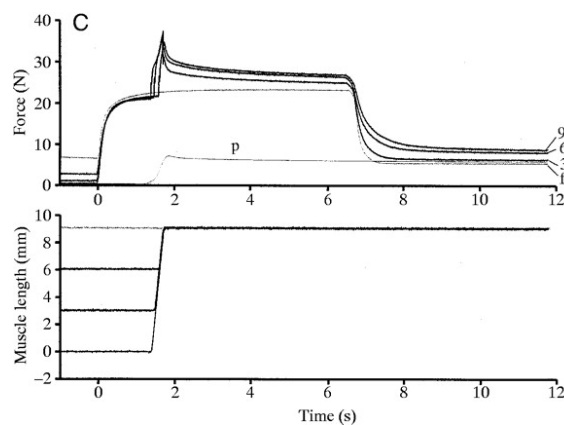


Figure 2.18: The stretches of 9, 6, 3 mm conducted by speed of 27 mms^{-1} , f denotes reference isometric contraction. The picture was adapted from [41].

Steady-state force enhancement

When activated skeletal muscle is stretched from its initial isometric contraction state to the following isometric state after stretch, the force developed by sarcomere after stretch is greater than expected by classical theories [100], [40], [79], [43]. According to the classical cross-bridge theory, the expected value of isometric force after stretch might have the same value as the isometric force at the corresponding length of sarcomere. This is in contrary with experimentally observed data. The difference between expected value of force according to the cross-bridge theory and the value of force observable in experiments is called (steady-state) *force enhancement* (see figure 2.19).

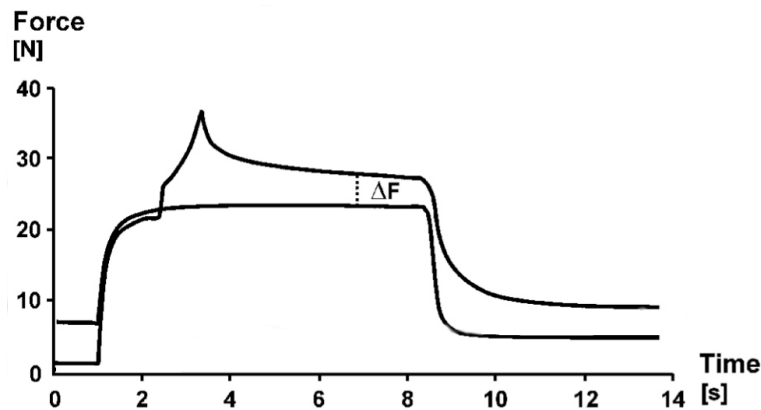


Figure 2.19: Force enhancement ΔF : the top line represents force-time relationship of eccentric contraction. The bottom line represents isometric contraction. The force produced by muscle after stretch is higher than the force produced during isometric contraction at corresponding (same) length. The picture was adapted from [35].

Force enhancement after active stretch can not be explained based on the classical cross-bridge theory and two sliding-filament theory. This contractile history-dependent property of muscles can not be explained by the degree of actin and myosin filaments overlap [100] or another reasons as "stuck cross-bridge" or "new unbound/bound state" leading to additional force producing step in cross-bridge cycle (the multi-step cycle model)[123].

A few theories were proposed to clarify the steady-state force enhancement. Among the others for example, it was suggested that the nature of force enhancement may arise

from non-uniformity of sarcomere lengths connected in series along myofibrile [86]. But, the experiments on the single sarcomere level precluded sarcomeres non-uniformities as a source of force enhancement [79].

The most apparent properties of steady-state force enhancement as observed in experiments are as follows. Force enhancement occurs on the ascending, descending limb also as on plateau region of the force-length relationship (Gordon's graph) [123]. Force enhancement seems to be permanent and its value depends on the magnitude of stretch [123]. The steady-state values of force enhancement after stretch remains the same for all velocities of stretch performed for the same length of stretch. Consequently, the two main properties of the steady-state force enhancement might be summarized as follows [37]:

1. the magnitude of steady-state force enhancement is increasing with magnitude of stretch (see figure 2.20),
2. the magnitude of steady-state force enhancement is independent on the magnitude of the speed of stretch.

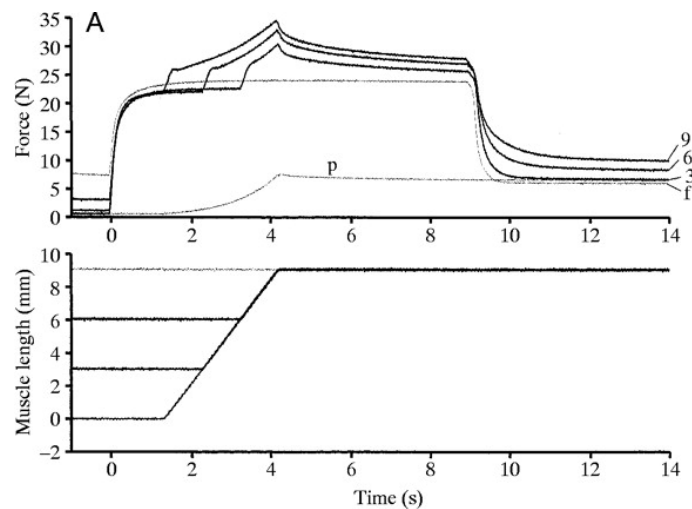


Figure 2.20: The dependence of the magnitude of force enhancement on the magnitude of stretch. f represents the reference isometric contraction. The lines 9, 6, 3 represent the force-time relationship for stretches conducted for 9, 6 and 3 mm . All stretches were conducted for the same speed of $3\text{ mm}\cdot\text{s}^{-1}$. The picture was adapted from [41].

Force enhancement at different levels of muscle hierarchical structure Force enhancement was observed at whole muscle scale, fibre scale and single sarcomere scale [79]. Force enhancement at muscle level was examined for instance in [106]. Force enhancement at single fibres level was observed for example in [19], [20]. At single isolated myofibrile it was observed in [59]. And at the lowest level of muscle structure, the force enhancement was observed also in experiments on a single sarcomere as published in [79].

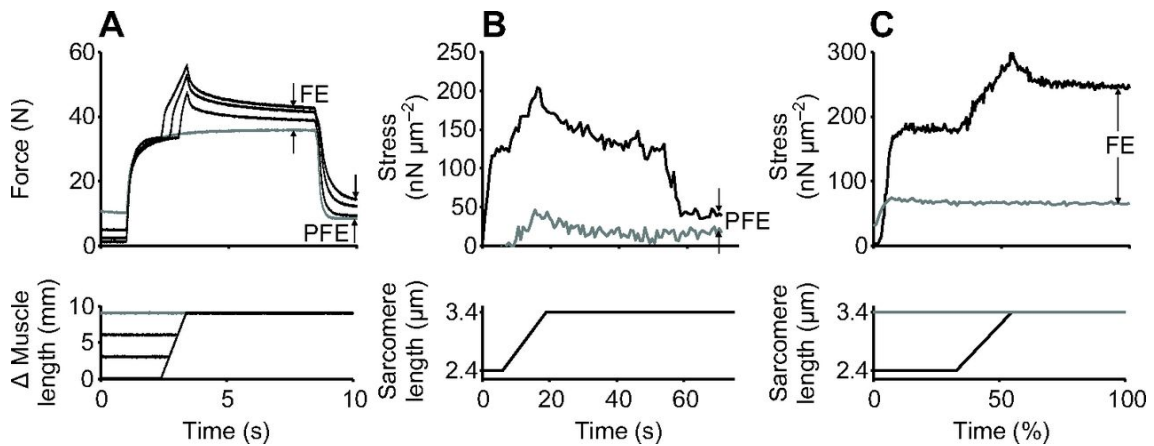


Figure 2.21: Force enhancement on three structural levels of skeletal muscle. **A** shows force enhancement in an entire muscle. **B** depicts force enhancement on isolated myofibril. **C** represents force enhancement in a single, mechanically isolated sarcomere. The grey lines in **A** refers to isometric reference force and length. The black lines in **A** represents course of force during stretches. The grey trace in **B** is a passive stretch while the black trace is an active stretch of a myofibril. The picture and the annotations are adapted from [37], [38], [43].

Passive force enhancement

The force enhancement does not occur in stretched passive (deactivated) muscles [123]. Nevertheless, passive force after deactivation of an actively stretched muscle is higher than the force produced after a purely passive stretch or after deactivation from an isometric contraction at the corresponding length [60]. The passive force enhancement is long lasting. It increases with stretch magnitude and initial muscle length. Passive force enhancement is independent of the speed of stretch [60], [41]. As the main source of passive force enhancement is believed to be titin [60]. See depicted passive force enhancement ΔP in

figure 2.22.

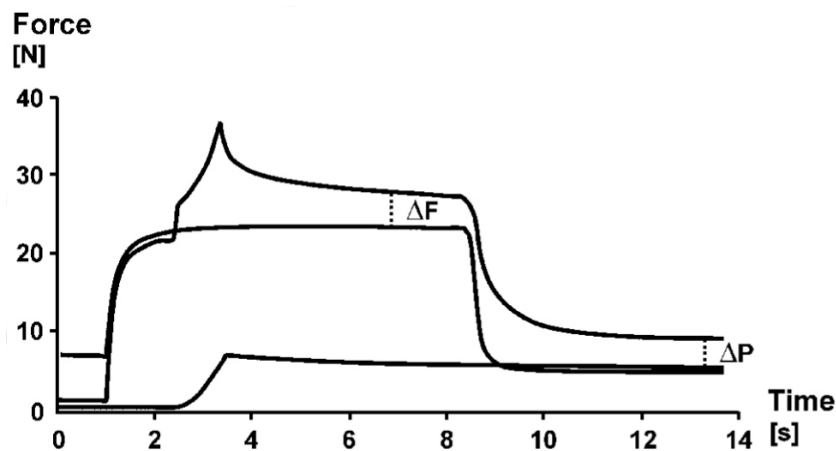


Figure 2.22: Illustration of passive force enhancement ΔP . ΔF is force enhancement after stretch. The top line represents eccentric contraction. The middle line represents isometric contraction at corresponding length of the final length of eccentric contraction. The bottom line represents stretch of passive muscle. Adapted from [35].

Sudden stretch

Sudden stretch is a special case of eccentric contraction. In this case the muscle is subjected to sudden short ramp stretch starting from isometric force production. The results of this stretch as experimentally observed by Huxley can be seen in figure 2.23.

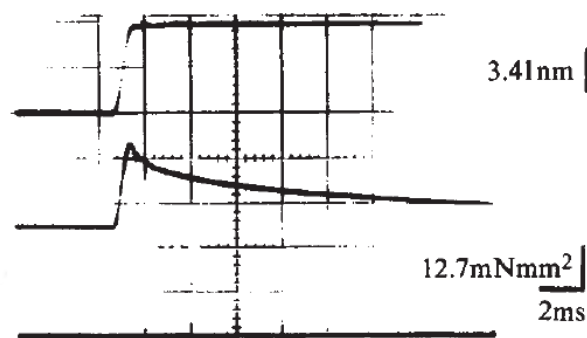



Figure 2.23: Sudden stretch of muscle as published by Huxley in 1971 [54]. The top line represents sudden change of muscle length - ramp stretch. The bottom line represents the corresponding force-time relationship during response on ramp stretch.

 **Quick summary of chapter**

Sarcomere is the basic contractile unit of skeletal and cardiac muscles. As a mechanical system in the range of units of μm , single sarcomere contractile activity is propelled by molecular motor myosin II. Sarcomere can only shorten not lengthen actively. Sarcomere force production on account of contraction is history dependent. Steady states of isometric force production following after transient states of concentric as well as eccentric contraction are accompanied by phenomena of force depression and force enhancement. In the case of force depression, the isometric force is decreased in comparison to isometric force achieved without previous contraction. In the case of force enhancement, the isometric force is increased in comparison to isometric force achieved without previous contractile activity. The phenomena of force enhancement was observed at every structural scale of muscles. Both of these history dependent properties of muscle/sarcomeres can not be explained by classical theories of contraction, i.e by cross-bridge theory and two sliding-filament theory.

Chapter 3

Myosin II - Muscle Molecular Motor

The main aim of the following pages is to introduce the muscle propelling molecular motor myosin II with its basic properties. At first, this chapter briefly summarizes the elementary properties of molecular motors in general. Then, the essential myosin II properties related to the muscle contraction are provided.

3.1 Molecular Motors in General

The beginning of understanding to molecular motors is closely related to the muscle science. It can be dated back in the year 1954 when two papers were published in Nature by two independent research groups [113]. The first paper was published by Hugh Huxley and Jean Hanson (Massachusetts Institute of Technology); *Changes in the cross-striations of muscle during contraction and stretch and their structural interpretation* [57]. The second paper was published by Andrew Fielding Huxley and Rolf Niedegerke (University of Cambridge); *Structural changes in muscle during contraction; interference microscopy of living muscle fibres* [53]. It might be worthwhile to mention that A.F. Huxley and H. Huxley were not relatives and the same surname Huxley of these two men is only coincidence. In their papers the authors proposed **sliding-filament theory** of muscle contraction. This theory was further extended theoretically by Andrew F. Huxley in paper *Muscle structure and*

theories of contraction [48] into **cross-bridge theory** in year 1957.

The cross-bridge theory is nowadays widely theoretically as well as experimentally admitted description of molecular motor myosin II activity in muscle tissues on molecular level. Except of muscle science, it also helped to describe activity of another types of molecular motors, which were discovered during the latest years in nature. These another molecular motors are namely families of kinesin and dynein molecular motors. Last years also emerged the first success in artificially synthesized molecular motors. Currently, the Nobel Prize in Chemistry 2016 awarded to synthesis of molecular machines". Jean-Pierre Sauvage, Sir J. Fraser Stoddart and Bernard L. Feringa was "for the design and Apart from muscle contraction, the molecular motors are involved in processes such as carrying cargo against physical field gradients or cell division and many other physiologically important processes.

During the 1950s, when the cross-bridge theory was proposed, it was related strictly to the muscle science. In first, this theory was suggested namely theoretically based on Huxley's mathematical model. In the following years, it took decades to submit convincing experimental results to support Huxley's cross-bridge theory, because no laboratory instruments were able to sufficiently capture and display the processes occurring at nano-scale, where the crucial activity of cross-bridge theory as well as of all molecular motors happens. Apart from cross-bridge theory, also another theoretical concepts and approaches were devised for better understanding of molecular motors. Among other, theoretical models based on Brownian ratchets, power-strokes, Langevin equation, Fokker-Planck equation, Markov models, Markov-Fokker-Planck models [76] are sufficiently used. The later mentioned are predominantly used to describe single molecular motor properties, whereas cross-bridge based models are used to describe the simultaneous activity of greater amount of molecular motors.

Individual molecular motors are enzymatic molecules that convert chemical energy into mechanical work and linear translational motion [71] or rotation. Molecular motors, as proteins, usually need the presence of another specific proteins, which serve as the tracks and usually determine the direction of their movement. For instance, molecular motors

walk on cytoskeleton proteins as microtubules and actin filaments.

Information about the structure of molecular motors is mostly obtained by diffraction-based techniques and cryomicroscopy [71]. Single motor proteins comprise typically of several subunits [76]. The most important part of the molecular motors are usually "heads", where the enzymatic activity takes place. These "heads" also bind specific places on molecular tracks (microtubules, actin filament, DNA or RNA molecules) [71].

Molecular motors are cyclic machines like a heat engines [88]. Their working cycle is closed series of chemical (conformational) states. In comparison to macromolecular motors (for instance combustion and diesel engines), one of the most striking features is that the thermal energy k_bT , of surroundings is much smaller for macromolecular motors. Whilst for the molecular motors, the thermal energy of surroundings is comparable. The kinetic energy of a molecular motor calculated using the average velocity is much smaller than the thermal energy $k_B T$ and the kinetic energy calculated using the instantaneous velocity is comparable to the thermal energy. In contrast, the kinetic energy of a macroscopic motor is much larger than the thermal energy [125].

3.1.1 Mechanochemical cycle - conformation states and power stroke

Many theoretical approaches to rotary and linear motor proteins are essentially the same [71]. One of them is the concept of biochemical or mechanochemical cycle and kinetic of this cycle. In order to produce force and work, molecular motors combine chemical cycle of ATP hydrolysis with a mechanical cycle of motor interaction with its tracks. This process can be found also under name mechano-chemical coupling or biochemical cycle.

The operation of molecular motor is strictly connected with its mechanochemical cycle. The results from experiments show that motor protein undergoes multiple conformations coupled in biochemical network [71] during its activity. Some of the pathways of biochemical cycle are dominant and control the overall dynamics [71].

The important concept related to the molecular motor's biochemical cycle is the term

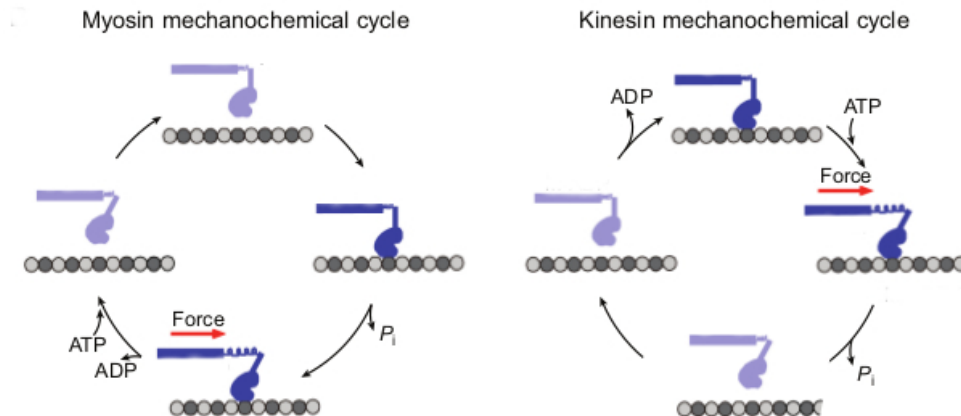


Figure 3.1: Mechanochemical cycles of myosin (left) and kinesin (right). The myosin force-producing step occurs with P_i release. In contrary, ATP binding is thought to be the force-producing step for kinesin based motors. Modified from [73].

power stroke. Understanding the phenomena of power-stroke is crucial to comprehend the biological motility achieved by molecular motors. It connects and include mechanical forces, movements, structural changes as well it is linked to ATPase cycle and hydrolysis of ATP. The power stroke is the most important conformational change in the globular motor domain of a molecular motor. During power stroke, the molecular motor can perform step on its track or shift another proteins as in the case of muscle contraction. This way molecular motors are able to perform work as a part of their biochemical cycle [88]. Series of conformational changes, including power strokes, are driven by biochemical reactions. Repetitive power strokes and conformational changes produced by molecular motor are generated as a result of periodical conformational rearrangements of protein structure driven by the enzymatic cycle of ATP hydrolysis [74]. Each biochemical cycle starts and ends at the same conformational state. Therefore, molecular motors are cyclic machines like a heat engines [88].

On account of biochemical cycle, another property called the **duty ratio** can be defined. The duty ration is the time of the biochemical cycle over which a motor head stays strongly attached to its track [8].

3.1.2 Movement on molecular motor tracks

Molecular motors move along linear, periodic, polar filaments [61] of the cytoskeleton. The usual filaments tracks are microtubules and actin filaments. Kinesins and dyneins move along microtubules. Myosins move along actin filaments [69]. Actin and tubulin filaments are formed by a polymerization process from identical monomers - actin and tubulin monomers [61]. During polymerization of these monomers units, the regular periodic track structure is prepared.

The important feature of filaments track is their polarity. The filaments are asymmetric with respect to their two ends [61]. The ends of macromolecular tracks are usually denoted as $+$, $-$, i.e. "plus end" and "minus end". This polar asymmetry is crucial for motor on account of the direction of motion. Depending on concrete molecular motors, molecular motors can move towards plus as well as to minus ends of particular tracks.

The movement is performed in discrete steps. For myosin V it is $36nm$ and $8nm$ for kinesin [69]. The periodicity along the motor's track is also one of the main factors determining the length of molecular motor step. Several classes of motors move on their tracks by repeatedly hydrolyzing one ATP molecules at rate of order one step per $10ms$ [71]. The catalytic activity of a motor domain is strongly diminished when it unbinds from from its linear filament [71].

Kinesin and Myosin V appear to move hand-over-hand fashion in which rear head detaches from the track and reattaches to the front [3]. Another type of movement is that whole molecular motor unbinds from its track once its biochemical cycle is finished (myosin II).

3.1.3 Processive vs. non-processive motors

One of the essential properties of molecular motors is the property called **processivity**. It refers to the manner how the molecular motors moves along their tracks. Processivity is a mechanochemical property that refers to the number of catalytic cycles a motor can perform before diffusing away from its track [92].

Processive molecular motors

Processive molecular motors typically undergo numerous steps along their tracks before they completely dissociate from their track filament. Highly processive motors can perform hundreds of rounds of ATP binding and hydrolysis before release from their tracks [92]. For instance myosin *VI* can move longer than 200 *nm* without detaching from actin. Myosin *Va* can go up to several microns [92] before detaching. Processive motors are often dimeric or even oligomeric forms [71]. Among processive motors are conventional kinesin, cytoplasmic dynein, and myosin *V* and *VI*[71].

Non-processive molecular motors

Unlike of processive motors, the non-processive motors complete only few steps or strokes before they completely detach from their filaments [71]. Non-processive motors bind their track once per ATPase cycle and release their track after their biochemical cycle [92] is finished. Many of non-processive motor proteins such as myosin II work in large groups and in assembly, although the detail of the cooperative mechanism is largely unresolved [71]. Non-processive motors are usually monomers forms [71].

3.1.4 Thermodynamics of molecular motors

The molecular motors operate in the environment of continuous stochastic thermal fluctuation [88]. Thermal fluctuations affect their behaviour and these effects must be often included in theoretical description [125]. This results also in assumption that unbounded molecular motors from their tracks are believed to perform Brownian motion in the surroundings fluid [69]. The binding energy of molecular motors to filaments is finite and can be overcome by thermal fluctuations [69].

Due to the small size and negligible inertia of molecular motors, the motors are often damped by high viscous friction during their activity and are subjects to large thermal excitation from the surrounding fluid environment [125]. Also therefore, for molecular motors the length scale over which inertial effects are important are much shorter than the

characteristic length scales of the motor motion [125]. Therefore inertial effect can be in many cases neglected.

In vast majority of literature, it is believed that molecular motors operate under isothermal conditions. At the nanoscale, where the molecular motors operate, the greater temperature gradient is hardly sustainable. Therefore, in comparison to macromolecular motors, the molecular motors activity is not achieved by temperature gradient. The origin of their activity comes from their biochemical cycle, which keeps molecular motors in non-equilibrium thermodynamic state. The information about how far from thermodynamic equilibrium molecular motors operate differs. Some papers say that molecular motors operate far from thermodynamic equilibrium in contrast to the texts that stated that the molecular motors operate close to thermal equilibrium.

Regarding the skeletal muscles, at the rest, the skeletal muscles use 18% of the body energy consumption rate (basal metabolic rate) [32]. The energy used for work by skeletal muscles during activity varies around 25% [32], which reflects the muscular efficiency. The resting 75% is released as heat, which is very important source of body heat [32].

Energy sources

Invention in muscle physiology before World War II led to the discovery of adenosine triphosphate (ATP) and to the idea that this substance is the energy source for muscle contraction [48]. The molecular motor's heads are an actin-activated adenosine triphosphatase (ATPase) [102]. Discovering the interaction of ATP with myosin was also one of the investigation that brought the research of muscle contraction in the right way [48]. The most common source of chemical energy for motor proteins is hydrolysis of ATP or related compounds [71] and second the polymerization of nucleic acids and proteins (tubulin) [71]. The energy of ATP hydrolysis is only about one order of magnitude larger than the average energy of thermal fluctuation. The hydrolysis of ATP maintains the system in non-equilibrium thermodynamic conditions and biases the random walk of molecular motors in one direction[74].

Although it is known that working step is directly coupled to the ATP hydrolysis step, the transfer of chemical energy to mechanical energy by molecular motors still remains object of intense research. The transformation of chemical energy into mechanical work and movement is typically the serie of biochemical reaction and physical processes [71].

ATP hydrolysis - source of energy Adenosine triphosphate molecules are abundant in cells and react with water (hydrolyse) to form the products ADP and P_i . Under physiological conditions, ATP hydrolysis can occur through a spontaneous pathway in solution (slow) or accelerated through an enzyme-catalysed pathway [4].

Through the uncatalysed reaction pathway, released Gibbs free energy ΔG_{ATP} is lost entirely as heat. Whereas through the catalysed reaction pathway ΔG_{ATP} is divided between heat and external work [4]. The work is here conducted by molecular motor as moving against the external force by distance δx and internal work performed by a motor in stretching out elastic elements (springs, cross-bridges) in the motor system [4].

Motor as the protein structures are dynamic. Within a given biochemical state they fluctuate about an energy minimum. Upon motor biochemical transition such as ATP binding and $ADP + P_i$ release, motors undergo dramatic structural changes [4]. The hydrolysis of ATP releases about $20k_bT$ [69], where the part of energy in used for work and a part of energy is also dissipated to heat.

Simplified form of ATP hydrolysis:



where ATP is adenotriphosphate, ADP is adenodiphosphate and P_i is inorganic phosphate. ATP hydrolysis is an exothermic reaction with a negative change in enthalpy ΔH that contributes to the reaction's negative ΔG [88].

$$\Delta G = \Delta G'_0 + kT \ln\left(\frac{[ADP][P_i]}{[ATP]}\right) \quad (3.2)$$

The free energy, ΔG , is available to motor via hydrolysis of ATP (or other nucleotides). Under the physiological conditions normally used for in vitro studies, it is concluded that [71]:

$$|\Delta G_{ATP}| \lesssim 25k_B T \quad (3.3)$$

The maximum force a motor taking a step d can exert can be formulated as [71]:

$$F_{max} = \frac{\Delta G}{d}. \quad (3.4)$$

3.1.5 Myosin family

Myosins are a large superfamily of actin-dependent molecular motors [109]. Myosins are found in most eukaryotic cells [101]. Myosins play structural and enzymatic roles in muscle contraction, intracellular motility, cell division and transport of organelles within cells [101], [27]. Myosins molecules can be also found in plants, some of them exclusively (myosin VIII, XI and XIII) [109]. Members of this class are hexameric enzymes composed of two heavy chains with a molecular weight of 171-244 kDa and pairs of light chains [109]. The myosin family consists of at least 18 [105] - 20 [92] distinct classes with a number approaching 100 unique myosins [18] distributed across plant and animal kingdoms and with great diversity of cellular functions [105]. Recent studies identified many more potential classes of myosins with a total number up to 40 [92]. Motor proteins of the myosin family drive various movements in biological environment by a multi-step power stroke.

Most majority of the myosins move toward the plus end of actin. The myosin properties of a myosin family are defined by a combination of its enzyme kinetics and structural characteristic [92].

The structure of myosins

Myosins are characterized by three domains; **head**, **neck** and **tail** domain [92], [27]:

1. N-terminal motor or "head" that binds actin and ATP,
2. a "neck" domain consisting of one or more light chain,
3. C-terminal tail, also known as α helix.

The tail connects the myosin motor to its cargo or myosin filament. In myosin family, there is a considerable sequence and structural diversity in the tail part of the molecule. Whereas the domain motor or head of the molecule is well conserved [105]. Therefore it is assumed that throughout the myosin family the basic mechanism of movement and force generation remains the same [105].

Lever-arm hypothesis

Lever-arm hypothesis has received much experimental support [27]. This theory suggests that conformational changes in myosin's heads are amplified by the adjoining part serving as lever-arm. Mentioned conformational changes produce large displacement at far end of the neck, which is translated into the movement of the whole protein [27] (see figure 3.2). The size of motor displacement then depends (also) on the length of the lever arm, which turns around its fulcrum.

For the same lever arm length the size of the apparent power stroke can vary among different myosins [8]. The apparent stroke size is proportional to the length of the light chain domain [8]. The power stroke is multi-step and comprises of series of structural changes within the actin-myosin complex after the myosin motor domain has attached an actin filament [8]. Without external load the total movement generated by one head of a myosin molecule during an ATPase cycle is expected to be equal to the sum of the individual structural changes of the multi-step power stroke [8].

Velocity of single myosin molecules

Myosins move along their track with a wide range of velocities. The slowest myosin 9b moves with velocity in the range of $15 - 40nm/s$. On the other hand, one of the fastest

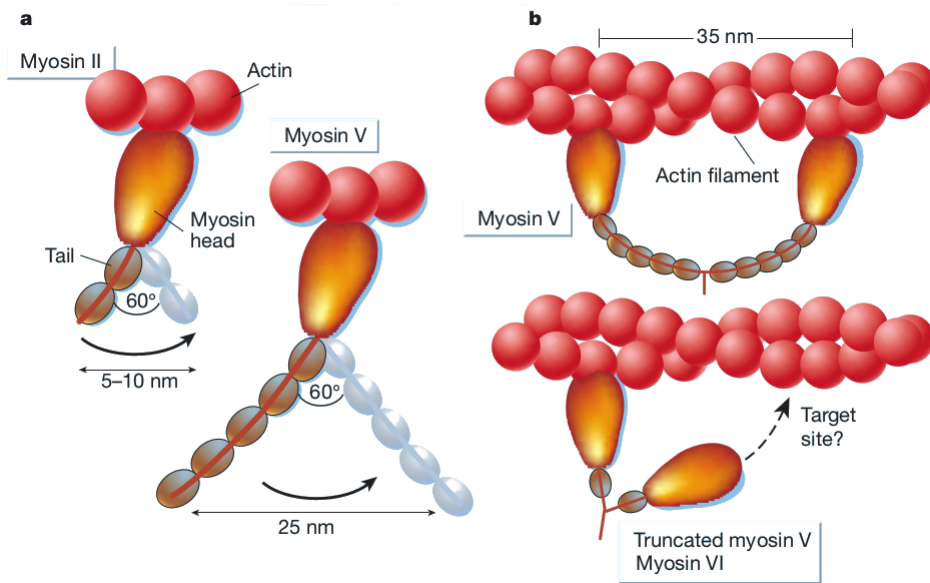


Figure 3.2: a) Lever arm movement of myosin molecular motors. b) Movement of myosins in hand-over-hand fashion. The picture was adapted from [27].

as myosin XI "runs" $60\mu\text{m/s}$ [92]. Myosin Ia moves with velocity of $50 - 100\text{nm/s}$ [92]. Velocity of single myosins is also adjusted to physiological functions. Smooth muscle myosin velocity ($\mu\text{m/s}$) in vitro is $> 10x$ slower than skeletal muscle myosin ($6.6\mu\text{m/s}$) [92].

3.2 Myosin II - Muscle Propelling Engine

Myosin II was first extracted from muscle by Kühne, who named it and characterize it in *Untersuchungen über das Protoplasma und die Contractilität (1864)* [48], [10]. It took approximately to the year 1930 that it was shown that the length of the myosin filaments is approximately the same length as the length of A-band in sarcomeres. Although some nowadays studies show that the length of myosin part of sarcomere slightly changes as well, that time it was crucial results which helped to distinguish among the sarcomere parts. Till now, myosin II is also the best studied molecular motor from myosin family also for the reason of intensive research in muscle science and its crucial role in contraction [27]. Therefore, myosin II is sometimes referred as "convictional" myosin since it was the only

class of myosin known for decades [109], [18].

Myosin II as a molecular motor propelling muscle contraction is a pico-Newton force generator, which is able to shift actin filaments. The myosin II head is an actin-activated adenosine-triphosphatase[102]. The part of myosin molecules, which protrudes out of the myosin filaments, is able to form a transient connection (cross-bridges) between actin and myosin filaments. This is the main assumption and principle of the **cross-bridge theory** based on **two-sliding-filament theory**, where the results of cyclical binding of cross-bridges is sliding of myosin and actin filaments along each other. Myosin II molecular motors are optimized for a wide range of contractile activity including rapid repetitive contraction cycles of insect flight muscles to the extremely slow contraction of tonic smooth muscle [105].

Among the most common factors influencing the properties of contraction are geometry of filaments in sarcomere, the mechanical properties of the filaments and cross-bridges, the kinetics of thin filament activation by Ca^{2+} and the kinetic of cross-bridge cycling [114].

3.2.1 Single myosin II molecule

Single myosin II molecule can be divided into discrete functional domains.

Structure of a single myosin molecule

Skeletal muscle myosin consists of two heavy chains of molecular weight $220kDa$ each and two pairs of light chains. Light chains have molecular weights in the range $15 - 22kDa$ [101]. Each myosin molecule is highly asymmetric composed of two globular heads joined to a long tail. It is a complex hexameric structure, which is composed from

- two heavy chains,
- two essential light chains,
- two regulatory light chains.

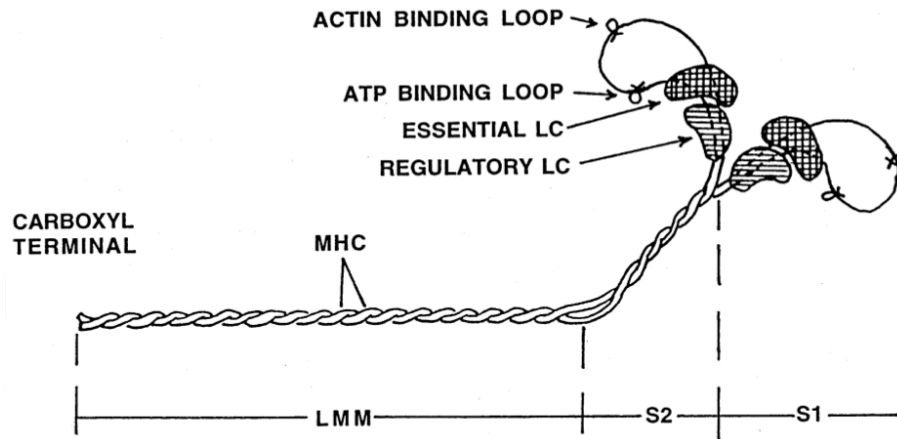


Figure 3.3: The two headed structure of single myosin molecule (single cross-bridge). The scheme depicts following parts: MHC - myosin heavy chains, essential light chains (LC), regulatory light chains (LC), ATP binding loop, actin binding loop, carboxyl terminal subfragment-1 (S1) part, subfragment-2 part(S2). MHC can be cleaved to into α -helical light meromyosin (LMM), S2 and S1. The picture adapted from [18].

One essential light chain and one regulatory light chain is associated with each myosin heavy chain and with one head (see figures 3.3 and 3.4). The terms "essential" and "regulatory" light chains might be considered as historical. Based on the identification of their electrophoretic mobility, they can be identify as follows [10]: the essential light chains have been classified as myosin light chain-1 (MLC_1) and myosin light chain-3 (MLC_3). The regulatory light chain has been classified as myosin light chain-2 (MLC_2). It is assumed that the two heads of myosin act independently from each other [87]. Only one myosin II head is necessary for production of motion and force [87].

Myosin head - Subfragment-1

Myosin head is also known as Subfragment-1 (S1). The globular head of myosin heavy chain contains the actin binding site and the ATP binding site. Globular part of the myosin molecule is responsible for the generation of force. S1 keeps its motor functionality in vitro, i.e. the ability to produce motility and force in vitro [105].

A neck domain of myosin head consists of essential and regulatory light chains bound to

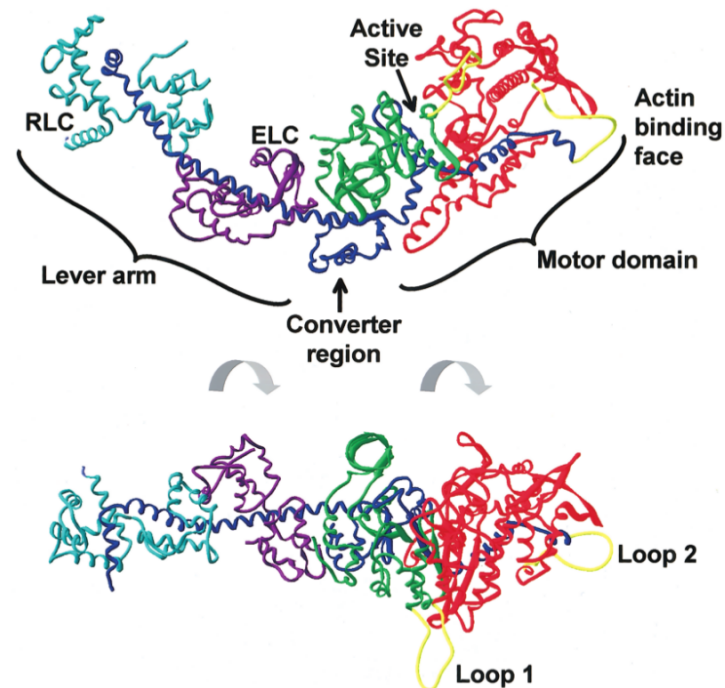


Figure 3.4: The N-terminal 25-kDa domain is labeled green. The upper and lower 50-kDa domains are red. The C-terminal 20-kDa is blue. The regulatory light chain is (RLC) light blue. The essential light chain (ELC) is purple. The picture with its description was adapted from [120].

a long α -helical portion of the heavy chain. The myosin head is an actin-activated adenosine triphosphatase (ATPase) [102]. Chicken skeletal myosin subfragment-1 as published in [101] has dimensions: overall length 165 Å, width 65 Å and thickness of 40 Å. S1 can be further distinguished into three fragments according to their apparent molecular weights [105]:

1. an amino-terminal nucleotide-binding region of molecular weight 25 *kDa*, called NH_2 - terminal, it is catalytic (or motor) domain containing the actin-binding sites and the ATPase catalytic site,
2. a central segment of molecular weight 50 *kDa*,
3. carboxy-terminal portion of molecular weight 20 *kDa*, called $COOH$ - terminal.

The length of Subfragment-2 (S2) as depicted in figure 3.3 is approximately 40nm [63].

The light chains Essential and regulatory light chains share considerable amino acid sequence similarity with troponin-C and calmodulin. The experiments suggested that regulatory light chains are important in controlling the myosin and cross-bridge kinetics [28]. The regulatory light chain is located at the end of the subfragment-1 head at distal part from the nucleotide binding site [101]. Essential light chain wraps around an approximately linear section of the long α -helix of the myosin heavy chain. Molecular weight of essential and regulatory light chains is approximately $20kDa$.

The arrangement of the regulatory and essential light chains, relative to the nucleotide-binding pocket and actin-binding site of S1 head, suggests that one of their function might be to create a longer molecule, thereby amplifying the power-stroke [101]. In contrary to striated muscle, in smooth muscle the phosphorylation of the regulatory light chains is essential for contraction. In striated muscle, phosphorylation of regulatory light chains enhances the force and force development rate at low Ca^{2+} activation [28].

The heavy chains The myosin heavy chain (MHC) constitutes the entire thick portion of the myosin head and contains both the nucleotide-binding site and actin-binding region [101]. Molecular mass of heavy chains is approximately $200kDa$ each [28]. The heavy chains form a parallel two-chain coiled structure over most of their length except for heads [28]. The coiled region of myosin forms filaments. The MHC can be proteolytically cleaved to generate α -helical light meromyosin (LMM), an S2 α -helical section and the S1 globular head region [18](see figure 3.3).

3.2.2 Power-stroke and myosin II conformation cycle

In detached state, the myosin head is subjected to unbiased thermal fluctuations. Whereas in activated state, when the myosin head is attached at actin binding sites, the myosin head is source of force production able to shift actin filaments in directed motion.

Lever-arm theory or neck-lever model

X-ray diffraction studies of muscle led to the proposal of the swinging cross-bridge model of contraction in which the myosin induced movement of actin occurs through the rotation of some structural components of the actin-bound myosin followed by release of the actin filament [56]. Swinging lever-arm theory was proposed and introduced in 1969 by H.E. Huxley in article *The mechanism of muscular contraction* [56].

On the basis of crystal structures, it has been hypothesized that the cross-bridge force is produced by an angular movement of the myosin regulatory domain about a fulcrum in the so-called converter region of the myosin head [105]. The swinging neck-lever model assumes that a swinging motion is the origin of the movement [121]. Due to the length and C-terminal location (see dark blue α -helix in figure 3.4), it was suggested that it may play a role as lever arm that could amplify a small conformational changes of motor domain [120]. This model assumes that the step size and the concentric contraction velocity are linearly related to the length of the neck [121]. The angular movement, which leads to the shortening of single cross-bridge resulting in force production and shifting of actin filament, is called **power-stroke** in cross-bridge theory. For instance, in myosin II of chicken or species *Dictyostelium discoideum* converter domain is rotated about 70° [8] or 65° [120].

Myosin II biochemical cycle

The transformation of chemical energy into mechanical work and movement is typically the serie of biochemical reaction and physical processes [71]. These processes are traditionally called by terms mechano-chemical cycle, conformational cycle or biochemical cycle. During these processes each myosin II molecule undergoes the set of cyclical conformational changes (isomerization). Most of these conformational changes, also denoted as states, are chemically indistinguishable. During this process the main change is the spatial rearrangement of the molecule parts.

During myosin biochemical cycle, single cross-bridge interacts with actin filament form-

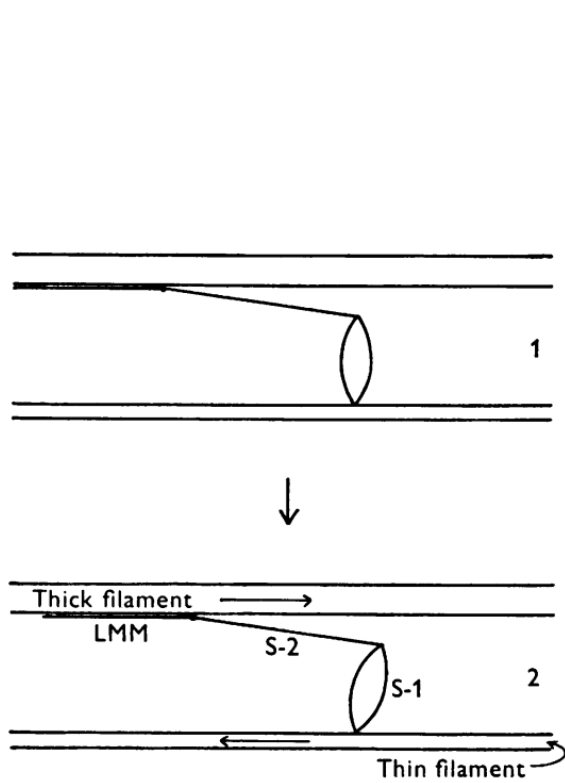


Figure 3.5: Myosin power-stroke mechanism as proposed by H. E. Huxley in 1969. He proposed that the source of force production is rotation of head S1, where the movement of rotation is transmitted to the actin filament by the S-2 part of single myosin molecule. The picture is adapted from [56], [49].

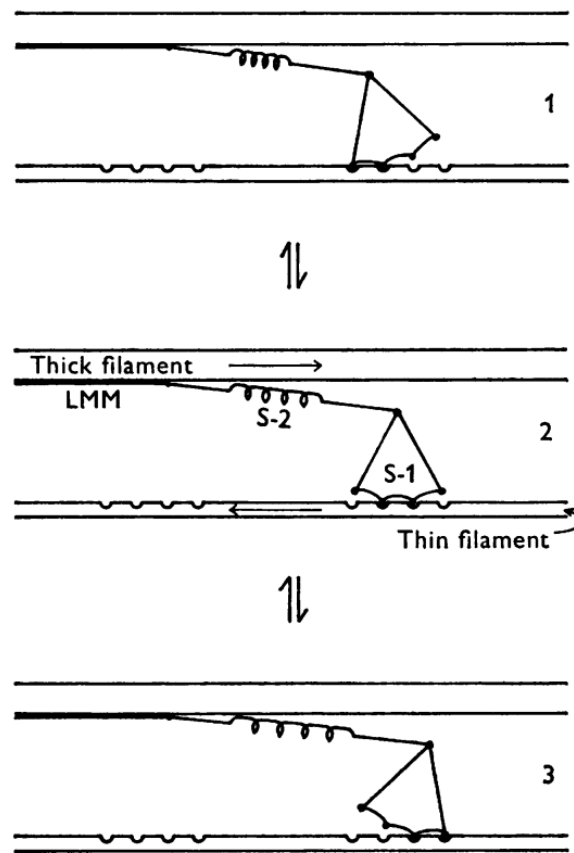


Figure 3.6: A.F. Huxley and Simmons further enhanced proposals [54] on mechanism as depicted in figure 3.5. They incorporated elastic element and stepwise-shortening elements into force-producing model. The picture is adapted from [49].

ing actomyosin complex. In each cyclical interaction of myosin with actin, one molecule of ATP is hydrolyzed by the myosin head into ADP and inorganic phosphate P_i [105]. Each myosin II motor domain spends most of its ATPase cycle time detached from actin [87]. Kinetic studies showed that the rate-limiting step of the myosin ATPase cycle is the release of hydrolysis products or an isomerization after ATP cleavage but before P_i release [28].

The relation between force-generation step and phosphatase release is still poorly understood [87]. The release of P_i and its relation to power-stroke still remains the subject of intensive research. It is still not obvious, if the release of P_i occurs before or after power

stroke. In literature, both of these cases can be found (see review article [87]).

For better comprehension of cycle and deeper insight into problem, see figures 3.7, 3.8 and 3.9. The biomechanical cycle can be described step by step as follows (mainly [15], [82], [87], [102]):

1. The cycle starts in rigor state. Binding of ATP to myosin motor domain causes unbinding from actin and a structural change with a swing of the myosin lever arm - a **recovery stroke** from previous power-stroke,
2. subsequently ATP is hydrolysed by free myosin to ADP and inorganic phosphate P_i , but the hydrolysis products remain bound to the active site of myosin,
3. myosin recombines with actin filament forming cross-bridge in a weak form,
4. subsequently, the release of P_i follows, which is associated with strong increase of actomyosin affinity and a large drop in free energy,
5. further follows an appreciable structural change - the **power stroke**,
6. the cycle is finished. The next detachment from strongly bound is linked again with the binding of ATP [120].

The rate of ATP binding to myosin II is $1 \times 10^6 M^{-1} s^{-1}$ [28]. The ADP release is ATP independent [120]. The recovery stroke occurs in detached state [87]. During eccentric contraction, after formation of bound, the cross-bridge is pulled in opposite direction to its power-stroke. In this case cross-bridges might be forcibly detached. This leads to the situation, where the whole biochemical cycle is uncompleted without release of *ADP* [87].

Weakly and Strongly bound states

Myosin cycle contains weakly and strongly bound states at actin filament binding sites. The idea is that myosin first bounds in a weakly conformation [102] and than undergoes isomerization to a strongly binding form [102] - tight (rigor) bound. It is assumed that power stroke occurs while the myosin is in strongly bound state.

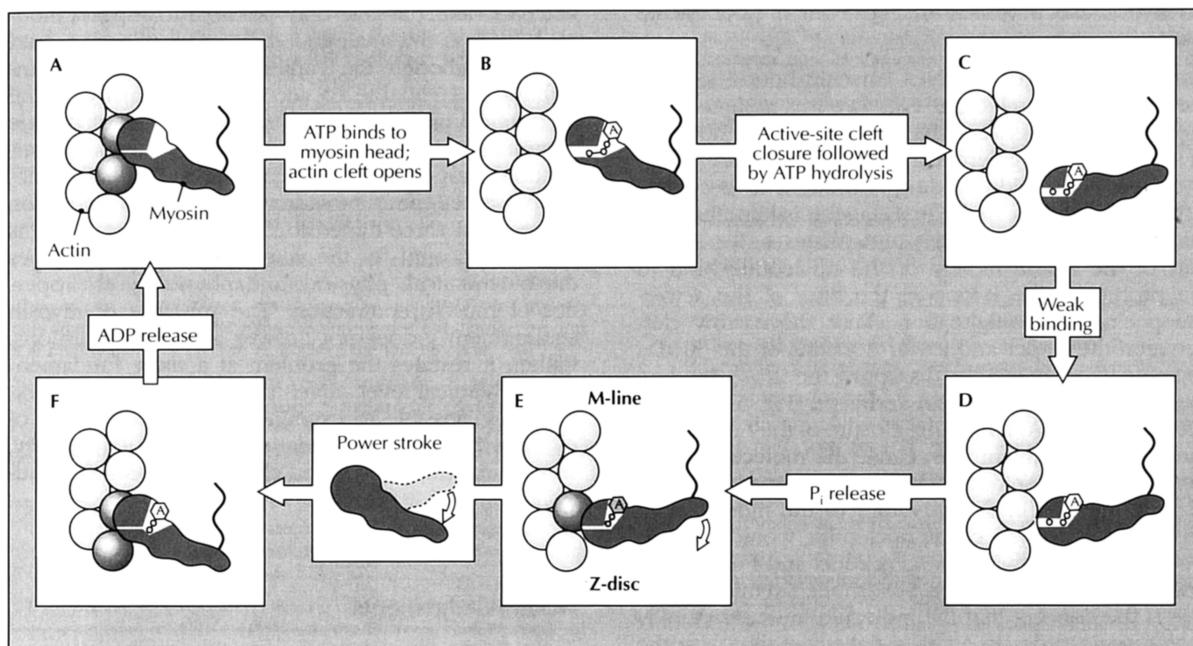


Figure 3.7: Schematic representation of cross-bridge cycle during contractile activity. The picture is adapted from [101].

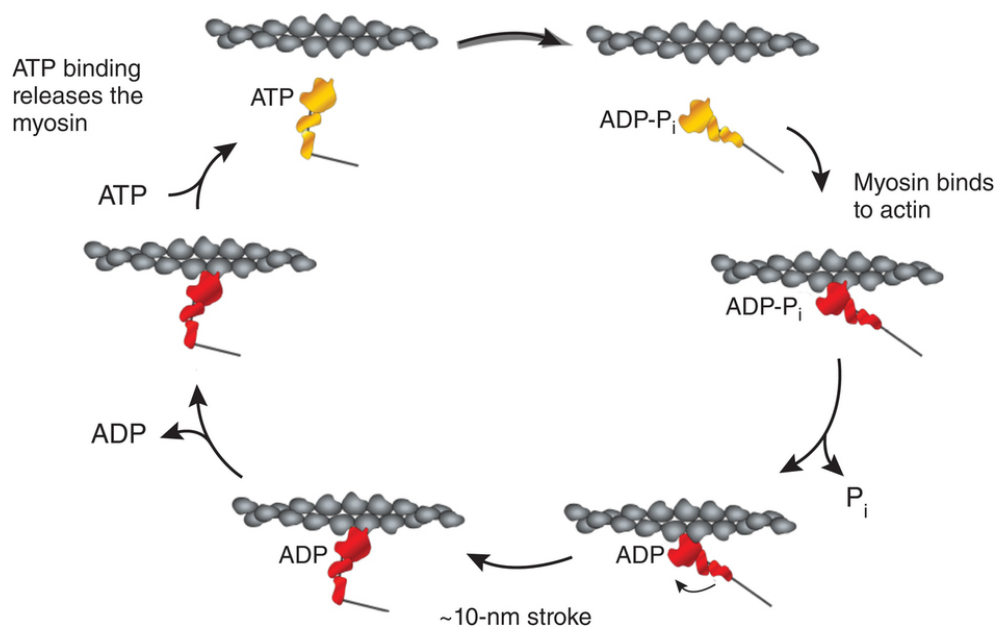


Figure 3.8: Myosin conformation cycle. Picture shows 10nm power-stroke. The picture is adapted from [113].

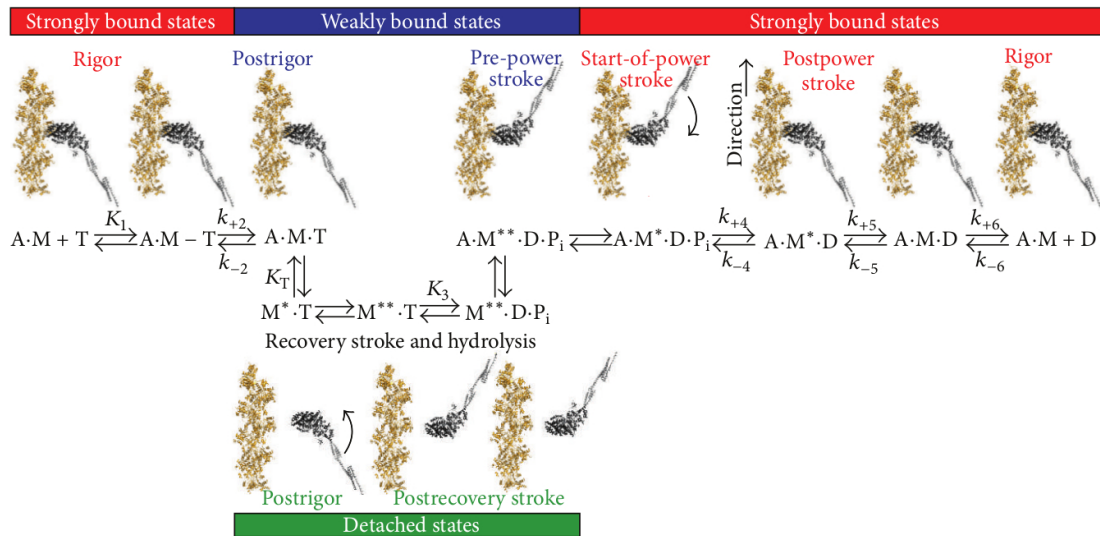


Figure 3.9: Biochemical and structural states of ATPase cycle. A = actin, M = myosin, T = ATP, D = ADP, P = P_i . Upper case K_i denotes equilibrium kinetics rates of state transitions, k_i denotes kinetics rates of various state transitions. Adapted from [87].

The initial weak binding is thought to be mainly electrostatic in nature with attached and detached states in rapid equilibrium [87]. Experiments suggested that the transition from weakly bound states to the strongly bound states involves a large change in free energy. Therefore, this change is associated with force generation performed by power stroke.

Smooth muscle and skeletal muscle myosins spend only a small fraction of their biochemical cycle time (5%) strongly bound to actin [120]. The information about exact time spent in rigor bound varies in literature. The lifetime of a rigor bond without a load and ATP has been reported to be $10^2 - 10^3 s$ [90]. In the presence of external load and without presence of ATP molecules the myosin detaches within 3s [90]. The duration of cross-bridge attachment during contraction, i.e. in the presence of ATP, is $< 5ms$ [28]. Or, depending on the myosin isoform, the duration of step may range from 1 – 100ms [120]. Cross-bridge detachment during isometric contraction is quite slow [87]. From experiments it is obvious that higher loads shorten lifetimes of rigor bond.

The structure of the actomyosin The actomyosin interaction is believed to be stochastic [12]. The initial binding is nonspecific and dynamically disordered with a range of azimuthal and axial angles relative to actin filament[87]. The motor domain of S1 binds to the actin filament at an angle of about 45° to the actin filament axis [102]. The structure of actomyosin is depicted in figures 3.10 and 3.11.

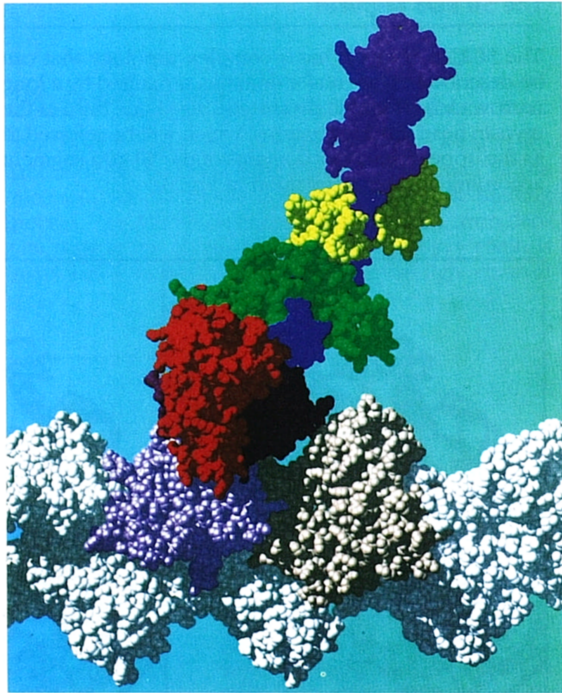


Figure 3.10: The interaction of myosin with actin. The green, red and blue segments represent the heavy chain. Yellow segment represent essential light chains. The magenta segment represent regulatory light chain. The picture is adapted from [101].

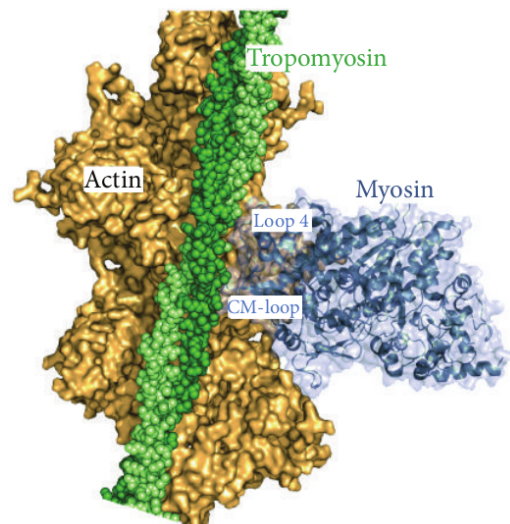


Figure 3.11: The structure of actomyosin. Adapted from [87].

3.2.3 Single myosin II molecule mechanics

In physiological conditions, the force and displacements produced by myosin head are heavily influenced by external load which dictates their functioning and mechanics [87]. Understanding single molecule mechanics of myosin II is crucial for comprehension to active

contraction of muscle. Finally in the last years, the progress in technology and developed techniques allowed to measure with precision of nanometers. Due to quick progress in technology, it is possible to measure mechanics properties of single cross-bridges as for example in [62], [63], [68], [90]. Before the description of mechanical properties of single cross-bridge, it is worth to recall here the the behaviour of single cross-bridge in attached states in the presence of three main types of contraction:

1. during isometric contraction, the length change of single cross-bridge is thought to be caused only by power-stroke,
2. during concentric contraction, the length change of single cross-bridge is a simultaneous effect of power stroke and activity of other cross-bridges on myosin filaments, which shortens considered cross-bridge by shift of actin filament. In this case, the power stroke has the same direction as contraction.
3. during eccentric contraction, the length change of single cross-bridge is a simultaneous effect of power stroke and the effect of external force, which stretches the sarcomere in opposite direction to contraction. Therefore in this case, the direction of power stroke is in opposite to the direction of "contraction" - eccentric contraction.

Power stroke size vs. size of step/shift/displacement

The length change of a single cross-bridge achieved by power-stroke is still a subject of debate. A wide range of myosin II steps were measured since the actomyosin complex attracts attention. Measured steps vary in the range of $4 - 25 \text{ nm}$ [81], $1 - 17 \text{ nm}$ [120], up to $15 - 20 \text{ nm}$ [127]. The wide variety of measured results is without doubts also on account of precision of laboratory devices.

The data from fibers studies and protein crystallography predicts a stroke size about 10 nm , single molecule studies imply a stroke size for single myosins only about 5 nm [8], 5.3 nm [68], 11 nm [25], $5 - 10 \text{ nm}$ by an unloaded myosin [87]. For example, the observed stroke size for a lever arm length for species *Dictyostelium discoideum* is 5.5 nm , whereas

for smooth muscle myosin it is $9nm$ [8]. Further, according to results in [25], the ATP concentration does not affect the length of myosin step.

On account of the length of actin filaments shift, it is necessary to distinguish the exact **size of power stroke step** and exact **size of filament shift/step**. According to results in single myosin experiments, the power stroke seems to be independent on the load and its value is $8 - 10nm$ [62], [63]. In contrary to assumed static value of power-stroke, step-size as the observed sliding displacement can vary with different velocities and loads [63].

The load-dependent step size can be interpreted as follows [62]: the myosin head attaches to an actin filament and performs the working stroke d_w generated by conformational changes of the myosin head. If there is an external load then the elastic part of myosin is elongated by d_e . The resulted step size (shift of filament) d_s can be then expressed as [62]:

$$d_s = d_w - d_e. \quad (3.5)$$

Therefore, in contrary to power stroke, step sizes of single myosin heads as experimentally measured in [62] vary from 4 to $7nm$ in a load-dependent manner. Without external load the working stroke distance is equal to sliding step size and consequently the working stroke is in the maximum limit of myosin II sliding step.

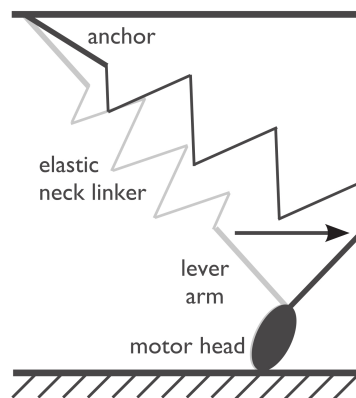


Figure 3.12: Stretch of elastic element by power stroke. The picture is adapted from [21].

Single myosin II molecule force and stiffness

Force As well as for the size of step, the data on exact magnitude of force production of single cross-bridge differs. On account of force production during muscle contraction and working properties of single cross-bridge, two magnitudes of force might attract attention. At first, it is the magnitude or better the range of force, which is single cross-bridge able to produce by itself. As second, it is the magnitude of force, which is single cross-bridge able to exert upon stretch of external force until it forcibly detaches from actin. Steady-states forces in the cross-bridge theory are thought to be independent of the history of contraction [48], [43].

Myosin II is pico-Newton force generator. Measured force per one single myosin head ranged from 1 to $7pN$ with average $3.4 \pm 1.2pN$ independent of ATP concentration [25], $1 - 10pN$ [87]. Recent experiments suggests maximum force per one myosin molecule to be approximately $12pN$ [63]. A maximum force of about $10pN$ is *actively* developed by a myosin motor domain [87]. For isometric contraction the average force per myosin molecule is assumed to be $6pN$ [63], $3 - 4pN$ [25].

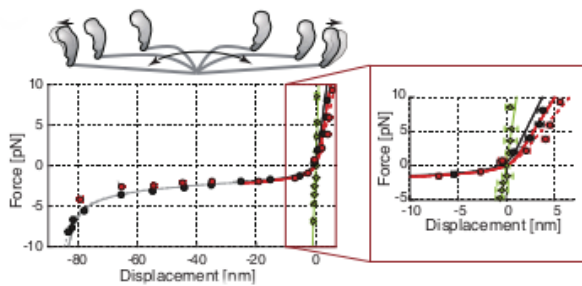


Figure 3.13: Force-length relationship for single myosin molecule as measured and published in [62].

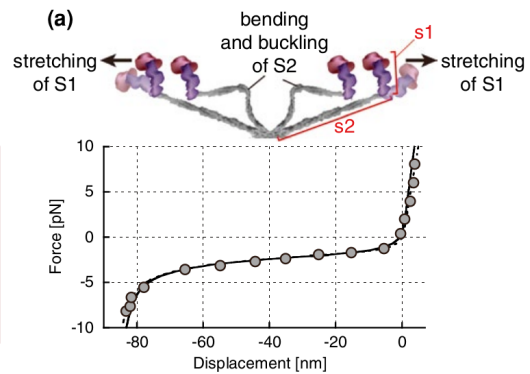


Figure 3.14: Force-length relationship for single myosin molecule as measured and published in [63].

Pulling cross-bridge in opposite direction to its power stroke lead to the stretching of myosin's elastic elements which results in higher force production until the cross-bridge detaches due to binding of ATP or due to forcible detach by external force. Pulling the

attached head to rupture the rigor state, the average unbinding force was 9.2 ± 4.5 [90]. This force is much smaller than other intermolecular forces, for example $110pN$ for actin-actin bound [90]. The maximum strain at which the rigor bond ruptures in experimental measurement in [90] was $69 \pm 27nm$. The measured force-length relationship of single cross-bridge is depicted in figure 3.13 and 3.14.

Stiffness of single cross-bridge The cross-bridges contribute significantly to the total compliance of muscle fibres: 50–70% [89]. The stiffness of one single myosin molecule varies in range of $1 - 3pN/nm$ [63], $0.58 \pm 0.26pN/nm$ [90], in the range $1.7 - 3.3pN/nm$ [87].

Since the measurements providing just strain showed the linear stiffness resulting from S1 domain, the nonlinearity is attributed to S2 region of myosin, i.e. buckled or bended part of myosin in figures 3.13 and 3.14. The experimentally measured stiffness-force relationship is depicted in figure .

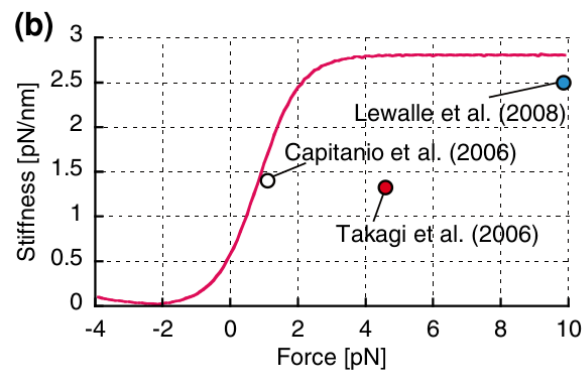


Figure 3.15: Stiffness-force relationship. Adapted from [63].

3.2.4 Myosin filament, thick filament

As notes already above, the myosin II motor is non-processive molecular motor and operates in cluster consisting of tens of myosin molecules. The α -helical tails of the myosin II molecules are packaged into the backbone of myosin filaments [96]. Individual motors

(cross-bridges) protrude from myosin filament at regular 14.5nm intervals. Single myosin filament is approximately $1.6\mu\text{m}$ in length. The whole filament in skeletal muscle, see figures 3.16 and 3.17, is bi-polar structure with central barezone, where no myosin heads are present. This barezone is situated in the middle of the sarcomere. The number of thick filaments in striated muscle is estimated to be $500/\mu\text{m}^2$ [28], $470/\mu\text{m}^2$ [117]. One of the internal structural part of myosin filament is also titin.

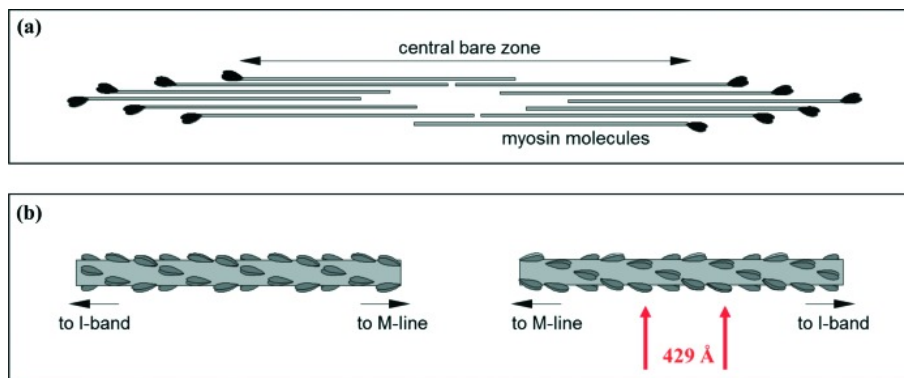


Figure 3.16: Myosin thick filament and its bipolar structure. Source of picture [2].

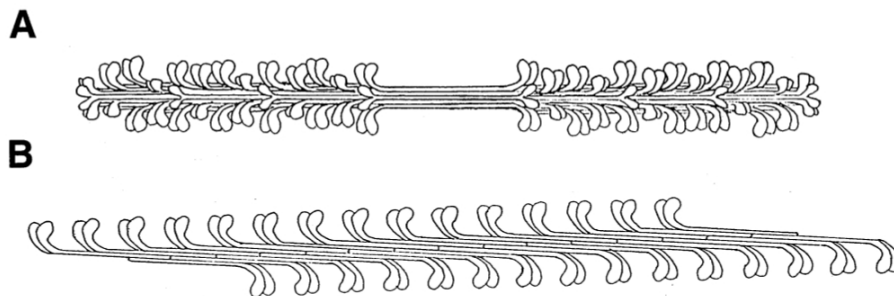


Figure 3.17: Comparison of skeletal muscle myosin filament (A) and smooth muscle myosin filament B. Skeletal muscle filament is a bipolar structure with a central bare zone without myosin heads. Myosin filament in smooth muscle is believed to be "side polar". Adapted from [18].

A large ensembles of motors acts as a functional unit, although it is assumed that each cross-bridge acts as independent force generator. Nevertheless, at least one kind of cooperation might be indentified. Since if they work in ensemble, single myosin can affect

the lengths of others by its power stroke activity. Therefore they "interact mechanically" as mentioned for example in [124]. As a result, the production of force and displacement by myosins in muscles is the cyclic interactions of billions of myosin motors [87].

Single filament mechanics

The myosin filament length was supposed to be constant in classic cross-bridge theory. Nowadays, it is experimentally confirmed that in unactivated state of sarcomere the length of thick filaments remains constant. Whereas in activated state of sarcomere, there is frequently reported that myosin filament shortens sometimes substantially [97].

Mechanical as well as X-ray studies demonstrated that the number of attached heads includes force-generating and non-force generating heads [63]. In studies, the estimated number of attached myosin heads producing force varies from 5 % up to 60 – 70% [25]. The results in [25] suggests that only 20 – 40% of the heads produce force at any time although the X-ray diffraction suggest values at any moment 75 – 90%. But these estimates may include attached cross-bridges not developing force. It is worth to notice, that some of these attached myosin head may be bounded under different angles, which could lower the ability to produce maximal force. X-ray measurement suggests a fraction of ordered heads in ideal direction is 0.2 – 0.3% [25].

3.2.5 Actin - A Linear Track for Molecular Motor Myosin, thin filament

Actin filaments with its regular structure serve to the myosin II motors as linear tracks. The experiments on single myosin molecule also established that the direction of contraction is determined by the actin filaments [50]. Myosin II moves along actin filament towards the plus end [61].

Structure of actin filament

Three main compounds comprise actin filament: actin monomer, troponin complex and two strands of tropomyosin molecules. Tropomyosin is approximately $42nm$ long molecule. It is formed as homodimer or heterodimer of two α -helical chains. Troponin complex consists further of three proteins: troponin-I, troponin-C and troponin-T. Actin has much higher stiffness (approximately $20pN/nm$) than myosin [63]. Actin filament in sarcomere is approximately $1.0\mu m$ long and has approximately 100 \AA in diameter. Its axial repeat is approximately 370 \AA [2]. Actin and myosin filaments have different rotational symmetry and helical symmetry [2].

Structural and biochemical studies suggest that the position of tropomyosin and troponin on the actin filament determines the interaction of myosin with the binding sites on actin [28]. In passive state of sarcomere, the binding sites on actin filaments are blocked by tropomyosin. Tropomyosin position on the actin filament is regulated by the occupancy of NH-terminal Ca^{2+} binding sites on TnC. The binding of Ca^{2+} at NH-terminals on TnC results in conformational change and movement of tropomyosin on actin surface. At the end, this process leads to the uncovering of cross-bridge binding sites. The states of binding sites on actin filament might be denoted as [28]:

1. **blocked**: cross-bridges are unable to bind the binding sites,
2. **closed**: cross-bridges are able to weakly bind the binding sites,
3. **open**: cross-bridges are able to create strong bound with power stroke.

Troponin C (TnC) binds Ca^{2+} , troponin I (TnI) binds to actin and inhibits the actomyosin ATPase. Troponin T (TnT) links the troponin complex to tropomyosin.

3.2.6 Spatial arrangement of myosin and actin filaments

The filaments arrangement in sarcomere varies from species to species. The impact of different arrangements of filaments in sarcomere on muscle contraction remain largely unknown [114]. To date, the most familiar arrangements are depicted in figure 3.20.

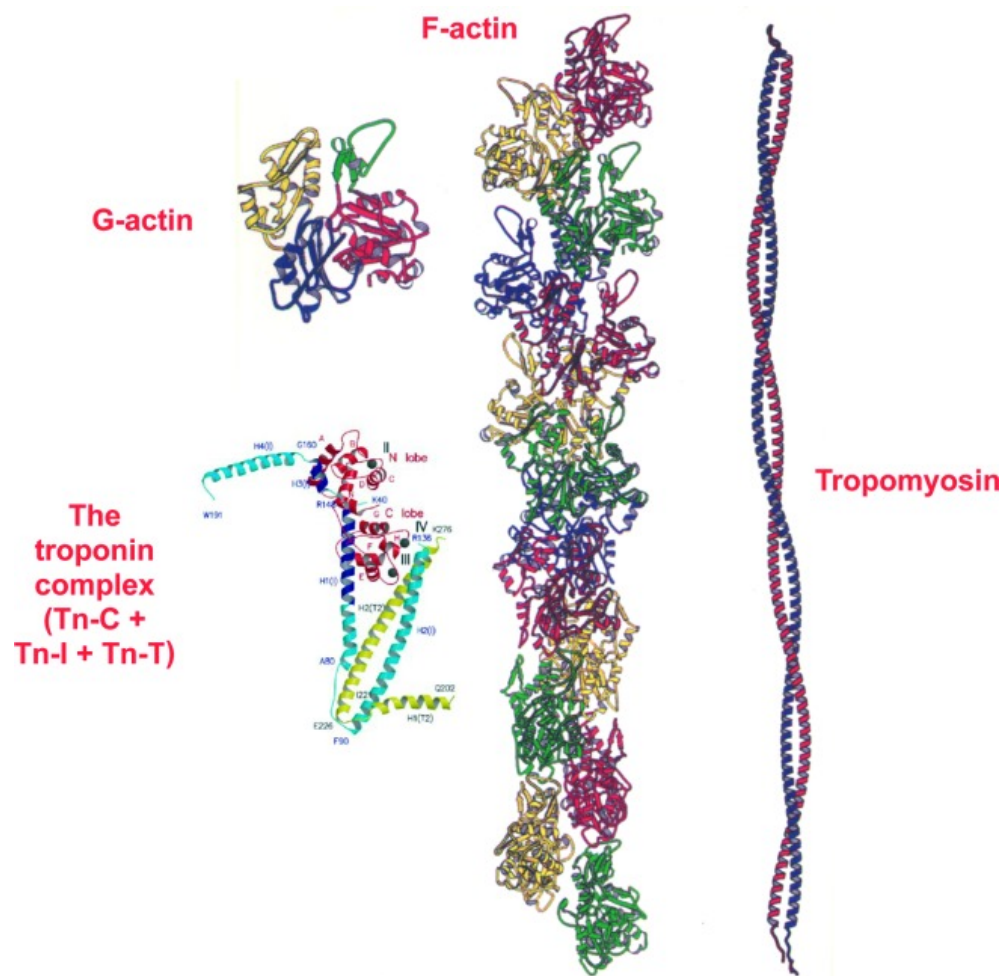


Figure 3.18: Structure of actin (F-actin, where "F" stands for filamentous). Four main components are: actin monomer (referred as G-actin), tropomyosin and troponin complex consisting of three components: troponin-C, troponin-I and troponin-T. The picture is adapted from [2].

In comparison to sarcomere, the arrangement of contractile proteins in smooth muscle cell is assumed to be random with prevailing direction along the longest "axis" of smooth muscle. Contractile proteins in smooth muscle cells are assumed to be anchored by so called dense bodies into cell membrane. For illustration see figure 3.21.

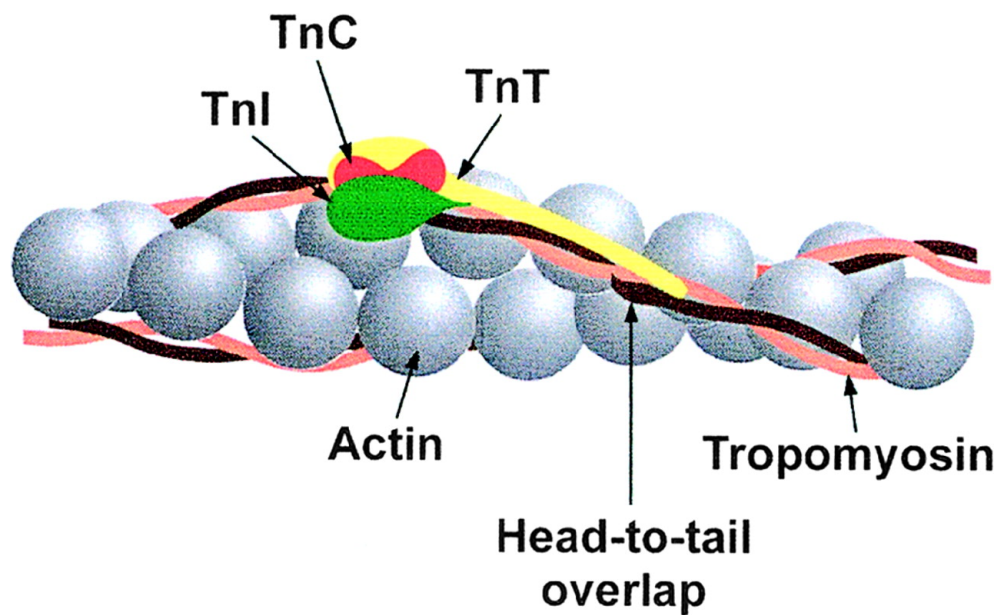


Figure 3.19: Atomic model of F-Actin filament. The arrangement of troponin (Tn), tropomyosin and actin in the skeletal muscle thin filament. The various troponin subunits are color coded - TnC(red), TnT(yellow) and TnI(green). The picture is adapted from [28].

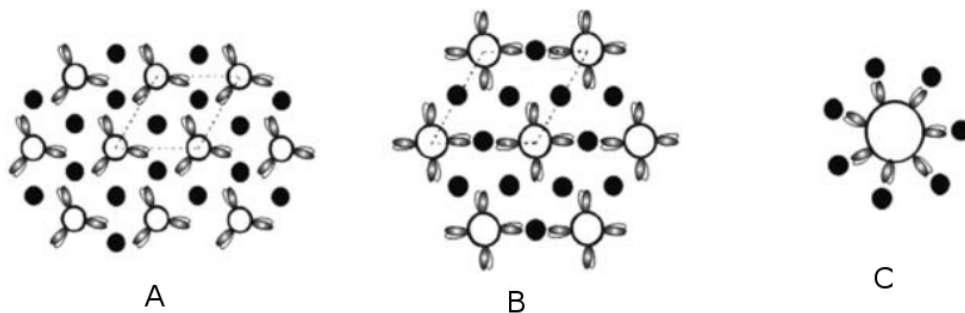


Figure 3.20: Schematic drawing of a cross-section through the myosin and action filaments lattices within the A-band parts of sarcomere. (A) fish skeletal muscle, (B) insect fibrillar flight muscle, (C) scallop pecten muscle. Adapted from [2].

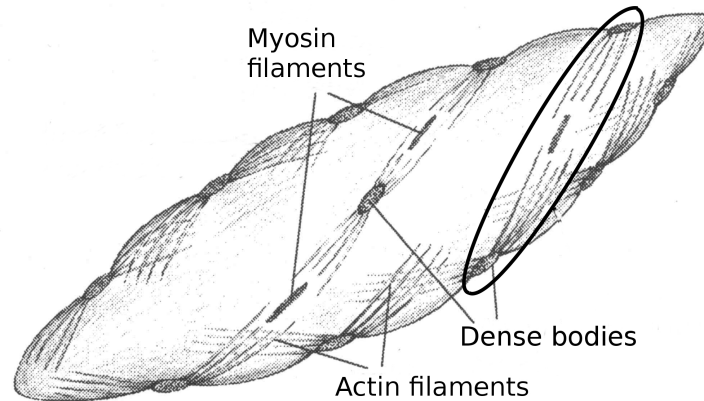


Figure 3.21: Assumed arrangement of myosin and actin filaments in smooth muscle cell. Modified from [104].

3.3 Contraction - Interaction between Myosin and Actin Filaments

3.3.1 Contraction velocity

Maximum shortening velocity depends on $[ATP]$, as emerged for instance in experiment presented in [81] as well as in other articles. Measured velocities on molecular level confirmed that in the presence of higher calcium concentration the velocities are also higher. The velocity of concentric contraction ranges from $0.5 - 5.0$ muscle length s^{-1} [18]. At maximal shortening velocity, the rate-limiting step in a cross-bridge cycle is the hydrolysis of ATP and the release of P_i and ADP from the myosin head [110]. Maximal velocity v_{max} is more temperature sensitive than maximal exerted force F_{max} . The measurements on single myosin molecules established that speed of contraction conducted by single myosin was close to the unloaded sliding speed of the filaments in the muscle from which the myosin was obtained [50].

3.3.2 Regulation of contraction - regulation of cross-bridge cycling activity

In vertebrate striated muscle, contraction is regulated primarily through Ca^{2+} effects on actin filament, where concentration of Ca^{2+} regulate strong cross-bridge binding to actin [28]. This regulation is often referred as thin filament regulation. The primary regulation of smooth muscle contraction is through the phosphorylation of myosin light chain by a calmodulin-kinase mechanism [18]. This regulation is often referred as thick filament regulation. In striated muscle, the main source of Ca^{2+} ions are primarily internal structures called sarcoplasmic reticulums. Whereas in smooth muscle the main source of Ca^{2+} is external environment of smooth muscle cell.


In striated muscle, the position of tropomyosin and troponin on the actin filament covers/uncovers binding sites for myosin heads (for cross-bridges). Tm position on the actin filament is regulated by the occupancy of NH-terminal Ca^{2+} binding sites on TnC. TnC then can be denoted as the Ca^{2+} sensor in skeletal and cardiac muscle contractile regulation. The expose of myosin-binding sites on actin increases the affinity of actin for myosin. The affinity of all actins for myosin is further increased when sufficient number of strongly attached cross-bridge displace (or stabilize the displacement of) the tropomyosin further than occurs with Ca^{2+} binding alone [28].

The initial rate of force development depends mostly on the extent of Ca^{2+} activation of the thin filament and myosin kinetic properties [28]. The regulation of contraction might be further modified by the activity on myosin light chains. Essential light chains may modulate ATPase activity [10]. The regulatory chains can be reversibly phosphorylated which can influence the rates of tension development [10].

As stated in [28], physiological studies suggest the following process of regulation of contraction:

1. Ca^{2+} ions bind to troponin and tropomyosin which results in opening of the binding sites on the actin filaments. Myosin heads can consequently attach at these places.

2. Ca^{2+} regulates the strong binding of myosin to actin, which precedes the production of force and release of hydrolysis products.
3. A small number of strongly attached cross bridges can activate the actins in one unit and perhaps those in neighbouring units. This results in additional myosin binding and isomerization to strongly bound states and force production.
4. The cooperativity between neighboring regulatory units contributes to the activation by strong cross bridges of steady-state force but does not affect the rate of force development.
5. Strongly attached cross bridges can delay relaxation in skeletal muscle in a cooperative manner.
6. Strongly attached and cycling cross bridges can enhance $[Ca^{2+}]$ binding to cardiac TnC, but influence skeletal TnC to a lesser extent. Different Tn subunit isoforms can modulate the cross-bridge detachment rate as shown by studies with mutant regulatory proteins in myotubes and in vitro motility assays. These results and conclusions suggest possible explanations for differences between skeletal and cardiac muscle regulation.
7. In some cases, the light chains are believed to modulate the basic functions of the globular head [10].

 **Quick summary of chapter**

Molecular motors are molecular (protein) mechanisms that are able to cyclically convert chemical energy into mechanical energy. They operate in the realm of nanometers surrounded by stochastic behaviour induced by thermal noise. In contrary to macroscopic engines, they operate under isothermal condition. Their working cycle is powered by chemical reactions. The beginning of understanding to molecular motors is strictly connected with muscle science and its early research during 1950s. In all kinds of muscles, the main propelling source and force generator is molecular motor myosin II. Single myosin is able to exert the force in the range of units of pN . Myosin II is found at the lowest level of the muscles structural hierarchy. Myosin II is non-processive molecular which acts in ensemble. During its working cycle, it is able to attach and shift actin filaments in the direction to the centre of sarcomere. The crucial force generating step in its working cycle is called power stroke, which is the biggest conformational change in its mechano-chemical cycle.

Chapter 4

Titin - An Entropic Molecular Spring

Titin, also known as connectin, is the largest protein currently known in the natural world [80]. Titin molecules are formed from the largest polypeptides found in nature [118]. Titin is the third most abundant protein in sarcomere after actin and myosin [72]. It constitutes about 10% of the total muscle protein mass [64]. About 90% of titin's mass consists of repeating immunoglobulin-C2 (Ig-domains) and fibronectin-III (Fn-3) domains [72]. The resting 10% of its mass consists of non-repetitive sequences as N2B, N2A and PVEK region (see figures 4.2 and 4.1).

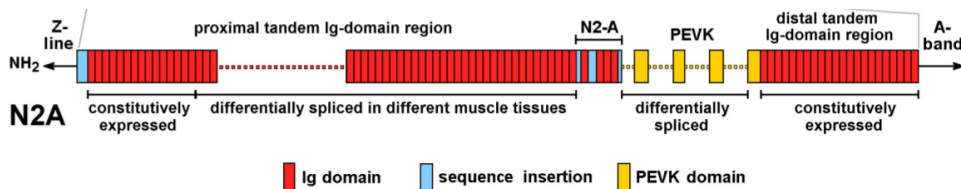


Figure 4.1: Titin's domains and titin's parts in its structure. Modified from [98].

The exact shape and properties of single titin molecules slightly varies with concrete species. On average, the main structure and characteristic properties remain similar. 90% of its polypeptide mass is organized into modular repetitive units. One molecule of titin can be up to $1\mu m$ long [118]. For instance in [66], the mean contour length of titin is stated as $0.87\mu m + / - 0.08$. The diameter of this protein is about $4nm$ [119]. Titin

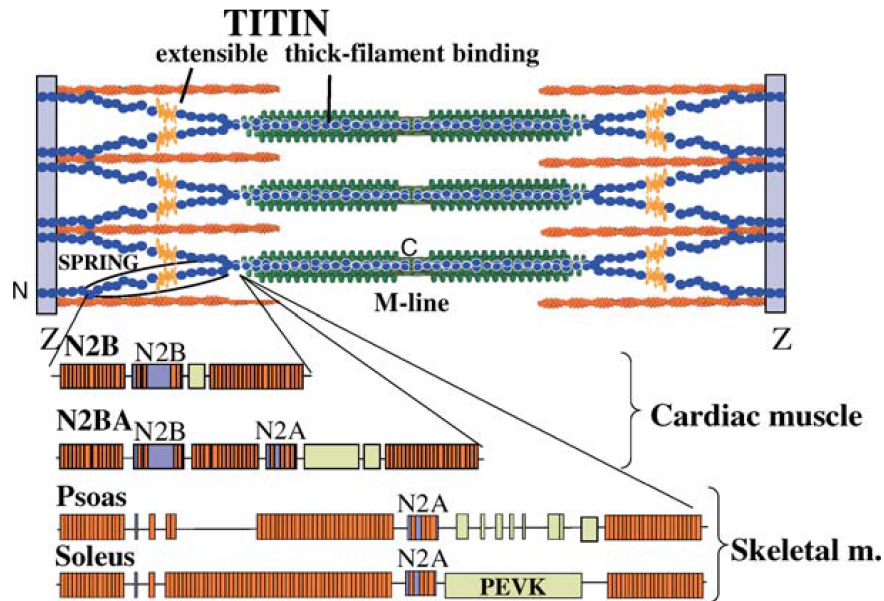


Figure 4.2: Sarcomere structure and the titin structure in the skeletal and heart muscle. The picture was adapted from [30].

weights 3.0 – 3.7 *MDa* (million-dalton) [66] or as published in [31] 4.2 *MDa*.

Titin plays a number of important roles in sarcomere. From a mechanical point of view, for its nature and the characteristic behaviour in sarcomere, titin is commonly denoted as a **molecular spring**. Titin as a molecular spring influences distinct biomechanical properties of sarcomere not only during contraction. As a spring, titin contributes significantly to the contraction, elasticity and viscous effect of sarcomere notwithstanding if the sarcomere is in activated or deactivated state. The diversity in myofibrillar passive elasticity among species is associated with different titin isoforms. Furthermore, in comparison among striated and cardiac muscles, the observed passive forces in cardiac muscle are higher in comparison to skeletal muscle [60].

Moreover, titin affects the rest lengths of sarcomere, operating range of sarcomere's lengths and passive elastic properties of sarcomere[119]. Titin as a passive force producer is responsible for restoring muscle length after release [67] of deactivated muscles. Titin is also important for maintaining structural integrity of sarcomere. In particular, it anchors and maintains myosin thick filaments in the central position of sarcomere and ensures a

balance of forces in the two halves of sarcomere during contractile cycles [31]. The crucial part of titin affecting the passive production of force in sarcomere is found in I-band region of sarcomere.

Besides other things, titin also interacts with a majority of sarcomere proteins [118]. Titin can be also involved in signal transduction [72]. Nowadays, titin is also believed to be important regulator of active force especially during eccentric contraction as explained at the end of this chapter.

4.1 Repetitive building blocks of titin

Immunoglobulin and fibronectin-3 domains are common building blocks of many extracellular proteins as well as group of intracellular proteins associated with the contractile apparatus of muscles [118]. Arrangement of Ig and Fn-3 domains is assumed to be serial as in chain. Titin isoforms in cardiac and skeletal muscle contain between 240 and 300 of Ig- and Fn-like domains [118] with each domain in length of $\sim 4nm$ [118], [31]. Ig and Fn-3 interdomain mobility and structural stability directly affect passive mechanical properties of muscles. As stated in [66], the only point of attachment among the titin's component (single oligomers) molecules are globular heads of single oligomers. The rest building parts along titin's contour length does not form any connections between neighbouring molecules among oligomers.

4.2 Titin in Sarcomere

In I-band part of sarcomere, the titin is anchored at one side to the Z-line. At the other side, the titin is anchored to M-line. In A-band, titin is strongly attached to the thick myosin filament.

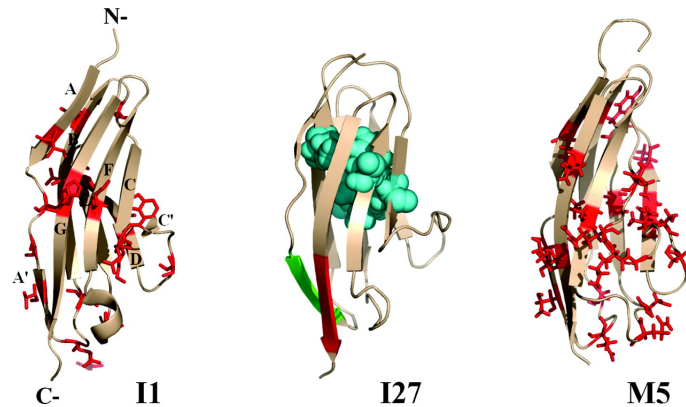


Figure 4.3: Structure of titin Ig domains as solved by x-ray crystallography. These domains are representative for proximal Ig domain segment *I1*, distal Ig domain segment *I27*, and the segment in A-band *M5*. The picture is adapted from [118].

4.2.1 Titin in I-band

In the I-band of sarcomere, the titin forms the elastic connection between the myosin filaments and Z-line. This part of titin strongly influences the passive force production (elasticity) in sarcomere namely during stretch notwithstanding if the sarcomere is activated or not. This part of titin comprises only from Ig domains and unique sequences. I-band part of titin does not contain Fn-3 domains [118]. Ig domains are arranged in tandem at two parts of titin: the **distal** region near to myosin filament and **proximal** region near to Z-line. The proximal tandem near to Z-disk contains of 15 Ig domains [31]. The distal tandem near to A-band contains of 22 Ig domains [31]. Between the distal and proximal region there is N2-PEVK region containing unique non-repetitive sequences of titin.

N2-PEVK region can be further divided into PEVK region and specific N2A, N2B regions. This part contains approximately 18-residue¹-containing PEVK segment. PEVK unique sequence comprises of a proline (P)-, glutamate (E)-, valine (V)- and lysine (K)-rich domains [66], [31]. The contour length of PEVK region is $\approx 826nm$ [31].

¹wikipedia:In chemistry, residue is the material remaining after distillation, evaporation, or filtration. Residue may also refer to an atom or a group of atoms that forms part of a molecule, such as a methyl group. It may also denote the undesired by-products of a chemical reaction.

All skeletal muscle isoforms contain in I-band the N2A element. All isoforms of muscle contain also variable number of additional Ig domains in proximal tandem Ig segment and variable number of additional PEVK residues. The cardiac muscle might contain in I-band region two types of titin: N2B titin, containing N2B specific segment, and N2BA titin, containing specific N2B and N2A segments. N2BA titins are less stiff [31].

Ig-domains in this part of titin are believed to serve as "molecular springs" and on the other hand N2-PEVK is believed to have the property of titin modulation.

4.2.2 Titin in A-band of sarcomere

In A-band region of sarcomere, the titin is the internal part of myosin filament. In this region, titin is mostly formed by Immunoglobulin and Fibronectin-3 domains [31]. The A-band region of titin does not participate in passive force production under physiological conditions [64].

4.3 Titin Mechanics

In the absence of external forces, the I-band region of titin is highly folded [72]. During the stretch, titin parts in I-band region extend and develop passive forces according to their characteristic elastic properties. Other parts of titin except the part of titin in I-band seem to be inextensible [72] under normal physiological conditions. Nevertheless, these parts have capability of extension in the presence of higher external forces.

Although, in some articles the titin is referred also as a bidirectional spring (for example in [72]) exerting force upon press, the titin molecule is mostly considered as **unidirectional spring** producing force only and virtually by stretch of external force - the case of eccentric contraction namely. If it is under the press, it is considered that it behaves as a free band - the case of concentric contraction. During the isometric contraction, the titin is considered as it does not change its length (approximately). Therefore, during isometric contraction it might contribute to the total sarcomere force production only in a case if it was stretched

before the sarcomere was activated or if the isometric contraction follows after eccentric contractions.

Titin's extensible region consists of tree spring-like subsegments (Ig-domains, PEVK and N2A,B regions) with distinct extensible properties [31]. Single molecule experiments as well as experiments with multiple titin molecules revealed that titin molecules exhibit properties of nonlinear entropic spring with partial unfolding during the stretch at high forces and refolding at low forces during the release [64]. In some cases and articles, the unfolding of titin parts are believed to be a cause of viscoelastic properties namely due to Ig-domains unfolding [85].

Measured data and theoretical models suggested that titin molecules behave as independent worm-like chains. Single experimental molecule studies confirmed that worm-like-chain model (WLC) can describe entropic elasticity of titin. Worm-like-chain model sufficiently describes the force-length relationship of titin. WLC model was with success applied to describe elasticity of single titin molecule, its parts, as well as bulk of titin molecules. The good compliance for data fit with WCL model suggest that multi-molecular titin chains act in parallel or nearly parallel arrangement of independent chains [66]. The mathematical WLC model is more profoundly introduced further in chapter 5.

4.3.1 Single titin molecule mechanics

The extension of titin's parts depends on the amount of external force and the amount of extension. Therefore, at specific extension of titin, the extension of particular parts dominate.

Ig-domain/segment extension - low forces

At low forces, i.e. at the start of stretch, the extension of tandemly connected Ig-domains dominates. Extension of the tandem Ig segments in short to intermediate long sarcomeres results from the unbending of sequences that serially link Ig domains [31]. During the stretch, the Ig-domains extend, unfold and straighten themselves [72]. It is assumed that

the Ig-domains extend, in average, uniformly. When the single sarcomere is stretched to the intermediate sarcomere lengths ($2.0 - 2.6\mu m$ for soleus muscle), the Ig-segments are found to be already greatly extended [31].

PVEK domain extension

As forces acting on titin arise, random coil sequences within the PEVK segment begin also extend. PEVK region is the major source of extensibility in titin in intermediate to long sarcomere lengths [31],[85]. In highly stretched sarcomeres, the PEVK region was found to extend up to $750nm$ [31].

Extension of N2B unique sequence

At higher forces, the random coil sequences in the N2B (cardiac specific segment) element extend also [72], [31]. N2B as the third spring element in cardiac titins is then the major source of extensibility at the upper range of physiological sarcomere lengths in the heart [31].

4.3.2 Unfolding and refolding of single protein

Individually folded domains are common parts of proteins [11]. Application of mechanical force to biological polymer produces conformations that are different in comparison to those which were investigated and achieved by chemical or thermal denaturation [26]. Mechanical force induced conformational transitions (unfolding) are therefore considered as physiologically important [26]. As individual domains unfold, the force produced by polymer chains relaxes. Hence, the viscoelastic properties of titin are believed to be namely due to Ig-domains unfolding [85].

Spontaneous unfolding

The native state of proteins is the most stable and therefore proteins rarely unfold spontaneously [11]. The spontaneous unfolding of isolated Ig domain and Fn-3 domain is esti-

ated to occur at rate 10^{-3} to $10^{-4}s^{-1}$ [11]. On the other hand, the refolding is typically much faster with rates in the range of 1 to $100s^{-1}$. Therefore, the spontaneous unfolding of individual Ig domains and other part of titin is highly unlikely.

Unfolding indicated by stretch

The single-molecule experiments showed that application of force by stretching the molecules of titin results in unfolding of Ig-domains by breaking the inter and intra-sheet bonds [31]. Unfolding of Ig domains during the stretch shows characteristic "saw-tooth" pattern in titin's force-length relationship (see fig. 4.4) .

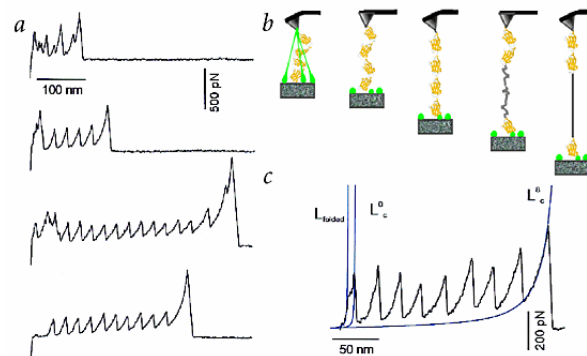


Figure 4.4: Typical response to force of protein unfolding achieved by Atomic force microscope. The graph is adapted from [26].

The measured data of force-extension relationship contains force peaks which correspond to individual domain unfolding [66]. These force peaks are typically roughly equidistant in single molecule stretching [66]. These peaks can be noticeable even in multi-molecular measurement [66]. Experimental measurements such as [64] indicate that various globular domains such as Ig domain, N2 region, PVEK region in titin require different unfolding forces due to differences in the activation energies for their unfolding [64].

The average force of unfolding is shown to depend on the pulling rate [11]. Unfolding force of Ig-domains varies with speed of stretch. The unfolding forces were measured in the range $150 - 300pN$ for stretches speed in the range $1 - 1000nms^{-1}$ [31].

The single molecule experiments suggested that unfolding of Ig-domains evince also

probabilistic behavior of unfolding without exceeding some force threshold value. Whereas the experiments on a bulk of titins molecules demonstrated that it is unlikely for Ig-domains to be unfolded under normal physiological conditions [85]. The Ig-domains unfold with a probability that increases with increasing force and passing time [30].

The exact properties of titin's domain is nowadays still a subject of intensive research. Due to this fact, the available information might be in contrary. Some authors therefore also assumed that the titin parts are already unfolded before the stretch (for example [67]). Or, as stated in [72], the unfolding of individual Ig domains is highly unlikely. Or, under physiological loading conditions, unfolding is unlikely to be major source of (visco)elasticity [117].

Refolding Refolding is not observed in presence of force [85]. Once the Ig-domain is unfolded, it remains in unfolded state until a low force is reached during release [31].

Hysteresis of titin/sarcomere

On account of unfolding/refolding of titin's domains during stretch, titin is also considered to be the main source of sarcomere hysteresis. Stretch and consequent release of single titin molecule show hysteresis properties [67]. This is likely due to the domain different folding/unfolding rates (see figure 4.5).

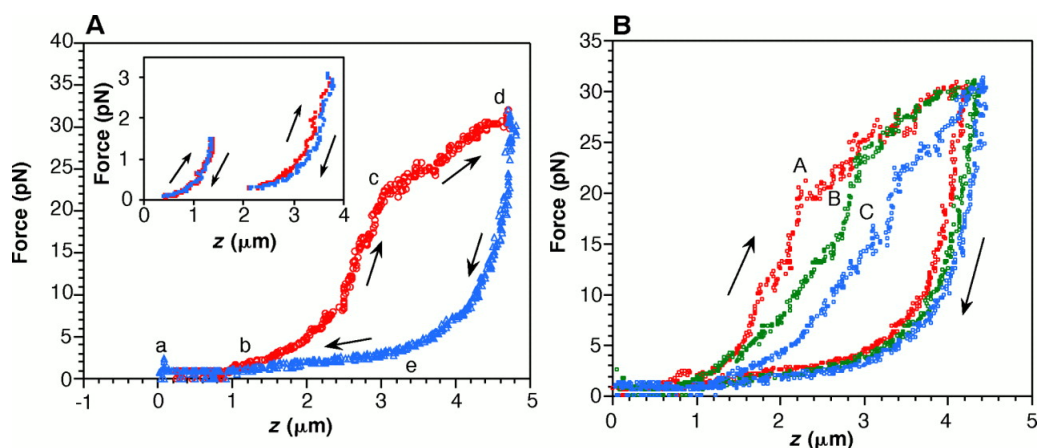


Figure 4.5: Measured single titin molecule hysteresis. The graph is adapted from [67].

4.3.3 Changing of mechanical properties of titin molecule

The performed experiments showed that mechanical properties of titin molecule are modulated by various factors. Titin interacts with a majority of sarcomere proteins [118] and chemicals, which leads to modulation of titin's mechanical properties. Before all, mechanical properties of titin can be modified by various Ca^{2+} concentration and by phosphorylation. Further, mechanical properties vary among the species on account of the number of unique sequences in sarcomeres.

Calcium binding

There is an evidence [17] that titin changes its mechanical properties upon chemical activation by calcium. According to latest available measurement and proposals (for example [17]), fluorescence microscopy showed that individual Ig domains change their mechanical properties and structure in the presence of calcium ions. Fluorescence microscopy showed that calcium binding is responsible of Ig 27 structure change [17]. A conformational change in I27 is attributed to enhanced mechanical stability. This can lead to the increase in a force demanded to extend and unfold the Ig domains. The measured difference in force production with and without calcium can be seen in figure 4.6.

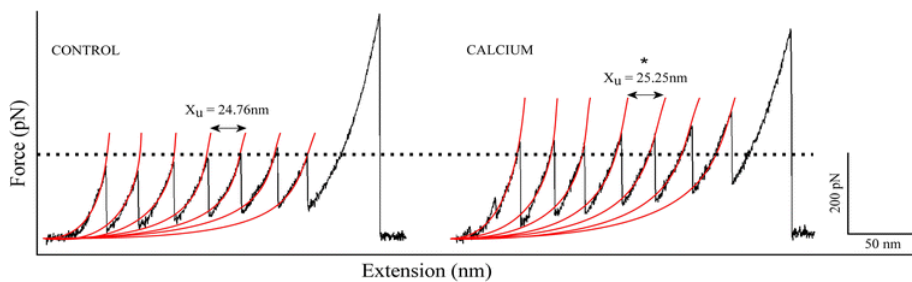


Figure 4.6: Unfolding of seven (of eight possible) distal cardiac Ig domains with atomic force microscopy. Broken line represent $200pN$. Left part of graph shows control force-length curve without presence of calcium. Right part of graph shows force-length curve with presence of calcium. The graph was adapted from [17].

The next structural domain of titin, the PEVK segment, binds calcium with high affinity [31]. After calcium is binded to PVEK, experiments showed that calcium induced

conformational changes reduced the bending rigidity of the PEVK segment[75].

4.4 Binding of titin to actin filament - a clue to modification of classical Huxley's cross-bridge model and hint to explanation of eccentric contraction

When activated sarcomere is stretched by external force (eccentric contraction), according to classical cross-bridge theory the force production should cease to exist behind the overlap of thin and thick filaments. This does not correspond with observed experiments, where the force rise up during the stretching of sarcomere. Further, when activated sarcomere is stretched and then left to relax to isometric contraction with new corresponding length, the new value of produced force is higher than predicted by classical cross-bridge theory. This phenomenon related to eccentric contraction and force enhancement phenomenon might be explained by nowadays observed and investigated "hidden" properties of titin.

The experimental measurements indicated that the behavior of passive forces differ in active and passive states of sarcomere, i.e. in presence of high resp. low calcium concentration. As discussed and experimentally observed in [80] and [40], although there are some changes in force regulation due to phosphorylation and calcium binding to titin domains, the resulted forces in and after stretch are still bigger than the forces expected by classical cross-bridge theory and purely stretched titin molecules.

As a crucial modification of titin's mechanical properties it seems to be that the titin is able to bind at actin by PVEK or N2A region [40], [80], [43]. This might be a result of modulation of "free spring" (titin) length. As a result of this assumption, sarcomere is able to produce more force during the eccentric contraction [40], [80], [43] since the local deformation achieved by stretch of titin parts is much higher than local deformation of detached and deactivated titin.

In brief summary, titin changes namely its material properties in activated sarcomere by the presence of calcium in two ways [43]:

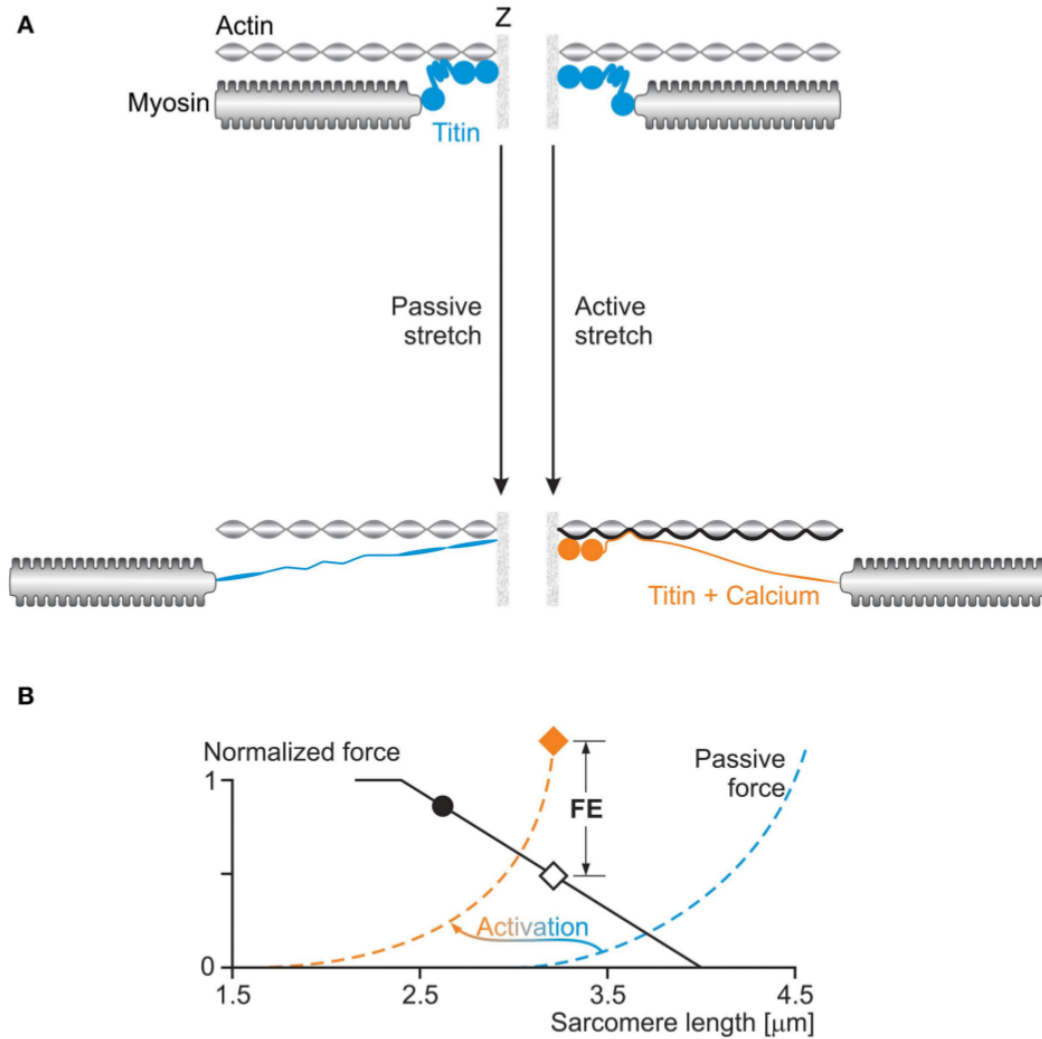


Figure 4.7: Titin-induced force enhancement. **A**: Left part of picture represents stretch of deactivated half-sarcomere. Right part of picture represents stretch of activated half-sarcomere (eccentric contraction). **B**: The effects of titin's modulated properties illustrated in force-length graph. Adapted from [43].

1. by changing its material properties,
2. by changing its free spring length.

The scheme of proposed titin mechanism is depicted in figure 4.7.

The theoretical model of the titin binding to actin is the main subject of this work and is discussed further in the text in chapters 5, 6, 7. In conclusion to this chapter,

it is important to highlight here how the titin contribution to the force production is considered regarding to the rest types of contraction. During concentric contraction, the titin is assumed to be attached at actin. But in this case, it is considered as it produces no force, since the distance of its both end is shortened and the titin is considered to behave as a free band. During isometric contraction, it is again considered as it is attached but is neither stretched or shortened, therefore produces again no force.



Quick summary of chapter

Titin is the third most abundant protein in sarcomere. It has various physiological and mechanical properties important for sarcomere. It maintains sarcomere structural integrity. It is virtually exclusively source of passive forces in sarcomere. Further, it is important stabilizer for sarcomere and regulator of active force. It anchors myosin in the sarcomere. Titin restores sarcomere relaxed length. Latest research indicated that the role of the titin during contraction might be much more important than originally thought. It seems like the titin can also actively contribute to the force regulation namely during eccentric contraction. Latest results found new properties of titin's force modulation namely by chemical modulation and further by binding to actin, which results in decrease of titin's free length.

Chapter 5

Mathematical Models - A Brief

Overview

Regular structure of muscles has always been a challenge and motivation to develop an easy and transparent model describing properties of muscle contraction. During the decades, a vast variety of models have been proposed in the range from molecular level to tissue level. More concretely, this range comprises from the scales of nanometers up to scale of centimeters/metres. Regardless the scale, the models at each level are (must be) still a compromise among inclusion of all aspects and mathematical model complexity. Especially, if the mathematical models should describe all muscle properties, then the muscle models need to contain mechanical, physiological and structural properties [34] as well as properties of chemical reaction.

On account of the models related to skeletal muscle contraction mechanics, there can be found at least one possible simplification of mathematical models regarding to the number of spatial variables. Since the molecular motors act on proteins in a shape of filaments, which imposes the movement on a "line", the mathematical models can be in most cases usually one dimensional in spatial variable with the second time variable. Besides this, another reason to develop models only with one spatial variable is also the fact that it is much easier to compare the theoretical results with experimental data, which were obtained

from the experiments conducted on contractile activity only in one direction as well [125].

This chapter is intended to present some of the selected important models for better comprehension of the aims of this work. The following introduced models are presented as published in literature with their achieved results.

5.1 Single myosin molecule mechanics

5.1.1 Force production of single cross-bridges

The mathematical descriptions of single myosin molecule elasticity are trivial models relating force-extension properties according to particular stiffness of single cross-bridges. But it is worthwhile to express it here, because then the comprehension namely of term of power-stroke might be much more clearer. Further, it might help to understand, why the single myosins acting in ensemble are able to produce different values of elastic forces by which they contribute to the resulting magnitude of the active forces in sarcomere.

Let's recall here the already presented model of magnitude of step-size of a single cross-bridge after power-stroke:

$$d_s = d_w - d_e, \quad (5.1)$$

where d_s is resulted step (shortening, shift of actin filaments) conducted by single cross-bridge after power-stroke, d_w is the magnitude of power-stroke (assumed to be constant) and d_e is the elongation of cross-bridge's elastic part. d_e depends on initial position of cross-bridge and on the external force. d_e can be zero and under special condition it might be negative to express the acting against the direction of active contractile activity.

The force F produced by single cross-bridge might be then simply expressed as:

$$F = k(d_e)d_e, \quad (5.2)$$

where k is the stiffness of single cross-bridge. Regarding to the value of d_e , the force might be zero or under special condition negative as explained above.

5.1.2 Strongly bound duration

One of the processes affecting the properties of contraction is the time, which single cross-bridge stays weakly and consequently strongly bounded to actin. This time might be expressed as [120] :

$$\tau_{on} = \tau_{-ADP} + \tau_{+ATP}, \tag{5.3}$$

where τ_{on} is time that myosin spends strongly bound to the actin filament, τ_{-ADP} is constant for ADP release and τ_{+ATP} is the time of ATP binding.

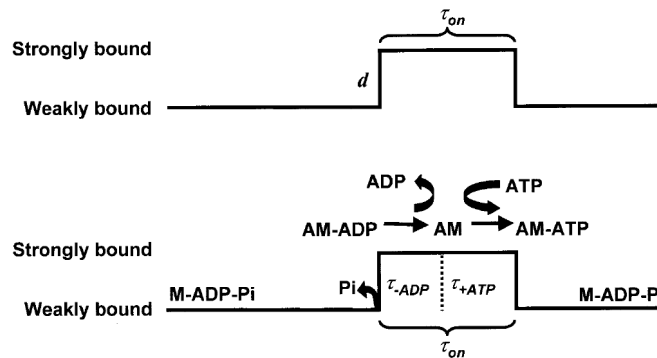


Figure 5.1: Strongly vs. weakly bound duration. The picture was modified from [120].

It can be further rewritten in the terms of rate constant k_{-ADP} , k_{+ATP} [120]:

$$\tau_{on} = \frac{1}{k_{-ADP} + \frac{1}{[ATP]k_{+ATP}}} \tag{5.4}$$

which says that at low concentration of $[ATP]$, the contraction is limited by unbinding, whereas at high concentration of $[ATP]$ the needed time spent at strong bound is

determined mainly by ADP release, which is consistent with measurements [120].

5.2 State models of molecular motors

Mathematical models of molecular motors describe mostly their properties on molecular level, i.e. on the scale of nanometers. There is a wide variety of different models. Among the most common approaches belong for instance models based on Langevin equation, Brownian (continuum) ratchets models, Fokker-Planck equation, discrete stochastic models, atom molecular dynamics and state models [74], [125]. Classical Huxley's cross-bridge theory is primarily based namely on *state models*. More concretely, classical Huxley's cross-bridge is two state model.

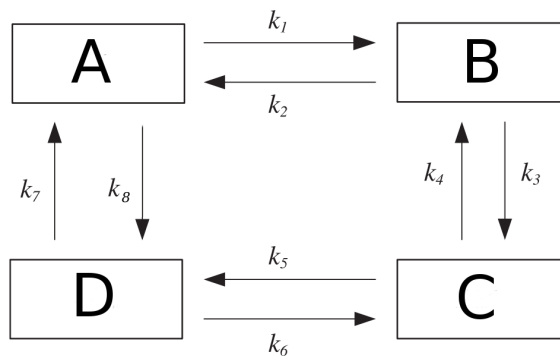


Figure 5.2: Diagram of a four state model with states A, B, C, D and kinetic rates $k_i, i = 1, \dots, 8$.

State models usually facilitate the description of the connection between biochemical cycle and movement of molecular motor. Therefore, these kinds of model are often called mechanochemical models. In general, the term "state" can be any property of molecular motor. The number of states in model depends only on the amount of the studied properties. States models then describe transitions among studied states. Although the transition between two states might behave as "discrete steps", the transitions are often treated as continuous.

The example of a four state model with states A, B, C, D is depicted in picture 5.2. This four state model can be easily described by a set of ordinary differential equations as in equations 5.5, where on the left side are time derivatives of states determined by the matrix of kinetic rates on the right side. The set of equations as 5.5 is often accompanied by the condition of conservation as in this case would be $A + B + C + D = 1$. More about state models can be found in [78], [77].

$$\frac{d}{dt} \begin{Bmatrix} A \\ B \\ C \\ D \end{Bmatrix} = \underbrace{\begin{bmatrix} -k_1 - k_8 & k_2 & 0 & k_7 \\ k_1 & -k_2 - k_3 & k_4 & 0 \\ 0 & k_3 & -k_4 - k_5 & k_6 \\ k_8 & 0 & k_5 & -k_6 - k_7 \end{bmatrix}}_{\text{matrix of kinetic rates}} \begin{Bmatrix} A \\ B \\ C \\ D \end{Bmatrix} \quad (5.5)$$

5.3 Hill's model of the force-velocity relationship

Notwithstanding the Hill's equation is not the main subject in presented work, it is worthwhile to introduce it here with more attention. One of the main reason to introduce here Hill's equation is among the others that the Hill's formula played also its key role, when Huxley has derived his mathematical model of cross-bridge. In particular, Huxley set the kinetic rates f, g in his model according to the results achieved by Hill in his article *The heat of shortening and the dynamic constant of muscle* from year 1938 [44]. Nowadays, it can be shown that these two models are closely related and the values of coefficients affecting the resulted shape of Hill's curve have their origin in actomyosin kinetics as can be seen for example more profoundly in [110].

Hill's model [44] relates force and velocity of isotonic concentric contraction of muscle fibre. Hill's force-relationship describes a steady-state property of muscle during isotonic concentric contraction. The example of force and length evolution during isotonic concentric contraction is depicted in figure 5.3. Hill's model was proposed before the sarcomere structure, i.e. filaments overlap and actomyosin interaction, was known. Therefore, this

type of model is often considered and used as purely empirical without deeper insight into molecular mechanism of muscle contraction.

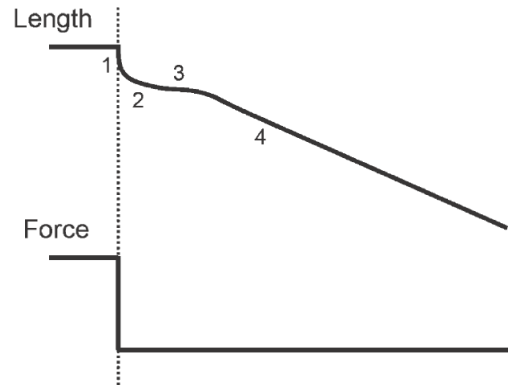


Figure 5.3: Length and force during isotonic contraction, which started from isometric contraction. Time course of the length response to a force step during an isotonic quick release. The shape of phases 1-2-3 is caused by transient behaviour of elastic element in muscle and cross-bridge transient behaviour. The phase 4 is characterized by linear slope during steady-state isotonic shortening. The picture was adapted from [110].

In the end of 1930s, Hill noticed in his experiments that during the *isotonic* contraction of muscle, the relation between *constant contraction velocity* of shortening and the load P (force) is sufficiently expressed by the force-velocity hyperbolic formula [44]:

$$(P + a)(v + b) = (P_0 + a)b = \text{const.}, \quad (5.6)$$

where P is the external load of muscle during isotonic concentric contraction, v is the constant rate of muscle shortening/contraction. Coefficients a and b are constants determined by experimental data. P_0 is maximum force achieved in isometric contraction ($v = 0$). a, b, P_0 coefficients are characteristic for studied type of muscle. Accordingly, the exact curve and the constants of Hill's equation are obtained from curve-fitting of measured force-velocity data. The exact shape of force-velocity relationship is affected by fiber type of a single species and actomyosin kinetics [110]. Further, the constant a was found to match closely to an empirically derived thermal constant of shortening heat [44]. At that

time, the form of Hill's equation impressed astonishingly by its simplicity.

The Hill's equation describes only the part capturing isotonic quick releases in the range of $0 - F_{max}$, where F_{max} (P_0) is maximal isometric force. Before an isotonic quick release, the muscle is activated at fixed length. Therefore, the initial state is isometric contraction. Then the muscle is suddenly released to a lower and constant external load, i.e. isotonic load. After a while and after characteristic transitional changes in velocity, the muscle reaches steady state with steady velocity moving against adjusted known constant external force (see fig. 5.3).

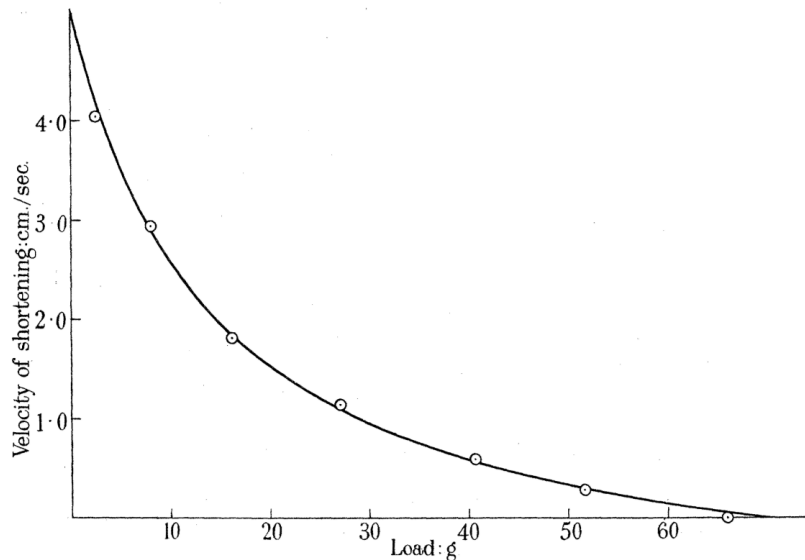


Figure 5.4: Relation between load and speed of shortening in isotonic contraction. The curve is calculated from the equation $(P + 14.35)(v + 1.03) = 87.6$. Hence $a = 14.35$, $b = 1.03\text{cm/sec} = 0.27\text{length/sec}$. The graph with its description is adapted from [44].

Hill's equation at low and high loads At low loads about $5\%F_{max}$, the measured velocities exceeded those predicted by the Hill's hyperbola. And contrary, at the extrapolated zero load, Hill's equation underestimates the value of v_{max} . Further, the Hill's formula does not describe accurately enough the force-velocity relationship for loads greater than 80% of isometric force [110].

To conclude, Hill's equation is still the predominant method used to characterize muscle

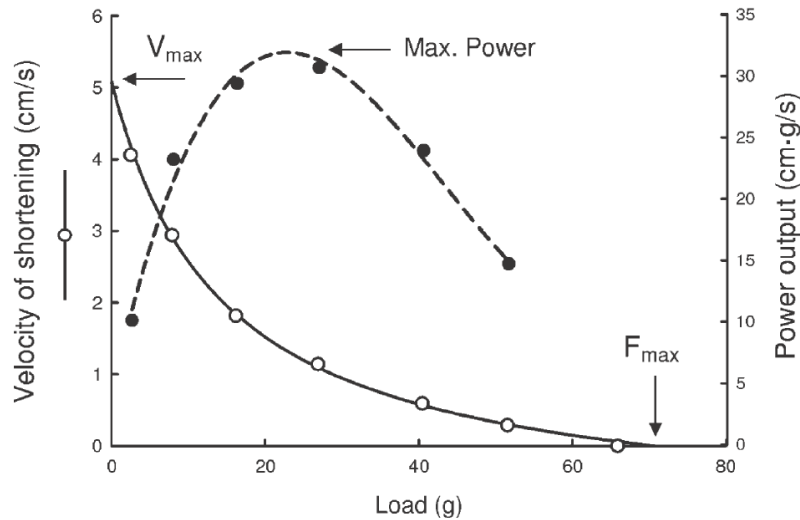


Figure 5.5: The dashed line and closed circles depict power output ($= F \cdot v$) of muscle. The solid line and open circles is force-velocity relationship. The graph is adapted from [110] where it was modified originally from [44].

performance, although it is purely empirical and lacks precision in predicting velocities at high and low loads [110]. Before all, this model captures the muscle property that the muscle shortens faster against light loads than it shortens against the heavy loads. The fact that the muscles shorten rapidly under light load and vice versa was known before Hill's work [10]. Although the Hill's equation was deduced purely out of empirical measurements, interestingly the latest measured data and cross-bridge kinetics gives to this equation meaningful sense [110].

Regardless the discrepancies as noted above, the Hill's equation is still accurate enough to describe the contraction velocities in the force range of $0.05 - 0.8F_{max}$ [110]. The property of muscle that is often searched by Hill's equation is maximum power output of muscle. This maximum lays close to $0.3F_{max}$ [110], which is in the range as noted above. Disadvantage of Hill type of mathematical model is that it does not reflect or connect microstructure of muscle. On the other hand, these type of models are still widely used to describe or simulate behaviour of skeletal muscle as "black box" since the numerical implementation is easier to compare to Huxley model.

In comparison to Huxley's model, the Hill's equation may stay popular till nowadays also because of its relative simplicity. Therefore it is still used to understand the basics of animal locomotion and to design of muscle-powered devices like bicycles [110], [32], where it helps to keep the shortening velocity near the value of the maximal power.

5.4 Huxley's cross-bridge model and Huxley type of models

The 1957 cross-bridge model of muscle contraction proposed by A. F. Huxley was primarily developed to help to explain the molecular origin of muscle contraction. Due to this reason, in comparison with Hill type of models, the models based on Huxley's approach have an advantage of better possibilities of integration of physiological properties on molecular level. Although the 1957 Huxley's theoretical proposals on molecular mechanism of contraction did not have the exact experimental support for next few decades, his work paved the way of muscle research direction. The main ideas of his work persisted till nowadays enriched and supported by actual results from experiments and theoretical proposals.

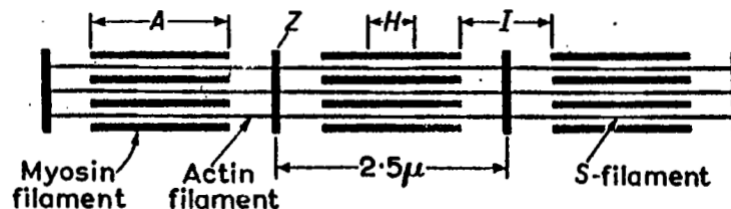


Figure 5.6: Historical diagram showing the arrangement of the filaments, which was suggested during the 1950s. Note that in comparison to recent schemes as in picture 2.3 on page 36 and in picture 4.2 on page 92 the titin filaments are completely missing. Further, the single actin filaments were assumed to connect both Z-lines across sarcomere. The pictures was adapted from Huxley's 1957 article [48].

Since Huxley published his original model in 1957, a lot of modifications of this model were published as reactions on actual state of art in physiology or as proposals on solution of unclear properties of muscle physiology. The importance of original Huxley's article

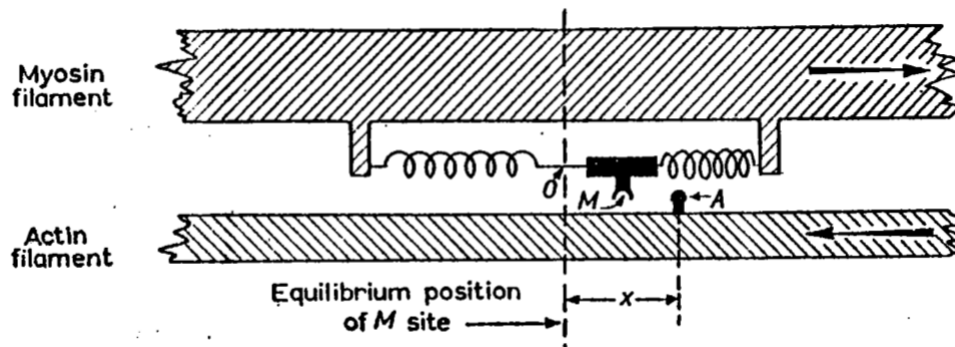


Figure 5.7: Diagram illustrating the mechanism of contraction (tension generation) as suggested by Huxley in 1957 [48]. The part of a fibril which is shown is in the right-hand half of an A band, so that the actin filament is attached to a Z line which is out of the picture to the right. The arrows give the direction of the relative motion between the filaments when the muscle shortens. The picture with its description is adapted from [48].

might be substantiated by the numbers of its citations. Till July 2016, it was 1704 times cited in Scopus or 2272 times cited in Web Of Science databases.

The common assumptions for the Huxley's type of models are [45], [48], [87], [128]:

- the assumption that the cross-bridges are independent force generators,
- the assumption that at any instant of time each cross-bridge has possibility to bind with significant probability (one binding site preferred) only one actin binding site,
- the myosin heads, even on the same myosin molecule (same cross-bridge), do not compete for the same binding site on actin,
- the binding of one head does not affect the kinetics for any transition of another head.

In original Huxley's 1957 paper, Huxley solved and presented results only for steady-states examples of isometric contraction and isotonic concentric contraction with constant velocity. The original Huxley's model as published in his 1957 article has a form as follows [48]:

$$\frac{\partial n}{\partial t} = (1 - n)f - ng \quad (5.7)$$

$$-v \frac{\partial n}{\partial x} = f - (f + g)n, \quad (5.8)$$

where variable n Huxley defined as the proportion (distribution) of all sites at which myosin is combined with the actin with corresponding variable x . The variable x Huxley defined as the position relative to the equilibrium position of myosin site (see figure 5.7). v is the velocity of contraction, where the positive values of contraction represent concentric contraction, zero velocity is isometric contraction and negative values of velocity represents eccentric contraction (stretch). t is obviously time. f and g express kinetic rates of binding respective unbinding of myosins to actin.

Through the literature, the Huxley's definition of variable x defined by word *equilibrium* might lead to confusing interpretation especially on account of the meaning of mechanical equilibrium in classical mechanic. Therefore, to clarify it, let's simply understand the variable x as the displacement of free end of spring from its relaxed state, i.e. as displacement in simple case of force F production described by 1D Hooke's law $F = kx$, where $k(x)$ is the stiffness of considered spring.

The equation 5.7 in Huxley's model represents nothing else than the state model with two states: bound and unbound states of considered cross-bridges. The second equation 5.8 in Huxley's model describes the steady-state form of distribution n of connected cross-bridges with considered value of contraction velocity v . The exact shape of distribution n might be denoted as one of the central points in cross-bridge theory because the shape of distribution n strongly affect the main mechanical properties of muscles.

Probably more famous form of Huxley's equation describing the distribution n is the equation in a form:

$$\frac{\partial n(x, t)}{\partial t} - v(t) \frac{\partial n(x, t)}{\partial x} = f(x)(1 - n(x, t)) - g(x)n(x, t). \quad (5.9)$$

This equation allows to simulate also transient states of muscle contraction. The source of this equation is again referred as the original Huxley's 1957 article [48] although the equation in this form is not presented in original Huxley's 1957 paper since Huxley considered (probably) only steady-state of muscle contraction as already mentioned above. On the other hand, the relation between equation 5.9 and equations 5.7, 5.8 is straightforward since in particular equation 5.8 express steady-state form of equation 5.9. Further, the equation 5.7 describes the time evolution of n distribution in a case of isometric contraction, i.e. in a case where $v = 0$.

On account of the mathematical forms of kinetic rates f, g , Huxley has chosen the kinetic rates of binding/unbinding rates to fit the experimental data of concentric contraction as measured by Hill in 1938 on myofibrils. The rates $f(x), g(x)$ then have forms as follows [48]:

$$f(x) = \begin{cases} 0 & -\infty < x < 0, \\ f_1 \frac{x}{h} & 0 < x < h, \\ 0 & h < x < \infty, \end{cases} \quad (5.10)$$

$$g(x) = \begin{cases} g_2 & -\infty < x < 0, \\ g_1 \frac{x}{h} & 0 < x < \infty, \end{cases} \quad (5.11)$$

where h represents the largest cross-bridge lengths at which a single myosin molecule can bind to an actin [48]. f_1, g_1, g_2 are constants. Depicted rates can be seen in figure 5.8. The meaning of the rates regarding the physiology might be expressed as the cross-bridges can bind only in range $x \in [0, h]$ with binding rate $f(x)$. Theoretically, once the cross-bridge is attached, its displacement x may change also to the values outside interval $[0, h]$ due to the contractile activity. Therefore and for mathematical convenience the unbound rate $g(x)$ is defined in interval $(-\infty, \infty)$. The increase of unbound rate defined by $g_2 \gg g_1$ has a meaning of rapid unbound to prevent the force production in reverse direction. Note, that

according to rates as defined by Huxley, it was not assumed that cross-bridge can not bind with zero displacement x .

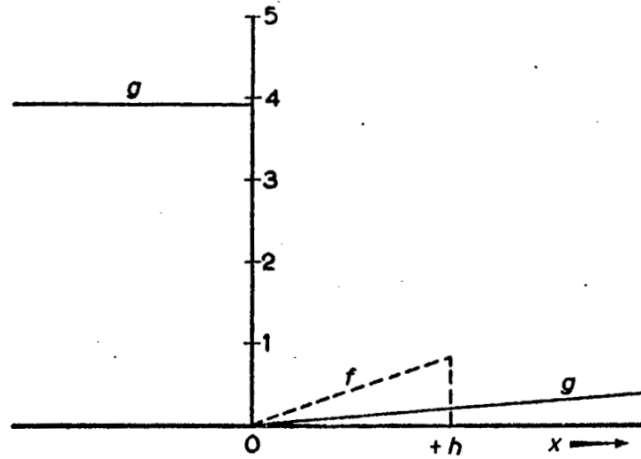


Figure 5.8: The shapes of kinetic rates: f - bounding rate, g unbinding rate as proposed by Huxley in [48].

Based on the defined cross-bridge distribution $n(x, t)$, Huxley derived the tension (force) production by muscle in a form [48]:

$$P = \frac{msk}{2l} \int_{-\infty}^{\infty} n(x, t)x dx, \tag{5.12}$$

where P is the tension (force) in muscle, m is the number of attached cross-bridges per cubic centimetre, l is the distance among binding sites on actin filaments. k is the stiffness of cross-bridge. s is the sarcomere length.

Further important relationship in cross-bridge theory is description of muscle energetics. The total rate of energy liberation, E , per cubic centimetre of muscle Huxley expressed as [48]:

$$E = \frac{me}{l} \int_{-\infty}^{\infty} f(x)(1 - n(x, t))dx, \tag{5.13}$$

where e is liberated energy per one site per one cross-bridge conformation cycle.

5.4.1 Common modifications of Huxley's model

Through the decades till now, the original Huxley's model was modified and improved in many ways. There can be found hundreds of articles since Huxley published his original work. It should be hard to summarize these results, but some of the modification appear more often than others.

The first common modification is related to the number of myosin head states. As demonstrated for example in [15], [16], more than two important states of myosin heads can be found through the myosin head working cycle. Therefore, one of the most common way of improvement is to take into account another states of myosin heads. This results to the expansion of the original Huxley's description of evolution of distribution n about another equations representing further considered states. This extension can be in general described by the set of equations in forms:

$$\frac{\partial n_i}{\partial t} - v(t) \frac{\partial n_i}{\partial x} = \sum_{j=1, j \neq i}^N f_{ji}(x) n_j - \sum_{j=1, j \neq i}^N f_{ij}(x) n_i, \quad (5.14)$$

$$\sum_i^N n_i = 1, \quad (5.15)$$

where n_i represents the distribution of the i -th state. f_{ij} represents the rate parameters of transition from i to j state. N is the number of studied states.

Another way of improvement can be determined by various physiological, physical, chemical restriction or thermodynamic restriction. These modification usually lead to special shapes of kinetic rates. As an example can be shown the modification with partial derivation of kinetic rates as used in [45]:

$$\frac{\partial n}{\partial t} - v(t) \frac{\partial n}{\partial x} = [f(x) + g'(x)](1 - n) - [g(x) + f'(x)]n \quad (5.16)$$

The next common modification is also to deal with Huxley equation as with material derivation:

$$\frac{Dn}{Dt} = \frac{\partial n}{\partial t} + v \frac{\partial n}{\partial x} \quad (5.17)$$

5.4.2 Results of Huxley's model

The results of Huxley's pioneering work are depicted in figures 5.9 and 5.10.

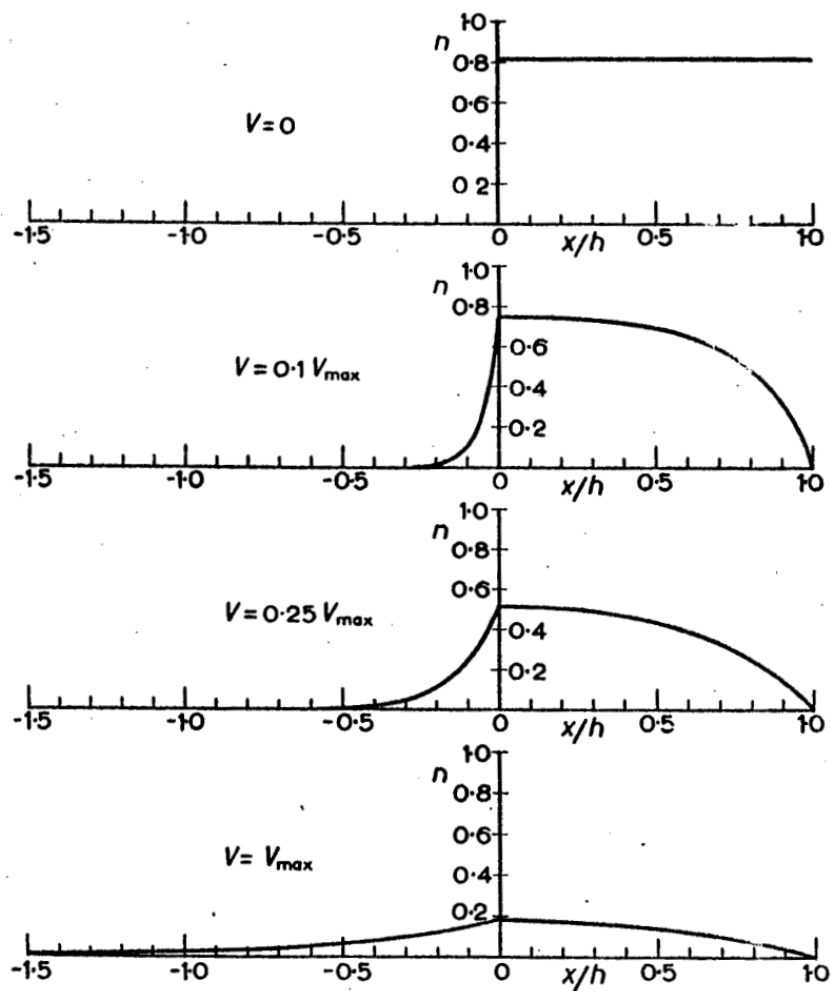


Figure 5.9: Results for Huxley's 1957 n distribution for various values of velocity v . The top part shows the distribution for $v = 0$, i.e. for isometric contraction. Adapted from [48].

The figure 5.9 shows the shapes of distribution during concentric contraction. The graph in top part depicts distribution for isometric case. The rest of graphs in figure 5.9 depicts the shape of distribution n for various magnitudes of velocity during concentric contraction.

The results in figure 5.10 compare the tension (force) of muscle during isotonic concentric contraction obtained from Huxley's model with results obtained by Hill's equation.

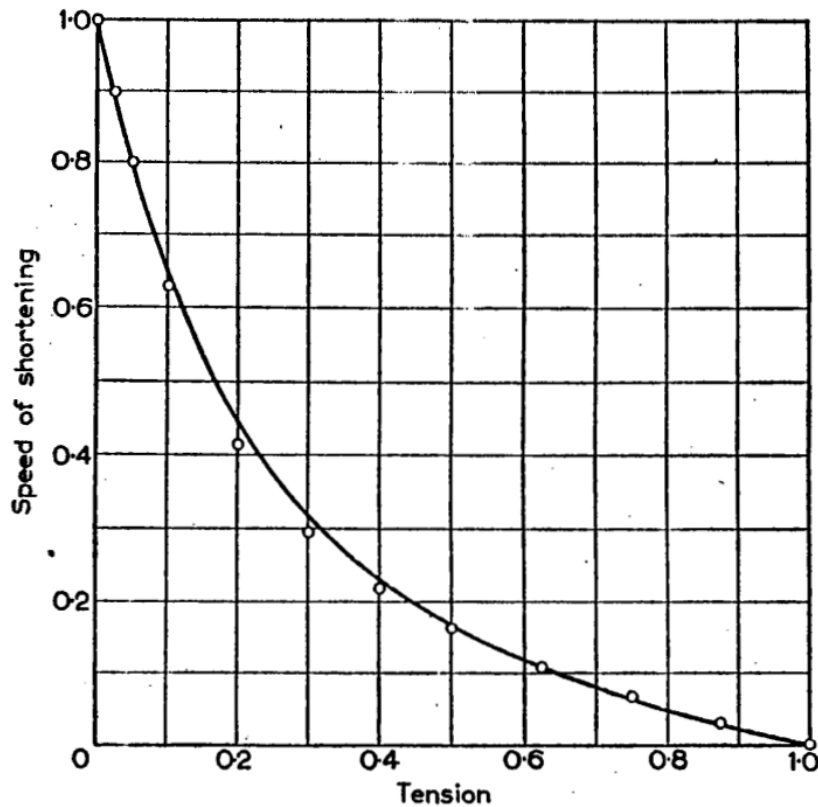


Figure 5.10: Huxley's model comparison to Hill's model as published in [48]. The continuous line is Hill's model. The circles are results of Huxley's model. The graph depicts results of concentric isotonic contraction.

5.4.3 Conclusion on Huxley's type of models

To conclude on Huxley type of models, it can be stated that these models more or less succeeded in the description of concentric contraction and isometric contraction including

main mechanical and energetic properties of skeletal and heart muscle. Huxley's type of models have great potential to sufficiently describe the molecular origin of mechanical processes at nanometres-scale and projects it up to micrometers-meters scale.

Till nowadays, the main problem of classical Huxley's model is the description of history-dependent properties of contraction. Namely it has a problem to sufficiently explain history-dependent properties as phenomena called force enhancement following after eccentric contraction and phenomena called force depression followed after concentric contraction.

5.5 Zahalak's Distribution Moment Model

Zahalak's model is based on classical Huxley's cross-bridge theory with two sliding filaments. His model, developed during 1980s, was proposed to better describe a response on muscle stretch (eccentric contraction). Among the main aims of his work was also to simplify the numerical solution of original Huxley's model consisting of partial differential equation(s) by the approximation of ordinary differential equations [128].

But still, it is worth to notice that Zahalak's model considered only two main filaments. The third the most abundant protein titin in sarcomere is in Zahalak's model still neglected due to the fact that the role of the titin in sarcomere was not exactly known in 1980s. In any case, this model is till nowadays one of the most successful in description of the eccentric contraction, which is the main reason to introduce here this model. Even though this model is widely used to successfully describe or simulate eccentric contraction, it does not explain the eccentric contraction sufficiently. Also, this model still considers linear elasticity of cross-bridges, even Zahalak mentioned the possible use of non-linear elasticity in [129]. Again, the exact non-linear elasticity properties of single cross-bridges were not known in 1980s.

The detailed derivation of Zahalak's distribution-moment model is in-depth introduced in [128]. In the following lines are presented the basic ideas of Zahalak's model. For better insight into this model, the texts [128], [129], [130], [132], [131] contain more detailed

information. In brief, the first pivotal proposal of original distribution-moment model as derived in [128] was an introduction of distribution-moments of Huxley's distribution $n(x, t)$ in a form:

$$M_\lambda(t) = \int_{-\infty}^{\infty} x^\lambda n(x, t) dx, \quad (5.18)$$

$$b_\lambda = \int_{-\infty}^{\infty} x^\lambda f(x) dx, \quad (5.19)$$

where M_λ is λ -th moment of bond-distribution $n(x, t)$ and b_λ is λ -th moment of bonding rate function for $\lambda = 0, 1, 2, \dots$. The second pivotal step in Zahalak's model is the approximation of Huxley's distribution $n(x, t)$ in a form of Gaussian distribution [128]:

$$n(x, t) \approx \frac{M_0(t)}{\sqrt{2\pi}\sigma(t)} e^{-\frac{[x-\mu(t)]^2}{2\sigma^2(t)}}, \quad (5.20)$$

where

$$\mu(t) = \frac{M_1(t)}{M_0(t)}, \quad (5.21)$$

$$\sigma(t) = \sqrt{\left\{ \frac{M_2(t)}{M_0(t)} - \left[\frac{M_1(t)}{M_0(t)} \right]^2 \right\}}. \quad (5.22)$$

After specific modification as in [128], the values of first three distribution-moments M_λ might be described by the set of ordinary differential equations:

$$\frac{dM_0}{dt} = b_0 - F_0(M_0, M_1, M_2), \quad (5.23)$$

$$\frac{dM_1}{dt} = b_1 - F_1(M_0, M_1, M_2) - v(t)M_0, \quad (5.24)$$

$$\frac{dM_2}{dt} = b_2 - F_2(M_0, M_1, M_2) - 2v(t)M_1, \quad (5.25)$$

where the exact forms of the functions F_1, F_2, F_3 depend on the forms of rate functions f, g and approximate form of $n(x, t)$ [128]. $v(t)$ represents the velocity of contraction.

Zahalak's Distribution-Moment model With the respect to proposed shape of $n(x, t)$ and the shapes of the kinetic rates in the forms [128]:

$$f(x) = \begin{cases} 0 & -\infty < x < 0, \\ f_1(\frac{x}{h}) & 0 < x < h, \\ 0 & h < x < \infty, \end{cases} \quad (5.26)$$

$$g(x) = \begin{cases} g_2 & -\infty < x < 0, \\ g_1(\frac{x}{h}) & 0 < x < h, \\ g_1(\frac{x}{h}) + g_3(\frac{x}{h} - 1) & h < x < \infty, \end{cases} \quad (5.27)$$

the final form of the set of the three ordinary differential equations might be written as [128], [129]:

$$\frac{dM_\lambda}{dt} = \beta_\lambda - \phi_\lambda - \lambda u(t)M_{\lambda-1}, \quad \lambda = 0, 1, 2, \dots \quad (5.28)$$

where M_{-1} is defined to be zero and

$$u = \frac{v}{h} \quad (5.29)$$

$$\xi = \frac{x}{h} \quad (5.30)$$

$$\beta_\lambda = \int_{-\infty}^{\infty} \xi^\lambda f(\xi) d\xi \quad (5.31)$$

$$\phi_\lambda = \int_{-\infty}^{\infty} \xi^\lambda [f(\xi) + g(\xi)] n(\xi, t) d\xi \quad (5.32)$$

$$n(\xi, t) \approx \frac{M_0(t)}{\sqrt{2\pi q(t)}} e^{-\frac{[\xi - p(t)]^2}{2q^2(t)}} \quad (5.33)$$

$$p(M_0, M_1) = \frac{M_1}{M_0} \quad (5.34)$$

$$q(M_0, M_1, M_2) = \sqrt{(M_2/M_0) - (M_1/M_0)^2} \quad (5.35)$$

In this approach M_λ , where $\lambda = 0, 1, 2$, have a following meanings [129]:

1. M_0 is proportional to the instantaneous stiffness of the contractile mechanism,
2. M_1 is proportional to the instantaneous force generated by the muscle,
3. M_2 is proportional to the total elastic energy instantaneously stored in the cross-bridges.

The results of distribution-moment model depicting the response of muscle on stretch is depicted in figure 5.11 as published in [128]. For comparison with measured data see figure 2.16 on page 50, figure 2.17 on page 51, figure 2.18 on page 51 and figure 2.19 on page 52.

To conclude on distribution-moment approximation of Huxley's model, lets cite here Zahalak [128]: *"The distribution moment approximation is, of course, no substitute for the full partial differential equations in cases where detailed and precise calculations of the complete kinetics model response are necessary."* From this citation is obvious that even the distribution-moment model claims good reputation on description of muscle contraction including eccentric contraction, it is still not the most appropriate model.

5.6 Mathematical Models of Titin

5.6.1 Worm-like-chain model

Worm-like chain model (WLC) is the most often used mathematical model as a force-length relationship for description of the titin filaments as well as for another proteins as DNA for example. The WLC model describes the molecule as a deformable continuum. Worm-like chain model describes purely elastic properties of titin in stretch. This model was

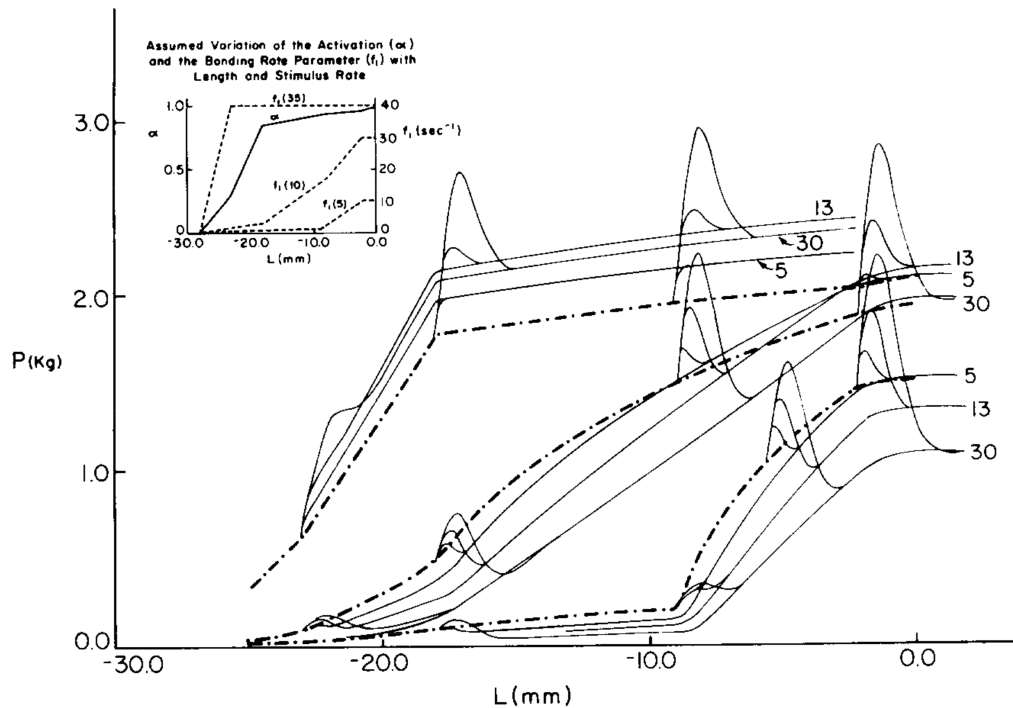


Figure 5.11: Results of Zahalak's distribution model as published in [128]. The picture depicts tension-length for a muscle subjected to constant-velocity stretches starting from isometric states corresponding to various initial lengths and stimulus rates. The interrupted curves represents isometric force of various activation. The thin curves are stretches labelled with corresponding velocities in $mm s^{-1}$.

successfully used to describe the bunch of filaments as well as single filaments (molecules) and as well as a single parts of titin molecule - for instance chain comprising just of a few Ig-domains [67], [64], [66], [17].

Worm-like-chain model was derived in a form [9], [84]:

$$F = \frac{k_B T}{A} \left(\frac{z}{L} + \frac{1}{4(1 - \frac{z}{L})^2} - \frac{1}{4} \right), \quad (5.36)$$

where F is the entropic restoring force, A is apparent persistence, L is chain's contour length, z is shortest end-to-end length among ends of chain ($z \in [0, L)$). k_B is the Boltz-

mann constant and T is absolute temperature. $\frac{z}{L}$ is the fractional extension of studied chain.

Through the literature, the definition of the quantity of persistence length A might be confusing. Sometimes, the persistence length is even wrongly mixed up with the quantity of stiffness. Therefore, for better comprehension of this quantity, lets cite here some definitions from literature:

- Persistence length is a measure of the bending rigidity of the chain [67].
- Persistence length is a measure of the distance over which the polymer retains memory of a direction [11].

The values of persistence length are of the size of a single amino acid [11]. For example, the mechanical data suggest that the apparent overall persistence length of full-length titin may be up to 1.5 nm . Fitting the WLC model to measured force-extension curve gives persistence length of I27 domain $A = 0.39 \pm 0.07 \text{ nm}$ [11]. The persistence length of PEVK varies in wide range $0.3 - 2.1 \text{ nm}$ [31] with mean value around 1.5 nm [31].

5.6.2 Unfolding and refolding of proteins

The biggest challenge in modelling of titin in sarcomere is the description of the dynamic of the Ig-domains unfolding and other titin's part unfolding. Further challenge is to connect this unfolding description with WLC model or another model describing mechanical properties of titin. The unfolding of titin's parts leads to the increase of contour length L of a chain which is followed by the decrease of force. The contour length increment ΔL , after Ig-domain unfolded, was measured as $\Delta L = 28.4 \pm 0.3 \text{ nm}$ [11].

Although some models of unfolding already exist for example based on energetics or probability approach, still no sufficient model exists (was not found in literature). In the most majority of cases, the unfolding of protein is simulated by Monte-Carlo simulation (for instance [11], [85]).

In trivial cases, the easiest way to model the titin's force decay during the stretch might be also modelled by exponential function as for example used in [85]:

$$F(t) = F_0 + A_1 e^{-\frac{t-t_0}{t_1}} + A_2 e^{-\frac{t-t_0}{t_2}} + A_3 e^{-\frac{t-t_0}{t_3}}, \quad (5.37)$$

where A_i are decay amplitudes, t is time, t_i are time constant.

Two state models - folded and unfolded states

According to [11], the increase or decrease in the number of unfolding and refolding states can be modelled as two-state Markovian process with folding rate k_f and unfolding rate k_u . These rates can be determined by the activation energies ΔG and reaction lengths Δx :

$$k_u(F) = \omega e^{\frac{-(\Delta G_u - F\Delta x_u)}{k_B T}}, \quad (5.38)$$

$$k_f(F) = \omega e^{\frac{-(\Delta G_f + F\Delta x_f)}{k_B T}}, \quad (5.39)$$

where ω is the natural frequency of oscillation and Δx is the distance of the reaction length over which the force must be applied to reach the transition state. F is external force. k_B is Boltzmann constant and T absolute temperature.

The formulas of kinetic rates k_u, k_f noted above have origin in Bell's [7] and Evans' [22] works. Based on these articles, the number of unfolding/folding domains might be simulated by mathematical formula [7], [22], [65], [117]:

$$dN = N\omega_0 e^{-\frac{E_a - F\Delta x}{k_B T}} dt, \quad (5.40)$$

where dN is the number of broken bonds or domains unfolded/ folded during the dt polling interval, N is the number of available bonds or folded domains. Δx is the distance along the unfolding/folding occurs, ω_0 is constant called attempt frequency or natural vibration frequency [22] with value $\omega_0 = 10^8 s^{-1}$ [7], F is the external force, E_a is the activation

energy for unfolding (energy barrier of bond [22]), T is absolute temperature and k_B is Boltzmann constant.

As the examples of the magnitude of the values of quantities defined above, the value of $E_a = 28pNnm$ was used in [65] for modelling of unfolding of 70 globular domain and 760– nm pre-unfolded segment analogous to skeletal muscle PEVK segment. For re-folding the value of E_a was set to $82pN nm$ [117]. The value of product of $k_B T$ was in [117] set to $4.14pNnm$. The value of Δx for unfolding was in [117] set to $0.28nm$ for the case of unfolding and $8nm$ in the case of re-folding.

Although this model has a strong physical background with aim of reflecting the bound force of molecules etc., in the comparison with experiments is often still "only fitted" by adjusting of variables noted above. The values of mentioned model variables varies through the literature. As can be seen for example [117], where the variables E_a and Δx are considered as "user-adjustable".

Refolding To complete the brief overview of folding/unfolding models, the refolding of Ig domains might be well described also by equation [11]:

$$\frac{N_{refolded}}{N_{total}} = 1 - e^{-tk_f^0}, \quad (5.41)$$

where k_f^0 corresponds to refolding rate under zero applied force.

5.6.3 Three filament model - stochastic model of IG domain unfolding

The first simulations and model considering three filament model was published in [108]. In this text [108], the Huxley's theory was extended with WLC model, where the unfolding/folding of titin IG domains was realized by proposed stochastic function and WLC parameters as contour length and persistence length were changed according to.

Stochastic model for the length of a half sarcomere was proposed in a form [108]:

$$HSL = N_u^{prox} l_u^{prox} + (N^{prox} - N_u^{prox}) l_f^{prox} + l^{PEVK} + l^{dist} + d, \quad (5.42)$$

where l_u^{prox} is the length of unfolded proximal IG domain, l_f^{prox} is the length of folded proximal IG domain. N_u^{prox} is the discrete random variable N_u^{prox} characterizing the unfolding process of the number of proximal IG domains. The parameter d represents half of the A-band length. l^{PEVK} is the length of the PEVK region. l^{dist} is the length of the inextensible end filaments. The computation of unfolding process using the equation 5.42 was realized by Monte-Carlo simulation.

The results of eccentric contraction simulations achieved by this approach can be seen in figure 5.12 as published in [108]. The results depict the simulation of sarcomere stretch from initial length of $2.4\mu m$ to final length of $3\mu m$. In figure 5.12, the resulting force is normalized to the corresponding isometric force at $3\mu m$. In mentioned text, the simulation was conducted for velocity of $100nm s^{-1}$ per sarcomere. For comparison with measured data see figure 2.16 on page 50, figure 2.17 on page 51, figure 2.18 on page 51 and figure 2.19 on page 52.

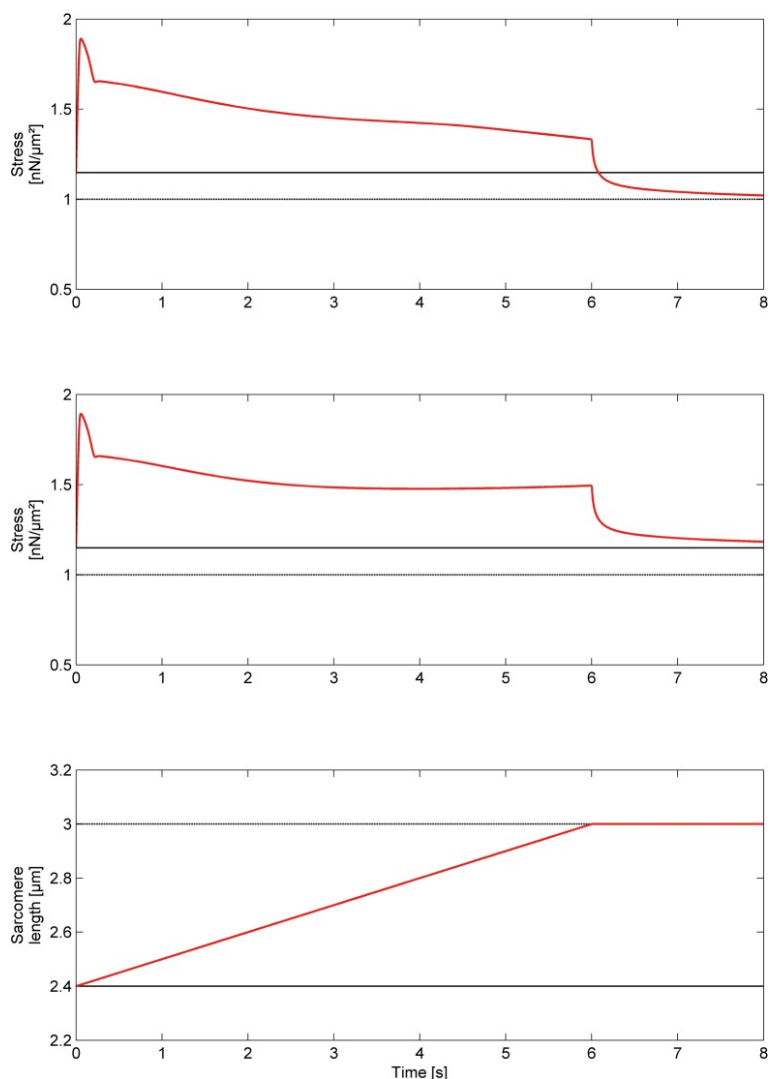



Figure 5.12: The results of eccentric contraction simulation as achieved with stochastic function as presented in [108]. The top panel depicts the forces from regular cross-bridge as simulated in [108]. The second panel depicts results considering three filaments. The last panel depict corresponding length of sarcomere. For comparison with measured data see figure 2.16 on page 50, figure 2.17 on page 51, figure 2.18 on page 51 and figure 2.19 on page 52.

 **Quick summary of chapter**

The most successful theoretical models explaining sarcomere (muscle) contraction are based on cross-bridge theory and two-sliding-filaments theory. The first mathematical model was proposed by A.F. Huxley in 1957. Since then, his model was modified in many ways to incorporate actual data arising from experiments and theoretical proposals during years. Up to now, the mathematical models based on classical Huxley's model more or less succeeded in description of concentric and isometric contraction.

Till nowadays, some phenomenons of muscle contraction are still not sufficiently explained based on cross-bridge theory and Huxley's model. These phenomenons are namely history-dependent properties of contraction as force decrease following after concentric contraction and force enhancement following after eccentric contraction and eccentric contraction itself. Although some models were proposed regarding noted problems, none of them was widely accepted as universal tool.

Recent experiments suggested that the role of the third structural protein of sarcomere, titin, might play more important role than originally thought in cross-bridge theory. These experiments also suggested the way and hint, which way the original cross-bridge theory and its mathematical model could be successfully enhanced.

Chapter 6

Proposed Three Filament Cross-Bridge Model

In the following lines, modified cross-bridge model was derived from scratch based on the summary in preceding introductory chapters. The main aims were to relate the active force production to the degree of actin-myosin overlap rather than to the sarcomere length as in classical cross-bridge theory. Further pivotal aim was to embody the non-linear elastic properties of single cross-bridges as measured in [62], [63] into the model. On account of this modification, the goal was also to include the "buckled" cross-bridges, which are attached to actin filaments but produce rather passive force than active force. One of the crucial and important intended modification was also that the classical cross-bridge theory was extended about titin properties as suggested in [40] (see figures 6.1 on page 132 and 4.7 on page 102).

6.1 Derivation of the Three Filament Cross-bridge Model

In the following text, the derivation of the model was related predominantly to the half-sarcomere level due to the fact that the sarcomere is symmetric. Nevertheless, the consid-

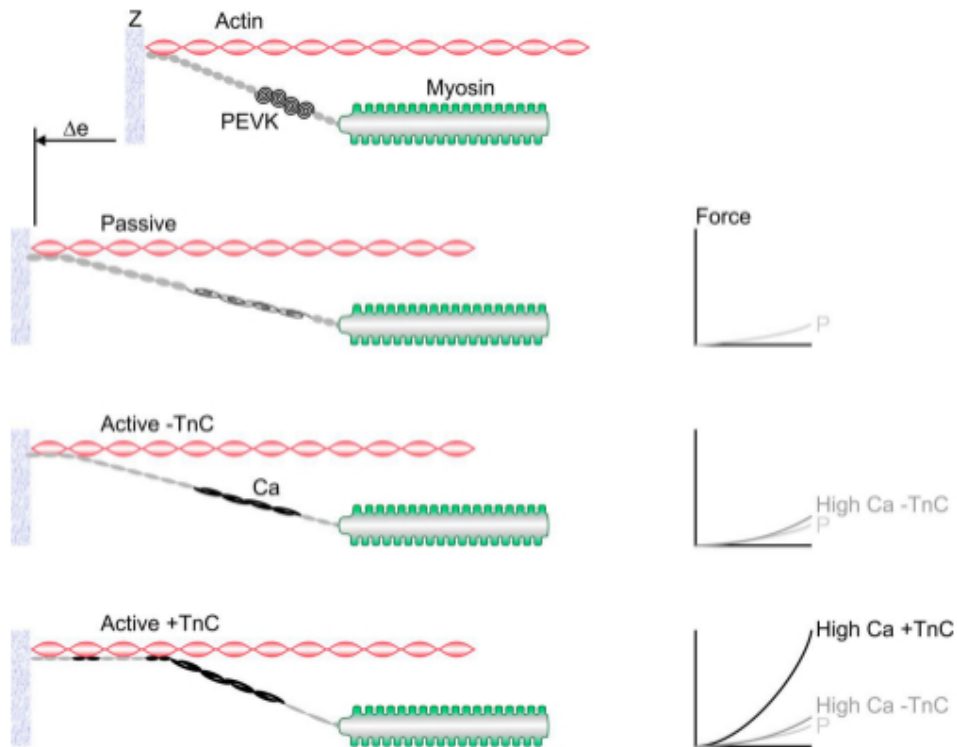


Figure 6.1: Conceptual model of titin's force regulation during eccentric contraction as proposed and published in [40]. Nowadays experimental research indicate that titin actively bind to actin and further titin increase its stiffness in the presence of calcium ions. Both of these new emerging properties give to the titin more important role than originally thought in classical cross-bridge theory.

eration of the whole sarcomere does not change the resulted mathematical model.

The main aim was to derive the mathematical model according to the cross-bridge theory, where the sarcomere is able to produce the force F_S . F_S denotes the force, which is the half-sarcomere able to develop on Z-line. It is assumed that force F_S is the sum of active force F_{CB} and passive force F_T . F_{CB} expresses the force, which is produced as a result of power-strokes of cyclically binding/unbinding cross-bridges and consequent shift of actin filaments in actin-myosin overlap. This force is also considered to include the forces emerging due to buckled/bended states of cross-bridges. F_T denotes the force, which is produced by bunch of titin filaments upon stretch. Derived model takes into account only active state of sarcomere. Therefore, titins are considered to be bounded to

actin as described in preceding chapters and depicted in figure 6.1. Force F_S produced by half-sarcomere can be then expressed as:

$$F_S = F_{CB} + F_T. \quad (6.1)$$

Forces F_S as well as F_{CB} and F_T are supposed to be perpendicular to Z-line. Directions of these forces are in the direction to the centre of sarcomere. Further, it can be introduced the external force F_E , which denotes the sum of the external forces acting on the same Z-line as the half-sarcomere force F_S . Forces F_S and F_E lie in one line, but these forces have opposite direction. Under assumptions noted above, three main types of contraction are traditionally stated regarding to the sarcomere contractile activity:

1. $F_S > F_E$ *concentric contraction* \Rightarrow shortening of the sarcomere.
2. $F_S = F_E$ *isometric contraction* \Rightarrow sarcomere develops the same amount of force as external force, no contraction/stretching of sarcomere occurs.
3. $F_S < F_E$ *eccentric contraction* \Rightarrow the sarcomere undergoes the stretching done by external force, which is higher than the mechanisms in sarcomere are able to exert.

6.1.1 Active force: force F_{CB} generated by cross-bridges in actin-myosin overlap

To describe the active force sufficiently, two levels of active force production had to be considered; at first, the properties of single cross-bridge force production, secondly, the properties of the force production exerted by the ensemble of cross-bridges. For the simplicity, it is assumed here that the stiffness of actin filaments is much higher than the stiffness of the ensemble of cross-bridges. Therefore, the consideration on actin elasticity can be neglected. This is also one of the standard simplifications of cross-bridge models.

Single cross-bridge mechanics

To describe the mechanical properties of single cross-bridge, the variable x is introduced. In comparison to classical Huxley's model, the variable x is here defined in little bit different manner. In the following text, x represents the shortest end-to-end distance between two ends of single cross-bridge. The first considered end is the end by which the cross-bridge is attached at myosin filament. The second end is the end of the cross-bridge which is able to attach at actin filaments.

When cross-bridge is fully stretched, the end-to-end variable x equals to the contour length of single cross-bridge. It might be to worth to notice that the contour length and therefore x as well are considered to be increased, when the cross-bridge is stretched. In comparison to classical cross-bridge model, the variable of x as defined above allows to include the force achieved by power-stroke and stretch of cross-bridges during contractile activity as in Huxley's model. In addition, it allows also to include the force produced by buckled or bended cross-bridges (see figure 3.13 on page 80).

Further, let's denote the force produced by single cross-bridge as $f_{cb} = f_{cb}(x)$. It is assumed here that $f_{cb}(x)$ expresses the force- x relationship of a single cross-bridge according to the experimental results presented in [62], [63], [90] and as depicted here in figure 6.2.

Since the single cross-bridge can be also oriented in the direction in which it produces the force against the direction of concentric contraction, the variable x must be further specified on account of its sign. Therefore, let's assume that in case where two ends of cross-bridge are one above the other, it is assumed here that $x = 0$. Further, it is assumed here that if the cross-bridge is in the wrong direction and therefore exerts the force against the direction to sarcomere's shortening, the value of end-to-end distance is $x < 0$. The most important values of end-to-end distance for contraction are when $x > 0$. In this case it is assumed here that the cross-bridge is oriented in the right way to produce force according to the sense of sarcomere shortening. In this case cross-bridge with $x > 0$ produces force in the direction to the centre of sarcomere.

To particularize the force $f_{cb}(x)$ production of cross-bridges with concrete values of x , it

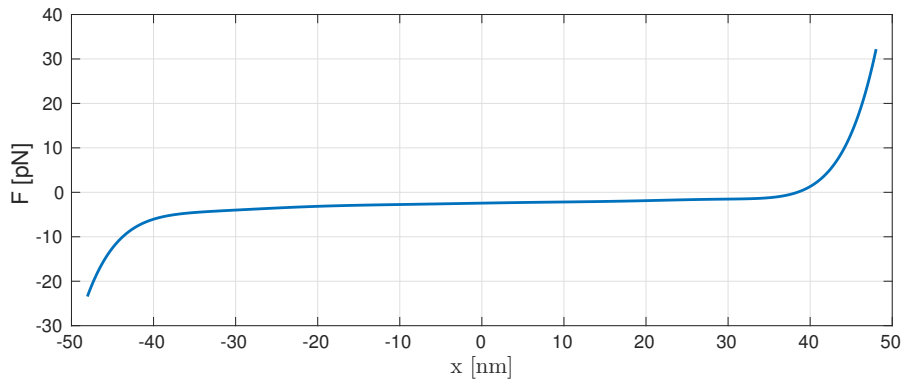


Figure 6.2: Force- x end-to-end relationship of single cross-bridge. In comparison to original measured data as published in [62], [63] the x -axis was moved according to the length of S2 part of cross-bridge. This modification allowed to use the end-to-end distance of cross-bridge's ends (compare with figures 3.13 and 3.14 on page 80).

is worth to state here another important assumption. At first, it is not assumed here that the cross-bridge with $x < 0$ can stretch its elastic element by the power-stroke against the shortening and this way produce the force against the direction of concentric contraction. But it is assumed here that single cross-bridge can produce the force in opposite direction to shortening by its buckled/bended state according to its force- x relationship (see fig. 6.2). Therefore, in this case, the elastic element of cross-bridge is not stretched once the cross-bridge gets attach. But is it considered here that the elastic element of cross-bridge with $x < 0$ can be stretched due to contractile activity namely by fast concentric contraction. On account of this, likely more probable situation is that the cross-bridge detaches before this situation can occur.

Further, the buckled/bended state of cross-bridge can be understand as the cross-bridge got attached with smaller distance x than its contour length. In this case the cross-bridge also undergoes power-stroke, but this power stroke can not contribute to active force generation because its elastic element was not stretched. A result in this case is only passive force due to cross-bridge's buckled state. This force acts against the mechanism of shortening as measured in [62], [63]. It is worth to notice also that it is thought here that even though buckled/bended cross-bridges can not contribute to active force, they

still consume ATP during their cycle.

Once the contour length of cross-bridge is the same as x end-to-end distance, the cross-bridge contributes to active force production by the stretch of its elastic element. According to figure 6.2, the cross-bridge starts to contribute to active force once its x end-to-end distance is approximately higher than $38 - 40[nm]$, which is approximately the length of its S2 part [62]. When the attached cross-bridge after power-stroke has the same distance as $38 - 40[nm]$, it is no more buckled, but its elastic element is still not stretched. In this case, the cross-bridge produce zero force - after power stroke it is just fully stretched.

Huxley's interval h : Further, to describe the binding properties of single cross-bridge sufficiently, two constants a, b must be introduced:

1. a is the maximal x end-to-end distance after the power-stroke by which the cross-bridge can be found in wrong (opposite) direction acting against the concentric contraction. Under assumptions as noted above $a < 0$.
2. b expresses the maximal x end-to-end distance after power-stroke by which the cross-bridge can be found in the right direction according to sarcomere active force production. Under assumption as noted above $b > 0$.

After an introduction of parameters a and b , another important parameter (interval) h can be introduced:

$$h = (a, b). \tag{6.2}$$

Interval h (Huxley's h parameter [48]) is the range of end-to-end distances $x \in h$ by which the single attached cross-bridge can be found immediately after power-stroke. The single cross-bridge with x distance outside of interval h can be found only due to contractile activity during concentric and eccentric contraction. In these cases x distance might be changed due to contractile activity when cross-bridge was already attached. In the case of isometric contraction, the distance x is not thought to be found outside of interval h . The

important thing is that during cross-bridge's working cycle, once the single cross-bridge detaches during any kind of contraction, it can rebind again only with x distance within interval h .

Based on these assumptions, theoretically and for the simplicity, the range of distances x is $(-\infty, \infty)$ with condition that immediately after power-stroke the values of x can be located only inside interval h . Whereas when the cross-bridge detaches, then it can be found theoretically with arbitrary value of x end-to-end distance $x \in (-\infty, \infty)$. The value of $x = x_0$ in case where the cross-bridge is only fully stretched but produces no force, i.e. $f_{cb}(x_0) = 0$, lies also inside h .

The exact values of parameters a, b might be the subject of discussion. But at least the value of b might be estimated based on the information noted in introductory chapters. Under assumption that in the case of x_0 which satisfies $f_{cb}(x_0) = 0$ and under assumption that the magnitude of power-stroke d_w is constant, the value of parameter b might be estimated as:

$$b = x_0 + d_w. \quad (6.3)$$

Hence, in the case $x = b$ the elastic element of cross-bridge is at maximal stretch exerting maximal force $f_{cb}(b)$ due to power-stroke activity. The values $x > b$ can be achieved only by external forces during eccentric contraction.

The exact value of a is hard to estimate. In literature might be found that sarcomere during activity contains cross-bridges in buckled state, but it is hard to propose any value of a based on these information. For simplicity, let's assume here that maximal possible value of $|a|$ equals to the contour length of S2, i.e. parameter a has approximately value of $-40nm$. The attach of single cross-bridge at $x = a$ is though to be here highly improbable but possible.

Single cross-bridge states: Further in this text, the attached cross-bridge with particular x end-to-end distance is assumed to be after power stroke, still attached and producing

force according to its force- x relationship. This presumption allows to use only two states model with attached and unattached states of cross-bridges. Although it is known that during the working cycle the cross-bridge undergoes a few of states, for simplicity it is considered here just two-state model. The model can be easily extended to capture more states as in equations 5.14 on page 117. It might be worthwhile to notice that in the case of addition of another bounded states as for example pre-power-stroke weak bound state, the range of particular intervals h must be adjusted to the length of cross-bridge according to considered state.

Two states mentioned here represent two states of myosin cross-bridge as follows:

1. N_{ux} unattached free cross-bridge before any conformation changes and before any activity,
2. N_{ax} attached strongly bound cross-bridge after power-stroke with its particular x end-to-end distance producing force according to its force- x end-to-end distance relationship.

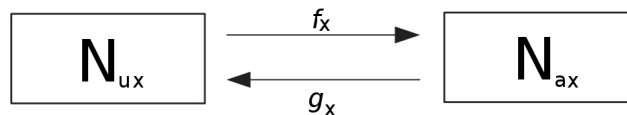


Figure 6.3: Diagram of two states model with states N_{ax} and N_{ux} with bound kinetic rate f_x and unbound kinetic rate g_x .

The schematic diagram of transition between attached and detached states is depicted in figure 6.3. The kinetic rates $f_x[s^{-1}]$ and $g_x[s^{-1}]$ describe the transition of amount (part) of cross-bridges between these two states. The values of kinetic rates are known to be dependent on various factors as concentration of Ca^{2+} , ATP and also, namely g_x , show load-dependent manner. The mathematical description of transition of amount of cross-bridges between two states N_{ax}, N_{ux} with particular x end-to-end distance and particular

rates f_x, g_x can be described by the set of equations in a form:

$$\frac{d}{dt}N_{ux} = g_x N_{ax} - f_x N_{ux}, \quad (6.4)$$

$$\frac{d}{dt}N_{ax} = f_x N_{ux} - g_x N_{ax}, \quad (6.5)$$

$$N_{ux} + N_{ax} = 1 \quad (6.6)$$

where the last equation 6.6 expresses the preservation condition of number of cross-bridges. In this case, the equation 6.6 defines that the N_{ax}, N_{ux} are proportions of attached, resp. unattached states at particular x distance.

For the description of sarcomere force production it is important only the proportion/number of attached cross-bridges N_{ax} . The consideration of only two states and condition as in equation 6.6 allows to simplify the description of N_{ax} in a form of one equation:

$$\frac{d}{dt}N_{ax} = (1 - N_{ax})f_x - g_x N_{ax}. \quad (6.7)$$

Mechanics of Ensemble of Cross-Bridges

Myosin II as non-processive molecular motor acts only in ensemble with another myosins (cross-bridges). Although it is assumed that every cross-bridge in ensemble acts independently, the resulted force production and contractile activity of sarcomere is an effect of simultaneous activity of a great amount of cross-bridges. More specifically, the number of attached cross-bridges on the level of single sarcomere is considered in the range of units. Whereas on the level of the whole muscle, the source of the resulted force generation is attachment of millions of cross-bridges.

x end-to-end distance distribution $n(x, t)$

To describe the great amount of attached cross-bridges, let's introduce here x end-to-end distance distribution $n_a(x, t)$. Distribution $n_a(x, t)$ describes the proportions of

cross-bridges which are attached to actin filaments with particular x end-to-end distances at concrete time t .

Under consideration that the cross-bridges bind with end-to-end distances x within range of interval $x \in h$, the equation 6.7 can be used to extend the description of attached cross-bridges along the interval h by distribution $n_a(x, t)$ in a form:

$$\frac{d}{dt}n_a(x, t) = \left(\frac{1}{|h|} - n_a(x, t) \right) f(x) - g(x)n_a(x, t). \quad (6.8)$$

The term $\frac{1}{|h|}$ in equation above help to guarantee the condition of number of cross-bridges which changed to:

$$\int_a^b n_a(x, t)dx + \int_a^b n_u(x, t)dx = 1, \quad (6.9)$$

where $n_u(x, t)$ is the distribution of x end-to-end distances of unattached cross-bridges. The equation 6.8 describes time-evolution of distribution of attached cross-bridges **only and purely during isometric contraction**. In comparison to classical Huxley description as in equation 5.7 on page 114, the equation satisfies the normalization condition 6.9. Let's denote further the distribution $n_a(x, t)$ only as $n(x, t)$.

From equation 6.8 follows that in steady state of isometric contraction the distribution of the number of attached cross-bridges with particular x can be computed as:

$$n_s(x) = \frac{1}{|h|} \frac{f(x)}{f(x) + g(x)}, \quad (6.10)$$

where $n_s(x)$ is the steady state distribution of a number (proportion) of attached cross-bridges with particular x end-to-end distances.

Velocity of contraction v

Before the mathematical formula 6.8 could be extended also for the cases of eccentric and concentric contraction, the variable of contraction velocity v and variable of length l of actin-myosin filaments overlap must be introduced.

In this text, the velocity of contraction $v(t)$ is related to the activity of sarcomere in the following common sense. The shortening speed of sarcomere is designated by positive values of velocity. Therefore, if the half-sarcomere undergoes concentric contraction, the velocity of contraction is $v > 0$. If the half-sarcomere is stretched by external force F_E (eccentric contraction), the velocity of contraction is described with negative values $v < 0$. Through the literature, some texts might be found that define the velocities just in opposite manner. Obviously, for the isometric contraction the velocity is $v(t) = 0$.

Effect of contractile velocity on a (half) sarcomere length The length change of a single (half) sarcomere is then:

$$\frac{dl_S}{dt} = v(t), \quad (6.11)$$

where l_S is a (half) sarcomere length.

Effect of contractile velocity on a single attached cross-bridge The direction of contractile velocity has following effect on a change of x end-to-end distance of a single attached cross-bridge. If the sarcomere undergoes concentric contraction, single cross-bridge shortens according to velocity v . On the other hand, if the sarcomere is stretched by velocity of v during eccentric contraction, the single cross-bridges are elongated according to time course of this velocity. By the definition of the sign of velocity as noted above, the change of x end-to-end distance of a single cross-bridge due to contractile activity can be simply expressed as:

$$\frac{dx}{dt} = -v(t). \quad (6.12)$$

Effect of contractile velocity on distribution $n(x, t)$ After assumptions noted above, the effect of contraction velocity on distribution of attached cross-bridges $n(x, t)$ might be expressed as:

$$-v(t) \frac{\partial n(x, t)}{\partial x}, \quad (6.13)$$

where the term 6.13 describes the change of the x end-to-end distances of a number of cross-bridges $n(x, t)$ by contraction velocity $v(t)$.

Effect of contractile velocity on a magnitude of actin-myosin overlap l The length l of actin-myosin filaments overlap changes according to sarcomere contractile activity. The degree of actin-myosin overlap is much more important for description of active force production than the length of sarcomere. The reason is that the degree of actin-myosin overlap is one of the crucial factors that dictates the number cross-bridges which can be attached.

The degree of actin-myosin overlap changes in the following manner. In the case of concentric contraction, the magnitude of actin-myosin overlap increases until it reaches its maximum. Due to the bare zone on myosin filaments (see figure 3.16 on page 82), this maximum does not increase once the actin filaments reach myosin filament bare zone, although the shortening of sarcomere can still continue. The effect of bare zone on myosin filaments is the plateau region in Gordon's graph (see figure 2.9 on page 45).

On the other hand, during the eccentric contraction the degree of actin-myosin overlap decreases until it reaches zero. Around the length of sarcomere about $3,4\mu m$ the actin-myosin overlap completely disappears.

On account of velocity definition and information noted above, the change of overlap l

during contractile activity can be described as:

$$\frac{dl}{dt} = \begin{cases} 0 & l \in (-\infty, 0), \\ v(t) & l \in [0, l_{max}], \\ 0 & l \in (l_{max}, l_{max} + l_{plateau}], \\ \text{not defined} & l > l_{max} + l_{plateau}, \end{cases} \quad (6.14)$$

where l denotes the magnitude of actin-myosin filaments overlap, l_{max} expresses the maximal possible value of actin-myosin overlap, $l_{plateau}$ denotes the (half) length of bare zone on myosin filament.

The range $l \in [0, l_{max}]$ represents the descending limb in Gordon's graph. The range $l \in (l_{max}, l_{max} + l_{plateau}]$ represents the plateau region of Gordon's graph. The region of overlap $l > l_{max} + l_{plateau}$ represents the ascending limb of Gordon's graph. Through the literature, it is not clear what exactly is happening in this region and there is only a few assumptions about it. In this region the actin filaments might encounter the actin filaments from counter part of sarcomere and consequently the Z-lines might encounter myosin filaments, which leads to the observable decrease in force production as showed by ascending limb of Gordon's graph. Due to the reason that the mentioned mechanisms of force decrease beyond $l > l_{max} + l_{plateau}$ are unclear, the range of overlap $l > l_{max} + l_{plateau}$ can not be considered in presented work.

Modified Huxley's equation

It is assumed that the shape of distribution $n(x, t)$ depends on the kinetics rates $f(x), g(x)$ and the velocity $v(t)$. By the use of previously derived mathematical forms 6.8 and 6.13, the time-evolution of distribution $n(x, t)$ during contractile activity of sarcomere with velocity $v(t)$ can be mathematically captured by transport equation with sources on right side in a form:

Modified Huxley's equation

$$\frac{\partial n(x,t)}{\partial t} - v(t) \frac{\partial n(x,t)}{\partial x} = \left(\frac{1}{|h|} - n(x,t) \right) f(x) - n(x,t)g(x) \quad (6.15)$$

In comparison to classical Huxley's equation 5.9 on page 114, the derived equation 6.15 differs only in one term $\frac{1}{|h|}$, which help to normalize the distribution $n(x,t)$ by the term 6.9 for the case of isometric contraction. But here, the equation 6.15 as well as original Huxley's equation encounters a problem.

The problem, and probably not widely known, of this equation is that due to the source term on right side, it violates the balance law of number of cross-bridges during concentric and eccentric contraction. In other words it means that condition 6.9 extended for the full theoretical possible range of $x \in (-\infty, \infty)$ is in general not valid:

$$\int_{-\infty}^{\infty} n(x,t)dx + \int_{-\infty}^{\infty} n_u(x,t)dx \neq 1. \quad (6.16)$$

Still, the original Huxley's equation is widely used in cross-bridge theory to model force production of muscles. In the same way, the equation 6.15 is in the following text used for the description of dynamic of attached cross-bridges during contractile activity of (half) sarcomere. The possible correction of mentioned error is proposed further in the text.

The shapes of kinetic rates $f(x)$ and $g(x)$ Through the history of the cross-bridge theory model evolution and related amount of published papers, the shapes of bounding and unbinding kinetics rates $f(x), g(x)$ might be denotes as one of the most common subjects of change. Therefore the great amount of proposals on the shapes of these rates can be found.

Unbound kinetic rate $g(x)$ In this text, the form of unbound rate $g(x)$ is assumed to be the sum of functions describing the unbinding of cross-bridges by *ATP* and due to unbinding of applied load on cross-bridges. Under assumption of uniformly distributed

concentration of ATP in sarcomere, the effect of ATP unbinding must be same for every cross-bridge. This leads to the description of this process by function:

$$g_{ATP}([ATP]), \quad (6.17)$$

where the value of $g_{ATP}([ATP])$ is dependent on the concentration of $[ATP]$ inside sarcomere.

From experiments is apparent that bound time of cross-bridge decreases with increased external load applied on cross-bridge. To capture this effect, let's assume here that this part of unbound rate can be described by formula:

$$g_L(f_{cb}(x)) = R|f_{cb}(x)|^Q \quad (6.18)$$

where g_L represents the part of $g(x)$ which is dependent on external load of single cross-bridges. R, Q are constants and $|f_{cb}(x)|$ is absolute value of cross-bridge's force. The final proposed form of unbinding kinetic rate $g(x)$ is assumed here in a form:

$$g(x, [ATP]) = g_{ATP}([ATP]) + R|f_{cb}(x)|^Q. \quad (6.19)$$

In comparison to classical Huxley description as unbound rate 5.11 on page 115, the equation 6.19 is able to distinguish among the cross-bridges, which are released by binding of ATP molecules, and among the cross-bridges, which were detached forcibly.

Bound kinetic rate $f(x)$ The estimation of bound kinetic rate $f(x)$ regarding to physiological background is much harder. At first, let's recall here assumption that cross-bridges can bind only within interval $x \in h$ and observation from experiments that the cross-bridges attached in wrong direction can be found in activated sarcomeres. Still, based on the summary in preceding introductory chapters, it is hard to propose any shape of kinetic rate $f(x)$. Therefore, let's tacitly assume that the probability of attachment decreases as the value of x approaches the value of the parameter a of interval $h = [a, b]$.

On the other hand, let's assume that the most of the cross-bridges attach in the proper direction according to concentric contraction. Based on these assumptions, the binding kinetic rate $f(x)$ is described here in a shape of log-normal distribution in a form:

$$f(x, [Ca^{2+}]) = \begin{cases} x \leq a & 0 \\ x \in h = (a, b) & f_{Ca}([Ca^{2+}]) \frac{1}{|x-b|\sigma\sqrt{2\pi}} e^{-\frac{(\ln|x-b|-\mu)^2}{2\sigma^2}} \\ x \geq b & 0 \end{cases}, \quad (6.20)$$

where f_{Ca} is considered to be constant dependent on the concentration of $[Ca^{2+}]$.

Dependency of rates $g(x), f(x)$ on concentration of ATP, Ca^{2+} The sarcomere activity is known to be dependent namely on the concentration of ATP and Ca^{2+} . In particular, the introduction of Ca^{2+} into sarcomere triggers the contraction. Briefly, it means that the kinetic rate $f(x)$ is dependent on Ca^{2+} . On the other hand, the detaching rate $g(x)$ is known to be dependent on the concentration of ATP . Again, through the literature, a lot of proposals about description of mentioned dependencies can be found. Therefore, let's assume that the these dependencies might be described in a forms (or by similar equations):

$$f_{Ca} = A_{Ca} \frac{[Ca^{2+}]}{[Ca^{2+}]_{max}} \quad \text{or} \quad f_{Ca} = A_{Ca}(1 - e^{-[Ca^{2+}]}), \quad (6.21)$$

$$g_{ATP} = A_{ATP} \frac{[ATP]}{[ATP]_{max}} \quad \text{or} \quad g_{ATP} = A_{ATP}(1 - e^{-[ATP]}), \quad (6.22)$$

where A_{Ca}, A_{ATP} are constants, $[Ca^{2+}]_{max}, [ATP]_{max}$ are maximal concentration of Ca^{2+}, ATP .

Active force F_{CB} in actin-myosin overlap

The active force F_{CB} , which is able to be exerted by cross-bridges in overlap of actin-myosin filaments, is here assumed to be dependent namely on these factors:

- the shape of the x end-to-end distance distribution $n(x, t)$,

- the magnitude of actin-myosin filaments overlap l ,
- the single cross-bridge force- x end-to-end distance relationship,
- the number of available cross-bridges m_{cb} in a whole (half) sarcomere.

Under these assumptions, the force F_{CB} , which is cross-bridge cycling capable to develop can be written as:

Active force F_{CB} produced by cross-bridges activity

$$F_{CB} = m_{cb} \frac{l}{l_{max}} \int_{-\infty}^{\infty} f_{cb}(x) n(x, t) dx, \quad (6.23)$$

where l represents the magnitude of actin-myosin overlap, $f_{cb}(x)$ describes force- x -distance relationship as presented in fig. 6.2. $n(x, t)$ is x -distance distribution.

Another form of force production can be defined as:

$$F_{CB} = m_{cb} \frac{l}{l_{max}} \int_{-\infty}^{\infty} x k_{cb}(x) n(x, t) dx, \quad (6.24)$$

where the term k_{cb} expresses the stiffness of single cross-bridge.

6.1.2 Another quantities describing properties of cross-bridge mechanism

Based on the preceding assumption can be proposed another quantities, which might help to allow better insight into sarcomere contractile activity.

Proportion of attached cross-bridges in cross-section of actin-myosin overlap

$$N(t) = m_{cb} \frac{1}{l_{max}} \int_{-\infty}^{\infty} n(x, t) dx \quad (6.25)$$

Number of attached cross-bridges

$$N_a(t) = m_{cb} \frac{l}{l_{max}} \int_{-\infty}^{\infty} n(x, t) dx, \quad (6.26)$$

Stiffness of cross-bridge mechanism

$$K(t) = m_{cb} \frac{l}{l_{max}} \int_{-\infty}^{\infty} k(x) n(x, t) dx \quad (6.27)$$

Potential elastic energy stored in cross-bridge mechanism

$$E_p(t) = m_{cb} \frac{l}{l_{max}} \int_{-\infty}^{\infty} |x| |k_{cb}(x) n(x, t)| dx, \quad (6.28)$$

where the absolute values refer to a fact that cross-bridges might be connected in wrong direction according to sense of (concentric) contraction.

ATP molecules input The number of consumed ATP molecules (power input) in particular time t is:

$$\frac{d}{dt} N_{ATP} = m_{cb} \frac{l}{l_{max}} \int_{-\infty}^{\infty} n(x, t) g_{ATP}([ATP]) dx. \quad (6.29)$$

The sum of consumed ATP molecules during the whole process of contractile activity is:

$$N_{ATP} = \frac{m_{cb}}{l_{max}} \int_0^{\tau} l(t) \int_{-\infty}^{\infty} n(x, t) g_{ATP}([ATP]) dx dt, \quad (6.30)$$

where τ is the end time of contractile activity (deactivation of sarcomere).

6.1.3 Preservation of cross-bridges error in classical Huxley's cross-bridge model

Although the correction of mentioned error is not the main aim of presented work, the following lines introduces the possible repair of this problem.

The reason of the error in balance law of conservation of cross-bridges in original Huxley's and modified Huxley's equation can be in brief demonstrated as follows. Let's recall here equations 6.4 and extend it formally for the range of $x \in (-\infty, \infty)$. Further, by the addition of equation 6.15, we get the following set of equations:

$$\frac{d}{dt}n_u(x, t) = g(x)n(x, t) - f(x)n_u(x, t), \quad (6.31)$$

$$\frac{\partial n(x, t)}{\partial t} - v(t)\frac{\partial n(x, t)}{\partial x} = \left(\frac{1}{|h|} - n(x, t)\right) f(x) - n(x, t)g(x). \quad (6.32)$$

This set of equations describes the dynamic of a number of attached cross-bridges $n(x, t)$ and simultaneously the dynamic of a number unattached cross-bridges $n_u(x, t)$ during contractile activity. Briefly, the balance error arises during concentric and eccentric contractile activity because the part of the cross-bridges unbind outside the interval h . By the definition of kinetic rate $f(x)$ above, the cross-bridges detached outside interval h can not attach again according to mathematical description in equations set above. Simultaneously, these cross-bridges are "substituted" by the cross-bridges "produced" by the source term on right side of equation 6.32. This leads to the fact that the number of cross-bridges in described system is increasing whenever the distribution $n(x, t)$ is shifted outside interval h . The increasing number of cross-bridges in sarcomere makes obviously no sense.

Further fact is that this error is unseen without the consideration of distribution of unattached cross-bridges, because the steady state distribution of attached cross-bridges contains again the same number of cross-bridges as before contractile activity due to the special form of source term on right side of equation 6.32.

The effect of this discrepancy might leads to various conclusions, which must be ex-

amined more properly. It is obvious that effect of this error influence the description of sarcomere activity namely during transient states. It might be also worthwhile to consider, if this error could have any impact on the shape of distribution $n(x, t)$ in steady states after contractile activity, which could lead to explanation of phenomenons as force depression.

The possible correction might be considered as follows. Let's consider equations 6.4, 6.5 and extend them formally again for the range of $x \in (-\infty, \infty)$.

$$\frac{d}{dt}n_u(x, t) = g(x)n(x, t) - f(x)n_u(x, t), \quad (6.33)$$

$$\frac{d}{dt}n(x, t) = f(x)n_u(x, t) - g(x)n(x, t). \quad (6.34)$$

The sum of unattached cross-bridges N_u at time t is:

$$N_u(t) = \int_{-\infty}^{\infty} n_u(x, t)dx. \quad (6.35)$$

Under strong simplification, let's assume that the cross-bridges which can bind inside interval h with particular x end-to-end distance are uniformly distributed along this interval. Therefore at any instant of time the distribution of unattached cross-bridges is $\frac{N_u(t)}{|h|}$. This assumption leads to the possible modification of equation 6.34 to the form

$$\frac{d}{dt}n(x, t) = f(x)\frac{N_u(t)}{|h|} - g(x)n(x, t). \quad (6.36)$$

Under the same assumption as noted in preceding part of this chapter, this equation can be formally extended to the form:

$$\frac{\partial}{\partial t}n(x, t) - v(t)\frac{\partial}{\partial x}n(x, t) = f(x)\frac{N_u}{|h|} - g(x)n(x, t). \quad (6.37)$$

To conclude on assumptions on correction of balance law error in classical Huxley's equation and modified Huxley's equation, the equation 6.15 might be substituted by the set of equations:

Modified Huxley's equation taking into account the preservation of cross-bridges in sarcomere

$$\frac{d}{dt}n_u(x, t) = g(x)n(x, t) - f(x)n_u(x, t), \quad (6.38)$$

$$N_u(t) = \int_{-\infty}^{\infty} n_u(x, t)dx, \quad (6.39)$$

$$\frac{\partial}{\partial t}n(x, t) - v(t)\frac{\partial}{\partial x}n(x, t) = f(x)\frac{N_u(t)}{|h|} - g(x)n(x, t). \quad (6.40)$$

6.1.4 Passive force: force F_T generated by the bunch of titin filaments

Single titin mechanics In sarcomere, as a main source of passive force are believed to be titin filaments. Recent experiments supported the idea that the role of titin is much more important in sarcomere than originally thought in classical cross-bridge theory. Based on experiments, it was proposed the way of titin's active regulation of sarcomere contractile activity. Let's recall here the two main ideas [40], [43]:

Titin's regulation mechanism of contractile activity

1. titin increases its stiffness in a presence of $[Ca^{2+}]$ (see results of experiments in figure 4.6 on page 100).
2. upon activation of sarcomere, titin actively binds at actin filaments by its specific segment N2A. This leads to the decrease of its free length (see scheme of this mechanism in figure 4.7 on page 102 and in figure 6.1 on page 132).

Both of mentioned titin's regulation mechanism have impact namely on eccentric contraction. At first, the force exerted upon titin stretch is higher because its stiffness is increased by $[Ca^{2+}]$. As the second, local deformation in activated sarcomere upon stretch of bounded titin is higher than the local deformation of the whole unattached titin filament in deactivated sarcomere. Therefore, although the much shorter part of titin takes a part

in contractile activity, the resulted force upon stretch is considered to be much higher than of unattached titin in deactivated sarcomere.

Obviously, this force can not be no more neglected namely during eccentric contraction. In comparison to classical two-sliding filament theory, there is a need to consider another important force arising from modified titin's properties namely during stretch of sarcomere.

To fulfil also the assumptions about other two kinds of contractile activity, let's assume that during isometric contraction titin changes its properties as described above. But in this case no length change of sarcomere occurs. Therefore also titin, although already attached, is not stretched and therefore its special properties can not be apparent. Further, because the titin is believed to behave like one-directional spring, during concentric contraction it is believed to behave as a free band producing no force or maybe producing negligible force acting against shortening by its buckled state.

The part of single titin filament with properties as discussed above might be then described as:

$$F_{wlc} = \begin{cases} 0 & l_T \leq 0, \\ \frac{k_B T}{A} \left(\frac{l_T}{L} + \frac{1}{4(1-\frac{l_T}{L})^2} - \frac{1}{4} \right) & l_T \in (0, L), \\ \text{not defined} & l_T \geq L, \end{cases} \quad (6.41)$$

where F_{wlc} is force described by wlc model, l_T is shortest end-to-end distance of titin's ends. L is titin's contour length. A is persistence length, k_B is Boltzmann constant and T is absolute temperature.

Single titin's part unfolding As noted in introductory chapters, the titin's parts as Ig domains unfold once these parts are stretched above some threshold value of stretch. The result of unfolding is the increase of contour length of studied chain, which results in decrease of produced force. Therefore, to describe the contour length L change of a single studied chain, let's assume that this can be captured by equations:

$$L = N_{fIg}L_f + N_{uIg}L_u, \quad (6.42)$$

$$N_{fIg} + N_{uIg} = N_{Ig}. \quad (6.43)$$

where N_{fIg} is number of folded Ig domains, L_f is contour length of single folded Ig domain, N_{uIg} is number of unfolded Ig domains, L_u is contour length of single unfolded Ig domain. N_{Ig} is a number of Ig domains.

As discussed in chapter 5.6.2, the simulation of unfolding and refolding of titin's parts is one of the most challenging part of considered problem. Based on the equation 6.43, the change $dN_{fIg} + dN_{uIg} = 0$ can be modelled for example by the equations presented in section 5.6.2. But this part of model must be still examined more properly.

Further, experiments on titin revealed that persistence length A of single titin chain also changes during unfolding/refolding. The change of persistence length is then function of grater amount of parameters as:

$$A = A(N_{fIg}, N_{uIg}, l_T, [Ca^{2+}], \dots) \quad (6.44)$$

Obviously, this relation must be subjected to more profound research.

Bunch of titin mechanics It is known that the all myosins filaments are not perfectly centered in sarcomere. From this fact follows that the single titins in bunch of titins does not have the same value of extension l_T at the beginning of contractile activity. Under assumption that the distribution of l_T at the beginning contractile activity might be described by normal distribution, the mechanics of bunch of titin filaments might be described as:

$$F_T = N_T \int_{-\infty}^{\infty} F_{wlc}(l_T) \frac{1}{\sigma_T \sqrt{2\pi}} e^{-\frac{(l_T - \mu_T)^2}{2\sigma_T^2}} dl_T, \quad (6.45)$$

where N_T is number of titins filaments in sarcomere.

6.2 Three Filament Cross-Bridge Model of Sarcomere

This section summarizes the presented deduced equations from the assumptions noted above into arranged sets of equations. The derived cross-bridge model can be written in two forms:

1. Dynamic model describing behaviour of (half) sarcomere during the contractile activity of any kind of contraction, where the type of contraction is determined by the value of contractile velocity,
2. steady-state model describing steady-state (relaxed) states of activated (half) sarcomere before and after contractile activity or reference steady-states during contractile activity.

6.2.1 Dynamic form of Three Filament Cross-Bridge Model

The dynamic form cross-bridge model is described by the set of equations in a form:

Three filaments cross-bridge model

$$F_S = F_{CB} + F_T \quad (6.46)$$

$$F_{CB} = m_{cb} \frac{l}{l_{max}} \int_{-\infty}^{\infty} f_{cb}(x) n(x, t) dx \quad (6.47)$$

$$F_T = N_T \int_{-\infty}^{\infty} F_{wlc}(l_T) \frac{1}{\sigma_T \sqrt{2\pi}} e^{-\frac{(l_T - \mu_T)^2}{2\sigma_T^2}} dl_T \quad (6.48)$$

$$\frac{\partial n(x, t)}{\partial t} - v(t) \frac{\partial n(x, t)}{\partial x} = \left(\frac{1}{|h|} - n(x, t) \right) f(x) - n(x, t) g(x) \quad (6.49)$$

$$f(x, [Ca^{2+}]) = \begin{cases} x \leq a & 0 \\ x \in h = (a, b) & f_{Ca}([Ca^{2+}]) \frac{1}{|x-b|\sigma\sqrt{2\pi}} e^{-\frac{(\ln|x-b|-\mu)^2}{2\sigma^2}} \\ x \geq b & 0 \end{cases} \quad (6.50)$$

$$g(x, [ATP]) = g_{ATP} + R|f_{cb}(x)|^Q \quad (6.51)$$

$$\frac{dl}{dt} = \begin{cases} 0 & l \in (-\infty, 0) \\ v(t) & l \in [0, l_{max}] \\ 0 & l \in (l_{max}, l_{max} + l_{plato}] \\ \text{not defined} & l > l_{max} + l_{plato} \end{cases} \quad (6.52)$$

$$\frac{dl_T}{dt} = \begin{cases} 0 & l_T \in (-\infty, 0) \\ -v(t) & l_T \in [0, L) \\ \text{not defined} & l_T \geq L \end{cases} \quad (6.53)$$

$$\frac{dl_S}{dt} = v(t) \quad (6.54)$$

$$F_{wlc} = \begin{cases} 0 & l_T \leq 0 \\ \frac{k_B T}{A} \left(\frac{l_T}{L} + \frac{1}{4(1-\frac{l_T}{L})^2} - \frac{1}{4} \right) & l_T \in (0, L) \\ \text{not defined} & l_T \geq L \end{cases} \quad (6.55)$$

$$L = N_{fIg}L_f + N_{uIg}L_u \quad (6.56)$$

$$\frac{d}{dt}N_{fIg} = N_{fIg}(l_T, E_a, F_{wlc}, \Delta x_f, \dots) \quad (6.57)$$

$$\frac{d}{dt}N_{uIg} = N_{uIg}(l_T, E_a, F_{wlc}, \Delta x_u, \dots) \quad (6.58)$$

$$A = A(N_{fIg}, N_{uIg}, l_T, [Ca^{2+}], \dots) \quad (6.59)$$

To employ the derived correction on error of conservation of number of cross-bridges in sarcomere, the equation 6.49 might be substituted by the following set of equations:

Three filaments cross-bridge model with corrected preservation of number of cross-bridges

$$\frac{d}{dt}n_u(x, t) = g(x)n(x, t) - f(x)n_u(x, t), \quad (6.60)$$

$$N_u(t) = \int_{-\infty}^{\infty} n_u(x, t) dx, \quad (6.61)$$

$$\frac{\partial}{\partial t}n(x, t) - v(t)\frac{\partial}{\partial x}n(x, t) = f(x)\frac{N_u(t)}{|h|} - g(x)n(x, t). \quad (6.62)$$

6.2.2 Steady-state model

Steady-state version of the model can be used to describe the steady-states before and after contractile activity, when the sarcomere stays still activated. This model can be also used to observe the "reference" relaxed states of sarcomere during dynamic simulations. Namely the comparison of force-time relationships of dynamic and steady-state simulation could enable more profound insight into considered problem.

The steady state form of the cross-bridge model has a form:

Steady-state three filaments cross-bridge model

$$F_{SS} = F_{CBS} + F_{TS} \quad (6.63)$$

$$F_{CBS} = m_{cb} \frac{l}{l_{max}} \int_{-\infty}^{\infty} f_{cb}(x) n_s(x) dx \quad (6.64)$$

$$F_{TS} = N_T \int_{-\infty}^{\infty} F_{wlc}(l_T) \frac{1}{\sigma_T \sqrt{2\pi}} e^{-\frac{(l_T - \mu_T)^2}{2\sigma_T^2}} dl_T, \quad (6.65)$$

$$n_s(x) = \frac{1}{|h|} \frac{f(x)}{f(x) + g(x)} \quad (6.66)$$

$$f(x, [Ca^{2+}]) = \begin{cases} x \leq a & 0 \\ x \in h = (a, b) & f_{Ca}([Ca^{2+}]) \frac{1}{|x-b|\sigma\sqrt{2\pi}} e^{-\frac{(ln|x-b|-\mu)^2}{2\sigma^2}} \\ x \geq b & 0 \end{cases} \quad (6.67)$$

$$g(x, [ATP]) = g_{ATP}([ATP]) + R|f_{cb}(x)|^Q \quad (6.68)$$

$$l = \begin{cases} 0 & l \in (-\infty, 0) \\ \int_0^\tau -v(t)dt + l_0 & l \in [0, l_{max}] \\ l_{max} & l \in (l_{max}, l_{max} + l_{plato}] \\ \text{not defined} & l > l_{max} + l_{plato} \end{cases} \quad (6.69)$$

$$l_T = \begin{cases} 0 & l_T \in (-\infty, 0) \\ \int_0^\tau -v(t)dt + l_{T0} & l_T \in [0, L) \\ \text{not defined} & l_T \geq L \end{cases} \quad (6.70)$$

$$l_S = \int_0^\tau v(t)dt + l_{S0} \quad (6.71)$$

$$F_{wlc} = \begin{cases} 0 & l_T \leq 0 \\ \frac{k_B T}{A} \left(\frac{l_T}{L} + \frac{1}{4(1-\frac{l_T}{L})^2} - \frac{1}{4} \right) & l_T \in (0, L) \\ \text{not defined} & l_T \geq L \end{cases} \quad (6.72)$$

$$L = N_{fIg}L_f + N_{uIg}L_u \quad (6.73)$$

$$N_{fIgS} = N_{fIgS}(l_T, E_a, F_{wlc}, \Delta x_f, \dots) \quad (6.74)$$

$$N_{uIgS} = N_{uIgS}(l_T, E_a, F_{wlc}, \Delta x_u, \dots) \quad (6.75)$$

$$A = A(N_{fIg}, N_{uIg}, l_T, [Ca^{2+}], \dots) \quad (6.76)$$

Maximal sarcomere active force F_{max} The maximal active force, which is the inner mechanism of sarcomere able to develop by itself, is at maximal overlap during isometric contraction. In this case $\frac{l}{l_{max}} = 1$. According to the equation 6.64 the maximal force per (half) sarcomere can be expressed as:

$$F_{max} = m_{cb} \int_{-\infty}^{\infty} f_{cb}(x)n_s(x)dx. \quad (6.77)$$

The maximal possible overlap of actin and myosin filaments is in the plateau region of Gordon's graph as shown in figure 2.9 on page 45. Therefore, this region is characteristic with maximal possible forces of isometric contraction.

Maximal concentric contraction velocity According to the force-velocity relationship as depicted for example in figure 2.6 on page 42, the maximal velocity of concentric contraction is at zero-load. Accordingly, the maximal velocity of (half) sarcomere shortening might be obtained from relationship:

$$v_{max} \iff m_{cb} \frac{l}{l_{max}} \int_{-\infty}^{\infty} f_{cb}(x)n(x,t)dx = 0 = F_{CB} \quad (6.78)$$

6.2.3 Initial and boundary conditions:

To accomplish especially the dynamic form of the model, the initial and boundary conditions and their meanings must be introduced. The initial and boundary conditions presented in next lines represent the case, where the sarcomere mechanism is activated from its relaxed state at particular length.

Initial and boundary conditions for equation 6.49 describing the dynamic of the number of attached cross-bridges are then:

$$n(x, 0) = 0 \quad \forall x, \quad (6.79)$$

$$n(-\infty, t) = 0, \quad (6.80)$$

$$n(\infty, t) = 0. \quad (6.81)$$

If the simulation should start from the steady-state of activated sarcomere, then the initial conditions for equation 6.49 has a form as expressed by equation 6.66.

Initial condition for equation 6.52 is l_0 , where l_0 is the initial overlap of actin-myosin filaments overlap. The initial condition for equation 6.54 is initial (half) sarcomere length l_{S0} . Note that l_0 and l_{S0} are dependent and must satisfy the the geometry of sarcomere. l_{S0} must be chosen according to initial overlap or vice versa.

Initial condition for equation 6.53 of titin stretch l_{T0} is a little bit tricky. It is obvious that with increasing initial length of deactivated sarcomere the initial length of titin increases as well. The problem is that under assumptions on self-modified activity of titin noted above the sarcomere once activated the titin changes its free length by binding to titin. Due to the fact that various segments of titin have different stiffness, the unattached titin might be expected to extend non-uniformly before attached. Therefore, the impact of this effect on initial length l_{T0} of attached titin need to be more examined. For the simplicity, l_{T0} is always assumed to be zero, which might be expected around ideal sarcomere length.

The last initial conditions are on account of equations 6.57 and 6.58. The initial con-

dition of these equations are values of folded and unfolded parts of titin. These initial condition must reflect the condition $N_{fIgs} + N_{UIgs}$.

Chapter 7

Simulation and results

The purpose of simulations was to test the derived three filament cross-bridge for all kind of contractions and special cases of these considered contractions at the scale of half-sarcomere. Obviously, according to the main goal of submitted thesis, the main aim was to simulate the properties of eccentric contraction and its intrinsic phenomenon called force enhancement. In addition, it was also necessary to simulate the cases of isometric and concentric contraction to show that the proposed three filament cross-bridge is in concordance with results, which are traditionally believed as sufficiently understood by classical Huxley's model and classical two sliding-filament theory.

The main aim was rather to test the concept of the model than to obtain the same absolute values of studied quantities as in wide variety of measured experimental data in literature. Also due to this reason, all results of forces were normalized according to maximal force as expressed by equation 6.77 on page 157.

In particular, the graphical results of following simulations are presented in next pages:

1. simulation of isometric contraction,
2. simulation isotonic concentric contraction,
3. simulation of sudden shortening (special case of concentric contraction),
4. simulation of eccentric contraction followed by phenomena of force enhancement,

5. simulation of sudden stretch (special case of eccentric contraction),
6. special cases and properties of force enhancement.

Namely on account of problematic models of titin's parts unfolding, the proposed three filament cross-bridge model had to be simplified. Therefore, the bunch of titins were substituted by single representative titin (wlc) description. Accordingly, all conducted simulations were simulated only for physiological condition, where the unfolding of titin domains are not considered. This applied restrictions namely on account of small stretches during eccentric contractions.

The simplified dynamic and steady-state model then have following forms:

Simplified Three Filaments Cross-Bridge Model

$$F_S = F_{CB} + F_T \quad (7.1)$$

$$F_{CB} = m_{cb} \frac{l}{l_{max}} \int_{-\infty}^{\infty} f_{cb}(x) n(x, t) dx \quad (7.2)$$

$$F_{wlc} = \begin{cases} 0 & l_T \leq 0 \\ \frac{k_B T}{A} \left(\frac{l_T}{L} + \frac{1}{4(1-\frac{l_T}{L})^2} - \frac{1}{4} \right) & l_T \in (0, L) \\ \text{not defined} & l_T \geq L \end{cases} \quad (7.3)$$

$$\frac{\partial n(x, t)}{\partial t} - v(t) \frac{\partial n(x, t)}{\partial x} = \left(\frac{1}{|h|} - n(x, t) \right) f(x) - n(x, t) g(x) \quad (7.4)$$

$$f(x, [Ca^{2+}]) = \begin{cases} x \leq a & 0 \\ x \in h = (a, b) & f_{Ca}([Ca^{2+}]) \frac{1}{|x-b|\sigma\sqrt{2\pi}} e^{-\frac{(ln|x-b|-\mu)^2}{2\sigma^2}} \\ x \geq b & 0 \end{cases} \quad (7.5)$$

$$g(x, [ATP]) = g_{ATP}([ATP]) + R |f_{cb}(x)|^Q \quad (7.6)$$

$$\frac{dl}{dt} = \begin{cases} 0 & l \in (-\infty, 0) \\ v(t) & l \in [0, l_{max}] \\ 0 & l \in (l_{max}, l_{max} + l_{plato}] \\ \text{not defined} & l > l_{max} + l_{plato} \end{cases} \quad (7.7)$$

$$\frac{dl_T}{dt} = -v(t) \quad (7.8)$$

$$\frac{dl_S}{dt} = v(t) \quad (7.9)$$

Simplified Steady-State Three Filaments Cross-Bridge Model

$$F_{SS} = F_{CBS} + F_{TS} \quad (7.10)$$

$$F_{CBS} = m_{cb} \frac{l}{l_{max}} \int_{-\infty}^{\infty} f_{cb}(x) n_s(x) dx \quad (7.11)$$

$$F_{TS} = F_T = \begin{cases} 0 & l_T \leq 0 \\ \frac{k_B T}{A} \left(\frac{l_T}{L} + \frac{1}{4(1-\frac{l_T}{L})^2} - \frac{1}{4} \right) & l_T \in (0, L) \\ \text{not defined} & l_T \geq L \end{cases} \quad (7.12)$$

$$n_s(x) = \frac{1}{|h|} \frac{f(x)}{f(x) + g(x)} \quad (7.13)$$

$$f(x, [Ca^{2+}]) = \begin{cases} x \leq a & 0 \\ x \in h = (a, b) & f_{Ca}([Ca^{2+}])([Ca^{2+}]) \frac{1}{|x-b|\sigma\sqrt{2\pi}} e^{-\frac{(ln|x-b|-\mu)^2}{2\sigma^2}} \\ x \geq b & 0 \end{cases} \quad (7.14)$$

$$g(x, [ATP]) = g_{ATP}([ATP]) + R|f_{cb}(x)|^Q \quad (7.15)$$

$$l = \begin{cases} 0 & l \in (-\infty, 0) \\ \int_0^\tau -v(t) dt + l_0 & l \in [0, l_{max}] \\ l_{max} & l \in (l_{max}, l_{max} + l_{plato}] \\ \text{not defined} & l > l_{max} + l_{plato} \end{cases} \quad (7.16)$$

$$l_T = \begin{cases} 0 & l_T \in (-\infty, 0) \\ \int_0^\tau -v(t) dt + l_{T0} & l_T \in [0, L) \\ \text{not defined} & l_T \geq L \end{cases} \quad (7.17)$$

$$l_S = \int_0^\tau v(t) dt + l_{S0} \quad (7.18)$$

Based on simplified sets of equations, the following properties and quantities of contraction were simulated:

Studied properties in simulations

- a) F_S force developed by half-sarcomere on Z-line, equation 7.1,
- b) F_{CB} force in actin-myosin overlap, equation 7.2,
- c) F_{dl} force in cross-section of actin-myosin overlap, i.e. $\frac{1}{l_{max}} \int_{-\infty}^{\infty} f_{cb}(x)n(x,t)dx$,
- d) F_T force exerted by attached titin filaments to actin, equation 7.3,
- e) $v(t)$ speed of contraction ($v(t)$ is input parameter of dynamic model),
- f) magnitude of contraction $\int_0^{\tau} v(t)dt$,
 - in the case of eccentric contraction, the value of titin stretch l_T equals to the absolute value of the magnitude of contraction,
- g) l magnitude of actin-myosin filaments overlap,
- h) F_{SS} sarcomere steady-state force according to particular magnitude of stretch and overlap, equation 7.10,
- i) F_{CBS} steady-state (reference isometric) cross-bridge force, equation 7.11,
- j) $\frac{N_{dl}}{m_{cb}}$ number of attached cross-bridges in cross-section of actin-myosin overlap, equation 6.25 on page 147,
- k) $\frac{N}{m_{cb}}$ number of attached cross-bridges in actin-myosin overlap, equation 6.26 on page 148,
- l) l_S length of half-sarcomere, equations 7.9 and 7.18,
- m) $n(x,t)$, time evolution of x end-to-end distribution during contractile activity, equation 7.4.

Table 7.1: Studied properties in simulations.

7.1 Model parameters and half-sarcomere properties

d_w	8 nm
a	-40 nm
b	47.61262352 nm
$ h $	87.61262352 nm
l_{max}	725 nm
$l_{plateau}$	550 nm
L	400 nm
A	$1.4895e - 19$
T	329.15 K
μ	1.55
σ	0.22
f_{Ca}	120
g_{ATP}	120
R	0.8
Q	2

Table 7.2: Parameters of three filament cross-bridge model related to half-sarcomere.

Approximation of single cross-bridge force $f_{cb}(x)$ The measured force- x relationship of single cross-bridges was approximated by following function:

$$f_{cb}(x) = \begin{cases} f_{cb}(x) = p_1x^9 + p_2x^8 + p_3x^7 + p_4x^6 + \\ + p_5x^5 + p_6x^4 + p_7x^3 + p_8x^2 + p_9x + p_{10}, & -\infty < x \leq x_0, \\ k_{cb}(x - x_0), & x_0 < x < \infty, \end{cases} \quad (7.19)$$

where

$$p_i = [1.268e - 13, 1.005e - 12, -4.022e - 10, -2.728e - 09, 4.298e - 07, \\ 1.998e - 06, -0.0001525, -0.0006885, 0.04358, -2.456], \quad (7.20)$$

$$k_{cb} = 1.4 \text{ pN/nm}, \quad (7.21)$$

$$x_0 = 39.6126235204314 \text{ nm}. \quad (7.22)$$

Initial and boundary conditions For all simulations were used following initial and boundary conditions.

Initial and boundary conditions for modified Huxley's equation 7.4:

$$n(x, 0) = 0 \quad \forall x, \quad (7.23)$$

$$n(-\infty, t) = 0, \quad (7.24)$$

$$n(\infty, t) = 0. \quad (7.25)$$

Initial overlap of actin-myosin filaments was set to the value corresponding to estimated edge of plateau and descending limb of Gordon's graph. This reflects the physiological situation, where the contraction starts at maximal overlap. Therefore, in the cases of concentric contractions, the overlap can not increase any further. On the other hand, in the case of eccentric contraction, the overlap immediately starts to decrease. The estimated value of initial actin-myosin overlap was then set to:

$$l_0 = 725 \text{ nm}. \quad (7.26)$$

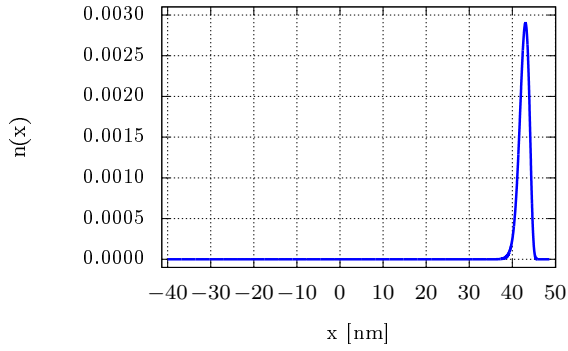
The initial value of titin stretch l_T was set to zero for all simulated cases:

$$l_{T0} = 0 \text{ nm}. \quad (7.27)$$

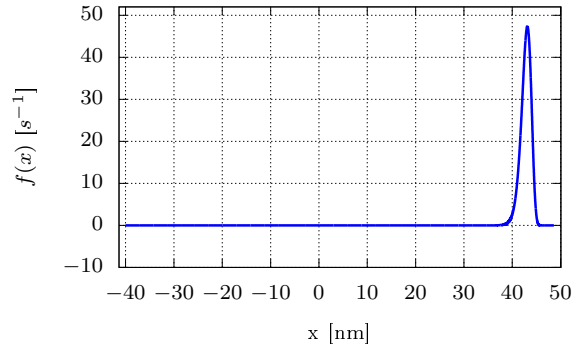
Half sarcomere initial length on account of initial actin-myosin overlap l_0 was estimated to:

$$l_{S0} = 1200 \text{ nm}. \quad (7.28)$$

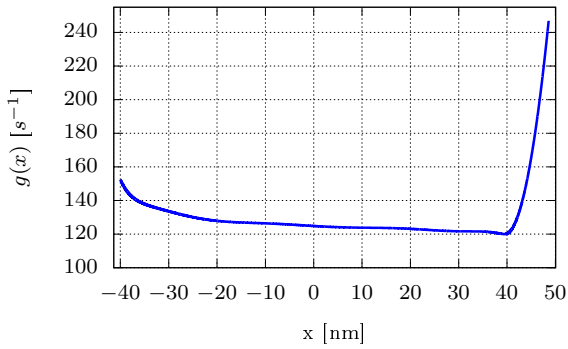
Basic properties Selected basic properties according to chosen parameters of sarcomere are depicted in figure 7.1.



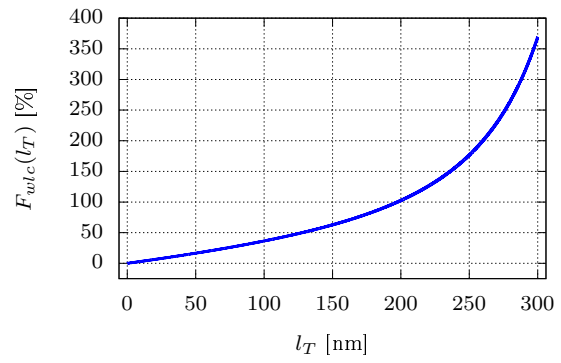
(a) Steady-state distribution $n_s(x)$ for $v = 0$.



(b) Bound rate $f(x)$.



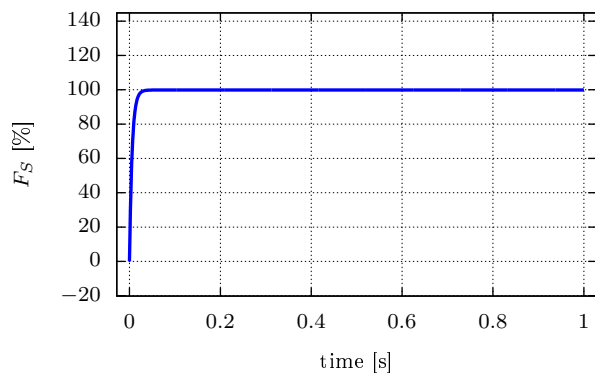
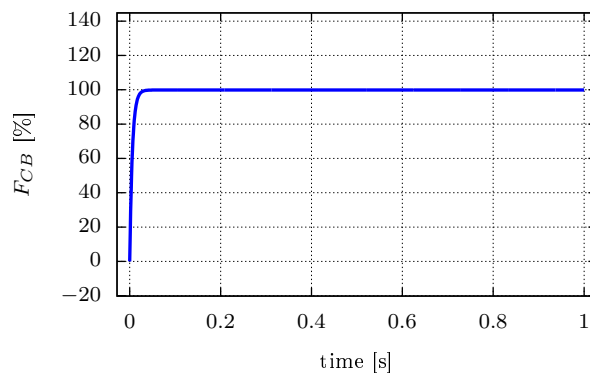
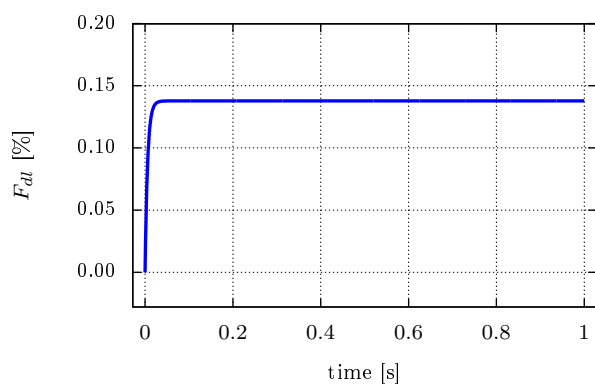
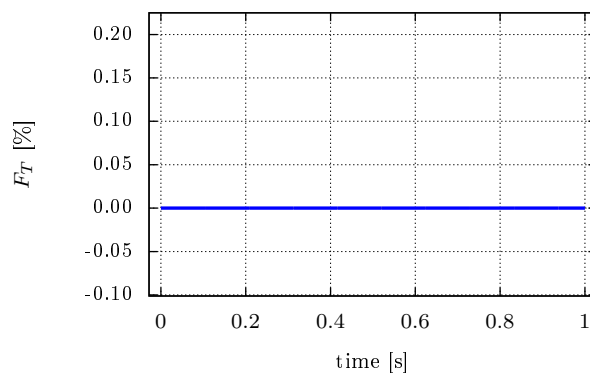
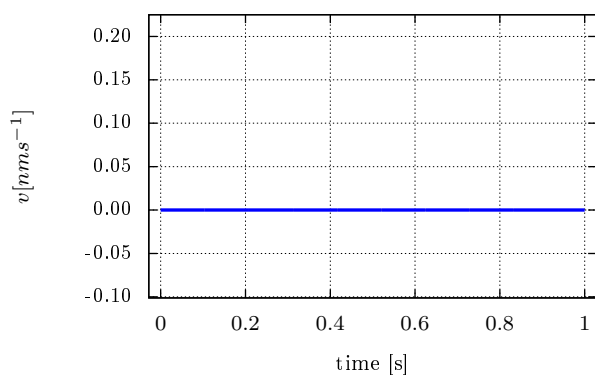
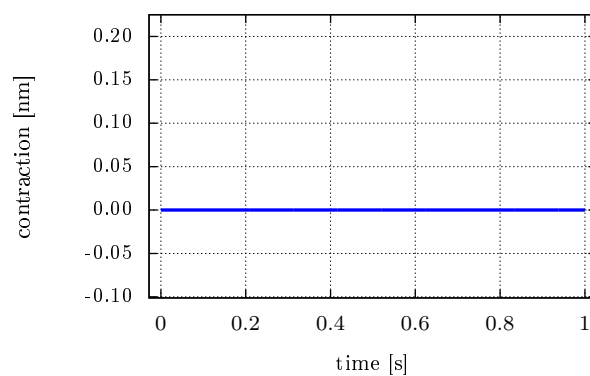
(c) Unbound rate $g(x)$.



(d) Titin force $F_{wlc}(l_T)$ up to 75% of contour length L .

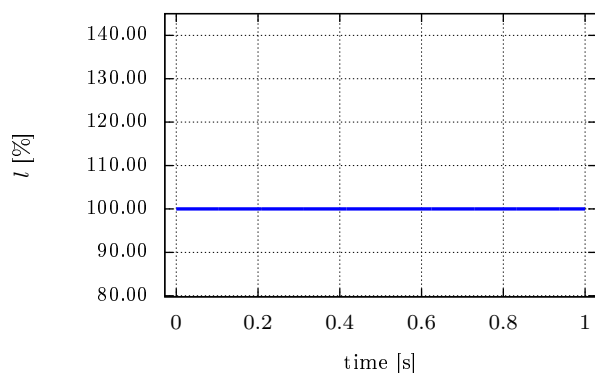
Figure 7.1: Selected properties of sarcomere and its parameters.

7.2 Isometric Contraction

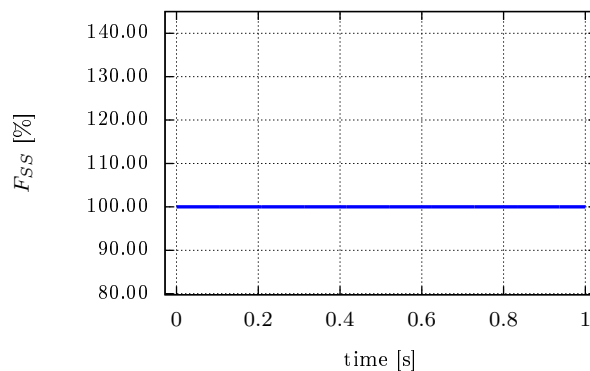
(a) F_S - half sarcomere force.(b) F_{CB} - force in overlap.(c) F_{dl} - force in a-m cross-section (per dl).(d) F_T - force exerted by titins.(e) $v(t)$ - velocity of contraction.

(f) Magnitude of contraction.

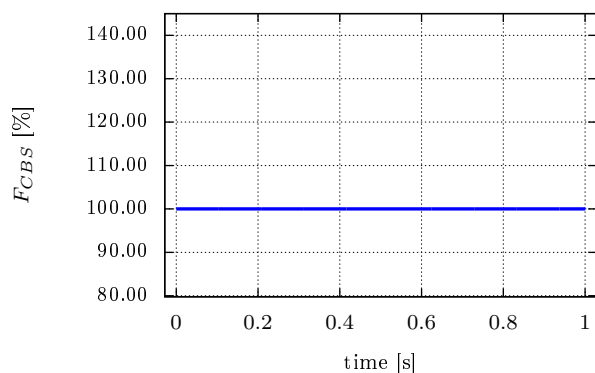
Figure 7.2: Properties of isometric contraction.



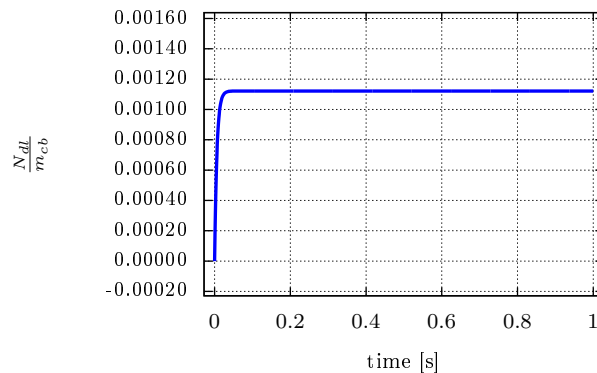
(g) l - magnitude of actin-myosin overlap.



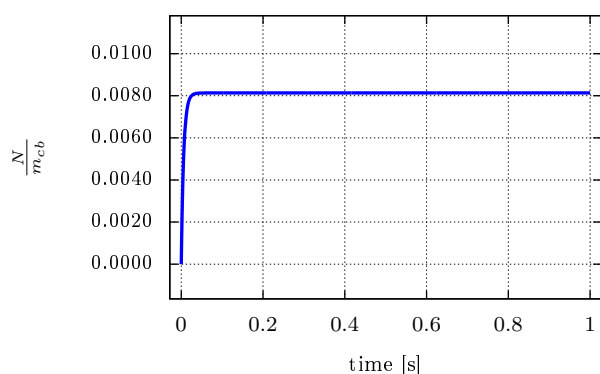
(h) F_{SS} - steady state force of half sarcomere according to degree of a-m overlap.



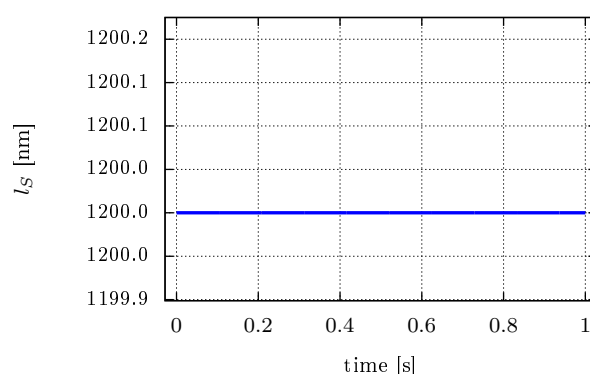
(i) F_{CBS} - steady state force in overlap according to degree of actin-myosin overlap.



(j) $\frac{N_{dl}}{m_{cb}}$ - number of attached cross-bridges in cross-section (per dl).

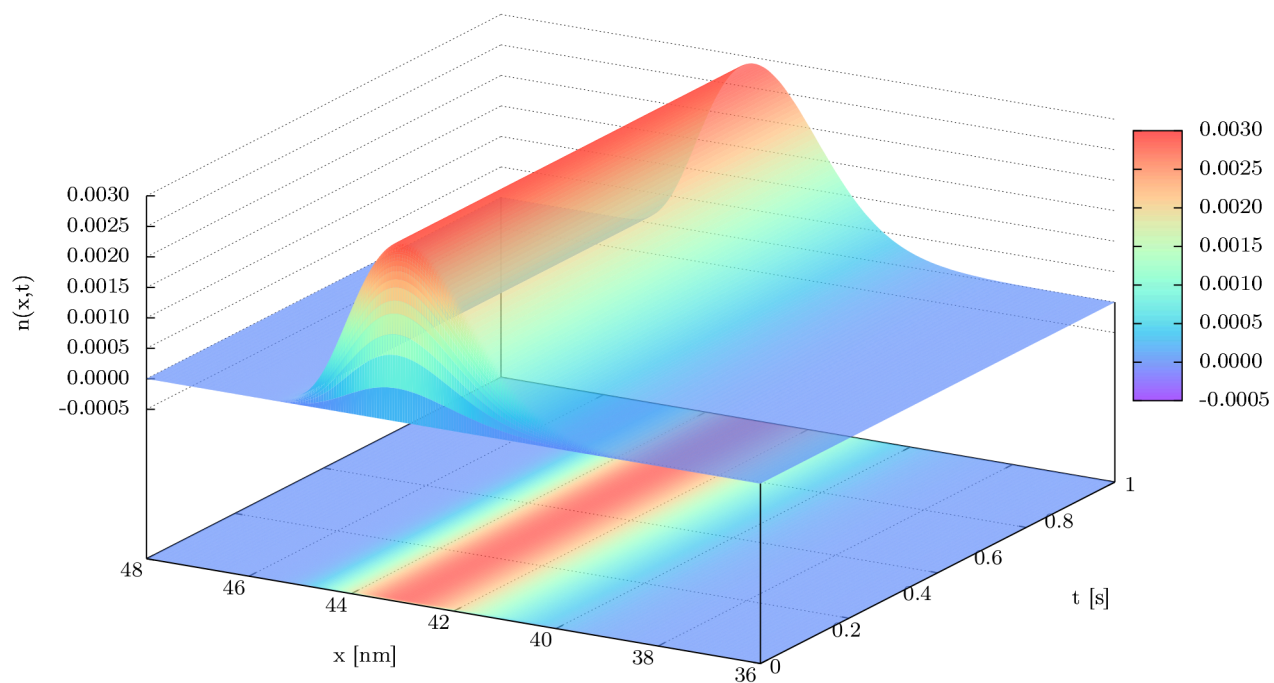
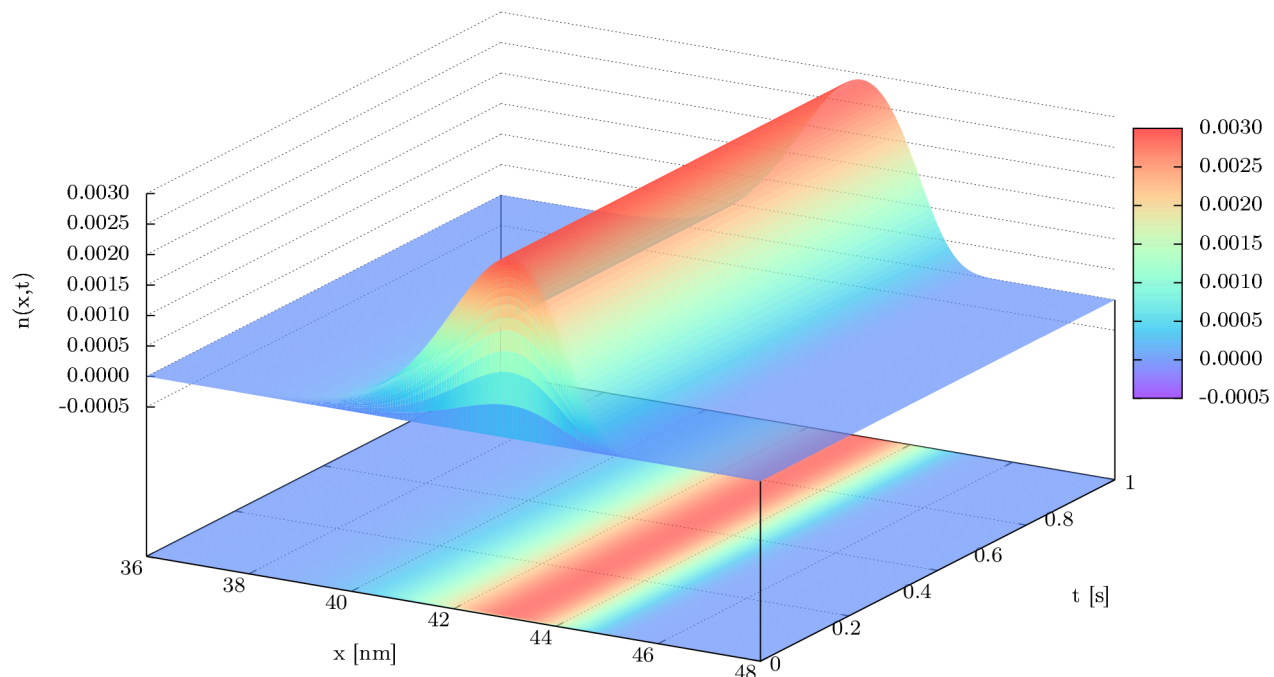


(k) $\frac{N}{m_{cb}}$ - number of attached cross-bridges.



(l) l_S - length of half-sarcomere.

Figure 7.2: Properties of isometric contraction.



(m) $n(x,t)$ time evolution during isometric contraction $v = 0 \text{ nm s}^{-1}$.

Figure 7.2: Properties of isometric contraction.

Comments on results of isometric contraction simulation

The graphical results of isometric contraction are presented namely to show that the modified three filament cross-bridge model does not break the parts of classical cross-bridge theory and two sliding filament theory, which are traditionally believed to be sufficiently explained by original Huxley's model. In the case of isometric contraction, the velocity of contraction is zero $v = 0$. Therefore, no geometrical properties as actin-myosin overlap l , titin stretch l_T , sarcomere length l_S changed. Accordingly, only dynamic properties, which can be observed, are sarcomere force F_S and $n(x, t)$ evolution in a course of time reaching their steady-state values after a while.

The force F_S as depicted in figure 7.2a is in this case only result of active force, i.e. of cross-bridge cycling, without any contribution of passive forces exerted by titins. Although the titin filaments are believed to be also modified according to proposed mechanism in [40], they are not stretched and therefore exert no force. The graphical results of sarcomere force F_S during isometric contraction can be compared for example to measured results as in figure 2.8 on page 44.

7.3 Concentric Isotonic Contraction

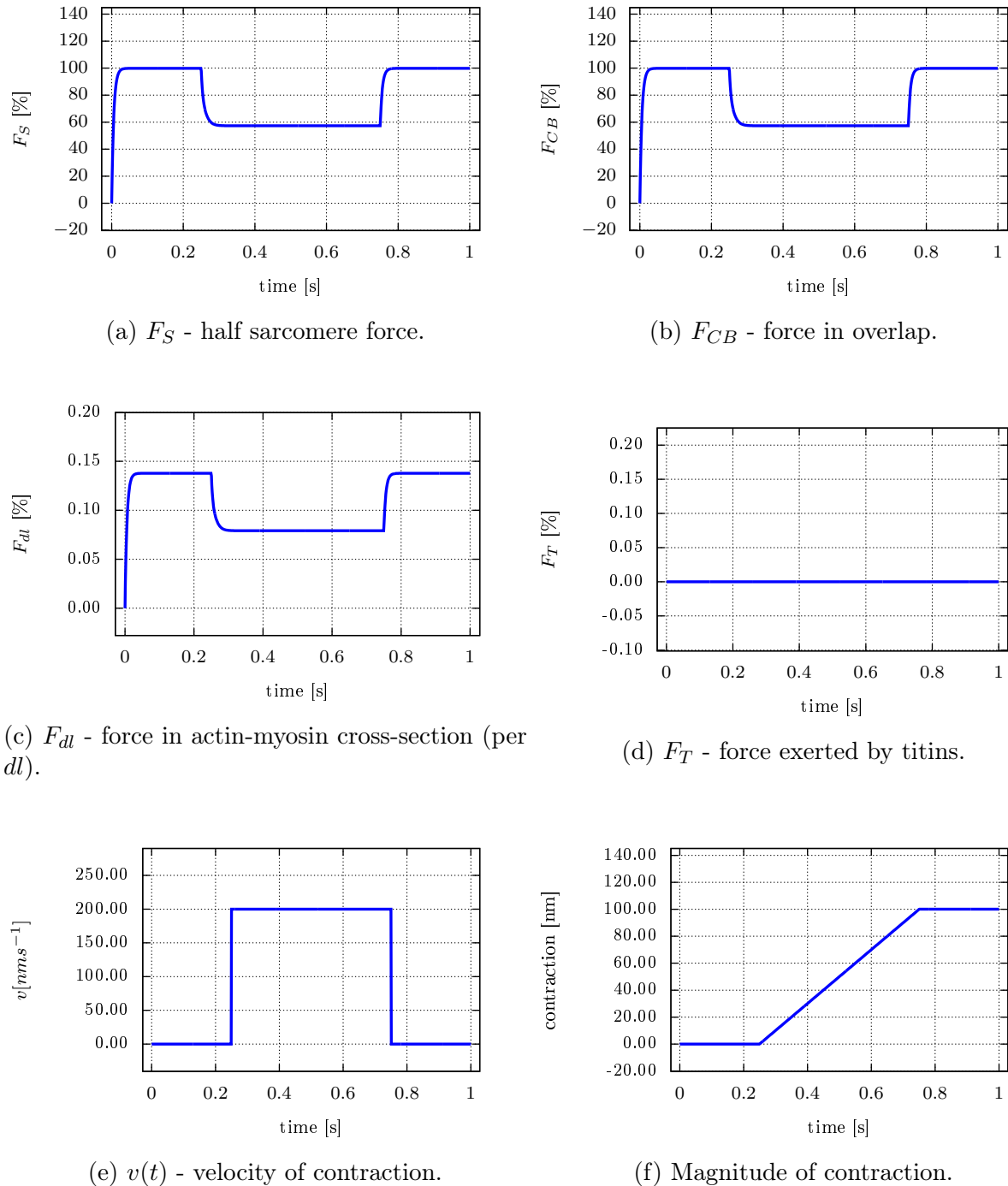
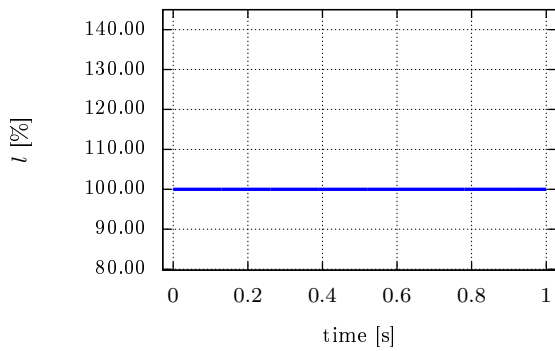
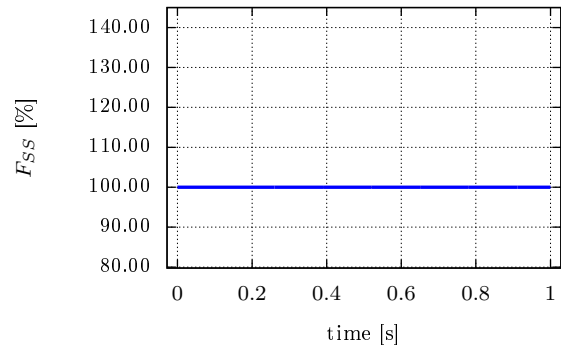


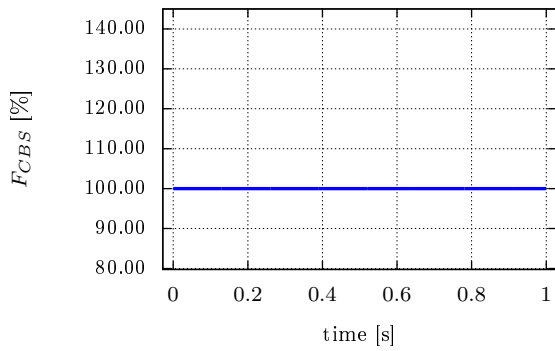
Figure 7.3: Properties of concentric contraction.



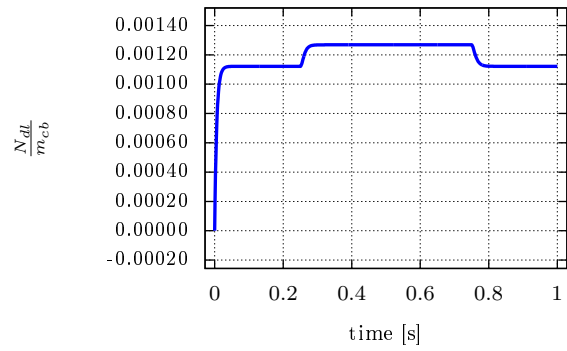
(g) l - magnitude of actin-myosin overlap.



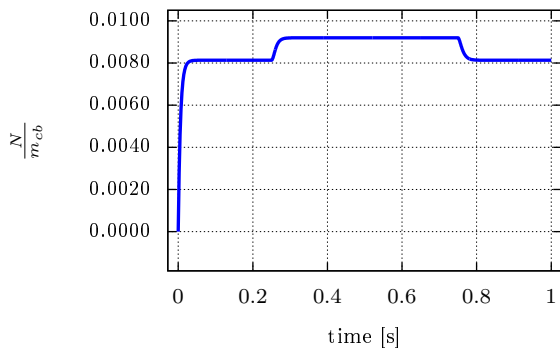
(h) F_{SS} - steady state force of half sarcomere according to degree of a-m overlap.



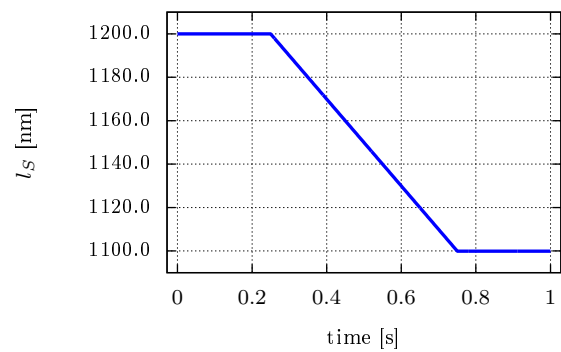
(i) F_{CBS} - steady state force in overlap according to degree of actin-myosin overlap.



(j) $\frac{N_{dl}}{m_{cb}}$ - number of attached cross-bridges in cross-section of overlap.

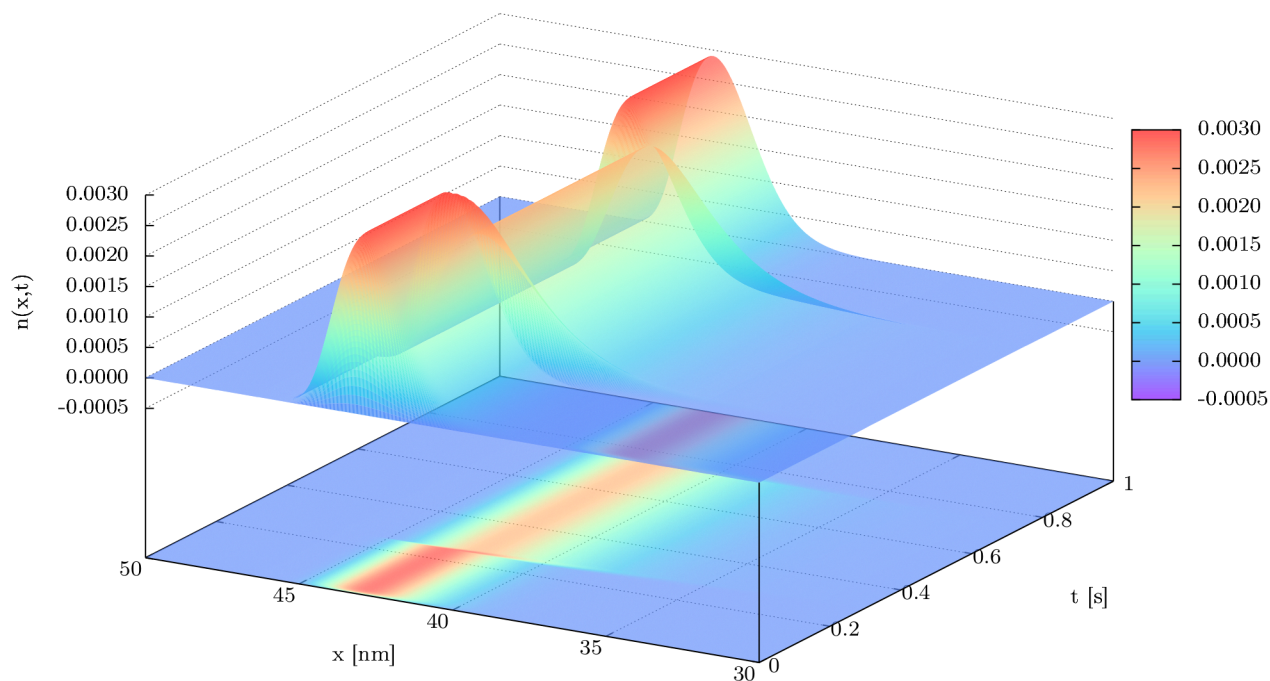
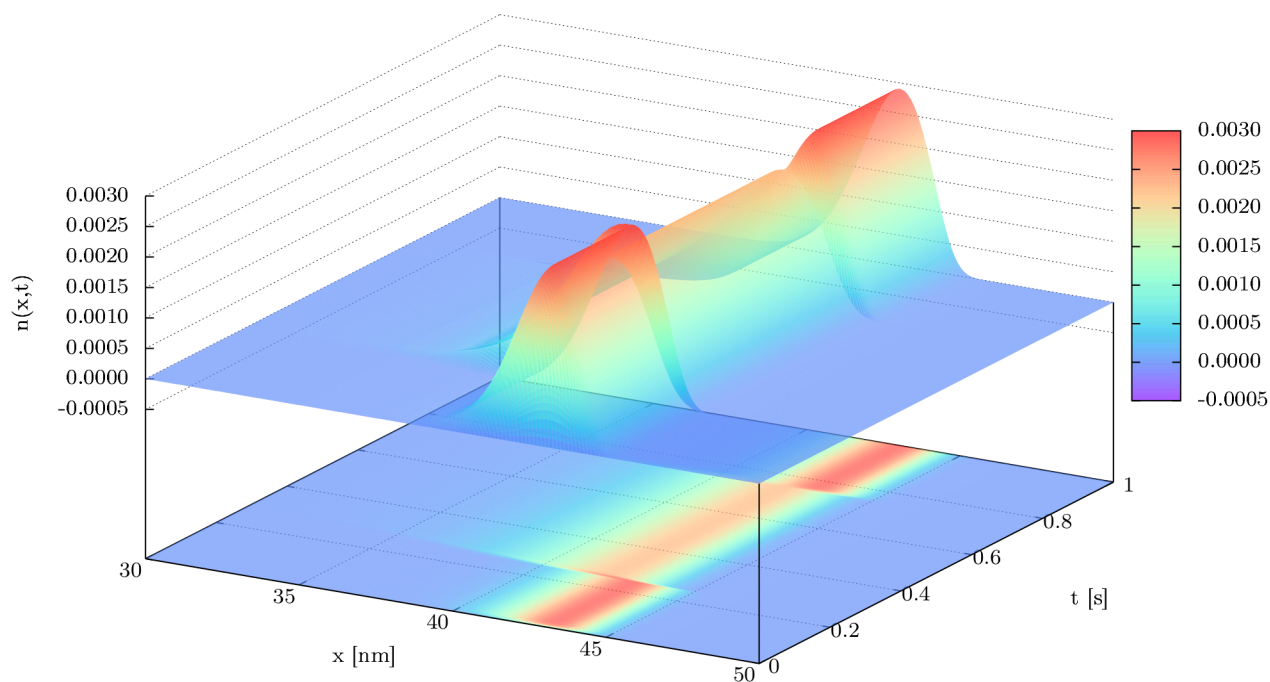


(k) $\frac{N}{m_{cb}}$ - number of attached cross-bridges.



(l) l_S - length of half-sarcomere.

Figure 7.3: Properties of concentric contraction.



(m) $n(x,t)$ evolution during concentric contraction with velocity of $v = 200 \text{ nm s}^{-1}$.

Figure 7.3: Properties of concentric contraction.

Comments on the results of isotonic concentric contraction simulation

The concentric contraction of muscles is characterized with force decrease once the contraction is triggered from initial isometric state. The parameters in original Huxley's model were tuned up according to Hill's curve depicting force-velocity relationship of isotonic concentric contraction. On account of results of Huxley's model, the concentric contraction is traditionally regarded as sufficiently understood in cross-bridge theory and two sliding filaments theory. The exception in sufficient explanation of this kind of contractile activity is the history dependent phenomenon called force depression following after concentric contraction, where the resulted force is smaller than the isometric force at corresponding sarcomere length (actin-myosin overlap).

The main aim of presented simulation results of concentric contraction was to show that the derived three filament cross-bridge model is in concordance with already achieved results and does not break the parts of cross-bridge theory, which are already considered to be sufficiently understood. Unfortunately, it is worth to notice here that the derived three filament cross-bridge model also do not contribute to the explanation of force depression.

The force-time relationship of simulated isotonic concentric contraction with a speed of 200 nms^{-1} of half-sarcomere is depicted in figure 7.3a. The force decrease is a result of the effect of $n(x, t)$ distribution change due to applied velocity. More concretely, the impact of velocity on $n(x, t)$ distribution is that the cross-bridges are shifted to the region of x end-to-end distances, where the resulted summarized force of single cross-bridges is smaller than in distribution of isometric state.

The time evolution of distribution $n(x, t)$ of the number of attached cross-bridges with particular x distances during concentric contraction is depicted in figure 7.3m. Beside other results, the time evolution of $n(x, t)$ distribution showed that after contractile activity, the shape of distribution reached the same shape as before the contractile activity was triggered from isometric state. It might be worthwhile to notice here that the shape of distribution during contractile activity and after contractile activity might be skewed by the mentioned

balance error on the conservation of the number of cross-bridges. The results of force-time relationship in figure 7.3a might be compared with experimentally measured results as in figure 2.12 on page 47 and in figure 2.13 on page 47.

Since the simulation represented the contraction in the region of the plateau of Gordon's graph, the actin-myosin filaments overlap stayed constant at its maximal value all the time - see figure 7.3g. Therefore, after the contractile activity ceased, the sarcomere force increased again to its maximal value. This not reflects the measured data which is characteristic with mentioned force depression. This discrepancy in comparison to measured data also indicates the direction of possible next research.

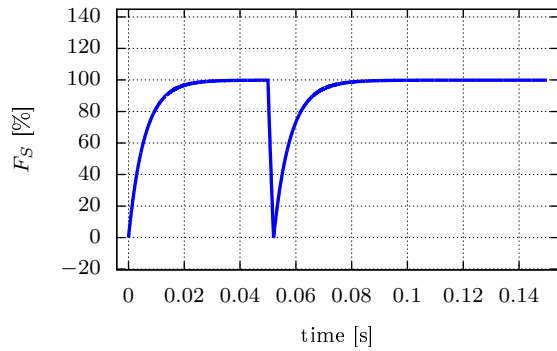
The results depicted in figures 7.3j and 7.3k might look as a paradox, because they showed that during the course of concentric contraction the number of attached cross-bridges is higher in comparison to isometric state, but the force is smaller than in isometric state. The explanation of this is as indicated above. Although the model predicted more attached cross-bridges than in isometric state, the distribution of the number of these cross-bridge is shifted by velocity to such extent of x distances that the resulted force is still smaller. The results of this is a fact that in a representative cross-section of actin-myosin overlap is produced less force - see the figure 7.3c than in isometric state.

Note that exactly these results of the number of attached cross-bridges as in figures 7.3j and 7.3k are skewed by the mentioned error on the conservation of cross-bridges in proposed model as well as in classical Huxley's model. Nevertheless, the nature of the force decrease by shifted $n(x, t)$ distribution is valid and showed the principle of force decrease during transient state of concentric contraction.

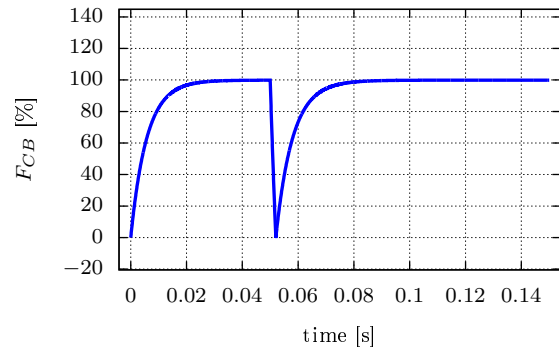
On account of integrated modified properties of titin filaments into derived three filament cross-bridge model, the force as predicted by model during the concentric contraction is still only the result of cross-bridges activity. The titin, although considered modified by Ca^{2+} and attached to actin filaments, is considered to produce no force, because it is rather buckled as a free band (one-directional spring) than stretched during this kind of contraction. Therefore it produces zero force - see figure 7.3d. Obviously, it might be considered that the buckled states of titins might contribute to the phenomenon of force

depression. But this effect must be studied more profoundly on account of its physiological background.

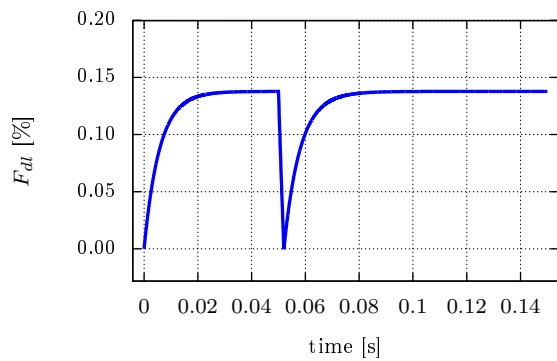
7.3.1 Sudden shortening



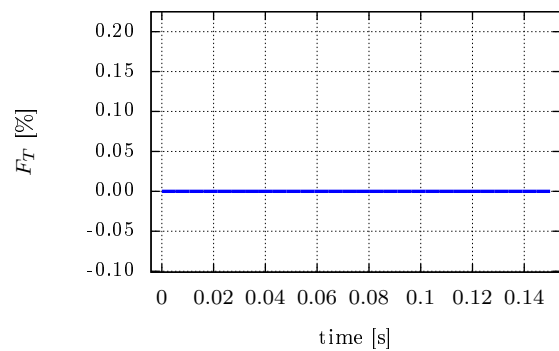
(a) F_S - half sarcomere force.



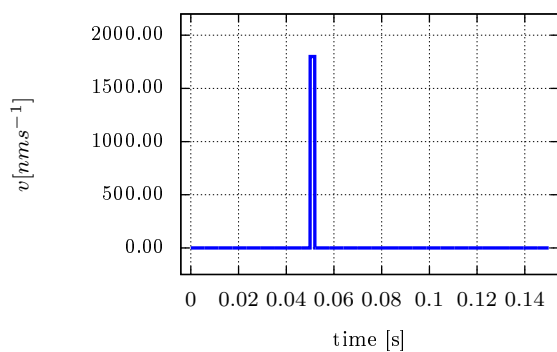
(b) F_{CB} - force in overlap.



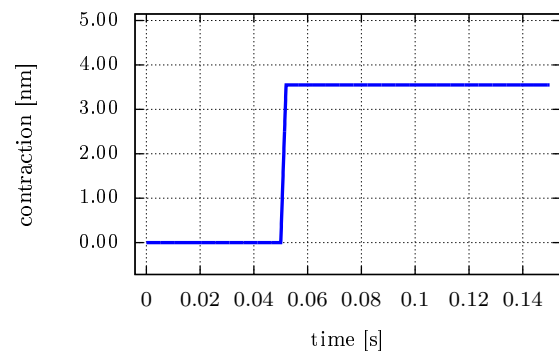
(c) F_{dl} - force in cross-section of actin-myosin overlap (per dl).



(d) F_T - force exerted by titins.

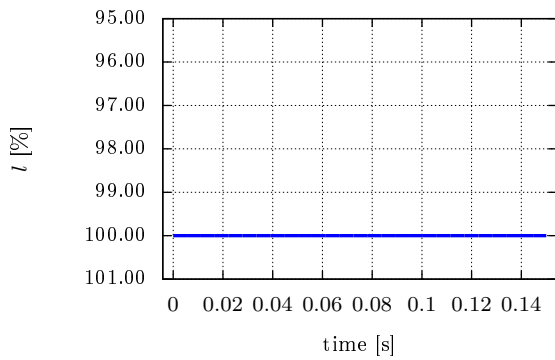


(e) $v(t)$ - velocity of contraction.

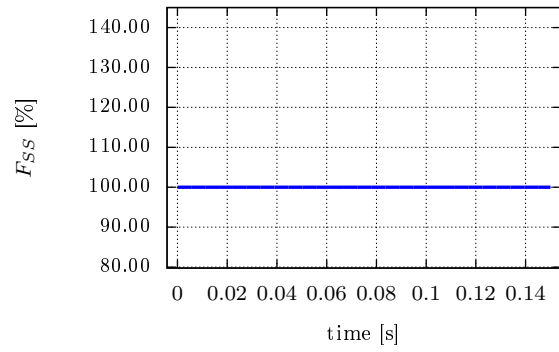


(f) Magnitude of contraction.

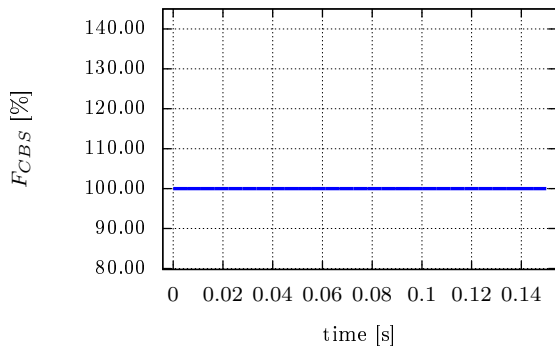
Figure 7.4: Properties of contraction during sudden shortening.



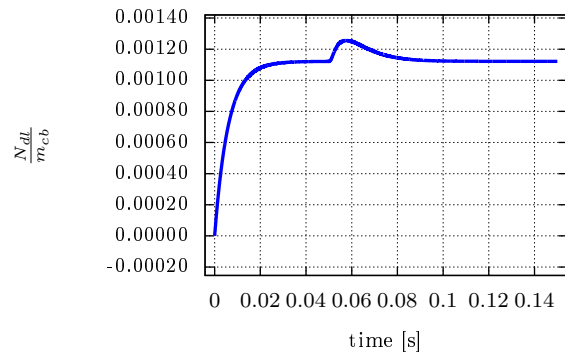
(g) l - magnitude of actin-myosin overlap.



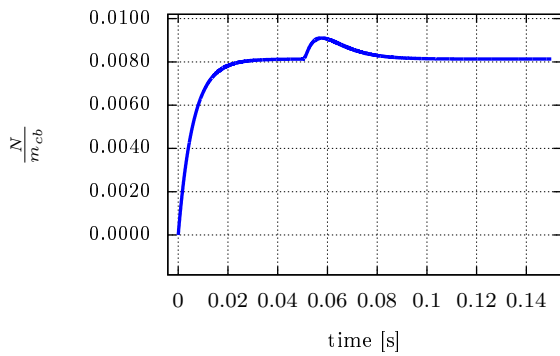
(h) F_{SS} - steady state force of half sarcomere according to degree of a-m overlap.



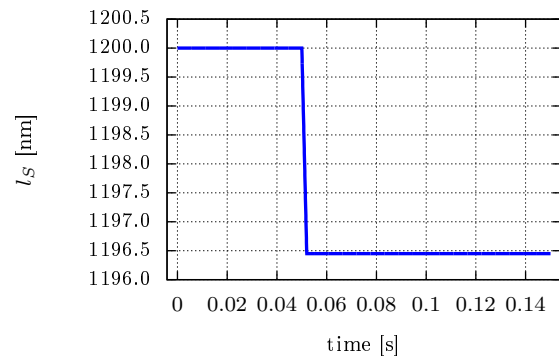
(i) F_{CBS} - steady state force in overlap according to degree of a-m overlap.



(j) $\frac{N_{dl}}{m_{cb}}$ - number of attached cross-bridges in cross-section of a-m overlap.

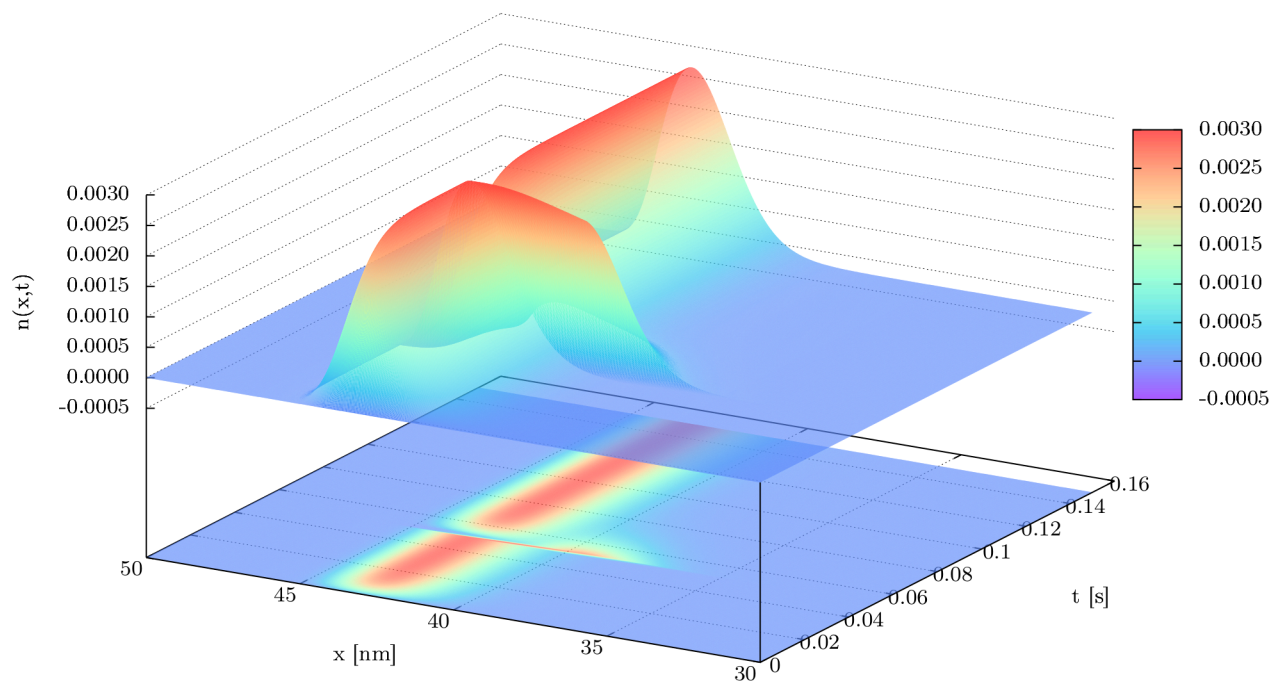
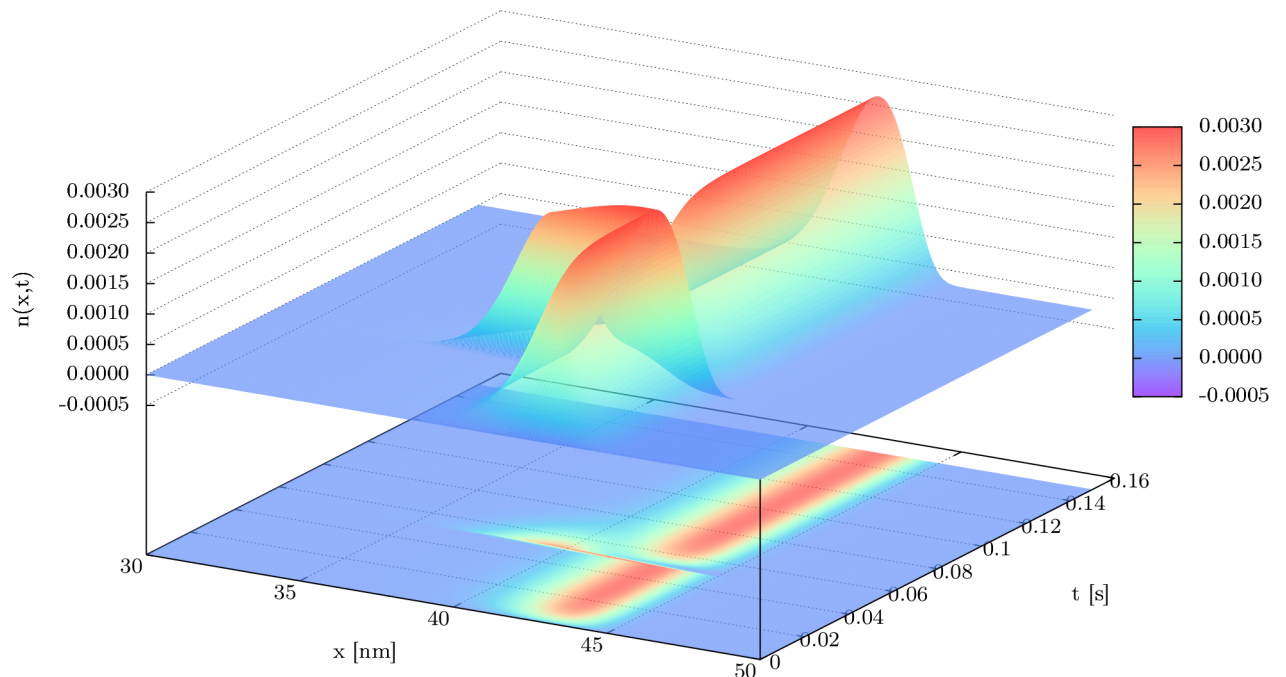


(k) $\frac{N}{m_{cb}}$ - number of attached cross-bridges.



(l) l_S - length of half-sarcomere.

Figure 7.4: Properties of contraction during sudden shortening.



(m) $n(x,t)$ time evolution during simulation of sudden shortening with $v = 1800 \text{ nm s}^{-1}$.

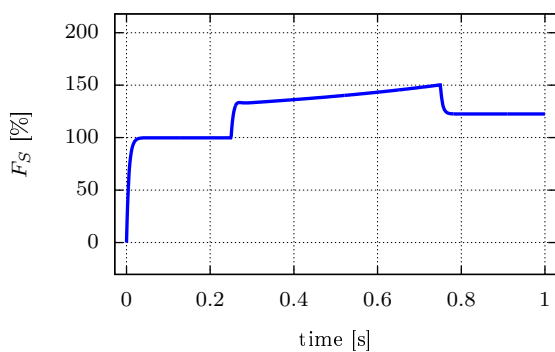
Figure 7.4: Properties of contraction during sudden shortening.

Comments on results of sudden shortening of a half-sarcomere

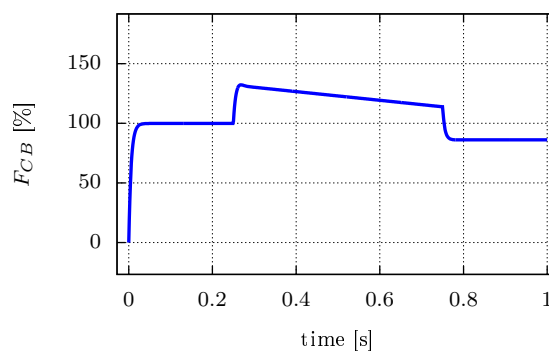
Sudden shortening is a special case of concentric contraction, where the sarcomere is suddenly subjected to quick shortening change starting from its initial isometric contraction state. After this quick release, the sarcomere undergoes quick shortening in its length with simultaneous quick decrease of force. Since the sudden shortening is the special case of concentric contraction, all depicted graphs describe basically the same properties as in discussion on preceding results of concentric contraction.

Again, the main aim of these results was to show that proposed three filament cross-bridge model is also able to simulate this special case of contraction. The results of force evolution during sudden shortening as in figure 7.4a and sarcomere length change as in figure 7.4l can be compared to experimentally obtained results as in figure 2.15 on page 49.

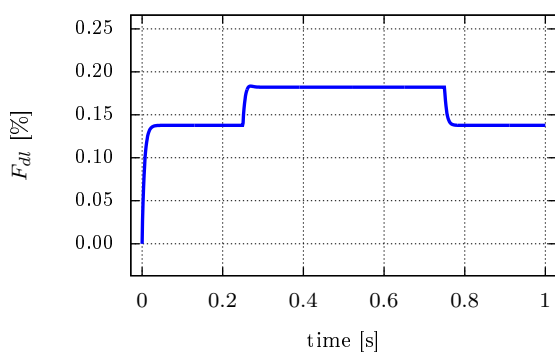
7.4 Eccentric Contraction (stretch of half-sarcomere)



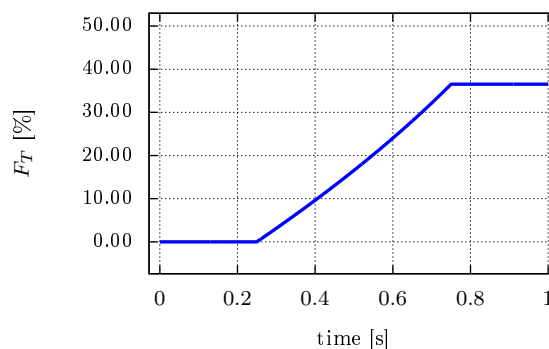
(a) F_S - half sarcomere force.



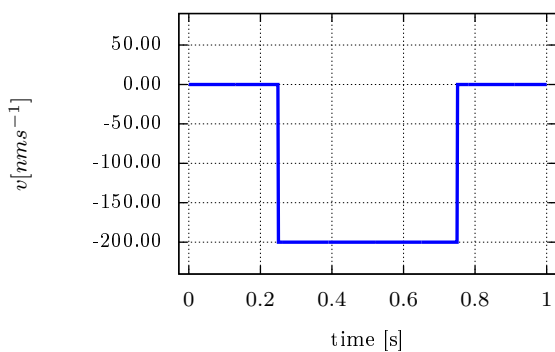
(b) F_{CB} - force in overlap.



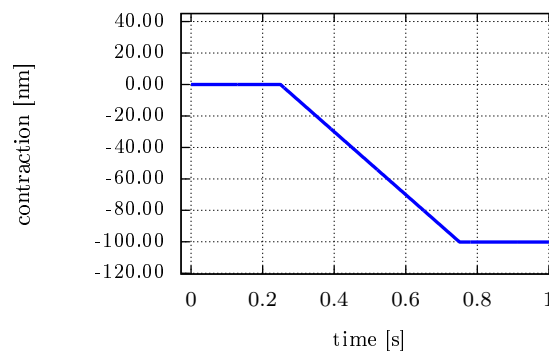
(c) F_{dl} - force in cross-section of a-m overlap (force per dl).



(d) F_T - force exerted by titins.

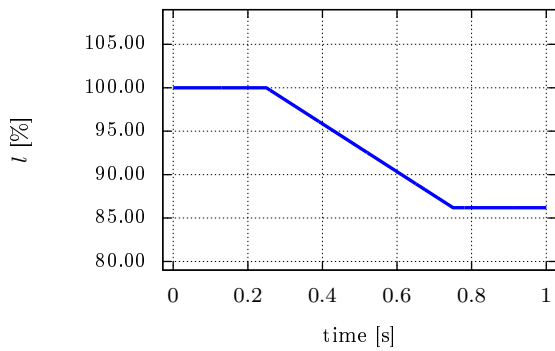


(e) $v(t)$ - velocity of contraction.

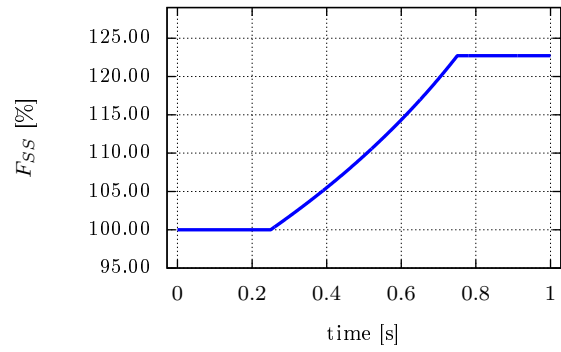


(f) Magnitude of contraction.

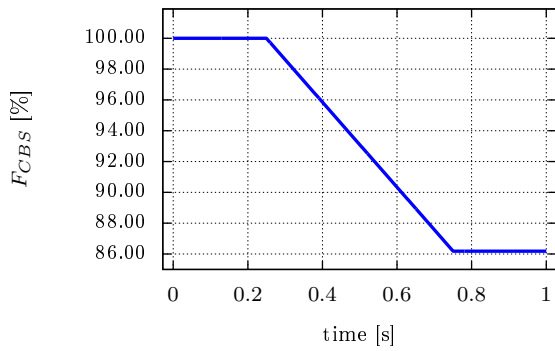
Figure 7.5: Properties of eccentric contraction.



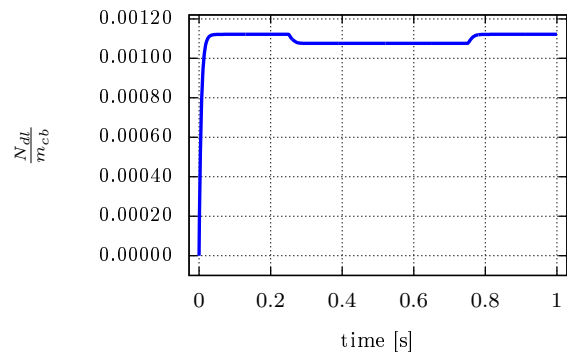
(g) l - magnitude of actin-myosin overlap.



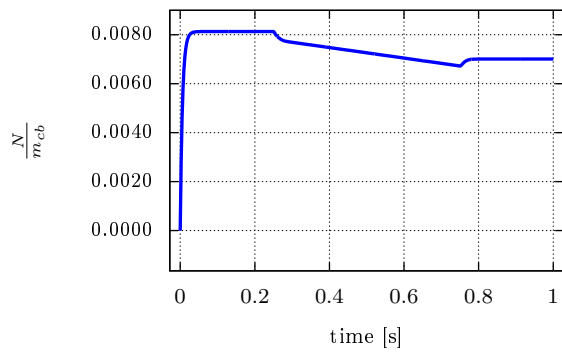
(h) F_{SS} - steady state force of half sarcomere according to magnitude of contraction.



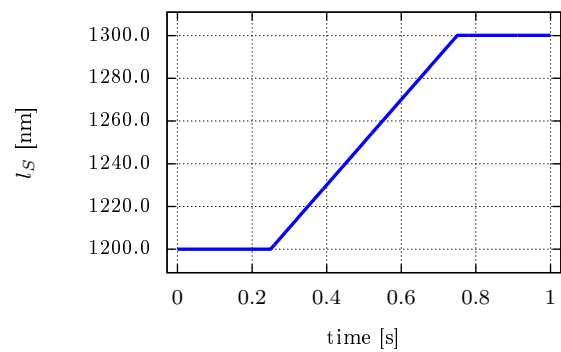
(i) F_{CBS} - steady state force in overlap according to degree of actin-myosin overlap.



(j) $\frac{N_{dl}}{m_{cb}}$ - number of attached cross-bridges in cross-section of a-m overlap.

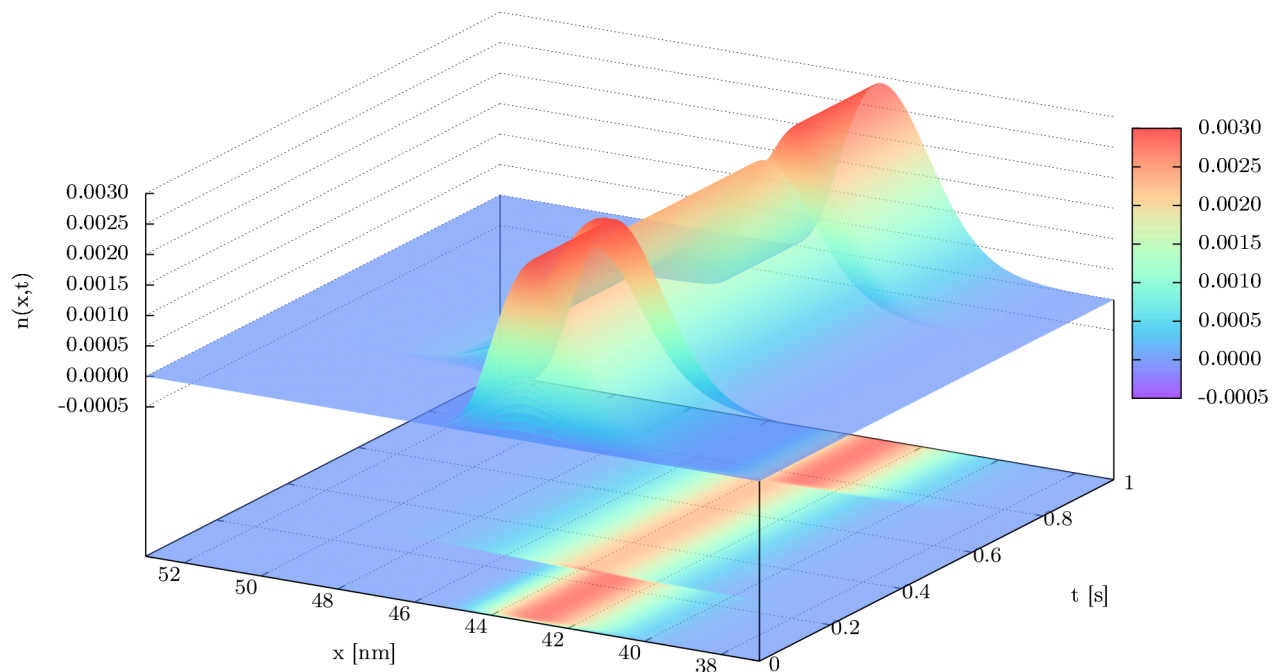
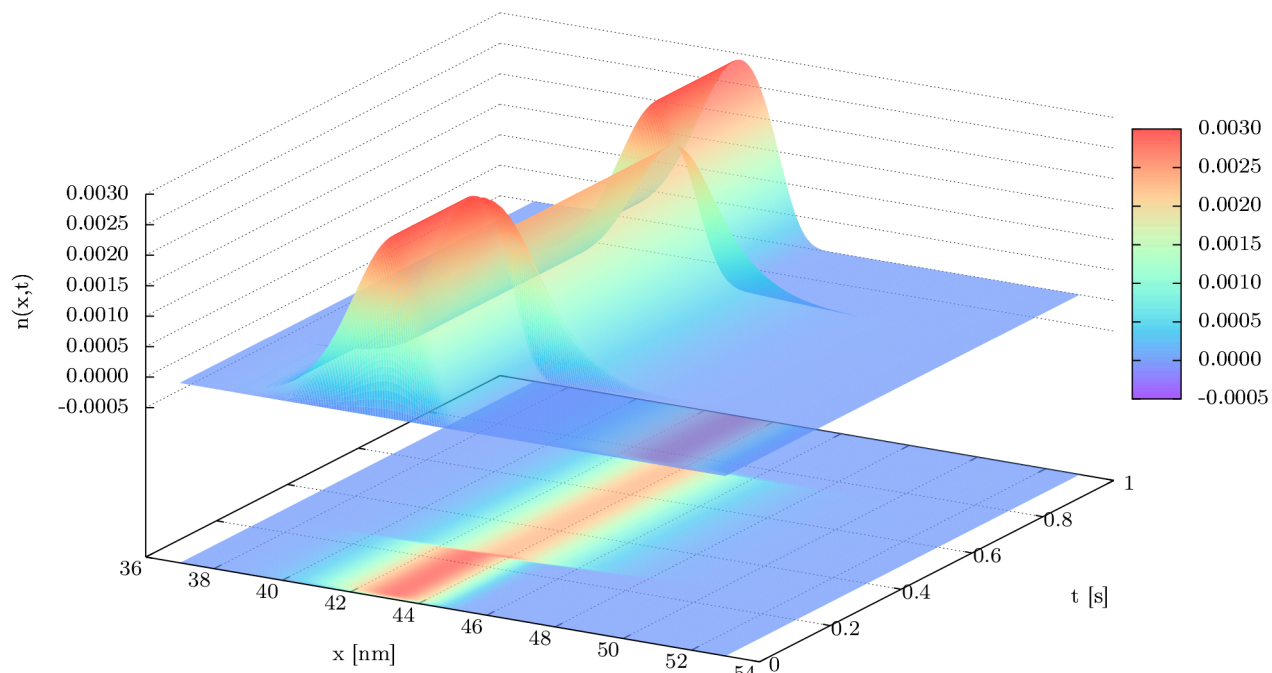


(k) $\frac{N}{m_{cb}}$ - number of attached cross-bridges.



(l) l_S - length of half-sarcomere.

Figure 7.5: Properties of eccentric contraction.



(m) $n(x,t)$ time evolution during eccentric contraction with $v = -200 \text{ nm s}^{-1}$.

Figure 7.5: Properties of eccentric contraction.

Comments on graphical results of eccentric contraction simulation

The results of eccentric contraction simulation are the most important results of submitted dissertation thesis. To recall the basic properties in brief, the eccentric contraction as observed in experiments on all hierarchical levels of skeletal muscles is characterized with force increase once the contraction is triggered from its initial isometric contraction. As soon as the contractile activity ceases, the force is characterized with force decay to lower steady-state magnitude of force - see experimental results as in figures 2.16 on page 50, 2.17 on page 51, 2.18 on page 51, 2.20 on page 53. In experiments, the value of steady-state force following after eccentric contraction is higher than the reference isometric force at corresponding length of sarcomere (actin-myosin overlap).

The explanation of force in a course of time during transient state of eccentric contraction and the following magnitude of steady-state force after eccentric contraction remains insufficiently understood in classical cross-bridge theory and two-sliding filaments theory till nowadays. By the use of the derived three filament cross-bridge model, the main aim of presented following results of simulation of eccentric contraction was to contribute to the explanation of the underlying mechanism that affect the shape of force-time relationship during stretch of skeletal muscles as measured in experiments.

The results of simulation of eccentric contraction (stretch) performed by external force with speed of $v = -200nm\ s^{-1}$ on half-sarcomere are depicted in figures 7.5a - 7.5m. Whereas in preceding simulations of isometric and concentric contraction the titin force F_T remained zero because the titin was not stretched or it was rather buckled (one-directional spring), in the case of eccentric contraction the attached titin part as proposed in [40] is supposed to exert force F_T upon stretch.

The resulted force-time relationship $F_S(t)$ of eccentric contraction of a half-sarcomere is depicted in figure 7.5a. Since the titin force F_T is not zero in this case, the resulted force F_S is a sum of active force F_{CB} (see figure 7.5b) and passive force F_T (see figure 7.5d). The magnitude of titin stretch is here supposed to be equal to the absolute value of the magnitude of stretch (contraction) - see figure 7.5f, where is depicted the magnitude of contraction. Although at first glance the titin force F_T might look linear, in a fact it is

described by the non-linear worm-like chain model (equation 7.3 on page 161). Therefore, for small stretches the titin force might be also approximated with linear elastic model.

Simultaneously with the increasing titin force during the half-sarcomere stretch, the cross-bridge mechanism exerts the force F_{CB} as depicted in figure 7.5b. The force-time relationship of force F_{CB} is in this case affected namely by two factors:

- by the velocity of stretch,
- by the change of the degree of actin-myosin overlap during contraction.

As can be seen in figure 7.5b, the cross-bridge force F_{CB} firstly quickly increases. This is a result of the shift of the attached cross-bridges to the extent of x -end-to-end distances, where the single cross-bridges produce higher force according to their force(f_{cb})- x end-to-end distance relationship (as measured in [62], [63], described by equation 7.19 on page 164). Therefore during eccentric contraction, the force in a representative cross-section through the actin-myosin overlap (force per dl) is higher than the force in a representative cross-section of actin-myosin overlap during isometric contraction - see figure 7.5c. The shift of $n(x, t)$ distribution to range of x end-to-end distances with higher values of x is depicted in figure 7.5m, where is presented the $n(x, t)$ distribution evolution during eccentric contraction.

The shift of the distribution $n(x, t)$ to the range of x end-to-end distances with higher values of x has an impact also on the number of the attached cross-bridges. In particular, since the cross-bridges are more stretched and according to the definition of unfolding rate $g(x)$ (equation 7.16 on page 162), greater amount of cross-bridges starts to unfold quicker than in isometric state. This leads to the decrease in a number of attached cross-bridges. This is depicted in figure 7.5j, where is depicted the proportion of the attached cross-bridges in a representative cross-section of actin-myosin overlap (number of attached cross-bridges per dl).

Although the less of cross-bridges are attached in a representative cross-section of actin-myosin overlap during eccentric contraction, the force per cross-section (per dl) of actin-myosin overlap is higher than in isometric state - see figure 7.5c. This is the result of the

shift of the cross-bridges to the such extent of x end-to-end distances, where the sum of forces generated by single cross-bridges is higher than in isometric state, although less of cross-bridges is attached. This effect is further explained and showed in figures 7.6 and 7.7.

More particular, the figure 7.6 shows the shapes of $n(x, t)$ distribution of the number (proportion) of attached cross-bridges during eccentric contraction for speeds of stretch $v = 100, 150, 200, 300 \text{ nm s}^{-1}$. For better comparison, the shape of distribution $n(x, t) = n_s(x)$ of isometric contraction is depicted as well. For the simplicity, the sum of the attached cross-bridges in isometric state is expressed and evaluated as $N_{iso} = 100\%$. As can be seen in figure 7.6, the numbers of attached cross-bridges $N_{100}, N_{150}, N_{200}, N_{300}$, where the subscripts denote the associated speed, are decreasing with the increasing speeds of stretch.

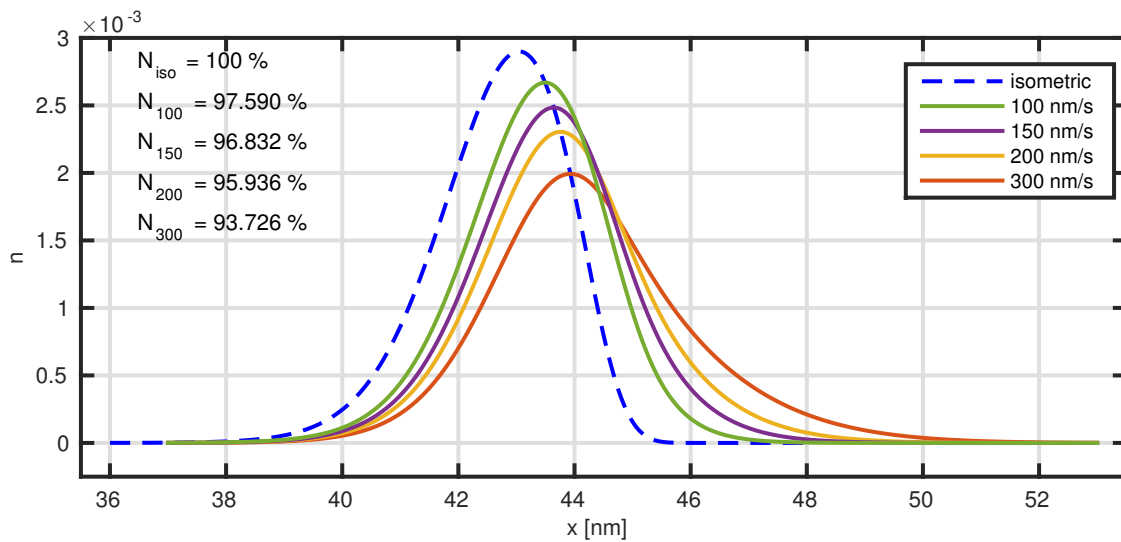


Figure 7.6: Proportion of the number of cross-bridges in $n(x, t)$ distribution during stretches of speeds $v = 0, 100, 150, 200, 300 \text{ nm s}^{-1}$.

Simultaneously with the increasing speed of stretch, the shape of distribution $n(x, t)$ is shifted to the range of x end-to-end distances with higher values of x . The figure 7.7 demonstrates that although the number of cross-bridges is decreasing with the increasing

speed of stretch, the sum of force distribution expressed as:

$$\int_{-\infty}^{\infty} f_{cb}(x)n(x,t)dx \quad (7.29)$$

is increasing with the speed of stretch. Again for the simplicity, the value of the force of the reference isometric distribution was denoted as $F_{iso} = 100\%$. The values of $F_{100}, F_{150}, F_{200}, F_{300}$ for speed of stretches $v = 100, 150, 200, 300 \text{ nm s}^{-1}$ show increasing manner (see results in figure 7.7). Obviously, it might be expected that after some threshold value of speed, the force $\int_{-\infty}^{\infty} f_{cb}(x)n(x,t)dx$ would begin to decrease until zero because of the likely decreasing number of attached cross-bridges to zero. The results from figures 7.6 and 7.7 are also summarized in table 7.3.

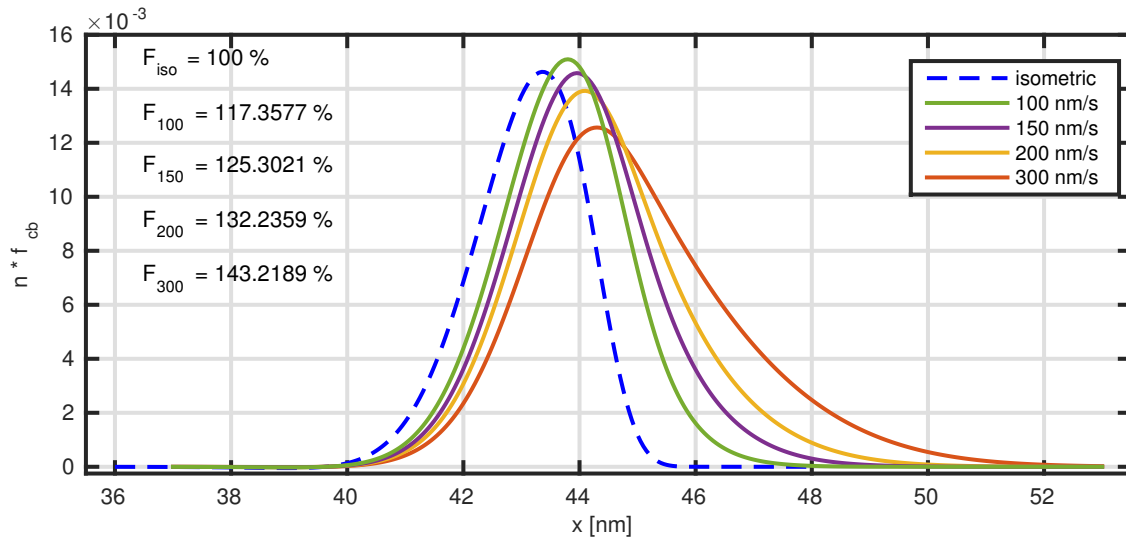


Figure 7.7: Force distribution $f_{cb}(x)n(x,t)$ during stretches of speeds $v = 0, 100, 150, 200, 300 \text{ nm s}^{-1}$.

Besides the shift of distribution $n(x,t)$ due to contractile activity, the second important effect on account of force F_{CB} evolution during eccentric contraction is that the degree of actin-myosin overlap decreases as the sarcomere is being stretched by velocity $v(t)$. The increase in sarcomere length by stretch is depicted in figure 7.5l and the associated decrease of actin-myosin overlap is depicted in figure 7.5g. This has the second important effect on

the evolution of F_{CB} , namely that the number of cross-bridges that can attach decreases - see figure 7.5k. Consequently, once the force F_{CB} is quickly increased due to the distribution shift, it starts to decrease due to the decreasing number of attached cross-bridges. This effect of decreasing force F_{CB} as depicted in figure 7.5b can not be observed in experiments on muscles, myofibrils and sarcomeres due to the fact that the decrease in F_{CB} due to decreasing a-m overlap is "hidden" by the increase of force F_T due to stretch of titin.

speed of stretch	N number of attached cross-bridges	force in distribution
$v [nm s^{-1}]$	$N = \int_{-\infty}^{\infty} n(x, t) dx$	$F = \int_{-\infty}^{\infty} f_{cb}(x) n(x, t) dx$
0	100%	100%
100	97.590%	117.3577%
150	96.832%	125.3021%
200	95.936%	132.2359%
300	93.726%	143.2189%

Table 7.3: The number and force of attached cross-bridges in a representative cross-section through the actin-myosin overlap for different values of speed of stretch of a half-sarcomere.

As already noted above, the eccentric contraction begins with quick increase of force once the muscle is stretched from its initial isometric state. The magnitude of this quick increase depends on the value of speed. For comparison, this can be seen in figures 7.8a - 7.8d, where are the results of half-sarcomere eccentric contraction simulations for speed of stretches of $v = 100, 150, 200, 300 nm s^{-1}$ for the magnitudes of stretches (contraction) of 60, 120, 180nm. From these results, it is apparent that magnitude of the quick increase in force at the beginning of eccentric contraction is increasing with the increasing speed of stretch.

The results 7.8a - 7.8d also show that the magnitude of force decay after the contractile activity ceases is higher for higher speeds of stretch. This effect can be clarified again on account of the magnitude of distribution shift to the higher values of x end-to-end distances. Therefore, as showed in figures 7.6 and 7.7, the difference between force produced by isometric distribution and force produced by distribution in stretch is increasing with speed of stretch. Consequently, the magnitude of force decay that is a results of $n(x, t)$

distribution recovery (relax) to its isometric state is greater for higher speeds. The shape of force-time relationships in figures 7.8a - 7.8d can be compared to the experimentally achieved results as presented in figures 2.17 on page 51, 2.18 on page 51, 2.20 on page 53.

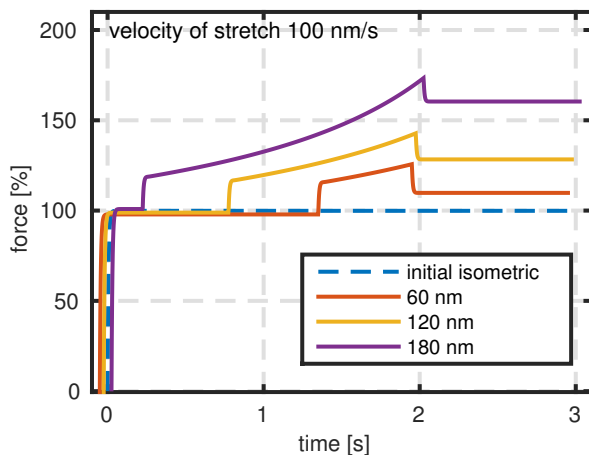
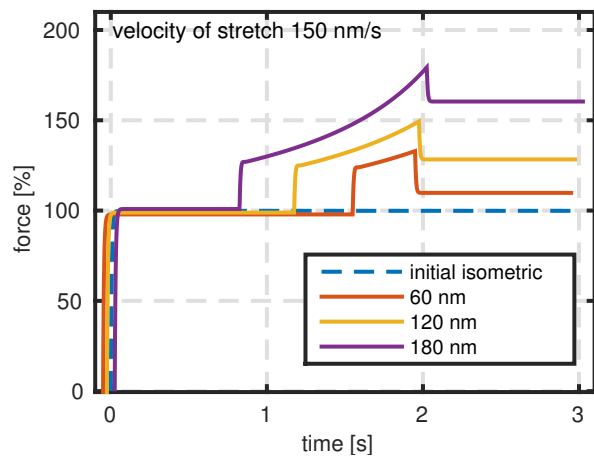
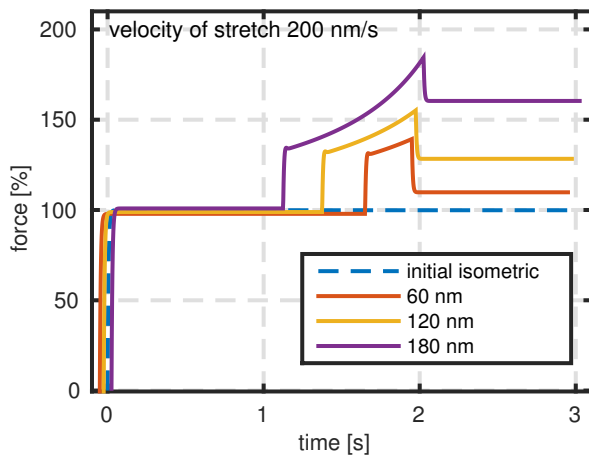
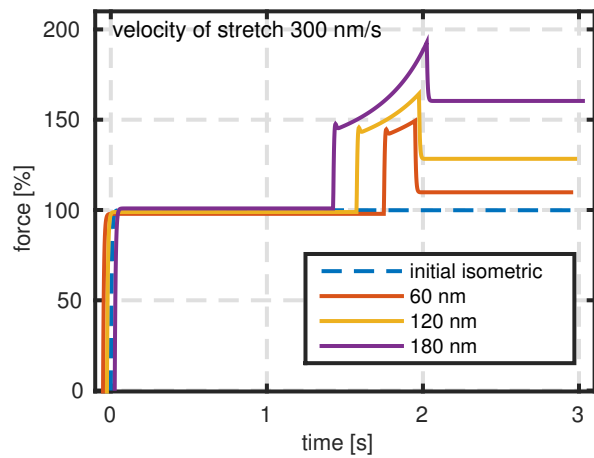
(a) $v = -100 \text{ nm s}^{-1}$ (b) $v = -150 \text{ nm s}^{-1}$ (c) $v = -200 \text{ nm s}^{-1}$ (d) $v = -300 \text{ nm s}^{-1}$

Figure 7.8: Simulation of eccentric contraction for length of stretches 60, 120, 180 nm with speeds of $-100, -150, -200, -300 \text{ nm s}^{-1}$.

Comparison between classical Huxley's approach based on the two-sliding filament and derived three filament cross-bridge model

Regarding the results of eccentric contraction, it might be worthwhile to depict the differences between classical Huxley's two sliding filaments approach and presented three filaments approach. The difference between those two approaches is demonstrated in figure 7.9. This figure depicts the simulation of eccentric contraction performed by derived three filament model with blue line. The black line shows the result of simulation without considering the titin, i.e. the black line depicts the classical two sliding filament approach.

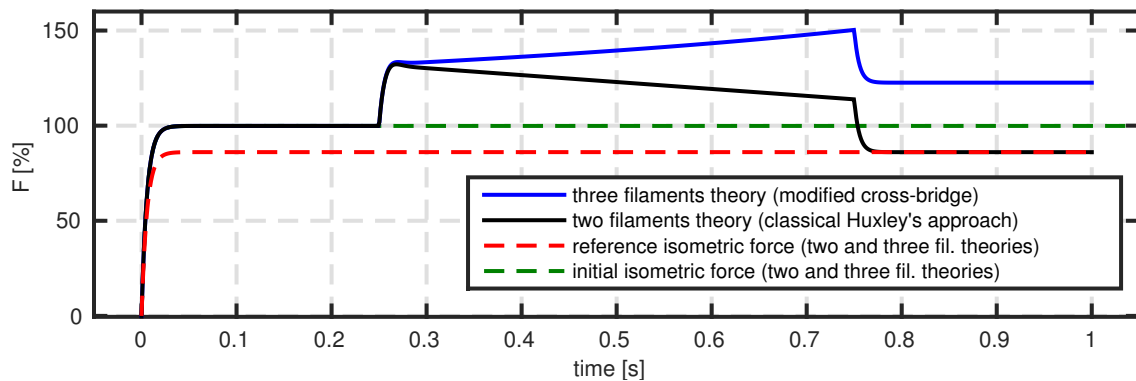


Figure 7.9: Comparison between classical two sliding filament theory (classical Huxley's approach) and three filament theory (proposed three filament cross-bridge model).

As can be seen in this figure, both of these approaches has the same initial isometric force (dashed green line). Further, both of these approaches have the same reference isometric force (dashed red line) at corresponding length of sarcomere (actin-myosin overlap) following after the contractile activity ceases. The difference between those two approaches shows that the simulation based on classical two-sliding filaments approach relaxes towards the steady-state value of force equalled to reference isometric force at corresponding length of sarcomere. This is not in concordance with observed measured results. Whereas the simulation based on proposed three filament approach as proposed in [40] ends with steady-state force which is higher than reference isometric force and even higher than initial isometric force, which better reflects the observed measured results in experiments on all levels of muscle hierarchy.

7.4.1 Properties of steady-state force enhancement

The intrinsic property associated with eccentric contraction is phenomenon called *force enhancement*. To recall this phenomenon, force enhancement is a steady-state property of muscle, where the stretched muscle produces higher force than at corresponding length during isometric contraction [35], [40], [43]. The difference between the value of steady-state force after stretch and the value of isometric force at corresponding length is a value of steady-state force enhancement. The force enhancement is depicted in the result of simulation in figure 7.10 or in experimentally achieved results as in figure 2.19 on page 52.

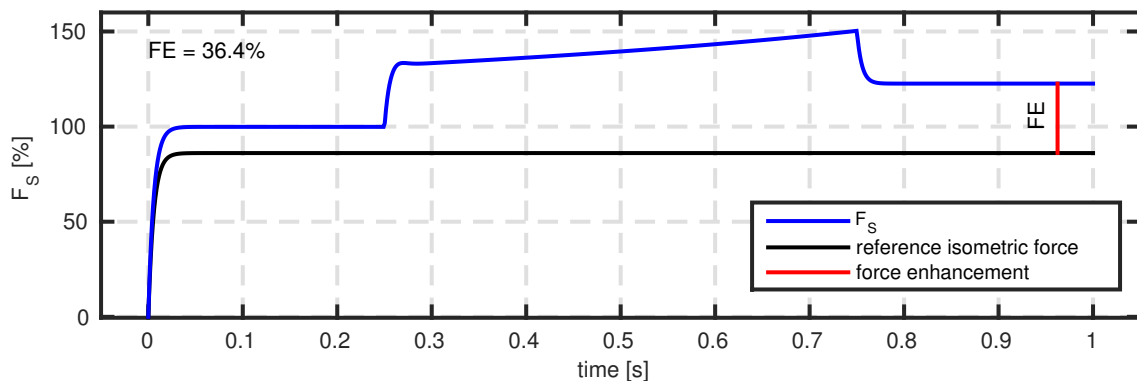


Figure 7.10: Demonstration of force enhancement achieved in simulation. The blue line represents the force-time relationship during eccentric contraction. The black line represents the isometric force at sarcomere length corresponding to the length of sarcomere after stretch.

To test the derived three filament cross-bridge model also on account of basic properties of steady-state force enhancement, the following two main properties of steady-state force enhancement were tested [37]:

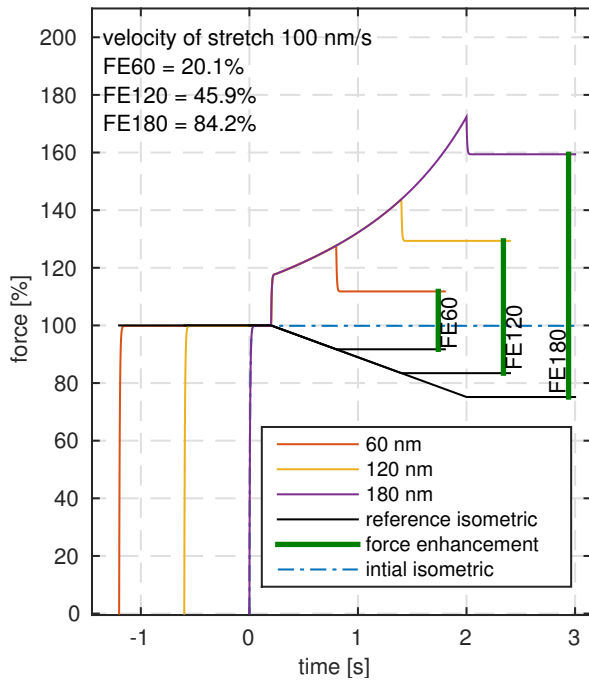
1. the magnitude of steady-state force enhancement is increasing with magnitude of stretch,
2. the magnitude of steady-state force enhancement is independent on the magnitude of the speed of stretch.

The simulation of first mentioned property is depicted in figures 7.11a - 7.11d. The figures are results of simulations, where the half-sarcomere was stretched for the magnitude of stretches 60, 120, 180 nm with various speeds of $v = 100, 150, 200, 300 nm s^{-1}$. The red, yellow and violet lines represent the force-time relationships of eccentric contraction performed for 60, 120, 180 nm . The dashed blue line represents the initial isometric force. The black line represents the reference steady-state isometric force at corresponding length of half-sarcomere (actin-myosin overlap). The green lines represent achieved values of steady-state force enhancements associated to particular magnitudes of stretch. The values $FE_{60}, FE_{120}, FE_{180}$ of achieved force enhancements for mentioned magnitude of stretches are normalized according to maximal isometric force. The figures 7.11a - 7.11d clearly show that the value of force enhancement is increasing with magnitude of stretch. This is consistent with measured experiments. The summary of the values of force enhancement for various stretches is presented in table 7.4.

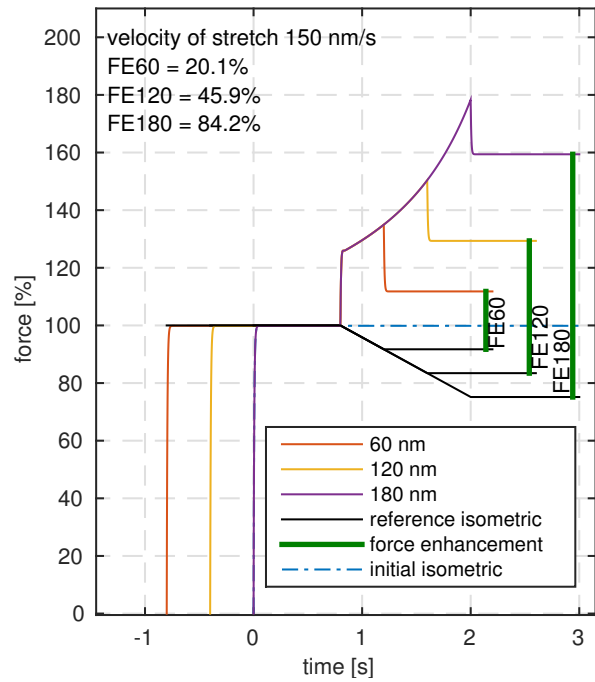
magnitude of stretch nm	steady state force enhancement
60	20.1%
120	45.9%
180	84.2%

Table 7.4: Summary on the values of force enhancement for magnitudes of stretches of 60, 120, 180 nm simulated with speeds of stretches of $v = 100, 150, 200 nm s^{-1}$.

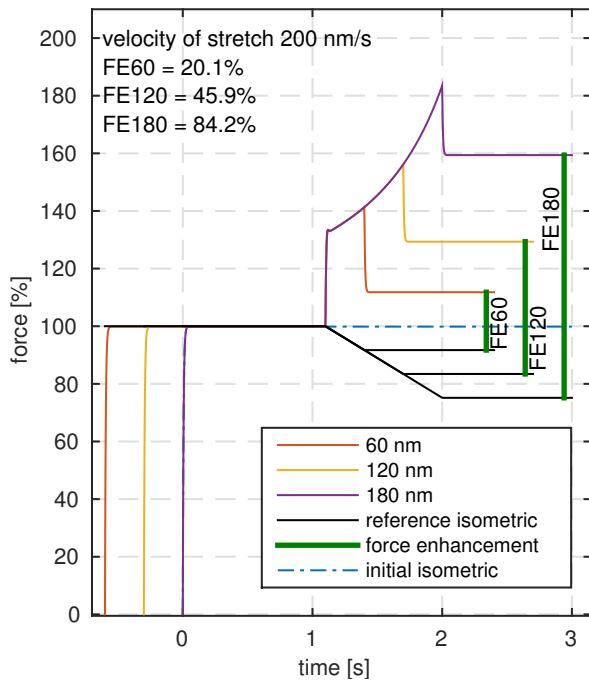
The second mentioned property of steady-state force enhancement that the value of steady-state force enhancement is independent on the speed of stretch is depicted in figures 7.12a - 7.12c. In particular, these figures show that the forces during transient state of eccentric contraction simulated for the same magnitude of stretch but with various speeds relax to the same value of steady-state force after stretch. The figures 7.12a - 7.12c also clearly show that the magnitude of initial quick increase in force during eccentric contraction increases with the magnitude of speed as already mentioned above. This is also valid for the size of force decay after the contractile activity ceases. Therefore in figures 7.12a - 7.12c can be seen that the size of force decay increases with the increasing speed of stretch.



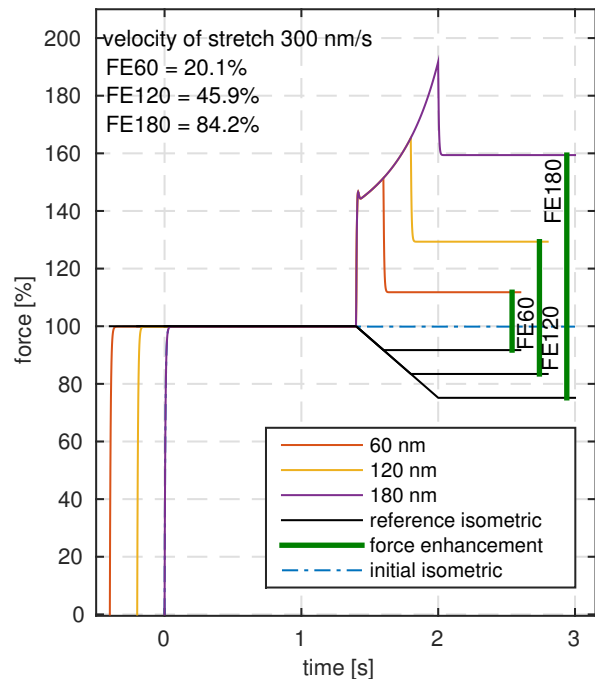
(a) Force enhancements achieved by speed $v = -100 \text{ nm s}^{-1}$ for stretches of magnitudes 60, 120, 180 nm .



(b) Force enhancements achieved by speed $v = -150 \text{ nm s}^{-1}$ for stretches of magnitudes 60, 120, 180 nm .

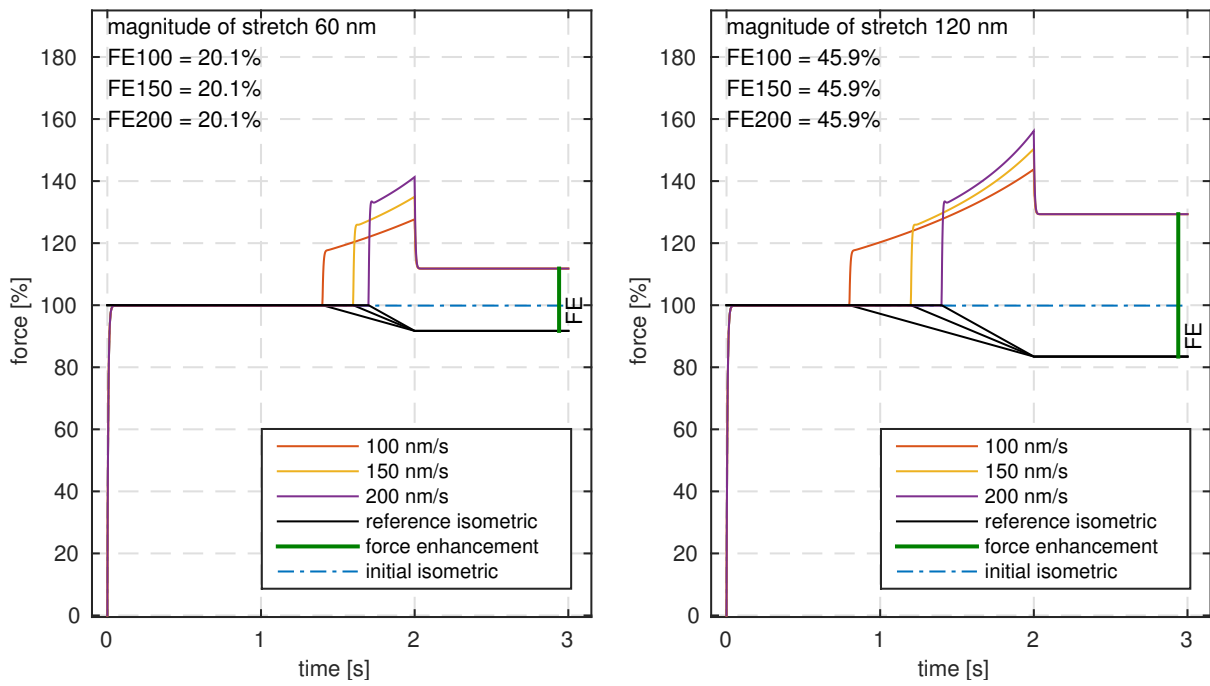


(c) Force enhancements achieved by speed $v = -200 \text{ nm s}^{-1}$ for stretches of magnitudes 60, 120, 180 nm .

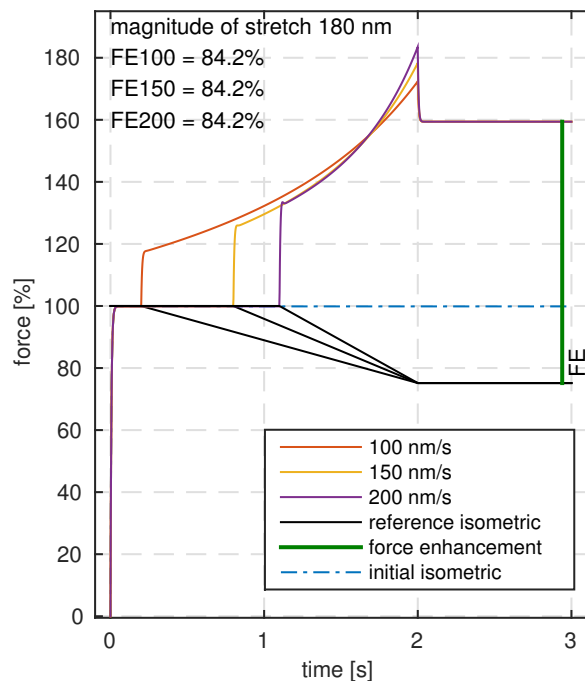


(d) Force enhancements achieved by speed $v = -300 \text{ nm s}^{-1}$ for stretches of magnitudes 60, 120, 180 nm .

Figure 7.11: Simulation of force enhancements conducted for stretches of 60, 120, 180 nm with speeds $-100, -150, -200, -300 \text{ nm s}^{-1}$.



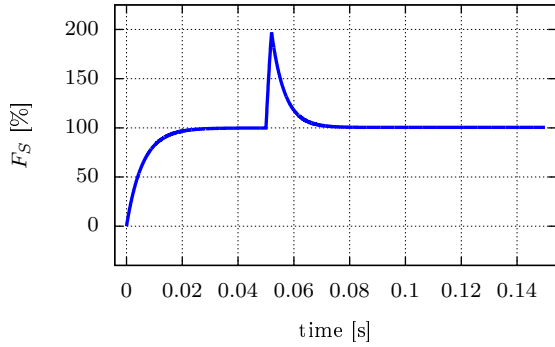
(a) 60nm stretches performed with speeds $-100, -150, -200 \text{ nm s}^{-1}$. (b) 120nm stretches performed with speeds $-100, -150, -200 \text{ nm s}^{-1}$.



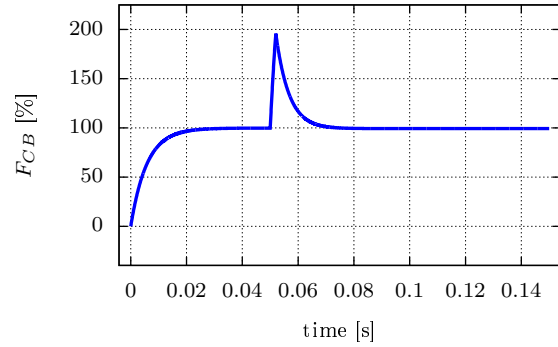
(c) 180nm stretches performed with speeds $-100, -150, -200 \text{ nm s}^{-1}$.

Figure 7.12: Force enhancements performed for stretches of 60nm, 120nm, 180nm with speeds of $-100, -150, -200 \text{ nm s}^{-1}$.

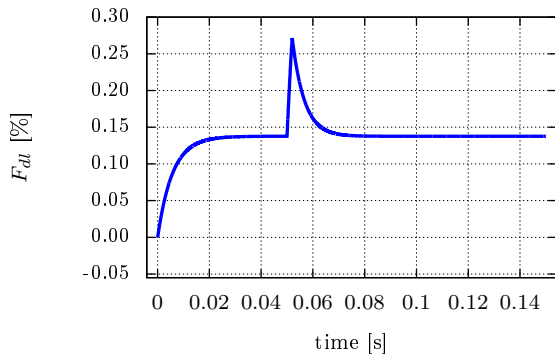
7.4.2 Sudden stretch



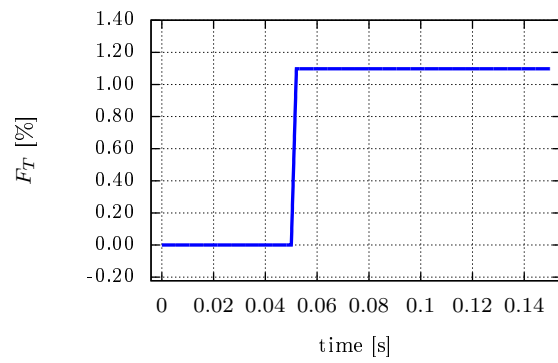
(a) F_S - half sarcomere force.



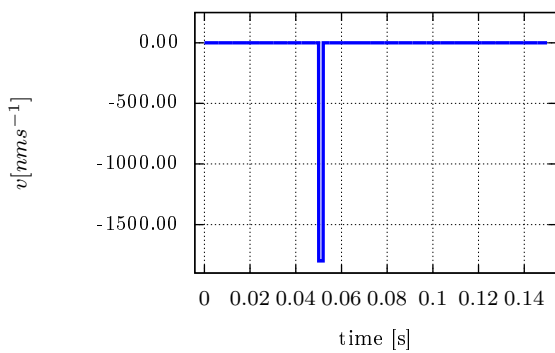
(b) F_{CB} - force in overlap.



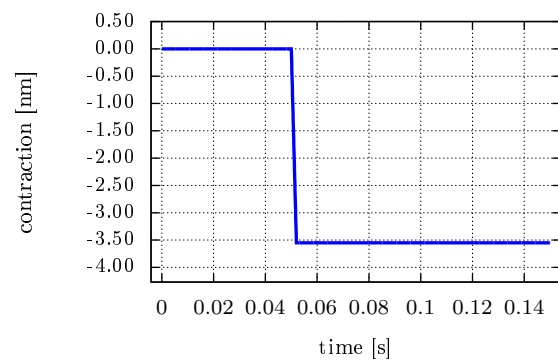
(c) F_{dl} - force in cross-section of actin-myosin overlap (per dl).



(d) F_T - force exerted by titins.

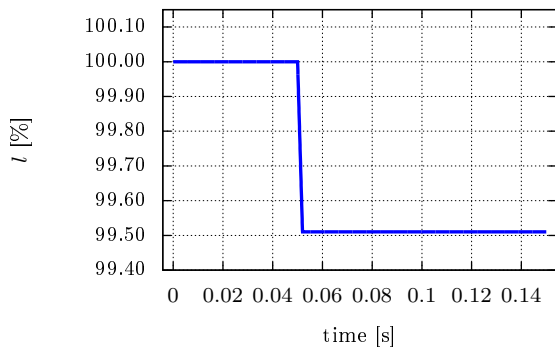


(e) $v(t)$ - velocity of contraction.

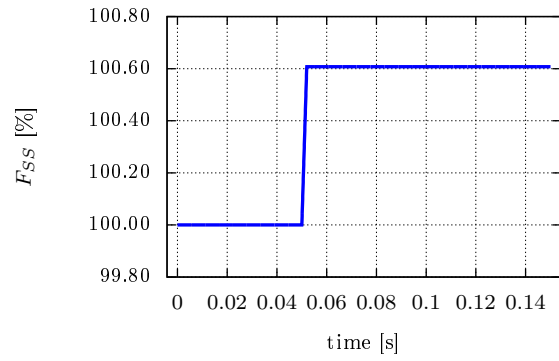


(f) Magnitude of contraction.

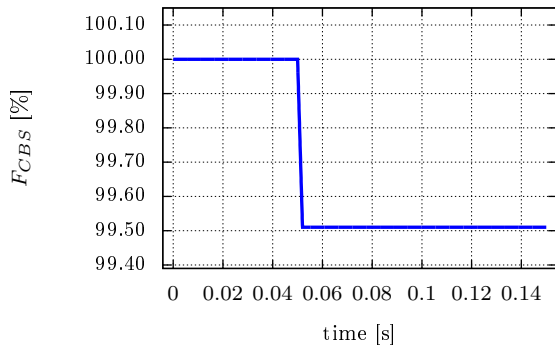
Figure 7.13: Properties of contraction during sudden stretch.



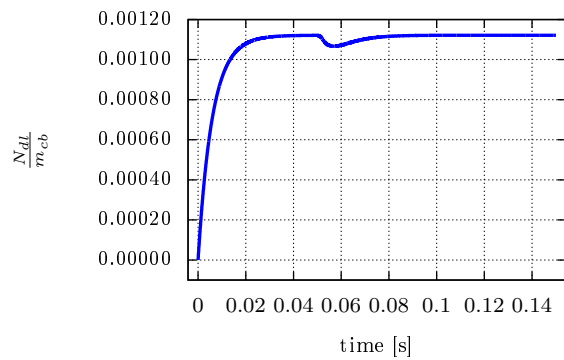
(g) l - magnitude of actin-myosin overlap.



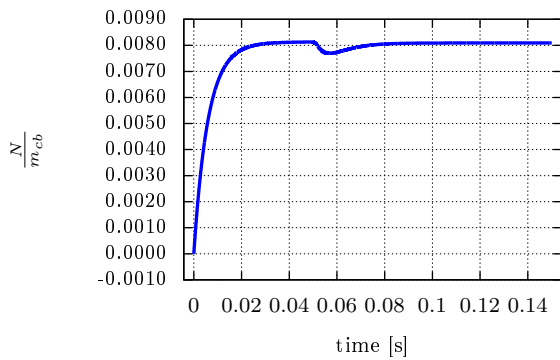
(h) F_{SS} - steady state force of half sarcomere according to magnitude of contraction.



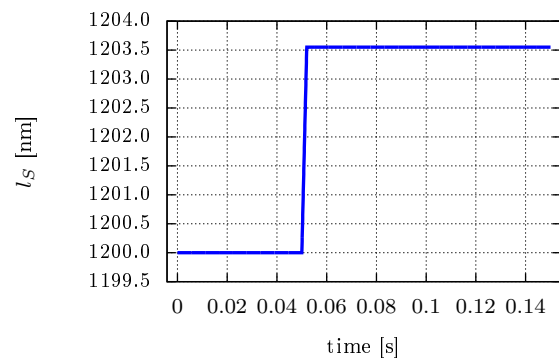
(i) F_{CBS} - steady state force in overlap according to degree of actin-myosin overlap.



(j) $\frac{N_{dl}}{m_{cb}}$ - number of attached cross-bridges per dl .



(k) $\frac{N}{m_{cb}}$ - number of attached cross-bridges.



(l) l_S - length of half-sarcomere.

Figure 7.13: Properties of contraction during sudden stretch.

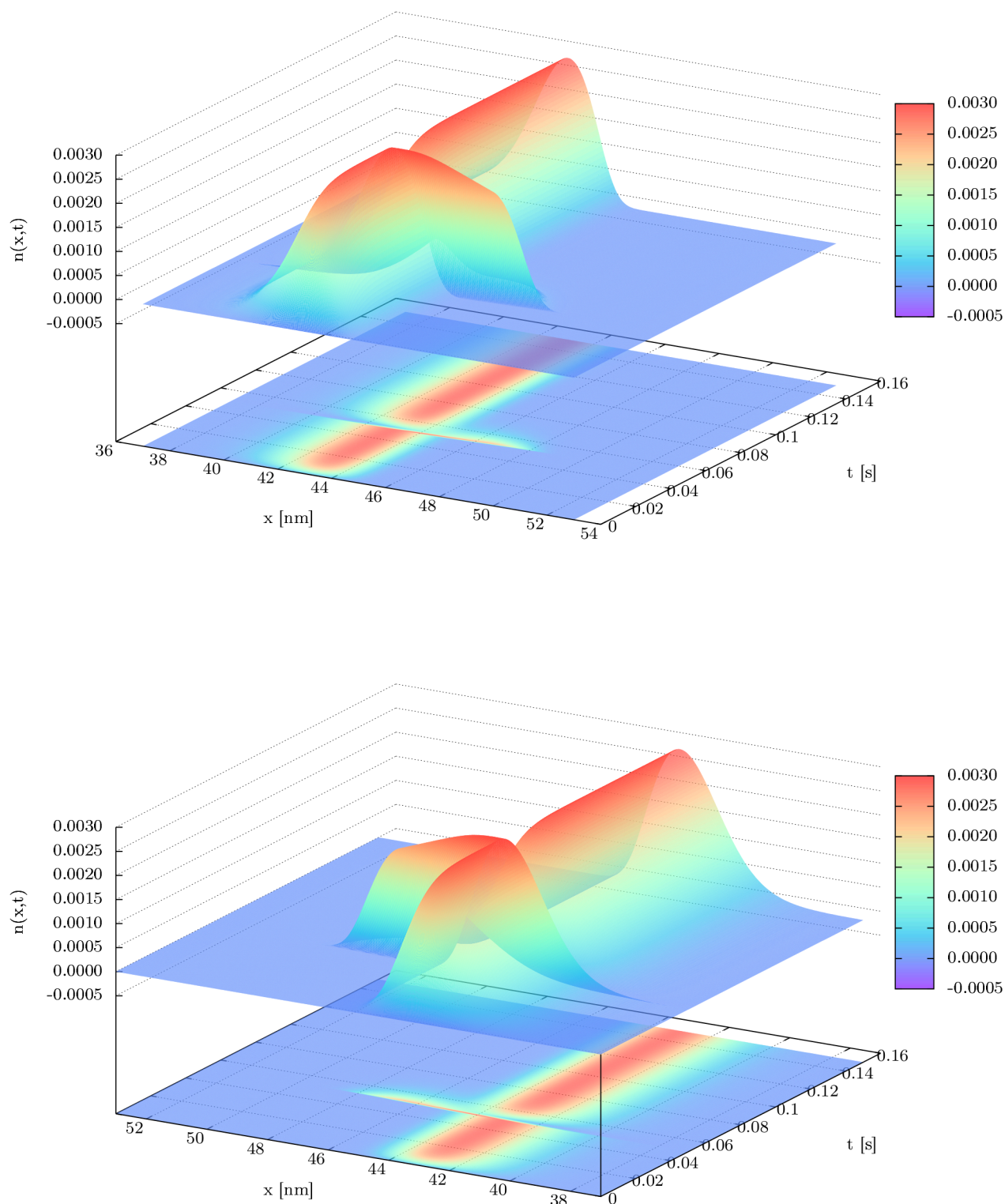


Figure 7.14: $n(x,t)$ time evolution during simulation of sudden stretch $v = -1800 \text{ nm s}^{-1}$.

Comments on the results of the sudden stretch of a half-sarcomere Sudden stretch is a special case of eccentric contraction, where the muscle is suddenly stretched from its initial isometric contraction. After quick stretch, the sarcomere undergoes quick increase in length - see figure 7.13l and simultaneously quick increase in force - see figure 7.13a. Since the sudden stretch is a special case of eccentric contraction, all properties described in preceding part on eccentric contraction are also valid for these results of simulation.

Because the sudden stretch is performed only for small length change of sarcomere (actin-myosin overlap) as well as for small titin stretch, the force that dominates in force-time relationship comes from the attached cross-bridges - see figure 7.13b. Although the titin is also stretched, its force increase is negligible - see figure 7.13d. Therefore, after stretch the force relaxes to the steady-state force, which is slightly higher than initial force. The results of simulation can be compared to the measured results as depicted in figure 2.23 on page 55.

Chapter 8

Conclusion and summary on the achieved results

In conclusion on the main topic of submitted work, let's quickly recall here the main aims of the thesis. The presented work dealt with theoretical model of skeletal sarcomere (muscle) contraction based on widely admitted classical cross-bridge theory and two sliding filament theory. The main topic of these classic theories is to explain the muscle contractile activity as it arises from the cyclical interaction of two proteins actin and myosin. The first mathematical model of cross-bridge theory was published by A.F. Huxley already in 1957. Since then, a lot of modifications of Huxley's original model were published to actual state of art in physiology at considered time.

To conclude on account of a long history of these models, it might be stated that models based on cross-bridge theory more or less succeeded in the description of concentric and isometric contraction including energetics of these contractions. Till nowadays, the most challenging part of cross-bridge theory remains the explanation of the nature of eccentric contraction and contraction history-dependent phenomenons as force enhancement following after eccentric contraction and force depression following after concentric contraction [35], [41], [43].

Therefore, the main effort of this dissertation thesis was to contribute to the possible

explanation of mentioned remaining problems of cross-bridge theory. Predominantly, the work was focused on the problems related to the explanation of the nature of eccentric contraction and its intrinsic phenomenon called force enhancement. Accordingly, one of the most necessary parts of presented work was also to carefully collect the actual information in physiology gained namely in last two decades in experiments on single sarcomeres, single cross-bridges (myosin II), single titin filament and its segments. Because the protein myosin II is molecular motor, a considerable part of text was devoted to the comprehension of these amazing natural mechanisms. The detailed collecting of mentioned information was also the most time-consuming part of work.

Consequently, based on the acquired information, the mathematical model based on Huxley's approach was derived from scratch with a strong attention to physiological background of considered problem. Therefore, one of the main results of presented work is also modified classical Huxley's cross-bridge model with precisely defined parameters regarding the latest possible results in physiology. The derived modified model in its dynamic form is on page 154. The steady-state form of proposed model is on page 156.

In comparison to classical cross-bridge theory and classical two-sliding filament theory, the classical Huxley's cross-bridge model was modified in particular in following manner:

1. the active force production in mathematical description was related directly to the degree of actin-myosin filaments overlap rather than to sarcomere length,
2. the experimentally measured mechanical properties of single cross-bridges [62], [63], [90] were used in the model,
3. the single cross-bridge elastic properties were described rather by shortest x end-to-end distances between single cross-bridge's ends than by spring with elongation x ,
4. the newly observed special properties of titin filaments were added to model as proposed in [17], [40], [43] - crucial modification related to eccentric contraction,

5. the Huxley's equation describing the evolution of distribution $n(x, t)$ of attached cross-bridges was slightly modified to allow the use of the normalized distribution $n(x, t)$,
6. probably not widely known the error of conservation law of the number of cross-bridges in classical as well as in modified model is discussed,
7. the kinetic rate $f(x)$ and interval h were proposed in manner to allow the attachment of cross-bridges oriented in wrong direction according the sense of the concentric contraction direction and in buckled/bended state,
8. the computation of consumed ATP molecules was connected rather with kinetic rate $g(x)$ than $f(x)$,
9. the form of considered kinetic rate $g(x)$ allows to compute forcibly detached cross-bridges vs. cross-bridges detached by ATPase activity,
10. the equations of another properties of mechanism were proposed for better insight into muscle contractile activity.

According to the first mentioned modification, the active force production was related directly to the degree of actin-myosin overlap in contrary to classical Huxley's model, where the force is related to the length of the whole (half) sarcomere including passive I-band region. It was believed here that this modification could contribute namely to the better estimation of the produced force by cross-bridges. Further it allows better estimation of the number of attached cross-bridges followed by the possible better estimation of energetic properties of the contractile processes as estimation of the number of consumed ATP molecules.

The second and third mentioned modifications were on a single cross-bridge level. Non-linear property of single cross-bridge elasticity as measured in [90], [62], [63] was integrated into the cross-bridge model. According to this modification, the variable x was defined as the shortest end-to-end distance of single cross-bridge's ends rather than as spring with

elongation x . The description of mechanical properties with end-to-end distance is also common approach in physics of proteins. The description with end-to-end distance also allows to incorporate into model the cross-bridges, which are attached in bended/buckled states and in wrong direction according to the sense of concentric contraction.

The fourth mentioned modification is the crucial step for the support of the newly proposed explanation of the nature of eccentric contraction. Regarding to this modification, the pivotal adjustment of classical model was the inclusion of the third filament titin into the classical cross-bridge model as proposed in [40]. This crucial modification supposes that during the all kind of contraction the resulted force, which is the inner mechanism in sarcomere able to develop, is always sum of active and passive force sources. More specifically, it is sum of forces produced by cross-bridges cycling and newly observed titin elastic properties, which play more significant role in sarcomere than originally considered in classical cross-bridge theory and two sliding filament theory. This modification resulted in enhancement of classical cross-bridge model especially on account of still challenging explanation of eccentric contraction, which is followed by the phenomena of force enhancement, where the steady-state force of activated sarcomere after stretch is much higher than in related isometric state with the same length of sarcomere (with the same degree of actin myosin overlap).

The fifth and sixth modifications were proposed on classical Huxley's equation for description of the dynamic of attached cross-bridges. The original equation was changed in a manner to allow normalization of distribution $n(x, t)$ of attached cross-bridges according to the sum of the number of attached and detached cross-bridges in (half) sarcomere. In connection with this modification, it was pointed out that classical Huxley's equation and modified Huxley's equation in a mathematical form of transport equation with sources violates the balance law on the preservation of the number of cross-bridges. On account of this problem, the possible way of correction of this error was proposed. Still, this problem need to be examined with more attention, because it might be the key for the resolution of another remaining problems of cross-bridge theory as for example of phenomena of force depression. The equations proposed for this correction are on page 155.

The seventh, eight and ninth modifications were related to the bound and unbound kinetic rates $f(x), g(x)$. The proposed bound rate $f(x)$ can be considered as the weakest part of proposed model because it was proposed rather phenomenologically. Nevertheless, the shape of this function as proposed here allows to include the cross-bridges with wrong orientation according to the sense of concentric contraction, which are often reported in literature. In comparison to classical Huxley's model, the use of this form of $f(x)$ also allows to describe the distribution $n(x, t)$ as continuous function. The resulted shape of distribution then might look more "physically" although this assumption is very arguable since the shape of distribution is probably impossible to verify with measured data.

The unbound kinetic rate $g(x)$ was proposed as the sum of the effects describing cross-bridge unbinding due to APTase activity on single cross-bridges and due to the effect of load, where the single cross-bridges might be forcibly detached before completion of their biochemical cycle. On account of this modification, the computation of consumed ATP molecules during contractile activity was related rather to function $g(x)$ in contrary to classical Huxley's model. The proposed shape of kinetic rate $g(x)$ thus allows to estimate the number of cross-bridges detached by ATP molecules and number of cross-bridges forcibly detached by external load.

Similarly to classical model, the last modifications of model were on account of description of another mechanical properties. Namely, the relationships for stiffness, elastic energy etc. were derived and changed to satisfy the mathematical form of proposed three filament cross-bridge model.

To test the modified classical Huxley's cross-bridge model, the following numerical simulations were conducted:

1. simulation of isometric contraction,
2. simulation of isotonic concentric contraction,
3. simulation of sudden shortening (special case of concentric contraction),
4. simulation of eccentric contraction followed by phenomena of force enhancement,

5. simulation of sudden stretch (special case of eccentric contraction),
6. special cases and properties of force enhancement.

It must be emphasized that proposed model is too complex and had to be simplified namely on account of simulation of titin's part unfolding. Therefore, the simulated situations and ranges of contractile length were selected with respect on physiological conditions, where it is assumed that unfolding of titin's Ig-domains does not occur. The reason for this was the imperfections in models describing the unfolding of proteins, which usually at the end leads to "user adjustable" parameters. The simplified model with its parameters is on page 161.

Accordingly, the simulation of eccentric contraction was conducted only for small stretches, where the unfolding of titin's parts need not to be considered. The aim of all results was rather to test the concept of proposed model than to achieve the results with the same absolute values in comparison to wide variety of experimentally measured data.

Although the simulation of isometric and eccentric contraction were not the main topic of presented work, it was necessary to show that the modified cross-bridge model also conform to these parts of cross-bridge theory, which are traditionally considered as sufficiently explained by classical Huxley's model. The results of simulation of isometric contraction are depicted in figures 7.2 on page 167. The time-evolution of distribution of attached cross-bridges during isometric contraction is depicted in figure 7.2m on page 169. The results of simulation of concentric contraction are depicted in figures 7.3 on page 171. The time-evolution of distribution of attached cross-bridges during concentric contraction is depicted in figure 7.3m on page 173. The results of simulation of sudden shortening of sarcomere are depicted in figures 7.4 on page 177 and in figure 7.4m on page 179.

The main conclusion of the simulation results of isometric and concentric contraction is that the proposed three filament cross-bridge model does not break the parts of cross-bridge theory, which are traditionally considered as sufficiently understood by original classical Huxley's model. The shape of force-time relationships of sarcomere force production achieved by these simulations might be easily compared with experimentally measured

results on the scales of the whole muscle, myofibrile and single sarcomere. On account of concentric contraction, it must be pointed out that modified model as well as original Huxley's model does not describe phenomenon of force depression following after shortening of muscle.

The important results of eccentric contraction are introduced in section 7.4. The various properties of eccentric contraction are depicted in figures 7.5 on page 182 and in figures 7.8 on page 189. Besides other conclusions presented in discussion, the results clearly showed that fast increase in force during transient state of eccentric contraction is predominantly caused by the change of the shape of distribution $n(x, t)$. In this kind of contraction, the distribution $n(x, t)$ is moved to the ranges of x , where the single cross-bridges produce higher force upon stretch although less of cross-bridges are attached in this kind of contraction than in others types of contraction.

Another important result is that the simulations performed only for the ranges of physiological condition, where the unfolding of titin's segments are not considered, clearly shows that the force decay at the end of transient state of eccentric contraction arises from the gradual change of $n(x, t)$ distribution to steady-state. The model further showed that the steady state shape of distribution after contractile activity correspond to the shape of isometric distribution. Nevertheless it might be worthwhile to notice, that studied properties in transient state of contractions are skewed by the mentioned error of conservation of number of cross-bridges. In any case, it might be concluded that at small stretches of sarcomere, the unfolding of titin's Ig domains is not necessary to describe force decay at the end of contractile activity. Whereas at higher stretches, the force decay at the end of transient state of eccentric contraction is likely the simultaneous effect of titin part's unfolding together with gradual change of distribution as described above.

The most important results of presented work are simulations of properties of phenomena of force enhancement depicted in section 7.4.1 in figure 7.10 on page 191, further in figures in 7.11 on page 193 and in figures 7.12 on page 194. The main conclusions resulting from these graphical results of performed simulation on steady-state force enhancement are the main results of presented dissertation thesis and can be summarized into two points:

1. the concept of proposed modifications in classical cross-bridge theory and two sliding filament theory as proposed in [40] conforms to the basic observable properties of eccentric contraction. More specifically, the simulations of eccentric contraction show the two most characteristic properties of eccentric contraction. At first, the results show the mechanism of the property that the quick increasing magnitude of sarcomere's force during transient state of eccentric contraction depends on the speed of stretch, which significantly affects the shape of distribution $n(x, t)$. Secondly, the simulations of eccentric contraction are consistent with the fact that the resulted magnitude of steady-state force enhancement increases with increasing magnitude of stretch. This is consequence of the self-modified properties of titin as showed in achieved results.
2. The second important conclusion based on the results is that the phenomena of force enhancement experimentally measured at all levels of muscle structural hierarchy has its origin on the scale of half-sarcomere (scale of the hundreds of nm and units of μm). This conclusion overshadows the theories as sarcomere length non-uniformities in myofibriles or proposals on additional special states in cross-bridge's biomechanical cycle etc.

In conclusion, modified Huxley's cross-bridge model is able to contribute namely to the explanation of the eccentric contraction and its intrinsic phenomena of force enhancement. Further, on account of the proposed modifications, the processes already successfully explained by original Huxley's model remained unchanged or improved. The crucial modification of the classical model has showed the way of the addition of special properties of titin filaments into the classical cross-bridge model. In comparison to classical theories, this modification as proposed in [40] also changes the general view on the mechanism of eccentric contraction.

The mentioned imperfections of the model also define the direction of the next possible research. Especially, the model of the titin's part must be enhanced in the way to include namely kinetics of unfolding and refolding of Ig-domains. Further, the impact of the balance

law error of the number of cross-bridges in model should be more carefully examined. The main task of this discrepancy might be to resolve the question if the shape of distribution $n(x, t)$ in steady-states after contractile activity has really the same shape as in the case of initial state (isometric contraction).

The modification and proposals in presented three filament cross-bridge model were proposed with respect to the experimental results of force-time relationships of considered kind of contractile activities. It might be worthwhile to improve the model also with respect to the experimentally measured results of energetic properties of muscles. For instance, the comparison with measured consumption of ATP molecules could also help to better tune up the shape of binding/unbinding rate functions $f(x), g(x)$. Regarding to the description of force-length relationship of single cross-bridges, it might be worthwhile to consider the description of this property also by worm-like chain model since this model is in general successful in the description of forces generated by proteins.

Bibliography

- [1] R. Ait-Haddou and Walter Herzog. Force and motion generation of myosin motors: muscle contraction. *Journal of Electromyography and Kinesiology*, 12:435–445, 2002.
- [2] Hind A. AL-Khayat. Three-dimensional structure of the human myosin thick filament: clinical implication. *Global Cardiology Science and Practise*, 36:280–302, 2013.
- [3] R. Dean Astumian. Thermodynamics and kinetics of molecular motors. *Biophysical Journal*, 98:2401 – 2409, 2010.
- [4] Josh E. Baker. Free energy transduction in a chemical motor model. *Journal of Theoretical Biology*, 228:467–476, 2004.
- [5] C.J. Barclay, R.C. Woledge, and N.A. Curtin. Inferring crossbridge properties from skeletal muscle energetics. *Progress in Biophysics and Molecular Biology*, 2010.
- [6] Jan Baxa, Jan Beneš, Marek Brandner, Jan Brůha, Jiří Egermajer, Jiří Ferda, Alena Jonášová, Petra Kochová, Hana Kopincová, Stanislav Kormuda, Milena Králíčková, Jana Křečková, Jiří Křen, Václav Liška, Vladimír Lukeš, Hynek Mírka, Martin Pešta, Pavel Pitule, Eduard Rohan, Josef Rosenberg, Tomáš Skalický, Pavel Souček, Zbyněk Tonar, Vladislav Třeška, Radek Tupý, Jan Vimmr, and Ondřej Vyčítal. *Experimentální chirurgie - nové technologie v medicíně, II. díl: Biomechanika*. Univerzita Karlova v Praze, Lékařská fakulta v Plzni, Husova 3, 306 05 Plzeň, 2013.
- [7] George I. Bell. Models for the specific adhesion of cells to cells. *Science*, 200(618):618–627, 1978.
- [8] Bernhard Brenner. The stroke size of myosins: a reevaluation. *Journal of Muscle Research and Cell Motility*, 27:173–187, 2006.
- [9] C. Bustamante, J.F. Marko, E.D. Siggia, and S. Smith. Entropic elasticity of α -phage dna. *Science*, 9 September 1994.

- [10] Vincent J. Caiozzo. Plasticity of skeletal muscle phenotype: mechanical consequences. *Muscle & Nerve*, 26:740–768, August 9 2002.
- [11] Mariano Carrion-Vazquez, Andres F. Oberhauser, Susan B. Fowler, Piotr E. Marszalek, Sheldon E. Broedel, Jane Clarke, and Julio M. Fernandez. Mechanical and chemical unfolding of a single protein: A comparison. *Proceedings of the National Academy of Sciences of the United States of America*, 96(7):3694–3699, 1999.
- [12] Leslie Chin, Pengtao Yue, James J. Feng, and Chun Y. Seow. Mathematical simulation of muscle cross-bridge cycle and force-velocity relationship. *Biophysical Journal*, 91:3653–3663, November 2006.
- [13] Lenka Cihalova. *Biomechanical models of tissue and their implementation into human body*. PhD thesis, University of West Bohemia, Plzeň, Czech Republic, 2008.
- [14] Robert Cimrman. *Mathematical modeling of biological tissue*. PhD thesis, University of West Bohemia, Plzeň, Czech Republic, 2002.
- [15] Roger Cooke. The actomyosin engine. *The FASEB Journal*, 9:636–642, May 1995.
- [16] T.A.J. Duke. Molecular model of muscle contraction. *Proceedings of the National Academy of Sciences of the United States of America*, 96:2770–2775, March 1999.
- [17] Michael M. DuVall, Jessica L. Gifford, Matthias Amrein, and Walter Herzog. Altered mechanical properties of titin immunoglobulin domain 27 in presence of calcium. *European Biophysics Journal*, 42:301 – 307, 2013.
- [18] Thomas J. Eddinger. Myosin heavy chain isoforms and dynamic contractile properties: skeletal versus smooth muscle. *Comparative Biochemistry and Physiology Part B*, 119:425–434, 1998.
- [19] K. A. P. Edman, G. Elzinga, and M. I. M. Noble. Enhancement of mechanical performance by stretch during tetanic contraction of vertebrate skeletal muscle fibres. *Journal of Physiology*, 1978.
- [20] K.A.P Edman and T. Tsuchiya. Strain of passive elements during force enhancement by stretch in frog muscle. *Journal of Physiology*, 490(1):191–205, 1996.
- [21] Thorsten Erdmann, Philipp J. Albert, and Ulrich S. Schwarz. Stochastic dynamics of small ensembles of non-processive molecular motors: The parallel cluster model. *The Journal of Chemical Physics*, 139, 2013.

- [22] Evan Evans and Ken Ritchie. Dynamic strength of molecular adhesion bonds. *Biophysical Journal*, 72:1541–1555, 1997.
- [23] John A. Faulkner, Lisa M. Larkin, Dennis R. Clafflin, and Susan V. Brooks. Age-related changes in the structure and function of skeletal muscles. *Clinical and Experimental Pharmacology and Physiology*, 34:1091–1096, 2007.
- [24] Richard Phillips Feynman. There’s plenty of room at the bottom: An invitation to enter a new field of physics. *Caltech Engineering and Science*, 23(5):22–36, 1960.
- [25] Jeffrey T. Finer, Robert M. Simmons, and James A. Spudich. Single myosin molecule mechanics: piconewton forces and nanometer steps. *Nature*, 368:113–119, 1994.
- [26] Thomas E. Fisher, Piotr E. Marszalek, and Julio M. Fernandez. Stretching single molecules into novel conformation using the atomic force microscope. *Nature structural biology*, 7(9):719–724, September 2000.
- [27] Michael A. Geeves. Stretching the lever-arm theory. *Nature*, 415:129–128, January 10 2002.
- [28] A. M. Gordon, E. Homsher, and M. Regnier. Regulation of contraction in striated muscle. *Physiological Reviews*, 80(2):853–924, 2000.
- [29] A.M. Gordon, A.F. Huxley, and F.J. Julian. The variation in isometric tension with sarcomere length in vertebrate muscle fibre. *J. Physiol*, 184:170–192, 1966.
- [30] Henk Granzier, Yiming Wu, Labeit Siegfried, and Martin LeWinter. Titin: Physiological function and role in cardiomyopathy and failure. In *Heart Failure Reviews*, volume 10, pages 211–223. Springer Science + Business Media, 2005.
- [31] Henk L. Granzier and Siegfried Labeit. Titin and its associated proteins: the third myofilament system of the sarcomere. *Advances in Protein Chemistry*, 71:89–119, 2005.
- [32] Irving P. Herman. *Physics of the Human Body*. Springer, 2007.
- [33] Jens A. Herzog, Tim R. Leonard, Azim Jinha, and Walter Herzog. Are titin properties reflected in single myofibrils? *Journal of Biomechanics*, 45:1893 – 1899, 2012.
- [34] Walter Herzog. Consideration on the theoretical modelling of skeletal muscle contraction. In Walter Herzog, editor, *Skeletal Muscle Mechanics, From Mechanisms to Function*. John Wiley & Sons, LTD, 2000. ISBN 0-471-49238-8.

- [35] Walter Herzog. The nature of force depression and force enhancement in skeletal muscle contraction. *European Journal of Sport Science*, 2001.
- [36] Walter Herzog. History dependence of skeletal muscle force production: Implication for movement control. *Human Movement Science*, 23:591–604, 2004.
- [37] Walter Herzog. Mechanism of enhanced force production in lengthening (eccentric) muscle contraction. *Journal of Applied Physiology*, 116(11):1407–1417, June 1st 2014.
- [38] Walter Herzog. The role of titin in eccentric muscle contraction. *The Journal of Experimental Biology*, 217:2825–2833, 2014.
- [39] Walter Herzog and Rachid Ait-Haddou. Consideration on muscle contraction. *Journal of Electromyography and Kinesiology*, 12:425–433, 2002.
- [40] Walter Herzog, Tim Leonard, Venus Joumaa, Michael DuVall, and Appaji Panchangam. The three filament model of skeletal muscle stability and force production. *Tech Science Press*, 9(3):175–191, 2012.
- [41] Walter Herzog and Tim R. Leonard. Force enhancement following stretching of skeletal muscle: a new mechanism. *Journal of Experimental Biology*, 205:1275–1283, 2002.
- [42] Walter Herzog, Tim R. Leonard, and J. Z. Wu. The relationship between force depression following shortening and mechanical work in skeletal muscle. *Journal of Biomechanics*, 33(6):659–668, June 2000.
- [43] Walter Herzog, Krysta Powers, Kaleena Johnston, and Michael DuVall. A new paradigm for muscle contraction. *Frontiers in Physiology*, 6(174), 2015.
- [44] A. V. Hill. The heat of shortening and the dynamic constants of muscle. *Proceedings of the Royal Society of London B: Biological Sciences*, 126(843):136–195, October 10th 1938.
- [45] Terrell L. Hill, Evan Eisenberg, and YI-Der Chen. Some self-consistent two-state sliding filament models of muscle contraction. *Biophysical Journal*, 15:335–372, April 1975.
- [46] Johnatton Howard and James A. Spudich. Is the lever arm of myosin a molecular elastic element? *Proceedings of the National Academy of Sciences of the United*

- States of America*, 1996. Appendix to article: Taro Q. P. Uyeda, Paul D. Abramson, and James A. Spudich. The neck region of the myosin motor acts as a lever arm to generate movement. *Proceedings of the National Academy of Sciences of the United States of America*, pages 4459–4464, April 1996. Biophysics.
- [47] <http://biomhs.blogspot.cz>.
- [48] Andrew F. Huxley. Muscle structure and theories of contraction. *Progress in biophysics and biophysical chemistry*, 7:255–318, 1957.
- [49] Andrew F. Huxley. Review lecture: Muscular contraction. *Journal of Physiology*, 243:1–43, 1974.
- [50] Andrew F. Huxley. Biological motors: Energy storage in myosin molecules. *Current Biology*, 8:485–488, 1998.
- [51] Andrew F. Huxley. Cross-bridge action: present views, prospects, and unknowns. *Journal of Biomechanics*, 33:1189 – 1195, 2000.
- [52] Andrew F. Huxley. Mechanics and models of the myosin motor. *Philosophical Transaction of the Royal Society B: Biological Sciences.*, 355:433–440, 2000.
- [53] Andrew F. Huxley and R. Niedergerke. Structural changes in muscle during contraction; interference microscopy of living muscle fibres. *Nature*, 173(4412):971 – 973, 1954.
- [54] Andrew F. Huxley and R.M. Simmons. Proposed mechanism of force generation. *Nature*, 22:533 – 538, 1971.
- [55] Andrew F. Huxley and S. Tideswell. Filament compliance and tension transients in muscle. *Journal of Muscle Research and Cell Motility*, 17:507–511, 1996.
- [56] Hugh E. Huxley. The mechanism of muscular contraction. *Science*, 164:1356–1366, 1969.
- [57] Hugh E. Huxley and J. Hanson. Changes in the cross-striations of muscle during contraction and stretch and their structural interpretation. *Nature*, 173 (4412):971–973, 1954.
- [58] Hugh Esmor Huxley. Electron microscope studies of the organisation of the filaments in striated muscle. *Biochimica et Biophysica Acta*, 12:387–394, 1953.

- [59] V. Joumaa, T.R. Leonard, and Walter Herzog. Residual force enhancement in myofibrils and sarcomeres. *Proceedings of The Royal Society B*, 275:1411–1419, 2008.
- [60] Venus Joumaa, D.E. Rassier, Tim R. Leonard, and Walter Herzog. The origin of passive force enhancement in skeletal muscle. *American Journal of Physiology*, 2008.
- [61] Frank Jülicher. Force and motion generation of molecular motors: A generic description. In *Transport and Structure: Their Competitive Roles in Biophysics and Chemistry*. Springer, Berlin 1999.
- [62] Motoshi Kaya and Hideo Higuchi. Nonlinear elasticity and an 8-nm working stroke of single myosin molecules in myofilaments. *Science*, 329:686–689, 6 August 2010.
- [63] Motoshi Kaya and Hideo Higuchi. Stiffness, working stroke, and force of single-myosin molecules in skeletal muscle: elucidation of these mechanical properties via nonlinear elasticity evaluation. *Cellular and Molecular Life Sciences*, 70:4275–4292, 2013.
- [64] Miklos S.Z. Kellermayer, Steven B. Smith, Carlos Bustamante, and Henk L. Granzier. Complete unfolding of the titin molecule under external force. *Journal of Structural Biology*, 122:197–205, 1998.
- [65] Miklos S. Z. Kellermayer, Steven B. Smith, Carlos Bustamante, and Henk L. Granzier. Mechanical fatigue in repetitively stretched single molecules of titin. *Biophysical Journal*, 80:852–863, February 2001.
- [66] Miklos S.Z. Kellermayer, Carlos Bustamante, and Henk L. Granzier. Mechanics and structure of titin oligomers explored with atomic force microscopy. *Biochimica et Biophysica Acta*, 1604:105–114, 2003.
- [67] Miklos S.Z. Kellermayer, Steven B. Smith, Henk L. Granzier, and Carlos Bustamante. Folding-unfolding transitions in single titin molecules characterized with laser tweezers. *Science*, 276:1112–1116, May 16 1997.
- [68] Kazuo Kitamura, Makio Tokunaga, and Toshio Yanagida. A single myosin head moves along an actin filament with regular steps of 5.3 nanometers. *Nature*, 397, 14 January 1999.
- [69] Stefan Klumpp, Theo M. Nieuwenhuizen, and Reinhard Lipowsky. Movements of molecular motors: Ratchets, random walks and traffic phenomena. *Physica E: Low-dimensional Systems and Nanostructures*, 29, Issues 1-2:380–389, October 2005.

- [70] Hana Kockova. *Biomechanical models of living tissues and their industrial applications*. PhD thesis, University of West Bohemia, Plzeň, Czech Republic, 2007.
- [71] Anatoly B. Kolomeisky and Michael E. Fisher. Molecular motors: A theorist's perspective. *Annual Review of Physical Chemistry*, 58:675–95, 2007.
- [72] Aikaterini Kontrogianni-Konstantopoulos, Maegen A. Ackermann, Amber L. Bowman, Solomon V. Yap, and Robert J. Bloch. Muscle giants: Molecular scaffolds in sarcomerogenesis. *Physiological Reviews*, 89:1217–1267, 2009.
- [73] F. Jon Kull and Sharyn A. Endow. Force generation by kinesin and myosin cytoskeletal motor proteins. *Journal of Cell Science*, (126):9–19, 2013.
- [74] Alexei Kurakin. Self-organization versus watchmaker: Molecular motors and protein translocation. *BioSystems*, 84:15–23, 2005.
- [75] Dietmar Labeit, Kaori Watanabe, Christian Witt, Hideaki Fujita, Yiming Wu, Sunshine Lahmers, Theodor Funck, Siegfried Labeit, and Henk Granzier. Calcium-dependent molecular spring elements in the giant protein titin. *Proceeding of the National Academy of Sciences of the United States of America*, 100(23), November 11 2003.
- [76] Ganhui Lan and Sean X. Sun. Mechanical models of processive molecular motors. *Molecular Physics*, 110:1017–1034, May 2012.
- [77] Carlos A. Lazalde and Lloyd Barr. Four-state models of contraction of smooth muscle. ii. properties of the solution and identification. *Mathematical Biosciences*, 112:31–54, 1992.
- [78] Carlos A. Lazalde and Lloyd C. Barr. Four-state models and regulation of contraction of smooth muscle. i. physical consideration, stability, and solutions. *Mathematical Biosciences*, 112, Issue 1:1–30, 1992.
- [79] Tim R. Leonard, Mark DuVall, and Walter Herzog. Force enhancement following stretch in a single sarcomere. *American Journal of Physiology Cell Physiology*, 2010.
- [80] T.R. Leonard and W. Herzog. Regulation of muscle force in the absence of actin-myosin-based cross-bridge interaction. *Am J Physiol Cell Physiol*, 299:C14–C20, 2010.

- [81] Xiumei Liu and Gerald H. Pollack. Stepwise sliding of single actin and myosin filaments. *Biophysical Journal*, 86:353–358, January 2004.
- [82] R. W. Lymn and E.W. Taylor. Mechanism of adenosine triphosphate hydrolysis by actomyosin. *Biochemistry*, 10(25):4617–4624, 1971.
- [83] Lorenzo Marcucci and Toshio Yanagida. From single molecule fluctuation to muscle contraction: A brownian model of a.f. huxley’s hypotheses. *PloS ONE*, 7(7), 2012.
- [84] John F. Marko and Eric D. Siggia. Stretching dna. *Macromolecules*, 28:8759–8770, 1995.
- [85] Ave Minajeva, Michael Kulke, Julio M. Fernandez, and Wolfgang A. Linke. Unfolding of titin domains explains the viscoelastic behavior of skeletal myofibrils. *Biophysical Journal*, 80:1442–1451, 2001.
- [86] D.L. Morgan. New insight into the behavior of muscle during active lengthening. *Biophysical Journal*, 57(2):209–221, 1990.
- [87] Alf Månsson, Dilson Rassier, and Georgios Tsiavaliaris. Review article: Poorly understood aspects of striated muscle contraction. *BioMed Research International*, 2015:1–28, 2015.
- [88] Yasuhiro Imafuku Neil Thomas and Katsuhisa Tawada. Molecular motors: thermodynamics and the random walk. *Proc. Royal Society London*, B 268:2113 – 2122, 2001.
- [89] Benno M. Nigg and Walter Herzog. *Biomechanics of the Musco-skeletal System*. John Wiley & Sons, third edition edition, 2006.
- [90] Takayuki Nishizaka, Hidetake Miyata, Hiroshi Yoshikawa, Shin’ichi Ishiwata, and Kazuhiko Kinoshita. Unbinding force of a single motor molecule of muscle measured using optical tweezers. *Nature*, 377:251–254, September 21 1995.
- [91] Andres F. Oberhauser, Piotr E. Marszalek, Mariano Carrion-Vazquez, and Julio M. Fernandez. Single protein misfolding events captured by atomic force microscopy. *Nature structural biology*, 6(11):1025–1028, November 1999.
- [92] Christopher B. O’Connell, Matthew J. Tyska, and Mark S. Mooseker. Myosin at work: Motor adaptations for a variety of cellular functions. *Biochimica et Biophysica Acta*, 1773:615–630, 2007.

- [93] Gerald Offer and K. W. Ranatunga. A cross-bridge with two tension-generating steps simulates skeletal muscle mechanics. *Biophysical Journal*, 105:928–940, August 2013.
- [94] Ray W. Ogden, Giuseppe Saccomandi, and Ivonne Sgura. Computational aspects of worm-like-chain interpolation formulas. *Computers and Mathematics with Applications*, 53:276–286, 2007.
- [95] Ivan Pavlov, Rowan Novinger, and Dilson E. Rassier. The mechanical behaviour of individual sarcomeres of myofibrils isolated from rabbit psoas muscle. *American Journal of Physiology Cell Physiology*, 297:C1211–C1219, 2009.
- [96] Gabriella Piazzesi, Massimo Reconditi, Marco Linari, Leonardo Lucii, Pasquale Bianco, Elisabetta Brunello, Valerie Decostre, Alex Stewart, David B. Gore, Thomas C. Irving, Malcolm Irving, and Vincenzo Lombardi. Skeletal muscle performance determined by modulation of number of myosin motors rather than motor force or stroke size. *Cell*, 131:784–795, November 6 2007.
- [97] Gerald H. Pollack. *Muscles & Molecules Uncovering the Principles of Biological Motion*. Ebner & Sons Publishers, 1990. ISBN: 0-9626895-0-5.
- [98] Lucas G. Prado, Irina Makarenko, Christian Andresen, Martina Krüger, Christiane A. Opitz, and Wolfgang A. Linke. Isoform diversity of giant proteins in relation to passive and active contractile properties of rabbit skeletal muscles. *Journal of General Physiology*, 126(November 5):461–480, 2005.
- [99] Dilson E. Rassier. The mechanisms of the residual force enhancement after stretch of skeletal muscle: non-uniformity in half-sarcomeres and stiffness of titin. *Proceedings of The Royal Society*, 2012.
- [100] Dilson E. Rassier and Walter Herzog. Force enhancement following an active stretch in skeletal muscle. *Journal of Electromyography and Kinesiology*, 12:471–477, 2002.
- [101] Ivan Raymet and Hazel M. Holden. Myosin sibfragment-1: structure and function of a molecular motor. *Current Opinion in Structural Biology*, 3:944–952, 1993.
- [102] Ivan Raymet, Hazel M Holden, Michael Whittaker, Christopher B. Yohn, Michael Lorenz, Holmes C. Kenneth, and Milligan A. Ronald. Structure of the actin-myosin complex and its implication for muscle contraction. *Science*, 261:58–65, July 2 1993.

- [103] Matthias Rief, Mathias Gautel, Alexander Schemmel, and Hermann E. Gaub. The mechanical stability of immunoglobulin and fibronectin iii domains in the muscle protein titin measured by atomic force microscopy. *Biophysical Journal*, 75:3008 – 3014, 1998.
- [104] Richard Rokyta. *Fyziologie pro bakalářská studia v medicíně, přírodovědných a tělovýchovných oborech*. ISV nakladatelství, 2000. ISBN 80-85866-45-5.
- [105] Caspar Ruegg, Claudia Veigel, Justin E. Molloy, Stephan Schmitz, John C. Sparrow, and Rainer H.A. Fink. Molecular motors: Force and movement generated by single myosin ii molecule. *Physiology*, 17:213–218, October 2002.
- [106] C. J. De Ruiter, W. J. M. Didden, D. A. Jones, and A. De Haan. The force-velocity relationship of human adductor pollicis muscle during stretch and the effects of fatigue. *Journal of Physiology*, 526(3):671–681, 2000.
- [107] G. Schappacher-Tilp, A. Jinha, and W. Herzog. Mapping the classical cross-bridge theory and backward steps in a three bead laser trap setup. *Mathematical Biosciences*, 229:115–122, 2011.
- [108] Gudrun Schappacher-Tilp, Timothy Leonard, Gertrud Desch, and Walter Herzog. A novel three-filament model of force generation in eccentric contraction of skeletal muscles. *PLoS ONE*, 10(3):e0117634, 03 2015.
- [109] James R. Sellers. Myosins: a diverse superfamily. *Biochimica*, 1496:3–22, 2000.
- [110] Chun Y. Seow. Hill’s equation of muscle performance and its hidden insight on molecular mechanism. *The Journal of General Physiology*, pages 561–573, 2013.
- [111] Ludmila Skubiszak. Geometrical conditions indispensable for muscle contraction. *International Journal of Molecular Sciences*, 12:2138–2157, 2007.
- [112] James A. Spudich. Molecular motors: forty years of interdisciplinary research. *Molecular Biology of the Cell*, 22(21):3936–9, 2011.
- [113] James A. Spudich. One path to understanding energy transduction in biological systems. *Nature Medicine*, 18:1478 –1482, 2012.
- [114] Bertrand C. W. Tanner, Thomas L. Daniel, and Michael Regnier. Sarcomere lattice geometry influences cooperative myosin binding in muscle. *PLoS Computational Biology*, 3(7):1195–1211, July 2007.

- [115] Cambridge Institute for Medical Research The Myosin Home Page hosted by the Myosin Group at RC Laboratory of Molecular Biology. <http://www.mrc-lmb.cam.ac.uk/myosin/myosin.html>.
- [116] D. De Tommasi, N. Milliardi, G. Puglisi, and G. Saccomandi. An energetic model for macromolecules unfolding in stretching experiments. *Journal of The Royal Society*, 10(88), 2013.
- [117] K. Trombitás, Y. Wu, M. McNabb, M. Greaser, M. S. Z. Kellermayer, S. Labeit, and H. Granzier. Molecular basis of passive stress relaxation in human soleus fibers: Assessment of the role of immunoglobulin-like domain unfolding. *Biophysical Journal*, 85:3142–3153, November 2003.
- [118] Larissa Tskhovrebova and John Trinick. Properties of titin immunoglobulin and fibronectin-3 do. *Journal of Biological Chemistry*, 279:46351–46354, November 5 2004.
- [119] Larissa Tskhovrebova and John Trinick. Roles of titin in the structure and elasticity of the sarcomere. *Journal of Biomedicine and Biotechnology*, 2010:7, 2010.
- [120] Matthew J. Tyska and David M. Warshaw. The myosin power stroke. *Cell Motility and the Cytoskeleton*, 51:1–15, 2002.
- [121] Taro Q. P. Uyeda, Paul D. Abramson, and James A. Spudich. The neck region of the myosin motor acts as a lever arm to generate movement. *Proceedings of the National Academy of Sciences of the United States of America*, pages 4459–4464, April 1996. Biophysics.
- [122] Roanald D. Vale and Ronald A. Milligan. The way things move: Looking under the hood of molecular motor proteins. *Science*, 88:88–95, 2000.
- [123] Sam Walcott and Walter Herzog. Modeling residual force enhancement with generic cross-bridge models. *Mathematical Biosciences*, 216:172–186, 2008.
- [124] Sam Walcott, David M. Warshaw, and Edward P. Debold. Mechanical coupling between myosin molecules causes differences between ensemble and single-molecule measurements. *Biophysical Journal*, 103:501–510, August 2012.
- [125] Hongyun Wang. Several issues in modeling molecular motors. *Journal of Computation and Theoretical Nanoscience*, 5:1–35, 2008.

- [126] C. David Williams, Michael Regnier, and Thomas L. Daniel. Elastic energy storage and radial forces in the myofilament lattice depend on sarcomere length. *PLOS Computational Biology*, 8(11), November 2012.
- [127] T. Yanagida, S. Esaki, A. H. Iwane, Y. Inoue, A. Ishijima, K. Kitamura, H. Tanaka, and M. Tokunaga. Single-motor mechanics and models of the myosin motor. *Philosophical Transactions of the Royal Society B: Biological Sciences*, 355(1396):441–447, 2000.
- [128] George Ireneus Zahalak. A distribution-moment approximation for kinetic theories of muscular contraction. *Mathematical Biosciences*, 55:89 – 114, 1981.
- [129] George Ireneus Zahalak. A comparison of the mechanical behavior of the cat soleus muscle with a distribution-moment model. *Journal of Biomechanical Engineering*, 108:131–140, May 1986.
- [130] George Ireneus Zahalak. Muscle activation and contraction: Constitutive relations based directly on cross-bridge kinetics. *Journal of Biomechanical Engineering*, 112:52–62, 1990.
- [131] George Ireneus Zahalak. The two-state cross-bridge model as a link between molecular and macroscopic muscle mechanics. In Walter Herzog, editor, *Skeletal Muscle Mechanics; From Mechanisms to Function*. Wiley, 2000.
- [132] George Ireneus Zahalak and I. Motabarzadeh. A re-examination of calcium activation in the huxley cross-bridge model. *Journal of Biomechanical Engineering*, 119:20–29, February 1997.

Publikace autora

Publikace indexované ve scopus

1. Čibera, V., Matas, R., Sedláček, J. Parametric model of ventilators simulated in Open-FOAM and Elmer. Volume 114, EPJ Web of Conferences, 2016
2. Matas, R., Sedláček, J., Čibera, V. Preliminary study to the temperatures of the thermocouple probes affected by the environment of heated walls. Volume 114, EPJ Web of Conferences, 2016
3. Matas, R., Čibera, V., Syka, T. Modelling of flow in pipes and ultrasonic flowmeter bodies. Volume 67, EPJ Web of Conferences, 2014
4. Čibera, V., Lávička, D., Kňourek, J. 1D models of the thermohydraulic systems supported by CFD results and measured data. Volume 67, EPJ Web of Conferences, 2014
5. Čibera, V., Lávička, D. Investigation of the thermohydraulic systems in MATLAB & Simulink using developed library. Volume 45, EPJ Web of Conferences, 2013

Konferenční příspěvky

1. ČIBERA, V. Ecentrická kontrakce modelovaná cross-bridge modelem skládajícím se ze třech filament. In *21st Congress of the European Society of Biomechanics*. Praha: ČVUT, 2015, ISBN: 978-80-01-05777-3
2. ČIBERA, V., HERZOG, W. Force enhancement modeled by three filament model. Salzburg, Rakousko, 2015.
3. LÁVIČKA, D., ČIBERA, V., KŇOUREK, J. Termohydraulické systémy řešené pomocí 1D modelů s využitím získaných výsledků z CFD simulací a z naměřených dat. In *Power System Engineering, Thermodynamics and Fluid Flow, ES 2014*. Plzeň: Západočeská univerzita v Plzni, 2014. s. 1-6. ISBN: 978-80-261-0360-8
4. ČIBERA, V. Three filament model of sarcomere. In *Computational Mechanics 2014, Book of extended abstracts*. Plzeň: Západočeská univerzita v Plzni, 2014. s. 17-18. ISBN: 978-80-261-0429-2
5. ČIBERA, V. Work of Molecular Motors. In *Energetické stroje a zařízení, Termomechanika & Mechanika tekutin, ES 2014*. Plzeň: Západočeská univerzita v Plzni, 2014. s. 1-6. ISBN: 978-80-261-0348-6
6. ČIBERA, V., LÁVIČKA, D., KŇOUREK, J., KŮS, M. 1D models of the thermohydraulic systems supported by CFD results. In *Power System Engineering, Thermodynamics & Fluid Flow 2013*. Plzeň: Západočeská univerzita, 2013. s. 1-4. ISBN: 978-80-261-0230-4
7. ČIBERA, V. Design and numerical simulations of the thermohydraulic systems in Simulink. In *Energetické stroje a zařízení, termomechanika & mechanika tekutin*. Plzeň: Západočeská univerzita v Plzni, 2012. s. 1-4. ISBN: 978-80-261-0113-0
8. ČIBERA, V. Rough estimation of the coefficients in mathematical models describing ion flux through cellular membrane. In *SVK 2012, studentská vědecká konference 2012*. Plzeň: Západočeská univerzita v Plzni, 2012. s. 13-14. ISBN: 978-80-261-0127-7
9. ČIBERA, V. Mathematical model of the molecular motor myosin in the smooth muscle cell. In *Computational Mechanics 2011*. Plzeň: Západočeská univerzita v Plzni, 2011. s. 1-2. ISBN: 978-80-261-0027-0

Výzkumné zprávy

1. SEDLÁČEK, J., MATAS, R., ŠTUDENT, J., ČIBERA, V. *Analýza dynamického namáhání ventilátoru a spalínovodu*. 2015
2. SEDLÁČEK, J., MATAS, R., ŠTUDENT, J., ČIBERA, V. *Software pro CFD výpočet a následnou analýzu dynamického namáhání ventilátoru a spalínovodu*. 2015
3. ČIBERA, V., SEDLÁČEK, J., MATAS, R., LÁVIČKA, D., NOVÁK, M. *Analýza 1D modelu vícestupňového kompresoru*. 2014.
4. ČIBERA, V., MATAS, R., LÁVIČKA, D. *Matematické 1-D modely potrubí pro použití v rámci softwaru navrženého pro simulace termohydraulických systémů*. 2013.
5. KŇOUREK, J., ČIBERA, V., LÁVIČKA, D., SEDLÁČEK, J. *Cooling circuit 1D model analysis and preparation*. Volkswagen Aktiengesellschaft, 2012.
6. KŇOUREK, J., ČIBERA, V. *Measured data analysis and model creation of the heat exchanger*. Volkswagen Aktiengesellschaft, 2012.
7. KŇOUREK, J., ČIBERA, V. *1-D model of water-air radiator*. 2011.
8. KŇOUREK, J., LÁVIČKA, D., ČIBERA, V. *Heating and thermal response solved by CFD*. 2011.

Kvalifikační práce

1. Čibera Václav *Využití nerovnovážné termodynamiky při popisu růstu a přetvoření hladkého svalstva*. Diplomová práce, ZČU, 2011
2. Čibera Václav *Entropie a II. termodynamický zákon v netradičních situacích*. Bakalářská práce, ZČU, 2009